博士論文

論文題目

Mathematical analysis of the method of fundamental solutions with its application to fluid mechanics and complex analysis

（基本解近似解法の数学解析およびその流体力学，複素解析への応用）

氏名　　**榊原　航也**

Preface

Method of Fundamental Solutions (MFS) is a mesh-free numerical solver for linear homogeneous partial differential equations, and its idea is very simple. Let us consider the following problem.

$$\begin{cases} \mathcal{L}u = 0 & \text{in } \Omega, \\ \mathcal{B}u = f & \text{on } \partial\Omega, \end{cases} \tag{0.0.1}$$

where Ω is a bounded region in the plane with smooth boundary $\partial\Omega$, $\mathcal{L}$ denotes a linear partial differential operator, $\mathcal{B}u = f$ gives boundary condition such as Dirichlet, Neumann, or Robin conditions. MFS offers an approximate solution for the above problem as in the following procedure.

(i) Take N singular points $\{y_k\}_{k=1}^N$ "suitably" from the exterior of Ω.

(ii) Construct an approximate solution $u^{(N)}$ as follows:

$$u^{(N)}(x) = \sum_{k=1}^{N} Q_k E(x - y_k),$$

where E is the fundamental solution for the operator $\mathcal{L}$. Note that the function $u^{(N)}$ satisfies the first equation in (0.0.1) exactly, that is, $\mathcal{L}u^{(N)} = 0$ in Ω.

(iii) Determine coefficients $\{Q_k\}_{k=1}^N$ by the collocation method. Namely, take N collocation points $\{x_j\}_{j=1}^N$ "suitably" on $\partial\Omega$, and impose the following "approximate" boundary conditions.

$$\mathcal{B}u^{(N)}(x_j) = f(x_j), \quad j = 1, 2, \ldots, N.$$

This is the algorithm of MFS. Namely, MFS is a truly mesh-free numerical solver for linear homogeneous partial differential equations. Moreover, if we arrange the singular and collocation points "suitably", then the approximation error decays exponentially with respect to N. This is a remarkable property of MFS compared with popular numerical solver such as finite element method (FEM) and finite difference method (FDM), in which the approximation error decays polynomially with respect to the mesh size. Furthermore, implementation and extension to higher dimensional problems of MFS is easy. Therefore, MFS has been applied to several problems in the field of engineering, science, and so on. On the other hand, there are no satisfactory mathematical theory for MFS compared with FEM and FDM, since we cannot apply useful mesh-dependent arguments used in the mathematical analysis of FEM and FEM to MFS. Hence, although MFS is a numerical solver for PDEs, we cannot use usual arguments in numerical analysis. Also, we have to clarify what the "suitable" arrangements of the singular and collocation points in mathematical sense. This is one reason why there are no adequate mathematical theory for MFS. In contrast, MFS has been applied to several problems (see, for instance, [20, 44]), however, it is hard to find mathematical result in those results. The author believes that mathematical analysis of MFS must be done in order to assure the efficiencies of previous applied researches. Then, we can state that the aim of this thesis is

- to develop mathematical theory of MFS, and
- to construct reliable numerical scheme for problems in the field of complex analysis and fluid mechanics based on MFS.

The contents of this paper are summarized as follows.

Part I is devoted to constructing mathematical theory of MFS. In Chapter 1, several notions are introduced, which will be used in mathematical analysis of MFS. Particularly, we introduce a family of Hilbert spaces which contains Sobolev spaces (Section 1.1), the notion of peripheral conformal mapping which is a conformal mapping in the neighborhood of the region (Section 1.2), fundamental results in potential theory (Section 1.3), the notion of capacity which measures the size of the region (Section 1.4), a theorem related discrete Fourier transform (Section 1.5), and estimates of Fourier coefficients for function which is defined in the direct product of two annular regions (Section 1.6).

In Chapter 2, we develop mathematical theory for MFS applied to potential problems in doubly-connected regions. Let us state the target problem precisely. Let Ω be a nondegenerate doubly-connected region in the complex plane, that is, there exist two disjoint connected components K_1 and K_2 such that $\hat{\mathbb{C}} \setminus \Omega = K_1 \sqcup K_2$, K_1 is unbounded in the sense that $\infty \in \mathring{K}_1$ holds, and neither K_1 nor K_2 is reduced to a single point, where $\hat{\mathbb{C}}$ denotes the extended complex plane, and $\mathring{K}_\nu$ denotes the interior of K_ν. Then, we consider the following potential problem:

$$\begin{cases} \triangle u = 0 & \text{in } \Omega, \\ u = f_\mu & \text{on } \Gamma^\mu,\ \mu = 1, 2, \end{cases} \tag{0.0.2}$$

where Γ^μ is the boundary ∂K_μ of K_μ, and f_μ is a given function defined on Γ^μ for each $\mu = 1, 2$. Let Ψ_μ be a peripheral conformal mapping of Γ^μ with reference radius ρ_μ for each $\mu = 1, 2$, where $\rho_1 > \rho_2 > 0$ (see, for the definition of peripheral conformal mapping, Definition 1.2.1). Then, we define the singular points $\{y_{\nu k}\}_{\nu=1,2}^{k=1,2,\dots,N}$ and the collocation points $\{x_{\mu j}\}_{\mu=1,2}^{j=1,2,\dots,N}$ as

$$\begin{cases} y_{\nu k} = \Psi_\nu(R_\nu \omega^{k-1}), & \nu = 1, 2;\ k = 1, 2, \dots, N, \\ x_{\mu j} = \Psi_\mu(\rho_\mu \omega^{j-1}), & \mu = 1, 2;\ j = 1, 2, \dots, N, \end{cases}$$

and construct an approximate solution $u^{(N)}$ as follows:

$$u^{(N)}(x) = \sum_{\nu=1}^{2} \sum_{k=1}^{N} Q_{\nu k} E(x - y_{\nu k}),$$

where $E(x) = (2\pi)^{-1} \log |x|$ is the fundamental solution for the operator $\triangle$, and the coefficients $\{Q_{\nu k}\}_{\nu=1,2}^{k=1,2,\dots,N}$ are determined by the following "approximate" boundary conditions:

$$u^{(N)}(x_{\mu j}) = f_\mu(x_{\mu j}), \quad \mu = 1, 2;\ j = 1, 2, \dots, N.$$

Parameters R_1 and R_2 for the singular points are chosen as $R_1 \in]\rho_1, \kappa\rho_1[$ and $R_2 \in]\kappa^{-1}\rho_2, \rho_2[$, where κ is a constant appeared in the definition of peripheral conformal mapping. Then, we prove that an approximate solution $u^{(N)}$ actually exists uniquely and an approximation error decays exponentially with respect to N when the boundary data are analytic (Theorem 2.1.1). The above is the conventional scheme for MFS applied to potential problems. Incidentally, it is known that $u^{(N)}$ does not satisfy invariance properties while the exact solution u for (0.0.2) satisfies them. Then, Murota [73] proposed an invariant scheme for MFS in disk, which satisfies invariance properties. If we apply it to (0.0.2), then an approximate solution $u^{(N)}$ is given of the form

$$u^{(N)}(x) = Q_0 + \sum_{\nu=1}^{2} \sum_{k=1}^{N} Q_{\nu k} E(x - y_{\nu k}),$$

and the coefficients are determined by the collocation method together with the following invariance condition:

$$\sum_{\nu=1}^{2}\sum_{k=1}^{N} Q_{\nu k} = 0.$$

We also prove corresponding results for this invariant scheme (Theorem 2.1.2). This chapter is based on my paper [85].

In Chapter 3, we consider a variant of MFS, which is called the dipole simulation method (DSM). When we consider the potential problem, MFS offers an approximate solution as a linear combination of logarithmic potentials, that is, an approximate solution given by MFS can be regarded as a discretization of the single-layer potential representation of the exact solution in some sense. On the other hand, in potential theory, the solution for the potential problem is given using double-layer potential. Therefore, it is natural to consider a discretization of this double-layer potential representation. Then, we find the following approximate solution for the potential problem:

$$u^{(N)}(x) = \sum_{k=1}^{N} Q_k D(x, y_k; n_k), \quad D(x, y_k; n_k) = \frac{-1}{2\pi}\frac{(n_k \mid x - y_k)}{\|x - y_k\|^2}. \tag{0.0.3}$$

Here the potential problem is considered as a problem in the two-dimensional Euclidean plane, and n_k, which is called the dipole moment, represents the direction of the axis of dipole located at y_k. Hereafter, we identify $\mathbb{R}^2$ with $\mathbb{C}$ in the usual manner. Although the formulation of DSM looks more natural than that of MFS for the potential problem, the mathematical analysis has been done only in [45]. In this chapter, we consider the potential problem in Jordan region. The singular points, the collocation points, and the dipole moments are defined by using peripheral conformal mapping. Then, under some conditions, we prove that an approximate solution actually exists uniquely, and that an approximation error decays exponentially with respect to N (Theorem 3.1.1). This chapter is based on my paper [84].

In Chapter 4, we consider the boundary value problem for the biharmonic equation. Namely, let Ω be a bounded region in the plane with smooth boundary, and consider the following problem.

$$\begin{cases} \triangle^2 u = 0 & \text{in } \Omega, \\ u = f & \text{on } \partial\Omega, \\ \dfrac{\partial u}{\partial \nu} = g & \text{on } \partial\Omega, \end{cases}$$

where $\triangle^2 = \dfrac{\partial^4}{\partial x^4} + 2\dfrac{\partial^4}{\partial x^2 \partial y^2} + \dfrac{\partial^4}{\partial x^2 \partial y^2}$ is the biharmonic operator in the plane, and $\partial u/\partial \nu$ denotes the derivative of u along outward normal direction. The conventional scheme for MFS offers an approximate solution for the above problem as a linear combination of the fundamental solutions of the biharmonic operator and ones of the Laplace operator. Namely, $u^{(N)}$ is of the form

$$u^{(N)}(x) = \sum_{k=1}^{N} \left(Q_k^{(1)} E(x - y_k) + Q_k^{(2)} F(x - y_k) \right),$$

where $F(x) = (8\pi)^{-1}|x|^2 \log|x|$ is the fundamental solution for the biharmonic operator. Although the above is the conventional scheme for MFS applied to biharmonic equation, in this chapter, we consider the another scheme for MFS based on Almansi-type decomposition of biharmonic function. Namely, we seek an approximate solution for the above problem having the following form:

$$u^{(N)}(x) = \sum_{k=1}^{N} \left(Q_k^p + Q_k^q |x|^2 \right) E(x - y_k).$$

Since there are no mathematical result for MFS applied to biharmonic equation, we consider the case where Ω is a disk as a first step to establish mathematical theory, and then we prove that an approximate solution actually exists uniquely (Theorem 4.1.2) and that an approximation error decays exponentially with respect to N (Theorem 4.1.3). This chapter is based on my paper [86].

In Chapter 5, we try to modify the original MFS for the potential problem, by adding the dummy points and weighted average condition. Namely, we seek an approximate solution $u^{(N)}$ for the potential problem having the form of

$$u^{(N)}(x) = Q_0 + \sum_{k=1}^{N} Q_k E_k(x), \quad E_k(x) = E(x - y_k) - E(x - z_k).$$

Here, $\{z_k\}_{k=1}^N$ are the dummy points, which are taken from the exterior of Ω. We determine the coefficients by the collocation method together with the following weighted average condition:

$$\sum_{k=1}^{N} Q_k H_k = 0,$$

where $\{H_k\}_{k=1}^N$ are given weights. Adding the dummy points $\{z_k\}_{k=1}^N$ and replacing the original kernel function with the difference of logarithmic potential E_k, $u^{(N)}$ satisfies the invariance condition with no additional condition. Therefore, we can add one more another condition, which enables us to construct geometrical variational structure-preserving numerical scheme for the one-phase Hele-Shaw problem, which will be presented in Chapter 6. Also, in this chapter, we consider the case where Ω is a disk, and establish mathematical theory, unique existence of approximate solution (Theorem 5.1.1) and exponential convergence (Theorem 5.1.2). This chapter is based on my paper [91].

Part II is devoted to MFS applied to fluid mechanics and complex analysis. In Chapter 6, we consider applications of MFS to fluid mechanics, especially, one-phase Hele-Shaw problems. The classical one-phase Hele-Shaw problem describes a motion of viscous fluid in a quasi two-dimensional space, which was starting from a short paper [32] in 1898 by Henry Selby Hele-Shaw (1854-1941). In his experiment, viscous fluid is sandwiched by two parallel plates with a narrow gap, and the apparatus is called Hele-Shaw cell. He succeeded in visualizing streamlines by means of colored water in the cell. The classical one-phase Hele-Shaw problem is stated as follows:

$$\begin{cases} \triangle p(\cdot,t) = 0 & \text{in } \mathscr{D}(t),\ t \in [0,T), \\ p(\cdot,t) = \gamma k(\cdot,t) & \text{on } \mathscr{C}(t),\ t \in [0,T), \\ V(\cdot,t) = -\nabla p(\cdot,t) \cdot \boldsymbol{N}(\cdot,t) & \text{on } \mathscr{C}(t),\ t \in [0,T), \end{cases} \tag{0.0.4}$$

where $\mathscr{D}(t) \subset \mathbb{R}^2$ is a bounded region occupied by fluid, $\mathscr{C}(t)$ is the boundary of $\mathscr{D}(t)$ (positively oriented closed curve), $p(\cdot,t)$ is the pressure function in $\mathscr{D}(t)$, γ is the surface tension coefficient, $k(\cdot,t)$ is the curvature (sing convention is the way that $k = 1$ if $\mathscr{D}(t)$ is a unit disk), $\boldsymbol{N}(\cdot,t)$ is the unit outward normal vector, and $V(\cdot,t)$ is the normal velocity, on $\mathscr{C}(t)$. We have three marked properties of the classical Hele-Shaw problem (0.0.4): the total length of $\mathscr{C}(t)$ is decreasing in time, the enclosed area of $\mathscr{D}(t)$ is preserving, and the barycenter of $\mathscr{D}(t)$ is being fixed. These properties are called curve-shortening (CS), area-preserving (AP), and barycenter-fixed (BF), respectively. Thus it is natural to consider that the numerical solution should satisfy these geometrical variational structures in some discrete sense. However, there is no such numerical scheme to our best knowledge. The purpose of this chapter is to propose a simple numerical scheme by means of MFS with the uniform distribution method. As a result, we have succeeded to construct numerical scheme which satisfies CS-, AP-, and BF-properties exactly, in which we have to solve system of "quadratic" equations, and the one which satisfies CS-, AP-, and BF-properties asymptotically, in which we have to solve system of "linear" equations. We also apply our scheme to other variations: the one-phase exterior problem, and the

one-phase interior Hele-Shaw problem with sink/source points. This chapter is based on my papers [89] and [90].

In Chapter 7, we construct numerical scheme for conformal mapping based on DSM. Conformal mapping is basic and important notion in complex analysis, and it has wide range of application in engineering, computational fluid mechanics, and so on. Therefore, it would be required to obtain "analytic form" of conformal mapping in practical application. However, it is impossible to do so except for only a few cases. Thus, numerical scheme for conformal mapping has been studied as an important research topic worldwide. Among numerous methods, Amano [2] offered very simple numerical scheme for conformal mapping based on MFS. Let Ω be a Jordan region in the complex plane, and consider a problem to find a conformal mapping f of Ω onto the unit disk satisfying the normalized conditions $f(z_0) = 0$ and $f'(z_0) > 0$, where $z_0 \in \Omega$ is a given point. Then, we can reduce this problem to find a harmonic function and its conjugate harmonic function as follows:

(i) Find a solution u for the following potential problem:

$$\begin{cases} \triangle u = 0 & \text{in } \Omega, \\ u(z) = -\log|z - z_0| & \text{on } \partial\Omega. \end{cases} \tag{0.0.5}$$

(ii) Find a conjugate harmonic function v of u satisfying $v(z_0) = 0$.

(iii) Define a function f as $f(z) = (z - z_0)\exp[u(z) + \mathrm{i}v(z)]$.

Then, the function f thus defined is nothing but the conformal mapping of Ω onto the unit disk satisfying the normalized conditions. Therefore, applying MFS to the above problem, we can obtain the following numerical scheme for conformal mapping [2]:

(i) Construct an approximate solution $u^{(N)}$ for the problem (0.0.5) by MFS as follows:

$$u^{(N)}(z) = \sum_{k=1}^{N} Q_k \log|z - \zeta_k|,$$

where $\{\zeta_k\}_{k=1}^{N}$ are the singular points.

(ii) Construct an approximate function $v^{(N)}$ of v as follows:

$$v^{(N)}(z) = \tilde{v}^{(N)}(z) - \tilde{v}^{(N)}(z_0), \quad \tilde{v}^{(N)}(z) = \sum_{k=1}^{N} Q_k \arg(z - \zeta_k).$$

(iii) Define a function $f^{(N)}$ as $f^{(N)}(z) = (z - z_0)\exp[u^{(N)}(z) + \mathrm{i}v^{(N)}(z)]$.

This is an algorithm for computing conformal mapping numerically. However, in the expression for $v^{(N)}$, the arg function appears. Mathematically, the branch of the arg function is selected so that $v^{(N)}$ would be continuous in Ω. On the other hand, when we implement the above numerical scheme, we have to deal with the problem to assign appropriate value for arg function, since the existing function in programing language only outputs the principal value of the arg function. Therefore, the above scheme is not easy for non-specialist to implement. In this chapter, another numerical scheme for conformal mapping based on DSM is proposed. As a result, we are able to avoid the issue related to the arg function, but it offers high-precision numerical results as well as the scheme based on MFS. Moreover, we investigate the behavior of errors for $u^{(N)}$, $v^{(N)}$, and $f^{(N)}$ mathematically, of which the results tell us that the behaviors of errors are completely governed by the error for $u^{(N)}$. We show

several results of numerical experiments in order to verify the effectiveness of our numerical scheme. This chapter is based on my paper [88].

In Chapter 8, we develop an interpolation method for holomorphic function, the complex dipole simulation method (CDSM). The idea of CDSM can be explained as follows. DSM offers an approximate solution for the potential problem as in (0.0.3). We here note that the kernel function $D(x, y_k; n_k)$ is a real part of the holomorphic function. Indeed, we have

$$D(x, y_k; n_k) = -\frac{1}{2\pi} \Re \left(\frac{n_k}{z - \zeta_k} \right),$$

where z, and ζ_k are complex representation of x, and y_k, respectively, and the same symbol n_k is the point in the two-dimensional Euclidean plane in the left hand side, and the one in the complex plane in the right hand side of the above relation. Therefore, we have

$$u^{(N)}(x) = u^{(N)}(z) = -\frac{1}{2\pi} \Re \left(\sum_{k=1}^{N} \frac{Q_k n_k}{z - \zeta_k} \right).$$

This expression suggests a new method for finding approximate function for holomorphic function in the form

$$f^{(N)}(z) = \sum_{k=1}^{N} Q_k H(z, \zeta_k), \quad H(z, \zeta) = \frac{1}{z - \zeta}.$$

This is a concept of CDSM. Approximate function obtained by CDSM can regarded as a discretization of Cauchy integral representation in some sense. In this chapter, we develop fundamental mathematical theory for CDSM in the case where Ω is a disk or the exterior domain of a disk. As a result, we prove that approximate function exists uniquely (Theorems 8.2.2 and 8.2.5), and that an approximation error decays exponentially with respect to N (Theorems 8.2.3 and 8.2.6). This chapter is based on my paper [87].

These works were supported by the Program for Leading Graduate Schools, MEXT, Japan.

Acknowledgements

I would like to express my gratitude to Professor Norikazu Saito, who is my supervisor, for his valuable suggestion and encouragement throughout my Doctor's course in University of Tokyo. I am deeply grateful to Professor Hiroshi Matano, who is my vice-supervisor, for his several advice and encouragement. I am grateful to Professor Masashi Katsurada for his instruction with patience and tolerance throughout my Bachelor's and Master's course in Meiji University. I would like to express the deepest appreciation to Professor Shigetoshi Yazaki who led me to the field of fluid mechanics, especially Hele-Shaw problem, and discussions and collaborations with him have been illuminating. I would like to offer my special thanks to Professor Michal Beneš for accepting me as a visiting Ph. D student at Czech Technical University in Prague, which have a good atmosphere and the stay in there for three months was so meaningful. I would like to thank Dr. Hisasi Tani for discussion on Hele-Shaw problem. I owe a very important debt to Mr. Shotaro Kamo (master's course student at Yazaki laboratory) and Mr. Toshiyuki Munakata (past master's course student at Yazaki laboratory), who helped me with carrying out experiments on Hele-Shaw problems. I owe my deepest gratitude to Professor Kaname Amano, Professor Tetsuya Ishiwata, Professor Masato Kimura, Professor Kenta Kobayashi, Professor Hayato Nawa, Professor Hisashi Okamoto, Professor Dai Okano, Professor Takashi Ohe, Professor Takashi Sakajo, and Professor Karel Švadlenka for their valuable comments and suggestions. I would like to thank the members of Saito laboratory (The University of Tokyo) and Yazaki laboratory (Meiji University) for their kindness and supports. I would like to thank the Program for Leading Graduate School for a grant that made it possible to complete this study. Finally, I would also like to express the deepest appreciation to my family for their support and warm encouragement.

Contents

Part I

Mathematical analysis of the method of fundamental solutions

Chapter 1

Preliminaries

Abstract

In this chapter, we collect several mathematical notions which are used to analyze MFS and DSM mathematically in Chapters 2 and 3.

1.1 Function spaces

When we study MFS and DSM, the following family of Hilbert spaces is used, which was firstly introduced by Arnold [5], in which a spline-trigonometric Galerkin method is studied.

Let $\mathcal{T}$ be the space of finite Fourier series on $S^1 := \mathbb{R}/\mathbb{Z}$. Namely, an element g of $\mathcal{T}$ is expressed by

$$g(\tau) = \sum_{n\in\mathbb{Z}} \hat{g}(n)\mathrm{e}^{2\pi \mathrm{i} n\tau} \quad (\tau \in S^1),$$

where $\{\hat{g}(n)\}_{n\in\mathbb{Z}}$ are complex numbers, all but a finite number of which are zeros. For each $(\epsilon, s) \in]0, +\infty[\times\mathbb{R}$, define an inner product $(\cdot,\cdot)_{\epsilon,s}\colon \mathcal{T}\times\mathcal{T}\to\mathbb{C}$ and a norm $\|\cdot\|_{\epsilon,s}\colon \mathcal{T}\to\mathbb{R}$ as

$$(g,h)_{\epsilon,s} = \sum_{n\in\mathbb{Z}} \hat{g}(n)\overline{\hat{h}(n)}\epsilon^{2|n|}\underline{n}^{2s} \qquad (g,h\in\mathcal{T}),$$

$$\|g\|_{\epsilon,s} = \sqrt{(g,g)_{\epsilon,s}} = \sqrt{\sum_{n\in\mathbb{Z}} |\hat{g}(n)|^2\epsilon^{2|n|}\underline{n}^{2s}} \quad (g\in\mathcal{T}), \tag{1.1.1}$$

where $\underline{n} := \max\{2\pi|n|, 1\}$. Then a space $\mathscr{X}_{\epsilon,s}$ is defined as the completion of $\mathcal{T}$ with $\|\cdot\|_{\epsilon,s}$, which forms a Hilbert space. The fundamental properties of $\mathscr{X}_{\epsilon,s}$ are as follows. Define a relation $>$ on $]0, +\infty[\times\mathbb{R}$ as

$$(\epsilon_1, s_1) > (\epsilon_2, s_2) \overset{\text{def}}{\iff} \epsilon_1 > \epsilon_2 \vee (\epsilon_1 = \epsilon_2 \wedge s_1 > s_2).$$

Proposition 1.1.1 ([48, Lemma 4.1])**.** (i) *For each $n\in\mathbb{Z}$, the nth Fourier coefficient mapping*

$$\mathcal{T} \ni g \longmapsto \hat{g}(n) = \int_0^1 g(\theta)\mathrm{e}^{-2\pi \mathrm{i} n\theta}\,\mathrm{d}\theta$$

has a unique bounded linear extension to $\mathscr{X}_{\epsilon,s}$. Furthermore, a norm $\|g\|_{\epsilon,s}$ of $g\in\mathscr{X}_{\epsilon,s}$ is defined as (1.1.1).

(ii) *For* $(\epsilon_\mu, s_\mu) \in]0, +\infty[\times\mathbb{R}$ $(\mu = 1, 2)$, *if* $(\epsilon_1, s_1) > (\epsilon_2, s_2)$ *then there exists a natural inclusion* $i\colon \mathscr{X}_{\epsilon_1,s_1} \hookrightarrow \mathscr{X}_{\epsilon_2,s_2}$ *and it is a compact operator. In particular, the union* $\mathscr{X} := \bigcup_{\epsilon,s} \mathscr{X}_{\epsilon,s}$ *of all the spaces* $\mathscr{X}_{\epsilon,s}$ *can be defined.*

Here, we list several facts regarding $\{\mathscr{X}_{\epsilon,s}\}_{\epsilon,s}$, which enable us to gain a strong understanding. Further details are explained in [5, Section 3]. When $\epsilon = 1$, $H^s := \mathscr{X}_{1,s}$ is a periodic Sobolev space with period 1. Then, for an analytic Jordan curve Γ in the plane $\mathbb{C}$, $H^s(\Gamma)$ can be defined as the set of functions on Γ whose composition with an analytic parameterization of Γ belong to H^s, and the norm of an element in $H^s(\Gamma)$ is given by the H^s norm of the composition. When $\epsilon > 1$, an element in $\mathscr{X}_{\epsilon,s}$ is an analytic function that can be continued complex analytically to the strip $\{b+\mathrm{i}\beta \mid b \in \mathbb{R},\ |\beta| < \log\epsilon\}$, and the trace on the boundary of the strip belongs to H^s. When $s > 1/2$, an element in $\mathscr{X}_{1,s}$ is a Hölder continuous function on S^1. Finally, the dual space of $\mathscr{X}_{\epsilon,s}$ is isomorphic to $\mathscr{X}_{\epsilon^{-1},-s}$, therefore we identify them as $(\mathscr{X}_{\epsilon,s})' = \mathscr{X}_{\epsilon^{-1},-s}$. For example, the Dirac delta function δ on S^1 can be regarded as the member of $\mathscr{X}_{\epsilon^{-1},-s}$ for $(\epsilon, s) > (1, 1/2)$ (see also Propositions 2.2.1 (ii), 2.2.2 (ii), and 3.2.1 (ii)).

1.2 Peripheral conformal mapping

In the analysis of MFS for potential problems in doubly-connected region (Chapter 2) and that of DSM in Jordan region (Chapter 3), we use peripheral conformal mappings to arrange the singular and collocation points. We here give a definition of peripheral conformal mapping and show its existence. Set $\gamma_r := \{z \in \mathbb{C} \mid |z| = r\}$ with $r > 0$, and $\mathcal{R}_{r_2,r_1} := \{z \in \mathbb{C} \mid r_2 < |z| < r_1\}$ with $r_1 > r_2 > 0$.

Definition 1.2.1. For a given Jordan curve Γ in the complex plane $\mathbb{C}$ and a given positive constant ρ, a map Ψ from a neighborhood of γ_ρ to $\mathbb{C}$ is called a *peripheral conformal mapping* of Γ with the reference radius ρ, if the following two conditions are satisfied:

(i) Ψ maps γ_ρ onto Γ;

(ii) there exists some $\kappa > 1$ such that $\Psi\colon \overline{\mathcal{R}}_{\kappa^{-1}\rho,\kappa\rho} \to \mathbb{C}$ is a conformal mapping, that is, Ψ is holomorphic and injective.

Although it has been pointed out in [48, Remark 3.1] that there exist peripheral conformal mappings of real analytic regular Jordan curves with arbitrary reference radii, the proof has not given. We here prove a theorem which verifies the above statement when $\rho = 1$. The other cases can be reduced to this case by suitable scaling argument.

Theorem 1.2.2. *Let* Γ *be a real analytic regular Jordan curve in the plane. Then, there exist some* $\kappa > 1$*, some open neighborhood* U *of* Γ*, and a biholomorphic function* $\varphi\colon \mathcal{R}_{\kappa^{-1},\kappa} \to U$ *such that* $\varphi(\gamma_1) = \Gamma$ *holds.*

Proof. Since Γ is a real analytic regular Jordan curve, there exists a real analytic function $\varphi\colon \mathbb{R}/(2\pi\mathbb{Z}) \to \mathbb{C}$ such that the following hold:

- $\varphi'(\theta) \neq 0$ for all $\theta \in \mathbb{R}/(2\pi\mathbb{Z})$;
- For all $\theta_1, \theta_2 \in \mathbb{R}/(2\pi\mathbb{Z})$ with $\theta_1 \neq \theta_2$, it holds that $\varphi(\theta_1) \neq \varphi(\theta_2)$;
- $\varphi([0, 2\pi]) = \Gamma$.

Since φ is real analytic, there exists some $\kappa \in]1, \infty[$ such that

$$\sum_{n\in\mathbb{Z}} |c_n|\kappa^{|n|} < +\infty,$$

where c_n denotes the nth Fourier coefficient of φ:

$$c_n = \frac{1}{2\pi}\int_{-\pi}^{\pi} \varphi(\theta)\mathrm{e}^{-\mathrm{i}n\theta}\,\mathrm{d}\theta, \quad n \in \mathbb{Z}.$$

Since $\varphi'(\theta) \neq 0$ for all θ, we have

$$\sum_{n\in\mathbb{Z}} \mathrm{i}nc_n\mathrm{e}^{\mathrm{i}n\theta} \neq 0, \quad \theta \in \mathbb{R}/(2\pi\mathbb{Z}).$$

We then define

$$F(z) = \sum_{n\in\mathbb{Z}} c_n z^n, \quad \kappa^{-1} \leq |z| \leq \kappa.$$

The infinite series on the right hand side of the above equation uniformly converges absolutely. Therefore F is continuous on $\overline{\mathcal{R}}_{\kappa^{-1},\kappa}$, and holomorphic in $\mathcal{R}_{\kappa^{-1},\kappa}$. Taking κ small if necessary, F could be injective on $\overline{\mathcal{R}}_{\kappa^{-1},\kappa}$. In the following, we prove this assertion. Note firstly that

$$F(\mathrm{e}^{\mathrm{i}n\theta}) = \sum_{n\in\mathbb{Z}} c_n\mathrm{e}^{\mathrm{i}n\theta} = \varphi(\theta)$$

holds for all $\theta \in \mathbb{R}/(2\pi\mathbb{Z})$. We show the existence of $\kappa \in]1,+\infty[$ satisfying the above property by contradiction. Namely, suppose that for all $\kappa \in]1,+\infty[$, there exist some $z_1, z_2 \in \overline{\mathcal{R}}_{\kappa^{-1},\kappa}$ such that $z_1 \neq z_2$ and $F(z_1) = F(z_2)$. Therefore, for each $n \in \mathbb{Z}$, by setting $\kappa := 1 + 1/n$, there exist $z_{1n}, z_{2n} \in \overline{\mathcal{R}}_{\kappa^{-1},\kappa}$ such that $z_{1n} \neq z_{2n}$ and $F(z_{1n}) = F(z_{2n})$. Since $\{z_{1n}\}$ and $\{z_{2n}\}$ are bounded sequences, there exist convergent subsequences $\{z_{1n_k}\}$ and $\{z_{2n_k}\}$ of $\{z_{1n}\}$ and $\{z_{2n}\}$, and z_1 and z_2 such that

$$z_{1n_k} \longrightarrow z_1, \quad z_{2n_k} \longrightarrow z_2, \quad \text{as} \quad k \to \infty.$$

Since $F(z_{1n_k}) = F(z_{2n_k})$ and F is continuous, we obtain $F(z_1) = F(z_2)$ by taking the limit $k \to \infty$. The injectivity of φ implies that $z_1 = z_2$ because of $|z_1| = |z_2| = 1$. Incidentally, for any $z_0 = \mathrm{e}^{\mathrm{i}\theta_0} \in \gamma_1$, we have

$$F'(z_0) = \sum_{n\in\mathbb{Z}} nc_n z_0^{n-1} = \frac{1}{\mathrm{i}\mathrm{e}^{\mathrm{i}\theta_0}} \sum_{n\in\mathbb{Z}} \mathrm{i}nc_n\mathrm{e}^{\mathrm{i}n\theta_0} = \frac{1}{\mathrm{i}\mathrm{e}^{\mathrm{i}\theta_0}}\varphi'(\theta_0) \neq 0.$$

Therefore, by the inverse function theorem, there exists some neighborhood V of z_1 such that F is injective in V. On the other hand, for sufficiently large k, z_{1n_k} and z_{2n_k} belong to V and satisfy that $z_{1n_k} \neq z_{2n_k}$ and $F(z_{1n_k}) = F(z_{2n_k})$, which contradicts the injectivity of F in V. □

1.3 Potential theory

1.3.1 single-layer potential

The following propositions play important roles in the proof of Lemma 2.4.6, where we aim to prove that $A^{\mathrm{C,I}}$, which are some bounded linear extensions of $A^{\mathrm{C,I}}$ defined in Section 2.4, are homeomorphisms. Here and hereafter, the symbol $\mathsf{F}^{\mathrm{C,I}}$ means F^{C} or F^{I}. Likewise, the symbol $\mathsf{F}_{\mathrm{C,I}}$ means F_{C} or F_{I}. Details of the following propositions are given in [33, Theorem 16.6h] and [79, Lemma 7], respectively.

Proposition 1.3.1. *Suppose that Γ is a C^2-regular Jordan curve in the plane with $\mathrm{Cap}(\Gamma) \neq 1$, where $\mathrm{Cap}(\Gamma)$ denotes the capacity of Γ and is defined in the subsequent section, Ω is the interior simply-connected region of Γ, φ is a Hölder continuous function on S^1, and $\gamma\colon S^1 \to \mathbb{C}$ is a C^2 regular parameterization of Γ. If it holds that*

$$\int_0^1 E(x-\gamma(\theta))\varphi(\theta)\,\mathrm{d}\theta = 0, \quad x \in \Omega,$$

then $\varphi \equiv 0$.

Proposition 1.3.2. *Suppose that* Γ *is a* C^2*-regular Jordan curve in the plane,* Ω *is the interior simply-connected region of* Γ*,* φ *is a Hölder continuous function on* S^1*,* $\gamma\colon S^1 \to \mathbb{C}$ *is a* C^2 *regular parameterization of* Γ*, and* α *is a constant. If it holds that*

$$\alpha + \int_0^1 E(x - \gamma(\theta))(\varphi(\theta) - \alpha)\,\mathrm{d}\theta = 0, \quad x \in \Omega,$$

then $\alpha = 0$ *and* $\varphi \equiv 0$.

Remark 1.3.3. The assumption on the capacity of Ω does not appear in Proposition 1.3.2, which enables us to remove the condition on the capacity of Ω from Theorem 2.1.2 concerning the invariant scheme for MFS, while it appears in Theorem 2.1.1 concerning the conventional scheme for MFS.

1.3.2 double-layer potential

Similar property also holds for double-layer potential.

Proposition 1.3.4. *Suppose that* Γ *is a* C^2*-regular Jordan curve,* Ω *the interior simply-connected region of* Γ*, and* Q *a continuous function on* Γ*. If it holds that*

$$\int_\Gamma \frac{-1}{2\pi} \frac{(\boldsymbol{n_y} \mid \boldsymbol{x} - \boldsymbol{y})}{\|\boldsymbol{x} - \boldsymbol{y}\|^2} Q(\boldsymbol{y})\,\mathrm{d}s_{\boldsymbol{y}} = 0, \quad \boldsymbol{x} \in \Omega,$$

then $Q \equiv 0$*. Here,* $\boldsymbol{n_y}$ *denotes the unit outward normal vector of* Γ *at* $\boldsymbol{y} \in \Gamma$*, and the symbol* $(\cdot \mid \cdot)$ *denotes the usual two-dimensional Euclidean inner product.*

Although this proposition is stated in [81, Theorem 35.1], these authors did not include a rigorous proof. Therefore, we provide a brief proof for the above proposition using the results in [19].

Proof. Let u be a function in Ω defined as

$$u(\boldsymbol{x}) = \int_\Gamma \frac{-1}{2\pi} \frac{(\boldsymbol{n_y} \mid \boldsymbol{x} - \boldsymbol{y})}{\|\boldsymbol{x} - \boldsymbol{y}\|^2} Q(\boldsymbol{y})\,\mathrm{d}s_{\boldsymbol{y}}, \quad \boldsymbol{x} \in \Omega.$$

Because Q is a continuous function on Γ, owing to [19, Theorem 3.22], u has a continuous extension $\tilde{u}$ to $\overline{\Omega}$. Especially, $\tilde{u}$ is expressed on Γ as

$$\tilde{u}(\boldsymbol{x}) = \frac{1}{2} Q(\boldsymbol{x}) + \int_\Gamma \frac{-1}{2\pi} \frac{(\boldsymbol{n_y} \mid \boldsymbol{x} - \boldsymbol{y})}{\|\boldsymbol{x} - \boldsymbol{y}\|^2} Q(\boldsymbol{y})\,\mathrm{d}s_{\boldsymbol{y}}, \quad \boldsymbol{x} \in \Gamma.$$

Because $u \equiv 0$ in Ω and $\tilde{u}$ is a continuous extension of u to $\overline{\Omega}$, $\tilde{u} \equiv 0$ on Γ holds, which is equivalent to

$$Q(\boldsymbol{x}) = \int_\Gamma \frac{1}{\pi} \frac{(\boldsymbol{n_y} \mid \boldsymbol{x} - \boldsymbol{y})}{\|\boldsymbol{x} - \boldsymbol{y}\|^2} Q(\boldsymbol{y})\,\mathrm{d}s_{\boldsymbol{y}}, \quad \boldsymbol{x} \in \Gamma. \tag{1.3.1}$$

The statement of Proposition 1.3.4 can be proved by showing that the integral equation (1.3.1) has only the trivial solution. Owing to Fredholm's alternative, the integral equation (1.3.1) has only the trivial solution if and only if the transposed equation of (1.3.1)

$$Q(\boldsymbol{x}) = \int_\Gamma \frac{1}{\pi} \frac{(\boldsymbol{n_x} \mid \boldsymbol{y} - \boldsymbol{x})}{\|\boldsymbol{y} - \boldsymbol{x}\|^2} Q(\boldsymbol{y})\,\mathrm{d}s_{\boldsymbol{y}}, \quad \boldsymbol{x} \in \Gamma \tag{1.3.2}$$

has only the trivial solution. Let Q be a solution for (1.3.2). Then, we have

$$\int_\Gamma Q(\boldsymbol{y})\,\mathrm{d}s_{\boldsymbol{y}} = 0, \tag{1.3.3}$$

which can be justified as follows:

$$\begin{aligned}\int_\Gamma Q(\boldsymbol{x})\,\mathrm{d}s_{\boldsymbol{x}} &= \int_\Gamma \left[-2\int_\Gamma \frac{-1}{2\pi}\frac{(\boldsymbol{n}_x \mid \boldsymbol{y}-\boldsymbol{x})}{\|\boldsymbol{y}-\boldsymbol{x}\|^2} Q(\boldsymbol{y})\,\mathrm{d}s_{\boldsymbol{y}}\right]\mathrm{d}s_{\boldsymbol{x}} \\ &= -2\int_\Gamma Q(\boldsymbol{y})\left[\int_\Gamma \frac{-1}{2\pi}\frac{(\boldsymbol{n}_x \mid \boldsymbol{y}-\boldsymbol{x})}{\|\boldsymbol{y}-\boldsymbol{x}\|^2}\,\mathrm{d}s_{\boldsymbol{x}}\right]\mathrm{d}s_{\boldsymbol{y}} = -\int_\Gamma Q(\boldsymbol{y})\,\mathrm{d}s_{\boldsymbol{y}}.\end{aligned}$$

We here consider the single-layer potential

$$w(\boldsymbol{x}) = \int_\Gamma Q(\boldsymbol{y})\frac{1}{2\pi}\log|\boldsymbol{x}-\boldsymbol{y}|\,\mathrm{d}s_{\boldsymbol{y}}.$$

Then, we see that w vanishes at a point at infinity, that is, $w(\boldsymbol{x}) \to 0$ ($|\boldsymbol{x}| \to 0$), which can be justified by [19, Lemma 3.31] with (1.3.3). As Q is a solution for (1.3.2), $\partial_{\nu+} w \equiv 0$ on Γ follows from [19, Theorem 3.28], where $\partial_{\nu+}$ is the exterior normal derivative on Γ defined as

$$\partial_{\nu+} g(\boldsymbol{x}) = \lim_{\tau\downarrow 0} \nu(\boldsymbol{x})\cdot\nabla g(\boldsymbol{x}+\tau\nu(\boldsymbol{x}))$$

for $g \in C^1(\mathbb{R}^2 \setminus \overline{\Omega})$ and $\boldsymbol{x} \in \Gamma$. Here, ν denotes the unit outward normal vector on Γ. Therefore, w is a solution for the following Laplace equation with the homogeneous Neumann boundary condition:

$$\begin{cases} \triangle w = 0 & \text{in } \mathbb{R}^2 \setminus \overline{\Omega}, \\ \partial_{\nu+} w = 0 & \text{on } \Gamma. \end{cases}$$

Then, there exists a constant C such that $w \equiv C$ in $\mathbb{R}^2 \setminus \overline{\Omega}$, because the solution of the exterior Neumann problem is determined up to a constant. The constant C is indeed equal to 0 because $w(\boldsymbol{x}) \to 0$ ($|\boldsymbol{x}| \to \infty$). Using the continuity of single-layer potential [19, Proposition 3.25], we have $w \equiv 0$ on Γ. Thus, $w \equiv 0$ in Ω follows from the maximum principle for harmonic functions, which yields that $\partial_{\nu-} w(\boldsymbol{x}) = 0$ ($\boldsymbol{x} \in \Gamma$), where $\partial_{\nu-}$ is defined similarly to $\partial_{\nu+}$. Hence, we obtain $Q \equiv 0$ on Γ by applying [19, Theorem 3.28]. □

1.4 Capacity

We here define the capacity of the Jordan region in the complex plane, which measures the size of the region.

Definition 1.4.1. Let Γ be a Jordan curve in the plane $\mathbb{C}$. Then, there exists a conformal mapping g of $\hat{\mathbb{C}} \setminus \overline{D}_1$ onto $\hat{\mathbb{C}} \setminus \overline{\Omega}$ with the following Laurent series expansion about ∞:

$$g(z) = c_1 z + c_0 + \frac{c_{-1}}{z} + \frac{c_{-2}}{z^2} + \cdots,$$

where Ω denotes the interior simply-connected region surrounded by Γ. The absolute value $|c_1|$ of c_1 is a geometrical value determined by Γ only, and is called the *capacity* of Γ. This is denoted by $\mathrm{Cap}(\Gamma)$.

The following proposition provides a method for evaluating the capacity of a Jordan curve in the plane $\mathbb{C}$. Roughly speaking, $\mathrm{Cap}(\Gamma)$ is bounded from below by the radius of a circle enclosed by Γ, and bounded from above by that enclosing Γ.

Proposition 1.4.2. *Let Γ be a Jordan curve in the plane $\mathbb{C}$.*

(i) *If Γ is a circle with radius r, then* $\mathrm{Cap}(\Gamma) = r$.

(ii) *If Γ is enclosed by a circle with radius r, then* $\mathrm{Cap}(\Gamma) \le r$.

(iii) *If Γ encloses a circle with radius r, then* $\mathrm{Cap}(\Gamma) \ge r$.

1.5 Discrete Fourier transform

The following proposition, which is used to establish the unique existence of approximate solution for MFS in annular region, states that the discrete Fourier transform is an isomorphism.

Proposition 1.5.1. *Suppose that $g \in L^1(S^1)$ and g is Hölder continuous in some neighborhood of Δ_N. Then, the series $\sum_{m\equiv p} \hat{g}(m)$ is convergent for $p \in \Lambda_N$, and moreover, the following equivalence holds:*

$$g = 0 \quad \text{on } \Delta_N \iff \sum_{m\equiv p} \hat{g}(m) = 0 \quad \text{for all } p \in \Lambda_N.$$

The details can be found in [6, Lemma 2.1].

1.6 Estimates of Fourier coefficients of function which is harmonic in the direct product of annular regions

The following proposition plays a key role in the analysis of MFS for potential problems in doubly-connected regions.

Proposition 1.6.1. *Let $u\colon \overline{\mathcal{R}}_{\kappa^{-1},\kappa} \times \overline{\mathcal{R}}_{\kappa^{-1},\kappa} \to \mathbb{C}$ be continuous, and harmonic in $\mathcal{R}_{\kappa^{-1},\kappa} \times \mathcal{R}_{\kappa^{-1},\kappa}$. Then, u has the following Fourier series expansion:*

$$\begin{aligned} u(r\mathrm{e}^{\mathrm{i}\theta}, \rho\mathrm{e}^{\mathrm{i}\tau}) = &\sum_{l,m\in\mathbb{Z}^*} \left(a_{lm} r^{|l|}\rho^{|m|} + b_{lm} r^{|l|}\rho^{-|m|} + c_{lm} r^{-|l|}\rho^{|m|} + d_{lm} r^{-|l|}\rho^{-|m|}\right) \mathrm{e}^{\mathrm{i}(l\theta+m\tau)} \\ &+ \sum_{m\in\mathbb{Z}^*} \left(a_{0m}\rho^{|m|} + b_{0m}\rho^{-|m|} + c_{0m}\rho^{|m|}\log r + d_{0m}\rho^{-|m|}\log r\right) \mathrm{e}^{\mathrm{i}m\tau} \\ &+ \sum_{l\in\mathbb{Z}^*} \left(a_{l0} r^{|l|} + b_{l0} r^{|l|}\log\rho + c_{l0} r^{-|l|} + d_{l0} r^{-|l|}\log\rho\right) \mathrm{e}^{\mathrm{i}l\theta} \\ &+ a_{00} + b_{00}\log\rho + c_{00}\log r + d_{00}\log r\log\rho. \end{aligned}$$

The Fourier coefficients $\{a_{lm}\}$, $\{b_{lm}\}$, $\{c_{lm}\}$, and $\{d_{lm}\}$ can be bounded as follows:

$$\begin{aligned} &|a_{00}| \le M, \quad |b_{00}|,\ |c_{00}| \le \frac{M}{\log\kappa}, \quad |d_{00}| \le \frac{M}{(\log\kappa)^2}, \\ &|a_{l0}|, |b_{l0}| \le \frac{M}{1-\kappa^{-2}}\kappa^{-|l|}, \quad |c_{l0}|, |d_{l0}| \le \frac{M}{(1-\kappa^{-2})\log\kappa}\kappa^{-|l|} \quad (l \ne 0), \\ &|a_{0m}|, |c_{0m}| \le \frac{M}{1-\kappa^{-2}}\kappa^{-|m|}, \quad |b_{0m}|, |d_{0m}| \le \frac{M}{(1-\kappa^{-2})\log\kappa}\kappa^{-|m|} \quad (m \ne 0), \\ &|a_{lm}|, |b_{lm}|, |c_{lm}|, |d_{lm}| \le \frac{M}{(1-\kappa^{-2})^2}\kappa^{-|l|-|m|} \quad (l, m \ne 0), \end{aligned}$$

where

$$M = \max_{x,y\in\partial\mathcal{R}_{\kappa^{-1},\kappa}} |u(x,y)|.$$

Proof. Define quantities A_{lm}, B_{lm}, C_{lm}, and D_{lm} as the double Fourier coefficients for $(r,\rho)=(\kappa,\kappa)$, (κ,κ^{-1}), (κ^{-1},κ), and $(\kappa^{-1},\kappa^{-1})$, respectively, that is,

$$
\begin{aligned}
A_{lm} &= \frac{1}{(2\pi)^2}\int_0^{2\pi}\int_0^{2\pi} u(\kappa \mathrm{e}^{\mathrm{i}\theta}, \kappa \mathrm{e}^{\mathrm{i}\tau}) \mathrm{e}^{-\mathrm{i}(l\theta+m\tau)}\,\mathrm{d}\theta\,\mathrm{d}\tau \\
&= \begin{cases}
a_{00} + b_{00}\log\kappa + c_{00}\log\kappa + d_{00}(\log\kappa)^2 & \text{if } l=m=0, \\
a_{l0}\kappa^{|l|} + b_{l0}\kappa^{|l|}\log\kappa + c_{l0}\kappa^{-|l|} + d_{l0}\kappa^{-|l|}\log\kappa & \text{if } l\neq 0,\ m=0, \\
a_{0m}\kappa^{|m|} + b_{0m}\kappa^{-|m|} + c_{0m}\kappa^{|m|}\log\kappa + d_{0m}\kappa^{-|m|}\log\kappa & \text{if } l=0,\ m\neq 0, \\
a_{lm}\kappa^{|l|+|m|} + b_{lm}\kappa^{|l|-|m|} + c_{lm}\kappa^{-|l|+|m|} + d_{lm}\kappa^{-|l|-|m|} & \text{if } l,m\neq 0,
\end{cases} \\
B_{lm} &= \frac{1}{(2\pi)^2}\int_0^{2\pi}\int_0^{2\pi} u(\kappa \mathrm{e}^{\mathrm{i}\theta}, \kappa^{-1} \mathrm{e}^{\mathrm{i}\tau}) \mathrm{e}^{-\mathrm{i}(l\theta+m\tau)}\,\mathrm{d}\theta\,\mathrm{d}\tau \\
&= \begin{cases}
a_{00} - b_{00}\log\kappa + c_{00}\log\kappa - d_{00}(\log\kappa)^2 & \text{if } l=m=0, \\
a_{l0}\kappa^{|l|} - b_{l0}\kappa^{|l|}\log\kappa + c_{l0}\kappa^{-|l|} - d_{l0}\kappa^{-|l|}\log\kappa & \text{if } l\neq 0,\ m=0, \\
a_{0m}\kappa^{-|m|} + b_{0m}\kappa^{|m|} + c_{0m}\kappa^{-|m|}\log\kappa + d_{0m}\kappa^{|m|}\log\kappa & \text{if } l=0,\ m\neq 0, \\
a_{lm}\kappa^{|l|-|m|} + b_{lm}\kappa^{|l|+|m|} + c_{lm}\kappa^{-|l|-|m|} + d_{lm}\kappa^{-|l|+|m|} & \text{if } l,m\neq 0
\end{cases} \\
C_{lm} &= \frac{1}{(2\pi)^2}\int_0^{2\pi}\int_0^{2\pi} u(\kappa^{-1} \mathrm{e}^{\mathrm{i}\theta}, \kappa \mathrm{e}^{\mathrm{i}\tau}) \mathrm{e}^{-\mathrm{i}(l\theta+m\tau)}\,\mathrm{d}\theta\,\mathrm{d}\tau \\
&= \begin{cases}
a_{00} + b_{00}\log\kappa - c_{00}\log\kappa - d_{00}(\log\kappa)^2 & \text{if } l=m=0, \\
a_{l0}\kappa^{-|l|} + b_{l0}\kappa^{-|l|}\log\kappa + c_{l0}\kappa^{|l|} + d_{l0}\kappa^{|l|}\log\kappa & \text{if } l\neq 0,\ m=0, \\
a_{0m}\kappa^{|m|} + b_{0m}\kappa^{-|m|} - c_{0m}\kappa^{|m|}\log\kappa - d_{0m}\kappa^{-|m|}\log\kappa & \text{if } l=0,\ m\neq 0, \\
a_{lm}\kappa^{-|l|+|m|} + b_{lm}\kappa^{-|l|-|m|} + c_{lm}\kappa^{|l|+|m|} + d_{lm}\kappa^{|l|-|m|} & \text{if } l,m\neq 0,
\end{cases} \\
D_{lm} &= \frac{1}{(2\pi)^2}\int_0^{2\pi}\int_0^{2\pi} u(\kappa^{-1} \mathrm{e}^{\mathrm{i}\theta}, \kappa^{-1} \mathrm{e}^{-\mathrm{i}\tau})\,\mathrm{d}\theta\,\mathrm{d}\tau \\
&= \begin{cases}
a_{00} - b_{00}\log\kappa - c_{00}\log\kappa + d_{00}(\log\kappa)^2 & \text{if } l=m=0, \\
a_{l0}\kappa^{-|l|} - b_{l0}\kappa^{-|l|}\log\kappa + c_{l0}\kappa^{|l|} - d_{l0}\kappa^{|l|}\log\kappa & \text{if } l\neq 0,\ m=0, \\
a_{0m}\kappa^{-|m|} + b_{0m}\kappa^{|m|} - c_{0m}\kappa^{-|m|}\log\kappa - d_{0m}\kappa^{|m|}\log\kappa & \text{if } l=0,\ m\neq 0, \\
a_{lm}\kappa^{-|l|-|m|} + b_{lm}\kappa^{-|l|+|m|} + c_{lm}\kappa^{|l|-|m|} + d_{lm}\kappa^{|l|+|m|} & \text{if } l,m\neq 0.
\end{cases}
\end{aligned}
$$

Then, it clearly holds that

$$
|A_{lm}|,\ |B_{lm}|,\ |C_{lm}|,\ |D_{lm}| \leq M.
$$

By definition, $\{a_{lm}\}$, $\{b_{lm}\}$, $\{c_{lm}\}$, and $\{d_{lm}\}$ can be expressed in terms of $\{A_{lm}\}$, $\{B_{lm}\}$, $\{C_{lm}\}$, and $\{D_{lm}\}$ as follows:

$$
\begin{aligned}
&\begin{pmatrix} A_{00} \\ B_{00} \\ C_{00} \\ D_{00} \end{pmatrix} = \begin{pmatrix} 1 & \log\kappa & \log\kappa & (\log\kappa)^2 \\ 1 & -\log\kappa & \log\kappa & -(\log\kappa)^2 \\ 1 & \log\kappa & -\log\kappa & -(\log\kappa)^2 \\ 1 & -\log\kappa & -\log\kappa & (\log\kappa)^2 \end{pmatrix} \begin{pmatrix} a_{00} \\ b_{00} \\ c_{00} \\ d_{00} \end{pmatrix} \\
&\iff \begin{pmatrix} a_{00} \\ b_{00} \\ c_{00} \\ d_{00} \end{pmatrix} = \frac{1}{4}\begin{pmatrix} 1 & 1 & 1 & 1 \\ (\log\kappa)^{-1} & -(\log\kappa)^{-1} & (\log\kappa)^{-1} & -(\log\kappa)^{-1} \\ (\log\kappa)^{-1} & (\log\kappa)^{-1} & -(\log\kappa)^{-1} & -(\log\kappa)^{-1} \\ (\log\kappa)^{-2} & -(\log\kappa)^{-2} & -(\log\kappa)^{-2} & (\log\kappa)^{-2} \end{pmatrix} \begin{pmatrix} A_{00} \\ B_{00} \\ C_{00} \\ D_{00} \end{pmatrix}
\end{aligned}
$$

$$= \frac{1}{4}\begin{pmatrix} A_{00}+B_{00}+C_{00}+D_{00} \\ (\log\kappa)^{-1}(A_{00}-B_{00}+C_{00}-D_{00}) \\ (\log\kappa)^{-1}(A_{00}+B_{00}-C_{00}-D_{00}) \\ (\log\kappa)^{-2}(A_{00}-B_{00}-C_{00}+D_{00}) \end{pmatrix},$$

$$\begin{pmatrix} A_{l0} \\ B_{l0} \\ C_{l0} \\ D_{l0} \end{pmatrix} = \begin{pmatrix} \kappa^{|l|} & \kappa^{|l|}\log\kappa & \kappa^{-|l|} & \kappa^{-|l|}\log\kappa \\ \kappa^{|l|} & -\kappa^{|l|}\log\kappa & \kappa^{-|l|} & -\kappa^{-|l|}\log\kappa \\ \kappa^{-|l|} & \kappa^{-|l|}\log\kappa & \kappa^{|l|} & \kappa^{|l|}\log\kappa \\ \kappa^{-|l|} & -\kappa^{-|l|}\log\kappa & \kappa^{|l|} & -\kappa^{|l|}\log\kappa \end{pmatrix} \begin{pmatrix} a_{l0} \\ b_{l0} \\ c_{l0} \\ d_{l0} \end{pmatrix}$$

$$\iff \begin{pmatrix} a_{l0} \\ b_{l0} \\ c_{l0} \\ d_{l0} \end{pmatrix} = \frac{\kappa^{|l|}}{2(\kappa^{4|l|}-1)} \begin{pmatrix} \kappa^{2|l|} & \kappa^{2|l|} & -1 & -1 \\ \kappa^{2|l|}(\log\kappa)^{-1} & -\kappa^{2|l|}(\log\kappa)^{-1} & -(\log\kappa)^{-1} & (\log\kappa)^{-1} \\ -1 & -1 & \kappa^{2|l|} & \kappa^{2|l|} \\ -(\log\kappa)^{-1} & (\log\kappa)^{-1} & \kappa^{2|l|}(\log\kappa)^{-1} & -\kappa^{2|l|}(\log\kappa)^{-1} \end{pmatrix} \begin{pmatrix} A_{l0} \\ B_{l0} \\ C_{l0} \\ D_{l0} \end{pmatrix}$$

$$= \frac{\kappa^{|l|}}{2(\kappa^{4|l|}-1)} \begin{pmatrix} (A_{l0}+B_{l0})\kappa^{2|l|}-(C_{l0}+D_{l0}) \\ (\log\kappa)^{-1}[(A_{l0}-B_{l0})\kappa^{2|l|}-C_{l0}+D_{l0}] \\ -(A_{l0}+B_{l0})+(C_{l0}+D_{l0})\kappa^{2|l|} \\ (\log\kappa)^{-1}[-A_{l0}+B_{l0}+(C_{l0}-D_{l0})\kappa^{2|l|}] \end{pmatrix}, \quad l \neq 0,$$

$$\begin{pmatrix} A_{0m} \\ B_{0m} \\ C_{0m} \\ D_{0m} \end{pmatrix} = \begin{pmatrix} \kappa^{|m|} & \kappa^{-|m|} & \kappa^{|m|}\log\kappa & \kappa^{-|m|}\log\kappa \\ \kappa^{-|m|} & \kappa^{|m|} & \kappa^{-|m|}\log\kappa & \kappa^{|m|}\log\kappa \\ \kappa^{|m|} & \kappa^{-|m|} & -\kappa^{|m|}\log\kappa & -\kappa^{-|m|}\log\kappa \\ \kappa^{-|m|} & \kappa^{|m|} & -\kappa^{-|m|}\log\kappa & -\kappa^{|m|}\log\kappa \end{pmatrix} \begin{pmatrix} a_{0m} \\ b_{0m} \\ c_{0m} \\ d_{0m} \end{pmatrix}$$

$$\iff \begin{pmatrix} a_{0m} \\ b_{0m} \\ c_{0m} \\ d_{0m} \end{pmatrix} = \frac{\kappa^{|m|}}{2(\kappa^{4|m|}-1)} \begin{pmatrix} \kappa^{2|m|} & -1 & \kappa^{2|m|} & -1 \\ -1 & \kappa^{2|m|} & -1 & \kappa^{2|m|} \\ \kappa^{2|m|}(\log\kappa)^{-1} & -(\log\kappa)^{-1} & -\kappa^{2|m|}(\log\kappa)^{-1} & (\log\kappa)^{-1} \\ -(\log\kappa)^{-1} & \kappa^{2|m|}(\log\kappa)^{-1} & (\log\kappa)^{-1} & -\kappa^{2|m|}(\log\kappa)^{-1} \end{pmatrix} \begin{pmatrix} A_{0m} \\ B_{0m} \\ C_{0m} \\ D_{0m} \end{pmatrix}$$

$$= \frac{\kappa^{|m|}}{2(\kappa^{4|m|}-1)} \begin{pmatrix} (A_{0m}+C_{0m})\kappa^{2|m|}-(B_{0m}+D_{0m}) \\ -(A_{0m}+C_{0m})+(B_{0m}+D_{0m})\kappa^{2|m|} \\ (\log\kappa)^{-1}[(A_{0m}-C_{0m})\kappa^{2|m|}-B_{0m}+D_{0m}] \\ (\log\kappa)^{-1}[-A_{0m}+C_{0m}+(B_{0m}-D_{0m})\kappa^{2|m|}] \end{pmatrix}, \quad m \neq 0,$$

$$\begin{pmatrix} A_{lm} \\ B_{lm} \\ C_{lm} \\ D_{lm} \end{pmatrix} = \begin{pmatrix} \kappa^{|l|+|m|} & \kappa^{|l|-|m|} & \kappa^{-|l|+|m|} & \kappa^{-|l|-|m|} \\ \kappa^{|l|-|m|} & \kappa^{|l|+|m|} & \kappa^{-|l|-|m|} & \kappa^{-|l|+|m|} \\ \kappa^{-|l|+|m|} & \kappa^{-|l|-|m|} & \kappa^{|l|+|m|} & \kappa^{|l|-|m|} \\ \kappa^{-|l|-|m|} & \kappa^{-|l|+|m|} & \kappa^{|l|-|m|} & \kappa^{|l|+|m|} \end{pmatrix} \begin{pmatrix} a_{lm} \\ b_{lm} \\ c_{lm} \\ d_{lm} \end{pmatrix}$$

$$\iff \begin{pmatrix} a_{lm} \\ b_{lm} \\ c_{lm} \\ d_{lm} \end{pmatrix} = \frac{\kappa^{|l|+|m|}}{(\kappa^{4|l|}-1)(\kappa^{4|m|}-1)} \begin{pmatrix} \kappa^{2(|l|+|m|)} & -\kappa^{2|l|} & -\kappa^{2|m|} & 1 \\ -\kappa^{2|l|} & \kappa^{2(|l|+|m|)} & 1 & -\kappa^{2|m|} \\ -\kappa^{2|m|} & 1 & \kappa^{2(|l|+|m|)} & -\kappa^{2|l|} \\ 1 & -\kappa^{2|m|} & -\kappa^{2|l|} & \kappa^{2(|l|+|m|)} \end{pmatrix} \begin{pmatrix} A_{lm} \\ B_{lm} \\ C_{lm} \\ D_{lm} \end{pmatrix}$$

$$= \frac{\kappa^{|l|+|m|}}{(\kappa^{4|l|}-1)(\kappa^{4|m|}-1)} \begin{pmatrix} A_{lm}\kappa^{2(|l|+|m|)}-B_{lm}\kappa^{2|l|}-C_{lm}\kappa^{2|m|}+D_{lm} \\ -A_{lm}\kappa^{2|l|}+B_{lm}\kappa^{2(|l|+|m|)}+C_{lm}-D_{lm}\kappa^{2|m|} \\ -A_{lm}\kappa^{2|m|}+B_{lm}+C_{lm}\kappa^{2(|l|+|m|)}-D_{lm}\kappa^{2|l|} \\ A_{lm}-B_{lm}\kappa^{2|m|}-C_{lm}\kappa^{2|l|}+D_{lm}\kappa^{2(|l|+|m|)} \end{pmatrix}, \quad l,m \neq 0.$$

Hence $\{a_{lm}\}$, $\{b_{lm}\}$, $\{c_{lm}\}$, $\{d_{lm}\}$ can be evaluated as follows:

$$|a_{00}| \le \frac{1}{4}(|A_{00}| + |B_{00}| + |C_{00}| + |D_{00}|) \le M, \quad |b_{00}|, |c_{00}| \le \frac{M}{\log \kappa}, \quad |d_{00}| \le \frac{M}{(\log \kappa)^2},$$

$$|a_{l0}|, |c_{l0}| \le \frac{\kappa^{|l|}}{2(\kappa^{4|l|} - 1)} 2M(\kappa^{2|l|} + 1) = \frac{M\kappa^{-|l|}}{1 - \kappa^{-2|l|}} \le \frac{M}{1 - \kappa^{-2}} \kappa^{-|l|}, \quad |b_{l0}|, |d_{l0}| \le \frac{M}{(1 - \kappa^{-2}) \log \kappa} \kappa^{-|l|},$$

$$|a_{0m}|, |b_{0m}| \le \frac{M}{1 - \kappa^{-2}} \kappa^{-|m|}, \quad |c_{0m}|, |d_{0m}| \le \frac{M}{(1 - \kappa^{-2}) \log \kappa} \kappa^{-|m|},$$

$$|a_{lm}|, |b_{lm}|, |c_{lm}|, |d_{lm}| \le \frac{M\kappa^{|l|+|m|}}{(\kappa^{4|l|} - 1)(\kappa^{4|m|} - 1)} (\kappa^{2|l|} + 1)(\kappa^{2|m|} + 1) \le \frac{M}{(1 - \kappa^{-2})^2} \kappa^{-|l|-|m|},$$

which are the desired estimates. □

1.7 Notations

We conclude this chapter by stating some notations that will be used in Chapters 2 and 3. The relation $(\epsilon_1, s_1) > (\epsilon_2, s_2)$ on $]0, +\infty[\times\mathbb{R}$ is defined as $\epsilon_1 > \epsilon_2 \vee (\epsilon_1 = \epsilon_2 \wedge s_1 > s_2)$, and $(\epsilon_1, s_1) \ge (\epsilon_2, s_2)$ as $(\epsilon_1, s_1) > (\epsilon_2, s_2) \wedge (\epsilon_1, s_1) \ne (\epsilon_2, s_2)$. For a given $N \in \mathbb{N}$, define $\Lambda_N = \{0, 1, \ldots, N-1\}$, $\Lambda'_N = \{p \in \mathbb{Z} \mid -N/2 < p \le N/2\}$, and $\Delta_N = \{j/N \in S^1 \mid j \in \Lambda_N\}$. For $p \in \mathbb{N}$, define $I(p) = \{p + lN \mid l \in \mathbb{Z}^*\} = p + N\mathbb{Z}^*$, where $\mathbb{Z}^* = \mathbb{Z} \setminus \{0\}$. For $m, n \in \mathbb{Z}$, $m \equiv n$ always means that $m \equiv n \pmod N$. Finally, for a vector-valued function $v = (v_1, v_2)^{\mathrm{T}}$, define $\hat{v}(n) := (\hat{v}_1(n), \hat{v}_2(n))^{\mathrm{T}}$ for $n \in \mathbb{Z}$.

Chapter 2

Asymptotic analysis of the conventional and invariant schemes for the method of fundamental solutions applied to potential problems in doubly-connected regions

Abstract

The aim of this chapter is to develop mathematical theory of the conventional and invariant schemes for the method of fundamental solutions used to solve potential problems in doubly-connected regions. Particularly, we prove that an approximate solution actually exists uniquely under some conditions, and that the error decays exponentially when the boundary data are analytic, and algebraically when they are not analytic but belong to some Sobolev spaces. Moreover, we present results of several numerical experiments in order to show the sharpness of our error estimate. This chapter is based on the following accepted paper:

- K. Sakakibara, *Asymptotic analysis of the conventional and invariant schemes for the method of fundamental solutions applied to potential problems in doubly-connected regions*, accepted by Japan Journal of Industrial and Applied Mathematics.

2.1 Introduction and main results

Let Ω be a nondegenerate doubly-connected region in the complex plane $\mathbb{C}$. That is, assume that there exist two disjoint connected components K_1 and K_2 such that $\hat{\mathbb{C}} \setminus \Omega = K_1 \sqcup K_2$, K_1 is unbounded in a sense that $\infty \in \mathring{K}_1$ holds, and neither K_1 nor K_2 is reduced to a single point, where $\hat{\mathbb{C}} = \mathbb{C} \cup \{\infty\}$ denotes the extended complex plane and $\mathring{K}_\nu$ denotes the interior of K_ν. Then, we consider the following

potential problem:

$$\begin{cases} \triangle u = 0 & \text{in } \Omega, \\ u = f_\mu & \text{on } \Gamma^\mu, \ \ \mu = 1, 2, \end{cases} \tag{2.1.1}$$

where Γ^μ is the boundary ∂K_μ of K_μ, and f_μ is a given function defined on Γ^μ for each $\mu = 1, 2$. See, for the geometrical settings, Figure 2.1. In this chapter, assume that each Γ^μ is regular analytic and

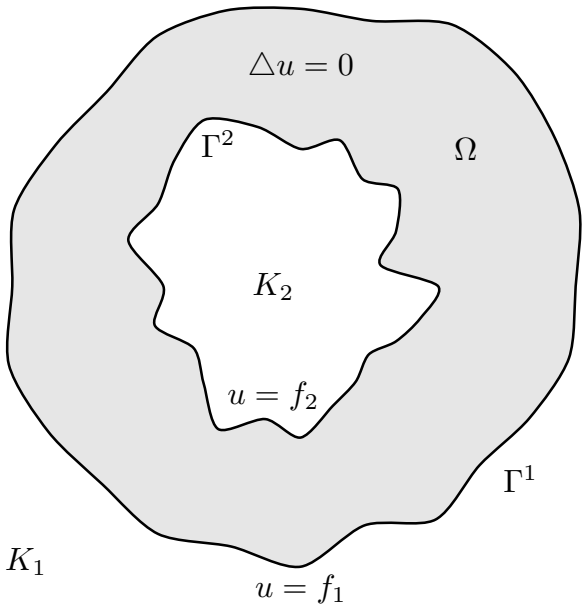

Figure 2.1: Graphic representation for the target problem

each boundary datum f_μ satisfies the following regularity condition:

f_μ is analytic, or belongs to Sobolev space $H^\sigma(\Gamma^\mu)$ for some $\sigma > 1/2$. (2.1.2)

The method of fundamental solutions (MFS) is a mesh-free numerical solver for partial differential equations that can be applied to the potential problem [64, 1, 22], the Helmholtz equation [16, 69, 14], higher order PDEs [39, 40, 65], the heat equation [59, 63], fluid dynamics [7, 60], the inverse problem [82, 103, 108, 37, 105], and so on. In addition, see the surveys [20, 44]. In the references given above, it can be seen that MFS has been investigated numerically by many authors. However, a satisfactory mathematical analysis has not been performed, because we cannot apply the mesh-dependent arguments that are used to analyze mesh-dependent numerical solvers such as the finite element method and finite difference method. The aim of this chapter is to develop a mathematical theory of MFS for the potential problems in doubly-connected regions.

The conventional scheme for MFS (C-MFS) offers an approximate solution for (2.1.1), as given by the following procedure.

(I) Take N points $\{y_{1k}\}_{k=1}^N$ in $\mathring{K}_1 \setminus \{\infty\}$ and $\{y_{2k}\}_{k=1}^N$ in $\mathring{K}_2$. That is, a total of $2N$ points are chosen from the exterior of Ω. In this chapter, these points are called the singular points.

(II) Construct an approximate solution $u_{\mathrm{C}}^{(N)}$ as follows:

$$u_{\mathrm{C}}^{(N)}(x) = \sum_{\nu=1}^{2} \sum_{k=1}^{N} Q_{\nu k} E(x - y_{\nu k}), \tag{2.1.3}$$

where $E(x) = -(2\pi)^{-1}\log|x|$ is the fundamental solution of the operator $-\triangle$.

(Ⅲ) Determine the coefficients $\{Q_{\nu k}\}_{\nu=1,2}^{k=1,2,\dots,N}$ using the collocation method. That is, take N points $\{x_{\mu j}\}_{j=1}^{N}$ on Γ^{μ} for each $\mu = 1, 2$, i.e., take a total of $2N$ points on the boundary of Ω, and impose the following boundary conditions:

$$u_{\mathrm{C}}^{(N)}(x_{\mu j}) = f_{\mu}(x_{\mu j}), \quad \mu = 1, 2;\ j = 1, 2, \dots, N. \tag{2.1.4}$$

In this chapter, these points are called the collocation points, and the equations (2.1.4) are the collcocation equations.

The above is one algorithm for C-MFS. We only choose the singular and collocation points, and solve the system of linear equations. That is, we do not need to perform mesh generation, which is required for popular numerical solvers such as the finite element method and finite difference method. Note that it is known that an approximate solution $u_{\mathrm{C}}^{(N)}$ is not invariant under affine transformations of coordinates or an origin shift of the boundary data, while the exact solution for (2.1.1) satisfies these properties. Murota [73, 74] proposed an invariant scheme for MFS (I-MFS), which gives an approximate solution $u_{\mathrm{I}}^{(N)}$ of the form

$$u_{\mathrm{I}}^{(N)}(x) = Q_0 + \sum_{\nu=1}^{2}\sum_{k=1}^{N} Q_{\nu k} E(x - y_{\nu k}), \tag{2.1.5}$$

as an alternative to (2.1.3). The coefficients are determined by the collocation method:

$$u_{\mathrm{I}}^{(N)}(x_{\mu j}) = f_{\mu}(x_{\mu j}), \quad \mu = 1, 2;\ j = 1, 2, \dots, N, \tag{2.1.6a}$$

with the constraint

$$\sum_{\nu=1}^{2}\sum_{k=1}^{N} Q_{\nu k} = 0. \tag{2.1.6b}$$

Such techniques are also applied in several papers (see, for instance, [96, 97]).

MFS has been widely applied in scientific fields. However, a satisfactory mathematical analysis of this technique has not yet been performed. Restricting to the Dirichlet problem for the Laplace equation, Katsurada and Okamoto [49] studied C-MFS in the case where Ω is a disk D_{ρ} with radius ρ, having the origin as its center. The boundary data are assumed to be analytic, and the singular points $\{y_k\}_{k=1}^{N}$ and the collocation points $\{x_j\}_{j=1}^{N}$ are chosen as $y_j = R\omega^{j-1}$ and $x_j = \rho\omega^{j-1}$ for $j = 1, 2, \dots, N$, respectively, where $R > \rho$ and $\omega = \exp(2\pi\mathrm{i}/N)$. Then, it has been proved that there uniquely exists an approximate solution by C-MFS, except for at most one value of N (cf. [49, Theorem 1]). Furthermore, the error decays exponentially with respect to N (cf. [49, Theorem 2]). Subsequently, Katsurada [45] extended this result to non-analytic boundary data (cf. [45, Theorem 2.3]), the case where Ω is the exterior of a disk (cf. [45, Theorem 4.1]), the Neumann problem (cf. [45, Theorems 6.1 and 6.2]), and the case where Ω is an annular region (cf. [45, Theorem 7.1]). Following these pioneering works, C-MFS has been comprehensively studied in the case where Ω is a Jordan region [46, 47, 50, 48], an annular region [74], and an elliptic region [76]. In addition to these works, [66] also studied C-MFS in annular shaped regions based on [13, 68, 17]. However, their work deals with the Trefftz method, rather than the collocation method. I-MFS has also been studied in [73] (Ω is a disk), [74] (Ω is an annular region), [76] (Ω is an elliptic region), and [79] (Ω is a Jordan region). Concerning other types of PDEs see, for example, [67] (biharmonic equation), [10, 78] (Helmholtz equation), [38] (Collocation method with delta functions for integral equations of the first kind), and [80, 102] (Cauchy problem).

Among previous studies concerning MFS for potential problems, there does not exists a mathematical result for multiply-connected regions other than in [74]. On the other hand, MFS has been applied to multiply-connected regions in order to construct conformal mappings numerically, and it offers satisfactory numerical results (see, for instance, [83, 3]). Therefore, it should be expected that a mathematical theory of MFS in multiply-connected regions can be established. This chapter aims to provide mathematical results regarding MFS in doubly-connected regions, as a first step toward a theory in regions with arbitrary connectivity.

In the unique existence and convergence analysis, the positions of the singular and collocation points play essential roles. In this chapter, we arrange these using peripheral conformal mappings (see, for the details of peripheral conformal mapping, Definition 1.2.1). Let Ψ_1 and Ψ_2 be peripheral conformal mappings of Γ^1 and Γ^2 with reference radii ρ_1 and ρ_2, respectively, where $0 < \rho_2 < \rho_1$. We suppose that the following two conditions hold:

$$\Psi_1(\overline{\mathcal{R}}_{\kappa^{-1}\rho_1,\kappa\rho_1}) \cap \Psi_2(\overline{\mathcal{R}}_{\kappa^{-1}\rho_2,\rho_2}) = \emptyset, \tag{2.1.7a}$$

$$\Psi_1(z) = \Psi_2(z), \quad z \in \overline{\mathcal{R}}_{\kappa^{-1}\rho_1,\kappa\rho_1} \cap \overline{\mathcal{R}}_{\kappa^{-1}\rho_2,\kappa\rho_2}. \tag{2.1.7b}$$

If $\overline{\mathcal{R}}_{\kappa^{-1}\rho_1,\kappa\rho_1} \cap \overline{\mathcal{R}}_{\kappa^{-1}\rho_2,\kappa\rho_2} \neq \emptyset$, then a map Ψ defined as

$$\Psi(z) = \begin{cases} \Psi_1(z) & \text{if } z \in \overline{\mathcal{R}}_{\kappa^{-1}\rho_1,\kappa\rho_1}, \\ \Psi_2(z) & \text{if } z \in \overline{\mathcal{R}}_{\kappa^{-1}\rho_2,\kappa\rho_2} \end{cases}$$

is a conformal mapping in a neighborhood of $\overline{\Omega}$. Thus the assumption (2.1.7b) seems natural. On the other hand, (2.1.7a) is a very technical assumption, and we do not know the way to remove it. These assumptions will be used to prove Lemma 2.4.1.

Let $R_1 \in]\rho_1, \kappa\rho_1[$ and $R_2 \in]\kappa^{-1}\rho_2, \rho_2[$. We then arrange the singular points $\{y_{\nu k}\}_{\nu=1,2}^{k=1,2,\dots,N}$ and the collocation points $\{x_{\mu j}\}_{\mu=1,2}^{j=1,2,\dots,N}$ as follows:

$$\begin{cases} y_{\nu k} = \Psi_\nu(R_\nu \omega^{k-1}), & \nu = 1,2;\ k = 1,2,\dots,N, \\ x_{\mu j} = \Psi_\mu(\rho_\mu \omega^{j-1}), & \mu = 1,2;\ j = 1,2,\dots,N. \end{cases} \tag{2.1.8}$$

See, for geometrical situation, Figure 2.2. Using these selections of the singular and collocation points, we prove that the unique existence and convergence of MFS.

Using a family of Hilbert spaces which is introduced in Section 1.1, the condition (2.1.2) on regularity of f_μ is equivalent to $F = (F_1, F_2)^{\mathrm{T}} \in \mathbb{X}_{\xi,\sigma}$ for some $(\xi, \sigma) > (1, 1/2)$, where F_μ is defined as $F_\mu(\tau) = f_\mu(\Psi_\mu(\rho_\mu \mathrm{e}^{2\pi \mathrm{i}\tau}))$ for $\tau \in S^1$.

We are now in a position to state the main results of this chapter.

Theorem 2.1.1 (Unique existence and convergence for C-MFS)**.** *Assume that for $\mu = 1, 2$, there exists a peripheral conformal mapping Ψ_μ of Γ^μ with the reference radius ρ_μ, where $\rho_1 > \rho_2 > 0$, and that they satisfy* (2.1.7)*. Let $R_1 \in]\rho_1, \sqrt{\kappa}\rho_1]$ satisfy $R_1 \neq 1$ and $\mathrm{Cap}(\Gamma_{R_1}) \neq 1$, and $R_2 \in [\sqrt{\kappa}^{-1}\rho_2, \rho_2[$, where $\mathrm{Cap}(\Gamma)$ denotes the capacity of a Jordan curve Γ, which is defined in Definition 1.4.1. Suppose that $F \in \mathbb{X}_{\xi,\sigma}$ for some $(\xi, \sigma) > (1, 1/2)$, (δ, t) satisfies*

$$1 \leq \delta \leq \min\{\xi, r^{-2}, \kappa\},$$
$$\text{if } \delta = 1 \text{ then } t > 1/2 \text{ and } s < t;\ \text{if } \delta = \kappa \text{ then } t < -1/2;\ \text{if } \delta = \xi \text{ then } t \leq \sigma,$$

and let the singular and collocation points be defined as in (2.1.8)*, where r is a positive number defined by $r = \max\{\rho_1/R_1, R_2/\rho_2\}$.*

(i) *For a sufficiently large $N \in \mathbb{N}$, there exists a unique $\{Q_{\nu k}\}_{\nu=1,2}^{k=1,2,\dots,N}$ satisfying* (2.1.3) *and* (2.1.4)*. Thus, an approximate solution of C-MFS actually exists uniquely.*

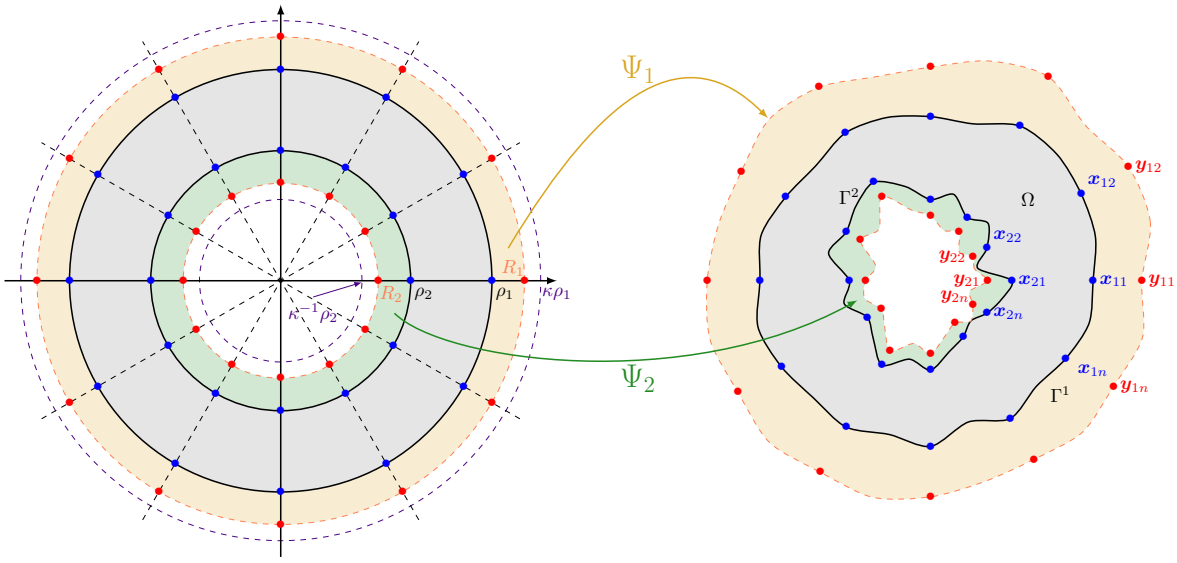

Figure 2.2: Arrangements of singular and collocation points by two peripheral conformal mappings

(ii) *The error estimate*

$$\|u - u^{(N)}\|_{H^s(\Gamma^1)\times H^s(\Gamma^2)} \le CN^{\tilde{P}(s,\delta,t)}\frac{1}{\delta^{N/2}}\|F\|_{\mathbb{X}_{\delta,t}}$$

holds true for a sufficiently large $N \in \mathbb{N}$, where C is a constant that is independent of N, and

$$\tilde{P}(s,\delta,t) = \begin{cases} \max\{s-t,-1,s-1\} & \text{if } \delta = r^{-2}\wedge(1,s) \ge (\gamma,3/2), \\ \max\{s-t,-t\} & \text{if } \delta = 1\wedge(1,s) \ge (\gamma,3/2), \\ s-t & \text{if } \delta \in]1,r^{-2}[\wedge(1,s) \ge (\gamma,3/2), \\ \max\{3/2-t,3/2\} & \text{if } \delta = r^{-2}\wedge 1 = \gamma\wedge s < 3/2, \\ 3/2-t & \text{if } \delta \in [1,r^{-2}[\wedge 1 = \gamma\wedge s < 3/2, \end{cases} \tag{2.1.9}$$

where $\gamma = \kappa^{-1}\max\{(R_1/\rho_1)^2,(\rho_2/R_2)^2\}$. This error estimate shows that the error decays exponentially with respect to N when both of boundary data f_μ are analytic, and that it decays algebraically with respect to N when at least one of boundary data f_μ is not analytic but belongs to some Sobolev space (in particular, they are Hölder continuous).

Theorem 2.1.2 (Unique existence and convergence for I-MFS)**.** *Suppose that the same hypotheses as in Theorem 2.1.1 hold, except that the assumptions that $R_1 \ne 1$ and $\mathrm{Cap}(\Gamma_{R_1}) \ne 1$ are removed.*

(i) *For a sufficiently large $N \in \mathbb{N}$, there exists a unique $\{Q_{\nu k}\}_{\nu=1,2}^{k=1,2,\dots,N}$ satisfying* (2.1.5), (2.1.6a), *and* (2.1.6b)*. Thus, an approximate solution of I-MFS actually exists uniquely.*

(ii) *The error estimate*

$$\|u - u_{\mathrm{I}}^{(N)}\|_{H^s(\Gamma^1)\times H^s(\Gamma^2)} \le CN^{\tilde{P}(s,\delta,t)}\frac{1}{\delta^{N/2}}\|F\|_{\mathbb{X}_{\delta,t}}$$

holds true for a sufficiently large $N \in \mathbb{N}$, where C is a constant that is independent of N, and $\tilde{P}(s,\delta,t)$ is defined as in (2.1.9)*.*

From the viewpoint of real computation, it is important to measure the errors in terms of L^∞ norms. Using the embedding relation $\mathscr{X}_{1,s} \subset C(S^1)$ for $s > 1/2$, we immediately obtain the following corollaries from Theorems 2.1.1 and 2.1.2. Here, $C(S^1)$ denotes the set of all continuous functions on S^1.

Corollary 2.1.3 (L^∞-error estimate for C-MFS)**.** *Under the same conditions as in Theorem 2.1.1, we have the following error estimate:*

$$\|u - u_{\mathrm{C}}^{(N)}\|_{L^\infty(\Gamma^1)\times L^\infty(\Gamma^2)} \le CN^{\tilde{P}(s,\delta,t)} \frac{1}{\delta^{N/2}} \|F\|_{\mathbb{X}_{\delta,t}},$$

for any $s > 1/2$, where C is a constant that is independent of N.

Corollary 2.1.4 (L^∞-error estimate for I-MFS)**.** *Under the same conditions as in Theorem 2.1.2, we have the following error estimate:*

$$\|u - u_{\mathrm{I}}^{(N)}\|_{L^\infty(\Gamma^1)\times L^\infty(\Gamma^2)} \le CN^{\tilde{P}(s,\delta,t)} \frac{1}{\delta^{N/2}} \|F\|_{\mathbb{X}_{\delta,t}},$$

for any $s > 1/2$, where C is a constant that is independent of N.

Theorems 2.1.1 and 2.1.2 can be obtained as the corollaries of Theorems 2.4.4 and 2.4.5, respectively, by setting $\epsilon = 1$ in both cases. Therefore, our aim is to prove Theorems 2.4.4 and 2.4.5, rather than Theorems 2.1.1 and 2.1.2 themselves. The strategies for the proofs are as follows. First, we consider the case where Ω is an annular region $\mathcal{R}_{\rho_2,\rho_1}$ with $\rho_1 > \rho_2 > 0$, and establish the unique existence (cf. Theorems 2.3.3 and 2.3.5) and convergence (cf. Theorems 2.3.7 and 2.3.8). Next, we consider the case where Ω is a nondegenerate doubly-connected region with boundary that is composed of two disjoint regular analytic Jordan curves. In fact, we can regard this problem as a compact perturbation of the problem in an annular region. Thus, we adopt the Riesz-Schauder theory, and analyze MFS using the results in annular region.

The contents of this chapter are as follows. In Section 2.2, integral operators and approximate function spaces are introduced, which will be used in the analysis. In Section 2.3, MFS in annular region is discussed. In Section 2.4, MFS in a nondegenerate doubly-connected region with boundary that is composed of two disjoint regular analytic Jordan curves is considered, and the most general versions of main results, Theorems 2.4.4 and 2.4.5, are proved. In Section 2.5, the results of some numerical experiments are presented, in order to exemplify the sharpness of our error estimate. In Section 2.6, we conclude the paper by providing some concluding remarks and conjectures describing future work.

2.2 Integral operators and approximate function spaces

2.2.1 Integral operators

2.2.1.1 Conventional scheme

In order to introduce integral operators for C-MFS, we suppose for the moment that there exists some function Q defined on $\Gamma_{R_1} \cup \Gamma_{R_2}$ such that the boundary datum f_μ can be represented as a linear combination of single-layer potentials, as follows:

$$f_\mu(x) = \sum_{\nu=1}^{2} \int_{\Gamma_{R_\nu}} E(x-y)Q(y)\,\mathrm{d}s_y^{(\nu)}, \quad x \in \Gamma^\mu$$

for each $\mu = 1, 2$, where $\Gamma_{R_\nu} = \Psi_\nu(\gamma_{R_\nu})$, and $\mathrm{d}s_y^{(\nu)}$ denotes the line element of Γ_{R_ν} $(\nu = 1, 2)$. Then, the exact solution u for (2.1.1) is represented as

$$u(x) = \sum_{\nu=1}^{2} \int_{\Gamma_{R_\nu}} E(x-y)Q(y)\,\mathrm{d}s_y^{(\nu)}, \quad x \in \Omega.$$

Considering S^1-parameterizations of Γ^μ, Γ_{R_ν}, f_μ, and Q as

$$\begin{aligned}
&\Gamma^\mu \colon S^1 \ni \tau \longmapsto \Psi_\mu(\rho_\mu \mathrm{e}^{2\pi \mathrm{i}\tau}) && (\tau \in S^1;\ \mu = 1, 2),\\
&\Gamma_{R_\nu} \colon S^1 \ni \theta \longmapsto \Psi_\nu(R_\nu \mathrm{e}^{2\pi \mathrm{i}\theta}) && (\theta \in S^1;\ \nu = 1, 2),\\
&F_\mu(\tau) = f_\mu(\Psi_\mu(\rho_\mu \mathrm{e}^{2\pi \mathrm{i}\tau})) && (\tau \in S^1;\ \mu = 1, 2),\\
&q_\nu(\theta) = Q(\Psi_\nu(R_\nu \mathrm{e}^{2\pi \mathrm{i}\theta}))|\Psi_\nu'(R_\nu \mathrm{e}^{2\pi \mathrm{i}\theta})| && (\theta \in S^1;\ \nu = 1, 2),
\end{aligned}$$

we have that

$$\begin{aligned}
F_\mu(\tau) &= \sum_{\nu=1}^{2} \int_0^1 E(\Psi_\mu(\rho_\mu \mathrm{e}^{2\pi \mathrm{i}\tau}) - \Psi_\nu(R_\nu \mathrm{e}^{2\pi \mathrm{i}\theta}))Q(\Psi_\nu(R_\nu \mathrm{e}^{2\pi \mathrm{i}\theta}))|2\pi \mathrm{i} R_\nu \Psi_\nu'(R_\nu \mathrm{e}^{2\pi \mathrm{i}\theta})|\,\mathrm{d}\theta\\
&= \sum_{\nu=1}^{2} A_{\mu\nu}^{\mathrm{C}} q_\nu(\tau) \quad (\tau \in S^1;\ \mu = 1, 2),
\end{aligned}$$

where $A_{\mu\nu}^{\mathrm{C}}$ are integral operators defined as

$$\begin{aligned}
&A_{\mu\nu}^{\mathrm{C}}\varphi(\tau) = \int_0^1 a_{\mu\nu}(\tau, \theta)\varphi(\theta)\,\mathrm{d}\theta && (\tau \in S^1;\ \mu, \nu = 1, 2),\\
&a_{\mu\nu}(\tau, \theta) = 2\pi R_\nu E(\Psi_\mu(\rho_\mu \mathrm{e}^{2\pi \mathrm{i}\tau}) - \Psi_\nu(R_\nu \mathrm{e}^{2\pi \mathrm{i}\theta})) && (\tau, \theta \in S^1;\ \mu, \nu = 1, 2),
\end{aligned}$$

for $\varphi \in C(S^1)$. Therefore, the boundary condition in (2.1.1) is equivalent to

$$A^{\mathrm{C}} q = F,$$

where

$$A^{\mathrm{C}} = (A_{\mu\nu}^{\mathrm{C}}) = \begin{pmatrix} A_{11}^{\mathrm{C}} & A_{12}^{\mathrm{C}} \\ A_{21}^{\mathrm{C}} & A_{22}^{\mathrm{C}} \end{pmatrix}, \quad q = \begin{pmatrix} q_1 \\ q_2 \end{pmatrix}, \quad F = \begin{pmatrix} F_1 \\ F_2 \end{pmatrix}.$$

Thus, our problem is reduced to finding an approximation for the above q.

2.2.1.2 Invariant scheme

Inspired by [5, Eq. (2.3)] and [79, Eq. (15)], we define the following integral operators for I-MFS:

$$A_{\mu\nu}^{\mathrm{I}}\varphi(\tau) = \frac{1}{2}\hat{\varphi}(0) + \int_0^1 a_{\mu\nu}(\tau, \theta)\left(\varphi(\theta) - \frac{1}{2}\hat{\varphi}(0)\right)\mathrm{d}\theta - \frac{1}{2}\int_0^1 a_{\mu,3-\nu}(\tau, \theta)\hat{\varphi}(0)\,\mathrm{d}\theta \quad (\tau \in S^1;\ \mu, \nu = 1, 2)$$

for $\varphi \in C(S^1)$. We also define $A^{\mathrm{I}} := (A_{\mu\nu}^{\mathrm{I}})$.

2.2.2 Approximate function space

2.2.2.1 Conventional scheme

We define the following approximate function space $\mathscr{D}_{\mathrm{C}}^{(N)}$ for C-MFS:

$$\mathscr{D}_{\mathrm{C}}^{(N)} = \left\{ \sum_{k=1}^{N} \begin{pmatrix} Q_{1k} \\ Q_{2k} \end{pmatrix} \delta\left(\cdot - \frac{k-1}{N} \right) \;\middle|\; Q_{\nu k} \in \mathbb{C} \ (\nu = 1,2;\ k = 1,2,\dots,N) \right\},$$

which is a natural extension of that for C-MFS in a Jordan region (see, for instance, [48, p. 202]), where δ is the Dirac delta function on S^1. For any $q^{(N)} \in \mathscr{D}_{\mathrm{C}}^{(N)}$, we formally have that

$$\begin{aligned} \sum_{\nu=1}^{2} A_{\mu\nu}^{\mathrm{C}} q_{\nu}^{(N)}(\tau) &= \sum_{\nu=1}^{2} \sum_{k=1}^{N} Q_{\nu k} \int_0^1 a_{\mu\nu}(\tau,\theta) \delta\left(\theta - \frac{k-1}{N} \right) \mathrm{d}\theta \\ &= \sum_{\nu=1}^{2} \sum_{k=1}^{N} 2\pi R_\nu Q_{\nu k} E(\Psi_\mu(\rho_\mu \mathrm{e}^{2\pi \mathrm{i} \tau}) - y_{\nu k}), \end{aligned}$$

which is the same as an approximate solution produced by C-MFS. Thus, we can infer that the definitions of the integral operators $A_{\mu\nu}^{\mathrm{C}}$ and the approximate function space $\mathscr{D}_{\mathrm{C}}^{(N)}$ are suitable for the analysis of C-MFS. The following proposition describes the fundamental properties of $\mathscr{D}_{\mathrm{C}}^{(N)}$.

Proposition 2.2.1. (i) *For $v = (v_1, v_2)^{\mathrm{T}} \in \mathscr{D}_{\mathrm{C}}^{(N)}$, $\{\hat{v}(n)\}_{n\in\mathbb{Z}}$ is a periodic vector sequence with respect to n with period N. That is, it holds that $\hat{v}(n) = \hat{v}(m)$ if $n \equiv m$.*

(ii) *If $(\epsilon_\mu, s_\mu) < (1, -1/2)$ for $\mu = 1, 2$, then it holds that $\mathscr{D}_{\mathrm{C}}^{(N)} \subset \mathscr{X}_{\epsilon_1,s_1} \times \mathscr{X}_{\epsilon_2,s_2}$.*

The above proposition can be found, for example, in [48, Lemma 4.3] and [79, Lemma 2].

2.2.2.2 Invariant scheme

We introduce the following approximate function space $\mathscr{D}_{\mathrm{I}}^{(N)}$ for I-MFS:

$$\mathscr{D}_{\mathrm{I}}^{N(} := \left\{ Q_0 \begin{pmatrix} 1 \\ 1 \end{pmatrix} + \sum_{k=1}^{N} \begin{pmatrix} Q_{1k} \\ Q_{2k} \end{pmatrix} \delta\left(\cdot - \frac{k-1}{N} \right) \;\middle|\; \begin{array}{l} Q_0, Q_{\nu k} \in \mathbb{C} \ (\nu = 1,2;\ k = 1,2,\dots,N) \\ \sum\limits_{\nu=1}^{2} \sum\limits_{k=1}^{N} Q_{\nu k} = 0 \end{array} \right\}.$$

This seems to be a natural extension of the one for I-MFS in a Jordan region (see, for instance, [79, p. 238]). For any $q^{(N)} \in \mathscr{D}_{\mathrm{I}}^{(N)}$, we formally have that

$$\begin{aligned} &\sum_{\nu=1}^{2} A_{\mu\nu}^{\mathrm{I}} q_{\nu}^{(N)}(\tau) \\ &\quad = \sum_{\nu=1}^{2} \left(\frac{1}{2} \hat{q}_{\nu}^{(N)}(0) + \int_0^1 a_{\mu\nu}(\tau,\theta) \left(q_{\nu}^{(N)}(\theta) - \frac{1}{2} \hat{q}_{\nu}^{(N)}(0) \right) \mathrm{d}\theta - \frac{1}{2} \int_0^1 a_{\mu,3-\nu}(\tau,\theta) \hat{q}_{\nu}^{(N)}(0) \, \mathrm{d}\theta \right) \\ &\quad = \frac{1}{2} (\hat{q}_1^{(N)}(0) + \hat{q}_2^{(N)}(0)) + \sum_{\nu=1}^{2} \int_0^1 a_{\mu\nu}(\tau,\theta) \left(q_{\nu}^{(N)}(\theta) - \frac{1}{2} (\hat{q}_1^{(N)}(0) + \hat{q}_2^{(N)}(0)) \right) \mathrm{d}\theta \\ &\quad = Q_0 + \sum_{\nu=1}^{2} \sum_{k=1}^{N} Q_{\nu k} \int_0^1 a_{\mu\nu}(\tau,\theta) \delta\left(\theta - \frac{k-1}{N} \right) \mathrm{d}\theta \\ &\quad = Q_0 + \sum_{\nu=1}^{2} \sum_{k=1}^{N} 2\pi R_\nu Q_{\nu k} E(\Psi_\mu(\rho_\mu \mathrm{e}^{2\pi \mathrm{i} \tau}) - y_{\nu k}), \end{aligned}$$

which is the same as an approximate solution obtained by I-MFS. Therefore, we can infer that the definitions of the integral operators $A^{\mathrm{I}}_{\mu\nu}$ and the approximate function space $\mathscr{D}^{(N)}_{\mathrm{I}}$ are appropriate for the analysis of I-MFS. Concerning $\mathscr{D}^{(N)}_{\mathrm{I}}$, the following proposition holds.

Proposition 2.2.2. (i) *For all $v = (v_1, v_2)^{\mathrm{T}} \in \mathscr{D}^{(N)}_{\mathrm{I}}$, $\{\hat{v}(n)\}_{n\in\mathbb{Z}^*}$ is a periodic vector sequence with respect to n with period N. That is, $\hat{v}(n) = \hat{v}(m)$ holds if $n \equiv m$ and $n, m \neq 0$. Moreover, $\hat{v}_2(0) = \hat{v}_1(0) - 2\hat{v}_1(n)$ and $\hat{v}_1(n) + \hat{v}_2(n) = 0$ hold for $n \in I(0)$.*

(ii) *If $(\epsilon_\mu, s_\mu) < (1, -1/2)$ for $\mu = 1, 2$, then it holds that $\mathscr{D}^{(N)}_{\mathrm{I}} \subset \mathscr{X}_{\epsilon_1,s_1} \times \mathscr{X}_{\epsilon_2,s_2}$.*

Proof. We only prove the latter half of the statement in (i). Concerning the remainder parts, see [79, Lemma 2].

Direct computation yields that for $v = (v_1, v_2)^{\mathrm{T}} \in \mathscr{D}^{(N)}_{\mathrm{I}}$, it holds that $\hat{v}_\nu(n) = 2^{-1}Q_0\delta_{n0} + \sum_{k=1}^{N} Q_{\nu k}$ for $\nu = 1, 2$ and $n \in I(0)$, where δ_{n0} denotes the Kronecker's delta. Therefore we obtain that

$$\hat{v}_1(n) + \hat{v}_2(n) = \sum_{\nu=1}^{2}\sum_{k=1}^{N} Q_{\nu k} = 0,$$
$$\hat{v}_1(0) - 2\hat{v}_1(n) = \frac{1}{2}Q_0 + \sum_{k=1}^{N} Q_{1k} - 2\sum_{k=1}^{N} Q_{1k} = \frac{1}{2}Q_0 - \sum_{k=1}^{N} Q_{1k} = \frac{1}{2}Q_0 + \sum_{k=1}^{N} Q_{2k} = \hat{v}_2(0)$$

for $n \in I(0)$. □

2.3 MFS in annular regions

In this section, we consider the case where Ω is an annular region, defined by $\Omega = \mathcal{R}_{\rho_2,\rho_1}$ with $\rho_1 > \rho_2 > 0$. Although there already exist mathematical results relating to this case (see [45, Section 7] and [74]), the settings of this paper are different from those. Therefore, we provide a mathematical analysis of MFS in the case of annular regions here.

Because we can take both of the peripheral conformal mappings Ψ_1 and Ψ_2 as the identity mappings, the integral operators $A^{\mathrm{C,I}}_{\mu\nu}$ are reduced to the following:

$$L^{\mathrm{C}}_{\mu\nu}\varphi(\tau) := \int_0^1 2\pi R_\nu E(\rho_\mu \mathrm{e}^{2\pi\mathrm{i}\tau} - R_\nu \mathrm{e}^{2\pi\mathrm{i}\theta})\varphi(\theta)\,\mathrm{d}\theta,$$
$$L^{\mathrm{I}}_{\mu\nu}\varphi(\tau) := \frac{1}{2}\hat{\varphi}(0) + \int_0^1 2\pi R_\nu E(\rho_\mu \mathrm{e}^{2\pi\mathrm{i}\tau} - R_\nu \mathrm{e}^{2\pi\mathrm{i}\theta})\left(\varphi(\theta) - \frac{1}{2}\hat{\varphi}(0)\right)\mathrm{d}\theta$$
$$- \frac{1}{2}\int_0^1 2\pi R_{3-\nu} E(\rho_\mu \mathrm{e}^{2\pi\mathrm{i}\tau} - R_{3-\nu}\mathrm{e}^{2\pi\mathrm{i}\theta})\hat{\varphi}(0)\,\mathrm{d}\theta$$

for $\varphi \in C(S^1)$, $\tau \in S^1$, and $\mu, \nu = 1, 2$. Introducing the functions

$$G_{\mu\nu}(\tau) := -R_\nu \log|\rho_\mu \mathrm{e}^{2\pi\mathrm{i}\tau} - R_\nu| \quad (\tau \in S^1;\ \mu, \nu = 1, 2),$$

we have that

$$L^{\mathrm{C}}_{\mu\nu}\varphi = G_{\mu\nu} * \varphi, \quad L^{\mathrm{I}}_{\mu\nu}\varphi = \frac{1}{2}\hat{\varphi}(0) + G_{\mu\nu} * \left(\varphi - \frac{1}{2}\hat{\varphi}(0)\right) - \frac{1}{2}G_{\mu,3-\nu} * \hat{\varphi}(0).$$

Then, it follows that

$$(L^{\mathrm{C}}_{\mu\nu}\varphi)^{\wedge}(n) = \hat{G}_{\mu\nu}(n)\hat{\varphi}(n),$$
$$(L^{\mathrm{I}}_{\mu\nu}\varphi)^{\wedge}(n) = \begin{cases} \dfrac{1}{2}(1+\hat{G}_{\mu\nu}(0)-\hat{G}_{\mu,3-\nu}(0))\hat{\varphi}(0) & \text{if } n=0, \\ \hat{G}_{\mu\nu}(n)\hat{\varphi}(n) & \text{if } n\neq 0, \end{cases}$$
$$\hat{G}_{\mu\nu}(n) = \begin{cases} -R_\nu \log\max\{\rho_\mu, R_\nu\} & \text{if } n=0, \\ \dfrac{R_\nu}{2|n|}\left(\min\left\{\dfrac{\rho_\mu}{R_\nu}, \dfrac{R_\nu}{\rho_\mu}\right\}\right)^{|n|} & \text{if } n\neq 0. \end{cases}$$

In order to deal with the function spaces $\mathscr{D}^{(N)}_{\mathrm{C}}$ and $\mathscr{D}^{(N)}_{\mathrm{I}}$, we need to extend the operators $L^{\mathrm{C,I}}_{\mu\nu}$ and $L^{\mathrm{C,I}} := (L^{\mathrm{C,I}}_{\mu\nu})$ to $\mathscr{X}$ and $\mathbb{Y} := \bigcup_{\epsilon,s}\mathbb{Y}_{\epsilon,s}$ which can be defined by virtue of Proposition 1.1.1 (ii).

Lemma 2.3.1. (i) *Define an operator $\mathscr{L}^{\mathrm{C}}_{\mu\nu}\colon \mathscr{X}_{\epsilon\xi(\mu,\nu),s-1} \to \mathscr{X}_{\epsilon,s}$ as $\mathscr{L}^{\mathrm{C}}_{\mu\nu}\varphi = G_{\mu\nu}*\varphi$ for each $(\epsilon,s)\in]0,+\infty[\times\mathbb{R}$, where $\xi(\mu,\nu) = \min\{\rho_\mu/R_\nu, R_\nu/\rho_\mu\}$. Then, $\mathscr{L}^{\mathrm{C}}_{\mu\nu}$ is a bounded linear extension of $L^{\mathrm{C}}_{\mu\nu}$.*

(ii) *Define an operator $\mathscr{L}^{\mathrm{I}}_{\mu\nu}\colon \mathscr{X}_{\epsilon\xi(\mu,\nu),s-1} \to \mathscr{X}_{\epsilon,s}$ as $\mathscr{L}^{\mathrm{I}}_{\mu\nu}\varphi = \dfrac{1}{2}\hat{\varphi}(0)+G_{\mu\nu}*\left(\varphi-\dfrac{1}{2}\hat{\varphi}(0)\right)-\dfrac{1}{2}G_{\mu,3-\nu}*\hat{\varphi}(0)$ for each $(\epsilon,s)\in]0,+\infty[\times\mathbb{R}$. Then, $\mathscr{L}^{\mathrm{I}}_{\mu\nu}$ is a bounded linear extension of $L^{\mathrm{I}}_{\mu\nu}$.*

(iii) *For each $(\epsilon,s)\in]0,+\infty[\times\mathbb{R}$, define an operator $\mathscr{L}^{\mathrm{C}}\colon \mathbb{Y}_{\epsilon,s}\to\mathbb{X}_{\epsilon,s}$ as $\mathscr{L}^{\mathrm{C}} = (\mathscr{L}^{\mathrm{C}}_{\mu\nu})$. Then, $\mathscr{L}^{\mathrm{C}}$ is a bounded linear extension of L^{C}. Moreover, if $R_1\neq 1$, then $\mathscr{L}^{\mathrm{C}}$ is a homeomorphism. That is, it is continuous, bijective, and has a bounded inverse.*

(iv) *For $(\epsilon,s)\in]0,+\infty[\times\mathbb{R}$, define an operator $\mathscr{L}^{\mathrm{I}}\colon \mathbb{Y}_{\epsilon,s}\to\mathbb{X}_{\epsilon,s}$ as $\mathscr{L}^{\mathrm{I}} = (\mathscr{L}^{\mathrm{I}}_{\mu\nu})$. Then, $\mathscr{L}^{\mathrm{I}}$ is a bounded linear extension of L^{I} and a homeomorphism.*

Proof. (i) For any $\varphi\in\mathscr{X}_{\xi(\mu,\nu),s-1}$, we have that

$$\begin{aligned}\|\mathscr{L}^{\mathrm{C}}_{\mu\nu}\varphi\|^2_{\epsilon,s} &= |-R_\nu\log\max\{\rho_\mu,R_\nu\}|^2|\hat{\varphi}(0)|^2 + \sum_{n\in\mathbb{Z}^*}\left|\frac{R_\nu}{2|n|}\left(\min\left\{\frac{\rho_\mu}{R_\nu},\frac{R_\nu}{\rho_\mu}\right\}\right)^{|n|}\right|^2 |\hat{\varphi}(n)|^2\epsilon^{2|n|}(2\pi|n|)^{2s} \\ &= R_\nu^2(\log\max\{\rho_\mu,R_\nu\})^2|\hat{\varphi}(0)|^2 + R_\nu^2\pi^2\sum_{n\in\mathbb{Z}^*}|\hat{\varphi}(n)|^2(\epsilon\xi(\mu,\nu))^2(2\pi|n|)^{2(s-1)} \\ &\leq R_\nu^2\max\{(\log\max\{\rho_\mu,R_\nu\})^2,\pi^2\}\|\varphi\|^2_{\epsilon\xi(\mu,\nu),s-1},\end{aligned}$$

which implies that $\mathscr{L}^{\mathrm{C}}_{\mu\nu}$ is a bounded linear extension of $L^{\mathrm{C}}_{\mu\nu}$.
(ii) For any $\varphi\in\mathscr{X}_{\epsilon\xi(\mu,\nu),s-1}$, we have that

$$\begin{aligned}&\|\mathscr{L}^{\mathrm{I}}_{\mu\nu}\varphi\|^2_{\epsilon,s} \\ &= \left|\frac{1}{2}(1+\hat{G}_{\mu\nu}(0)-\hat{G}_{\mu,3-\nu}(0))\right|^2|\hat{\varphi}(0)|^2 + \sum_{n\in\mathbb{Z}^*}\left|\frac{R_\nu}{2|n|}\left(\min\left\{\frac{\rho_\mu}{R_\nu},\frac{R_\nu}{\rho_\mu}\right\}\right)^{|n|}\right|^2|\hat{\varphi}(n)|^2\epsilon^{2|n|}(2\pi|n|)^{2s} \\ &\leq \max\left\{\frac{3}{4}(1+R_1^2(\log R_1)^2+R_2^2(\log\rho_\mu)^2), R_\nu^2\pi^2\right\}\|\varphi\|^2_{\epsilon\xi(\mu,\nu),s-1},\end{aligned}$$

which implies that $\mathscr{L}^{\mathrm{I}}_{\mu\nu}$ is a bounded linear extension of $L^{\mathrm{I}}_{\mu\nu}$.

(iii) Because $\mathscr{L}^{\mathrm{C}}_{\mu\nu}$ are bounded linear extensions of $L^{\mathrm{C}}_{\mu\nu}$, the boundedness of $\mathscr{L}^{\mathrm{C}}$ is clear. Suppose that $R_1 \neq 1$. Then, we will show that $\mathscr{L}^{\mathrm{C}}$ is a homeomorphism. Because $\{\phi_n\}_{n\in\mathbb{Z}}$, $\phi_n(\tau) = \mathrm{e}^{2\pi \mathrm{i} n\tau}\epsilon^{-|n|}\underline{n}^{-s}$ ($\tau \in S^1$, $n \in \mathbb{Z}$), forms a complete orthonormal basis of $\mathscr{X}_{\epsilon,s}$, $(\varphi_1, \varphi_2)^{\mathrm{T}} \in \mathbb{Y}_{\epsilon,s}$ belongs to $\operatorname{Ker}\mathscr{L}^{\mathrm{C}}$ if and only if it holds that

$$\underbrace{\begin{pmatrix} \hat{G}_{11}(n) & \hat{G}_{12}(n) \\ \hat{G}_{21}(n) & \hat{G}_{22}(n) \end{pmatrix}}_{=:\mathcal{G}^{\mathrm{C}}(n)} \begin{pmatrix} \hat{\varphi}_1(n) \\ \hat{\varphi}_2(n) \end{pmatrix} = \begin{pmatrix} 0 \\ 0 \end{pmatrix} \quad (\forall n \in \mathbb{Z}). \tag{2.3.1}$$

The determinants of $\mathcal{G}^{\mathrm{C}}(n)$ can be computed as

$$\det \mathcal{G}^{\mathrm{C}}(0) = \det \begin{pmatrix} -R_1 \log R_1 & -R_2 \log \rho_1 \\ -R_1 \log R_1 & -R_2 \log \rho_2 \end{pmatrix} = R_1 R_2 \log R_1 \log \frac{\rho_2}{\rho_1}$$

and

$$\det \mathcal{G}^{\mathrm{C}}(n) = \det \begin{pmatrix} \dfrac{R_1}{2|n|}\left(\dfrac{\rho_1}{R_1}\right)^{|n|} & \dfrac{R_2}{2|n|}\left(\dfrac{R_2}{\rho_1}\right)^{|n|} \\ \dfrac{R_1}{2|n|}\left(\dfrac{\rho_2}{R_1}\right)^{|n|} & \dfrac{R_2}{2|n|}\left(\dfrac{R_2}{\rho_2}\right)^{|n|} \end{pmatrix} = \frac{R_1 R_2}{4|n|^2}\left(\frac{R_2}{R_1}\right)^{|n|} \frac{\rho_1^{2|n|} - \rho_2^{2|n|}}{\rho_1^{|n|}\rho_2^{|n|}} \quad (n \in \mathbb{Z}^*),$$

from which we know that the $\mathcal{G}^{\mathrm{C}}(n)$ are nonsingular. Therefore, (2.3.1) has only the trivial solution. That is, it follows that $\hat{\varphi}(n) = \mathbf{0}$ for all $n \in \mathbb{Z}$, or $\varphi = \mathbf{0}$. Namely, $\mathscr{L}^{\mathrm{C}}$ is injective. Concerning the surjectivity of $\mathscr{L}^{\mathrm{C}}$, take any $\psi = (\psi_1, \psi_2)^{\mathrm{T}} \in \mathbb{X}_{\epsilon,s}$, and define $\varphi = (\varphi_1, \varphi_2)^{\mathrm{T}}$ as

$$\varphi_\mu(\tau) = \sum_{n\in\mathbb{Z}} \hat{\varphi}_\mu(n)\mathrm{e}^{2\pi \mathrm{i} n\tau} \quad (\tau \in S^1;\ \mu = 1, 2), \quad \hat{\varphi}(n) = \mathcal{G}^{\mathrm{C}}(n)^{-1}\hat{\psi}(n) \quad (n \in \mathbb{Z}),$$

that is,

$$\begin{pmatrix} \hat{\varphi}_1(0) \\ \hat{\varphi}_2(0) \end{pmatrix} = \begin{pmatrix} \dfrac{1}{R_1 \log R_1 \log(\rho_2/\rho_1)}(-\hat{\psi}_1(0)\log\rho_2 + \hat{\psi}_2(0)\log\rho_1) \\ \dfrac{1}{R_2 \log(\rho_2/\rho_1)}(\hat{\psi}_1(0) - \hat{\psi}_2(0)) \end{pmatrix},$$

$$\begin{pmatrix} \hat{\varphi}_1(n) \\ \hat{\varphi}_2(n) \end{pmatrix} = \begin{pmatrix} \dfrac{2|n|R_1^{|n|-1}}{\rho_1^{2|n|} - \rho_2^{2|n|}}(\rho_1^{|n|}\hat{\psi}_1(n) - \rho_2^{|n|}\hat{\psi}_2(n)) \\ \dfrac{2|n|\rho_1^{|n|}\rho_2^{|n|}}{R_2^{|n|+1}(\rho_1^{2|n|} - \rho_2^{2|n|})}(-\rho_2^{|n|}\hat{\psi}_1(n) + \rho_1^{|n|}\hat{\psi}_2(n)) \end{pmatrix} \quad (n \in \mathbb{Z}^*).$$

Then, we have that

$$\begin{aligned} \|\varphi_1\|^2_{\epsilon\rho_1/R_1, s-1} &= \frac{1}{R_1^2(\log R_1)^2(\log(\rho_2/\rho_1))^2}|-\hat{\psi}_1(0)\log\rho_2 + \hat{\psi}_2(0)\log\rho_1|^2 \\ &\quad + \sum_{n\in\mathbb{Z}^*} \frac{4|n|^2 R_1^{2(|n|-1)}}{(\rho_1^{2|n|} - \rho_2^{2|n|})^2}|\rho_1^{|n|}\hat{\psi}_1(n) - \rho_2^{|n|}\hat{\psi}_2(n)|^2 \left(\frac{\epsilon\rho_1}{R_1}\right)^{2|n|}(2\pi|n|)^{2(s-1)} \\ &\leq \frac{2}{R_1^2(\log R_1)^2(\log(\rho_2/\rho_1))^2}((\log\rho_2)^2|\hat{\psi}_1(0)|^2 + (\log\rho_1)^2|\hat{\psi}_2(0)|^2) \\ &\quad + \frac{2}{R_1^2\pi^2(1-(\rho_2/\rho_1)^2)^2}\sum_{n\in\mathbb{Z}^*}\left(|\hat{\psi}_1(n)|^2 + \left(\frac{\rho_2}{\rho_1}\right)^{2|n|}|\hat{\psi}_2(n)|^2\right)\epsilon^{2|n|}(2\pi|n|)^{2s} \\ &\leq \max\left\{\frac{2\max\{(\log\rho_1)^2, (\log\rho_1)^2\}}{(R_1\log R_1\log(\rho_2/\rho_1)))^2}, \frac{2}{(R_1\pi(1-(\rho_2/\rho_1)^2))^2}\right\}\|\psi\|^2_{\mathbb{X}_{\epsilon,s}}, \end{aligned} \tag{2.3.2}$$

and

(2.3.3)
$$\begin{aligned}\|\varphi_2\|^2_{\epsilon R_2/\rho_2} &= \frac{1}{R_2^2(\log(\rho_2/\rho_1))^2}|\hat{\psi}_1(0)-\hat{\psi}_2(0)|^2 \\ &\quad+\sum_{n\in\mathbb{Z}^*}\frac{4|n|^2\rho_1^{2|n|}\rho_2^{2|n|}}{R_1^{2(|n|+1)}(\rho_1^{2|n|}-\rho_2^{2|n|})^2}|-\rho_2^{|n|}\hat{\psi}_1(n)+\rho_1^{|n|}\hat{\psi}_2(n)|^2\left(\frac{\epsilon R_2}{\rho_2}\right)^{2|n|}(2\pi|n|)^{2(s-1)} \\ &\le \max\left\{\frac{2}{R_2^2(\log(\rho_2/\rho_1))^2},\frac{2}{R_2^2\pi^2(1-(\rho_2/\rho_1)^2)^2}\right\}\|\psi\|^2_{\mathbb{X}_{\epsilon,s}}.\end{aligned}$$

Therefore, $\varphi\in\mathbb{Y}_{\epsilon,s}$, and by definition $\mathscr{L}^{\mathrm{C}}\varphi=\psi$. The boundedness of $(\mathscr{L}^{\mathrm{C}})^{-1}$ follows from the inequalities (2.3.2) and (2.3.3).
(iv) The boundedness of $\mathscr{L}^{\mathrm{I}}$ immediately follows from (ii). $\varphi\in\mathbb{Y}_{\epsilon,s}$ belongs to $\operatorname{Ker}\mathscr{L}^{\mathrm{I}}$ if and only if it holds that

$$\frac{1}{2}\begin{pmatrix}1+\hat{G}_{11}(0)-\hat{G}_{12}(0) & 1+\hat{G}_{12}(0)-\hat{G}_{11}(0)\\ 1+\hat{G}_{21}(0)-\hat{G}_{22}(0) & 1+\hat{G}_{22}(0)-\hat{G}_{21}(0)\end{pmatrix}\begin{pmatrix}\hat{\varphi}_1(0)\\ \hat{\varphi}_2(0)\end{pmatrix}=\begin{pmatrix}0\\0\end{pmatrix}$$

and

$$\mathcal{G}^{\mathrm{I}}(n)\hat{\varphi}(n)=\mathbf{0}\quad(n\in\mathbb{Z}^*)$$

hold, where $\mathcal{G}^{\mathrm{I}}(n)=\mathcal{G}^{\mathrm{C}}(n)$ for $n\in\mathbb{Z}^*$. Because

$$\begin{aligned}\det\mathcal{G}^{\mathrm{I}}(0) &= \frac{1}{4}\det\begin{pmatrix}1-R_1\log R_1+R_2\log\rho_1 & 1-R_2\log\rho_1+R_1\log R_1\\ 1-R_1\log R_1+R_2\log\rho_2 & 1-R_2\log\rho_2+R_1\log R_1\end{pmatrix}\\ &= \frac{1}{4}\left[\det\begin{pmatrix}1-R_1\log R_1 & 1+R_1\log R_1\\ R_2\log\rho_2 & -R_2\log\rho_2\end{pmatrix}+\det\begin{pmatrix}R_2\log\rho_1 & -R_2\log\rho_1\\ 1-R_1\log R_1 & 1+R_1\log R_1\end{pmatrix}\right]\\ &= \frac{1}{2}R_2\log\frac{\rho_1}{\rho_2},\end{aligned}$$

we have that $\hat{\varphi}(n)=\mathbf{0}$ for all $n\in\mathbb{Z}$. That is, $\varphi=\mathbf{0}$. For any $\psi\in\mathbb{X}_{\epsilon,s}$, define φ as

$$\varphi_\mu(\tau)=\sum_{n\in\mathbb{Z}}\hat{\varphi}_\mu(n)\mathrm{e}^{2\pi\mathrm{i}n\tau}\quad(\tau\in S^1;\ \mu=1,2),\quad\hat{\varphi}(n)=\mathcal{G}^{\mathrm{I}}(n)^{-1}\hat{\psi}(n)\quad(n\in\mathbb{Z}),$$

that is,

$$\begin{pmatrix}\hat{\varphi}_1(0)\\ \hat{\varphi}_2(0)\end{pmatrix}=\frac{2}{R_2\log(\rho_1/\rho_2)}\begin{pmatrix}(1-R_2\log\rho_2+R_1\log R_1)\hat{\psi}_1(0)+(-1+R_2\log\rho_1-R_1\log R_1)\hat{\psi}_2(0)\\ (-1+R_1\log R_1-R_2\log\rho_2)\hat{\psi}_1(0)+(1-R_1\log R_1+R_2\log\rho_1)\hat{\psi}_2(0)\end{pmatrix}$$

and $\hat{\varphi}(n)$ for $n\in\mathbb{Z}^*$ are the same as that for $\mathscr{L}^{\mathrm{C}}$; i.e.,

$$\begin{pmatrix}\hat{\varphi}_1(n)\\ \hat{\varphi}_2(n)\end{pmatrix}=\begin{pmatrix}\dfrac{2|n|R_1^{|n|-1}}{\rho_1^{2|n|}-\rho_2^{2|n|}}(\rho_1^{|n|}\hat{\psi}_1(n)-\rho_2^{|n|}\hat{\psi}_2(n))\\ \dfrac{2|n|\rho_1^{|n|}\rho_2^{|n|}}{R_2^{|n|+1}(\rho_1^{2|n|}-\rho_2^{2|n|})}(-\rho_2^{|n|}\hat{\psi}_1(n)+\rho_1^{|n|}\hat{\psi}_2(n))\end{pmatrix}\quad(n\in\mathbb{Z}^*).$$

Then, we have that

(2.3.4)
$$\|\varphi_1\|^2_{\epsilon\rho_1/R_1,s-1},\ \|\varphi_2\|^2_{\epsilon R_2/\rho_2,s-1}\le C_\mu\|\psi\|^2_{\mathbb{X}_{\epsilon,s}}\quad(\mu=1,2),$$

which implies that $\varphi \in \mathbb{Y}_{\epsilon,s}$, where

$$C_\mu = \max\left\{ \frac{24}{(R_2 \log(\rho_1/\rho_2))^2}(1 + (R_1 \log R_1)^2 + R_2^2 \max\{(\log \rho_1)^2, (\log \rho_2)^2\}), \right. \\ \left. \frac{2}{(R_\mu \pi (1 - (\rho_2/\rho_1)^2))^2} \right\},$$

for $\mu = 1, 2$. By the definition of φ, it holds that $\mathscr{L}^{\mathrm{I}}\varphi = \psi$. The estimates (2.3.4) imply the boundedness of $(\mathscr{L}^{\mathrm{I}})^{-1}$. □

Remark 2.3.2. From the above proof, we can observe that the operator norms $\|\mathscr{L}^{\mathrm{C,I}}\|$ of $\mathscr{L}^{\mathrm{C,I}}$ and $\|(\mathscr{L}^{\mathrm{C,I}})^{-1}\|$ of $(\mathscr{L}^{\mathrm{C,I}})^{-1}$ can be bounded by constants depending only on ρ_μ and R_ν. Therefore, in the following context, the operator norms $\|\mathscr{L}^{\mathrm{C,I}}\|$ and $\|(\mathscr{L}^{\mathrm{C,I}})^{-1}\|$ do not appear explicitly.

We rewrite the collocation equation (2.1.4) for C-MFS and (2.1.6a) for I-MFS with the constraint (2.1.6b) in terms of the extended operators $\mathscr{L}^{\mathrm{C}}$ and $\mathscr{L}^{\mathrm{I}}$, respectively. For any $q^{(N)} \in \mathscr{D}_{\mathrm{C}}^{(N)}$, we have

$$\mathscr{L}^{\mathrm{C}}_{\mu\nu} q_\nu^{(N)}(\tau) = \sum_{k=1}^{N} Q_{\nu k} \mathscr{L}^{\mathrm{C}}_{\mu\nu} \delta\left(\cdot - \frac{k-1}{N}\right)(\tau) = \sum_{k=1}^{N} 2\pi R_\nu Q_{\nu k} E(\rho_\mu \mathrm{e}^{2\pi \mathrm{i}\tau} - y_{\nu k}).$$

Therefore, the unique solvability of (2.1.4) is equivalent to that of

$$\mathscr{L}^{\mathrm{C}} q^{(N)} = F \quad \text{on } \Delta_N \tag{2.3.5}$$

in $\mathscr{D}_{\mathrm{C}}^{(N)}$. Similarly, for any $q^{(N)} \in \mathscr{D}_{\mathrm{I}}^{(N)}$, we have

$$\begin{aligned} \sum_{\nu=1}^{2} \mathscr{L}_{\mu\nu} q_\nu^{(N)}(\tau) &= \sum_{\nu=1}^{2} \left(\frac{1}{2} \hat{q}_\nu^{(N)}(0) + G_{\mu\nu} * \left(q_\nu^{(N)} - \frac{1}{2} q_\nu^{(N)}(0) \right) - \frac{1}{2} G_{\mu,3-\nu} * \hat{q}_\nu^{(N)}(0) \right) \\ &= \sum_{\nu=1}^{2} \left(\frac{1}{2} \hat{q}_\nu^{(N)}(0) + G_{\mu\nu} * \left(q_\nu^{(N)} - \frac{1}{2} (\hat{q}_1^{(N)}(0) + \hat{q}_2^{(N)}(0)) \right)(\tau) \right) \\ &= Q_0 + \sum_{\nu=1}^{2} \sum_{k=1}^{N} 2\pi R_\nu Q_{\nu k} E(\rho_\mu \mathrm{e}^{2\pi \mathrm{i}\tau} - y_{\nu k}). \end{aligned}$$

Therefore, the unique solvability of (2.1.6a) with (2.1.6b) is equivalent to that of

$$\mathscr{L}^{\mathrm{I}} q^{(N)} = F \quad \text{on } \Delta_N \tag{2.3.6}$$

in $\mathscr{D}_{\mathrm{I}}^{(N)}$. The following theorem guarantees the unique existence of an approximate solution by C-MFS.

Theorem 2.3.3 (Stability of C-MFS in annular regions)**.** *Suppose that* $0 < R_2 < \rho_2 < \rho_1 < R_1$*, and* $F \in \mathbb{X}_{\xi,\sigma}$ *for some* $(\xi, \sigma) > (1, 1/2)$*. Then, for any* $N \in \mathbb{N}$ *satisfying*

$$\det \begin{pmatrix} \log|\rho_1^N - R_1^N| & \log|\rho_1^N - R_2^N| \\ \log|\rho_2^N - R_1^N| & \log|\rho_2^N - R_2^N| \end{pmatrix} \neq 0, \tag{2.3.7}$$

there exists a unique solution $q^{(N)} \in \mathscr{D}_{\mathrm{C}}^{(N)}$ *for* (2.3.5)*.*

Remark 2.3.4. The condition (2.3.7) on N is the same as in [74, Theorem 2.1]. Therefore, it seems natural for it to appear in this context.

Proof. Noting that $\sum_{\nu=1}^{2} \mathscr{L}^{\mathrm{C}}_{\mu\nu} q_\nu^{(N)} \in L^1(S^1)$ and it is Hölder continuous in some neighborhood of Δ_N for each $\mu = 1, 2$, we have that (2.3.5) is equivalent to the following equations, by virtue of Proposition 1.5.1:

$$\sum_{m\equiv p} \sum_{\nu=1}^{2} \hat{G}_{\mu\nu}(m) \hat{q}_\nu^{(N)}(m) = \sum_{m\equiv p} \hat{F}_\mu(m) \quad (p \in \Lambda_N;\ \mu = 1, 2).$$

Because $\hat{q}_\nu^{(N)}(m)$ are periodic with respect to m with period N (Proposition 2.2.1 (i)), the above are equivalent to

$$\Phi^{\mathrm{C}}(p) \hat{q}^{(N)}(p) = \sum_{m\equiv p} \hat{F}(m) \quad (p \in \Lambda_N), \tag{2.3.8}$$

where

$$\Phi^{\mathrm{C}}(p) = \begin{pmatrix} \Phi^{\mathrm{C}}_{11}(p) & \Phi^{\mathrm{C}}_{12}(p) \\ \Phi^{\mathrm{C}}_{21}(p) & \Phi^{\mathrm{C}}_{22}(p) \end{pmatrix}, \quad \Phi^{\mathrm{C}}_{\mu\nu}(p) = \sum_{m\equiv p} \hat{G}_{\mu\nu}(m).$$

Since

$$\Phi^{\mathrm{C}}_{\mu\nu}(0) = -R_\nu \log \max\{\rho_\mu, R_\nu\} + \sum_{m\in I(0)} \frac{R_\nu}{2|m|} (\xi(\mu,\nu))^{|m|} = -\frac{R_\nu}{N} \log |\rho_\mu^N - R_\nu^N|,$$

the determinant of $\Phi^{\mathrm{C}}(p)$ can be computed as

$$\begin{aligned}
\det \Phi^{\mathrm{C}}(0) &= \frac{R_1 R_2}{N^2} \det \begin{pmatrix} \log|\rho_1^N - R_1^N| & \log|\rho_1^N - R_2^N| \\ \log|\rho_2^N - R_1^N| & \log|\rho_2^N - R_2^N| \end{pmatrix}, \\
\det \Phi^{\mathrm{C}}(p) &= \det \begin{pmatrix} \displaystyle\sum_{m\equiv p} \frac{R_1}{2|m|} \left(\frac{\rho_1}{R_1}\right)^{|m|} & \displaystyle\sum_{l\equiv p} \frac{R_2}{2|l|} \left(\frac{R_2}{\rho_1}\right)^{|l|} \\ \displaystyle\sum_{m\equiv p} \frac{R_1}{2|m|} \left(\frac{\rho_2}{R_1}\right)^{|m|} & \displaystyle\sum_{l\equiv p} \frac{R_2}{2|l|} \left(\frac{R_2}{\rho_2}\right)^{|l|} \end{pmatrix} \\
&= \sum_{m\equiv p} \sum_{l\equiv p} \frac{R_1 R_2}{4|ml|} \frac{R_2^{|l|}}{R_1^{|m|}} \frac{\rho_1^{|m|+|l|} - \rho_2^{|m|+|l|}}{(\rho_1\rho_2)^{|l|}} > 0 \quad (p \in \Lambda_N \setminus \{0\}).
\end{aligned}$$

Hence it follows that the $\Phi^{\mathrm{C}}(p)$ are nonsingular. Therefore, the system (2.3.8) admits a unique solution. □

Concerning the unique existence of the approximate solution by I-MFS, the following theorem holds.

Theorem 2.3.5. *Suppose that $0 < R_2 < \rho_2 < \rho_1 < R_1$, and $F \in \mathbb{X}_{\xi,\sigma}$ for some $(\xi, \sigma) > (1, 1/2)$. Then, for any $N \in \mathbb{N}$, there exists a unique solution $q^{(N)} \in \mathscr{D}_{\mathrm{I}}^{(N)}$ for (2.3.6).*

Remark 2.3.6. The condition (2.3.7) on N in Theorem 2.3.3 for C-MFS is removed in the above theorem for I-MFS. This is the same as in [74, Theorem 2.3].

Proof. Owing to Proposition 1.5.1, (2.3.6) is equivalent to

$$\begin{cases}
\displaystyle\sum_{\nu=1}^{2} \left[\frac{1}{2} \left(1 + \hat{G}_{\mu\nu}(0) - \hat{G}_{\mu,3-\nu}(0)\right) \hat{q}_\nu^{(N)}(0) + \sum_{m\in I(0)} \hat{G}_{\mu\nu}(m) \hat{q}_\nu^{(N)}(m) \right] = \sum_{m\equiv 0} \hat{F}_\mu(m), \\
\displaystyle\sum_{\nu=1}^{2} \sum_{m\equiv p} \hat{G}_{\mu\nu}(m) \hat{q}_\nu^{(N)}(m) = \sum_{m\equiv p} \hat{F}_\mu(m) \quad (p \in \Lambda_N \setminus \{0\}),
\end{cases}$$

for $\mu = 1, 2$. Using the relations in Proposition 2.2.2 (i), $\hat{q}_\nu^{(N)}(m) = \hat{q}_\nu^{(N)}(N)$ if $m \equiv N$ and $m \neq 0$, $\hat{q}_2^{(N)}(0) = \hat{q}_1^{(N)}(0) - 2\hat{q}_1^{(N)}(N)$, and $\hat{q}_1^{(N)}(N) + \hat{q}_2^{(N)}(N) = 0$, the above are equivalent to

$$\begin{cases} \Phi^{\mathrm{I}}(0) \begin{pmatrix} \hat{q}_1^{(N)}(0) \\ \hat{q}_1^{(N)}(N) \end{pmatrix} = \sum_{m \equiv 0} \begin{pmatrix} \hat{F}_1(m) \\ \hat{F}_2(m) \end{pmatrix}, \\ \Phi^{\mathrm{I}}(p) \begin{pmatrix} \hat{q}_1^{(N)}(p) \\ \hat{q}_2^{(N)}(p) \end{pmatrix} = \sum_{m \equiv 0} \begin{pmatrix} \hat{F}_1(m) \\ \hat{F}_2(m) \end{pmatrix} \quad (p \in \Lambda_N \setminus \{0\}), \end{cases} \tag{2.3.9}$$

where

$$\Phi^{\mathrm{I}}(0) = \begin{pmatrix} 1 & -(1 + \hat{G}_{12}(0) - \hat{G}_{11}(0)) + \sum_{m \in I(0)} (\hat{G}_{11}(m) - \hat{G}_{12}(m)) \\ 1 & -(1 + \hat{G}_{22}(0) - \hat{G}_{21}(0)) + \sum_{m \in I(0)} (\hat{G}_{21}(m) - \hat{G}_{22}(m)) \end{pmatrix},$$
$$\Phi^{\mathrm{I}}(p) = \Phi^{\mathrm{C}}(p) \quad (p \in \Lambda_N \setminus \{0\}).$$

Because the determinant of $\Phi^{\mathrm{I}}(0)$ can be computed explicitly as

$$\begin{aligned} \det \Phi^{\mathrm{I}}(0) &= \hat{G}_{12}(0) - \hat{G}_{11}(0) - \hat{G}_{22}(0) + \hat{G}_{21}(0) + \sum_{m \in I(0)} \left(\hat{G}_{21}(m) - \hat{G}_{22}(m) - \hat{G}_{11}(m) + \hat{G}_{12}(m) \right) \\ &= -R_2 \log \rho_1 + R_2 \log \rho_2 + \frac{1}{N} \left[-R_1 \log \left(1 - \left(\frac{\rho_2}{R_1} \right)^N \right) \right. \\ &\quad \left. + R_2 \log \left(1 - \left(\frac{R_2}{\rho_2} \right)^N \right) + R_1 \log \left(1 - \left(\frac{\rho_1}{R_1} \right)^N \right) - R_2 \log \left(1 - \left(\frac{R_2}{\rho_1} \right)^N \right) \right] \\ &= \frac{R_1}{N} \log \left| \frac{\rho_1^N - R_1^N}{\rho_2^N - R_2^N} \right| + \frac{R_2}{N} \log \left| \frac{\rho_2^N - R_2^N}{\rho_1^N - R_2^N} \right|, \end{aligned}$$

which is negative, and $\det \Phi^{\mathrm{I}}(p) = \det \Phi^{\mathrm{C}}(p) > 0$ $(p \in \Lambda_N \setminus \{0\})$, the unique existence of a solution for (2.3.6) in $\mathscr{D}_{\mathrm{I}}^{(N)}$ has been shown. □

Next, we provide error estimates for C-MFS and I-MFS, which imply that the errors decay exponentially with respect to N when the boundary datum F is analytic, and algebraically when F is not analytic but belongs to some Sobolev space.

Theorem 2.3.7 (Error estimate for C-MFS in annular regions)**.** *Let $0 < R_2 < \rho_2 < \rho_1 < R_1$, $R_1 \neq 1$, and $F \in \mathbb{X}_{\xi,\sigma}$ for some $(\xi, \sigma) > (1, 1/2)$. Take any (δ, t) satisfying $(1, 1/2) < (\delta, t) \leq (\xi, \sigma)$, and suppose that (ϵ, s) satisfies the following conditions:*

$$\max \left\{ \delta r^2, \frac{1}{\delta} \right\} \leq \epsilon \leq \min \left\{ \frac{1}{\delta r^2}, \delta \right\}; \tag{2.3.10}$$

$$\text{if } \epsilon = \delta \text{ then } s \leq t; \quad \text{if } \epsilon = \frac{1}{r} \text{ then } s < -\frac{1}{2}. \tag{2.3.11}$$

Then, there exist some positive constant $C = C(\epsilon, s, \delta, t, \rho, R)$ and a real constant $P = P(\epsilon, s, \delta, t)$ such that, for all $N \in \mathbb{N}$ satisfying (2.3.7), the following error estimate holds:

$$\| F - \mathscr{L}^{\mathrm{C}} q^{(N)} \|_{\mathbb{X}_{\epsilon,s}} \leq C N^P \left(\frac{\epsilon}{\delta} \right)^{N/2} \| F \|_{\mathbb{X}_{\delta,t}},$$

where $q^{(N)} \in \mathscr{D}_{\mathrm{C}}^{(N)}$ is the unique solution for (2.3.5), the existence of which is assured by Theorem 2.3.3.

Theorem 2.3.8. *Under the same conditions as in Theorem 2.3.7, with the constraint $R_1 \neq 1$ is removed, there exist some positive constant $C = C(\epsilon, s, \delta, t, \rho, R)$ and a real constant $P = P(\epsilon, s, \delta, t)$ such that, for all $N \in \mathbb{N}$, the following error estimate holds:*

$$\|F - \mathscr{L}^{\mathrm{I}} q^{(N)}\|_{\mathbb{X}_{\epsilon,s}} \leq C N^P \left(\frac{\epsilon}{\delta}\right)^{N/2} \|F\|_{\mathbb{X}_{\delta,t}},$$

where $q^{(N)} \in \mathscr{D}_{\mathrm{I}}^{(N)}$ is the unique solution for (2.3.6)*, the existence of which is assured by Theorem 2.3.5.*

Remark 2.3.9. The condition (2.3.10) seems to be rather complicated. We employ a graph to show the region in which the condition (2.3.10) is satisfied. Define the following:

$$L_1 = \left\{(\delta,\epsilon) \;\middle|\; \frac{1}{r} \leq \delta \leq \frac{1}{r^2},\ \epsilon = \delta r^2\right\}, \quad L_2 = \left\{(\delta,\epsilon) \;\middle|\; 1 \leq \delta \leq \frac{1}{r},\ \epsilon = \delta\right\},$$
$$H_1 = \left\{(\delta,\epsilon) \;\middle|\; 1 \leq \delta \leq \frac{1}{r},\ \epsilon = \frac{1}{\delta}\right\}, \quad H_2 = \left\{(\delta,\epsilon) \;\middle|\; \frac{1}{r} \leq \delta \leq \frac{1}{r^2},\ \epsilon = \frac{1}{\delta r^2}\right\},$$
$$C_1 = \left(\frac{1}{r}, r\right), \quad C_2 = \left(\frac{1}{r^2}, 1\right).$$

Then, we denote by $\mathcal{J}$ the closed region surrounded by $H_1 \cup H_2 \cup H_2 \cup L_2$. It follows that (δ,ϵ) satisfies the condition (2.3.10) if and only if $(\delta,\epsilon) \in \mathcal{J}$. Moreover, defining $\mathcal{I} := \{(\delta,\epsilon) \in \mathcal{J} \mid \delta \leq \xi\}$, we have that (δ,ϵ) satisfies the conditions (2.3.10) and $\delta \leq \xi$ if and only if $(\delta,\epsilon) \in \mathcal{I}$. For the shape of $\mathcal{I}$, see Figure 2.3.

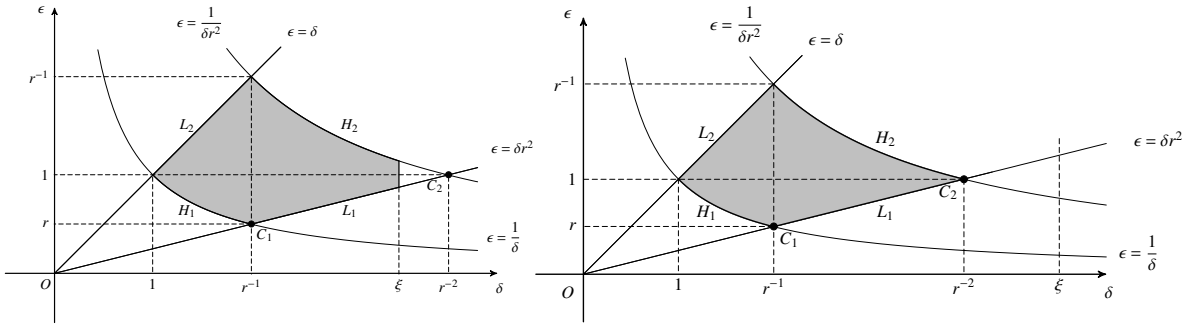

Figure 2.3: Graphic representation of the closed region $\mathcal{I}$ when (a) $\xi < r^{-2}$; (b) $\xi \geq r^{-2}$.

Remark 2.3.10. The exponent $P = P(\epsilon, s, \delta, t)$ in Theorem 2.3.7 and 2.3.8 can be written explicitly as

$$P(\epsilon, s, \delta, t) = \begin{cases} \max\{s-t, -1, -t\} & ((\delta,\epsilon) = C_1), \\ \max\{s-t, -1, s-1\} & ((\delta,\epsilon) = C_2), \\ \max\{s-t, -t\} & ((\delta,\epsilon) \in H_1 \setminus \{C_1\}), \\ \max\{s-t, s-1\} & ((\delta,\epsilon) \in H_2 \setminus \{C_2\}), \\ \max\{s-t, -1\} & ((\delta,\epsilon) \in L_1 \setminus \{C_1, C_2\}), \\ s-t & (\text{otherwise}). \end{cases}$$

Remark 2.3.11. The indices s and t can take any real values if (δ,ϵ) is in the interior of $\mathcal{I}$, while they must satisfy some conditions when $(\delta,\epsilon) \in \partial\mathcal{I}$. In particular, when we consider the case that $\epsilon = 1$,

which means that the errors $\|F-\mathscr{L}^{\mathrm{C,I}}q^{(N)}\|_{\mathbb{X}_{\epsilon,s}}$ are measured by $H^s\times H^s$ norm, $P(\epsilon,s,\delta,t)$ is reduced to

$$P(s,\delta,t)=\begin{cases}\max\{s-t,-t\} & (\delta=1),\\ \max\{s-t,-1,s-1\} & (\delta=r^{-2}),\\ s-t & (1<\delta<r^{-2}).\end{cases}$$

If $\xi=1$, then it holds that $\sigma>1/2$, $\delta=1$, $1/2<t\le\sigma$, and $s\le t$, yielding the error estimates

$$\|F-\mathscr{L}^{\mathrm{C,I}}q^{(N)}\|_{H^s\times H^s}\le CN^{\max\{s-t,-t\}}\|F\|_{H^t\times H^t}.$$

Therefore, the errors decay algebraically when the boundary datum F is not analytic, but belongs to some Sobolev spaces.

In order to prove the above Theorems 2.3.7 and 2.3.8 we will use the following Lemmas 2.3.12 and 2.3.13, respectively.

Lemma 2.3.12. *Under the same hypotheses as in Theorem 2.3.7, there exists some positive constant $C=C(\epsilon,s,\delta,t,\rho,R)$ such that the following estimate holds for $q\in\mathbb{Y}_{\xi,\sigma}$ with $\mathscr{L}^{\mathrm{C}}q=F$, the solution $q^{(N)}\in\mathscr{D}_{\mathrm{C}}^{(N)}$ for* (2.3.5)*, the unique existence of which is assured by Theorem 2.3.3, and all $N\in\mathbb{N}$ satisfying* (2.3.7)*:*

$$\|q-q^{(N)}\|_{\mathbb{Y}_{\epsilon,s}}\le CN^{P(\epsilon,s,\delta,t)}\left(\frac{\epsilon}{\delta}\right)^{N/2}\|q\|_{\mathbb{Y}_{\delta,t}}.$$

Lemma 2.3.13. *Under the same hypotheses as in Theorem 2.3.8, there exists some positive constant $C=C(\epsilon,s,\delta,t,\rho,R)$ such that the following estimate holds for $q\in\mathbb{Y}_{\xi,\sigma}$ with $\mathscr{L}^{\mathrm{I}}q=F$, the solution $q^{(N)}\in\mathscr{D}_{\mathrm{I}}^{(N)}$ for* (2.3.6)*, the unique existence of which is assured by Theorem 2.3.5, and all $N\in\mathbb{N}$:*

$$\|q-q^{(N)}\|_{\mathbb{Y}_{\epsilon,s}}\le CN^{P(\epsilon,s,\delta,t)}\left(\frac{\epsilon}{\delta}\right)^{N/2}\|q\|_{\mathbb{Y}_{\delta,t}}.$$

We defer the proofs of the above two lemmas to Section 2.7 and Section 2.8, and first apply them here to establish Theorems 2.3.7 and 2.3.8.

Proof of Theorem 2.3.7. For a given $F\in\mathbb{X}_{\xi,\sigma}$, there exists a unique $q\in\mathbb{Y}_{\xi,\sigma}$ such that $F=\mathscr{L}^{\mathrm{C}}q$, because $\mathscr{L}^{\mathrm{C}}$ is a homeomorphism (Lemma 2.3.1 (iii)). Then, by Lemma 2.3.12 we obtain that

$$\begin{aligned}\|F-\mathscr{L}^{\mathrm{C}}q^{(N)}\|_{\mathbb{X}_{\epsilon,s}}&\le\|\mathscr{L}^{\mathrm{C}}q-\mathscr{L}^{\mathrm{C}}q^{(N)}\|_{\mathbb{X}_{\epsilon,s}}\le C\|q-q^{(N)}\|_{\mathbb{Y}_{\epsilon,s}}\\&\le CN^{P(\epsilon,s,\delta,t)}\left(\frac{\epsilon}{\delta}\right)^{N/2}\|q\|_{\mathbb{Y}_{\delta,t}}\le CN^{P(\epsilon,s,\delta,t)}\left(\frac{\epsilon}{\delta}\right)^{N/2}\|F\|_{\mathbb{X}_{\delta,t}},\end{aligned}$$

which is the desire estimate. □

Proof of Theorem 2.3.8. This can be proved in the same manner as Theorem 2.3.7. □

2.4 MFS in doubly-connected regions

For the purpose of extending $A_{\mu\nu}^{\mathrm{C,I}}$ and $A^{\mathrm{C,I}}=(A_{\mu\nu}^{\mathrm{C,I}})$, we define perturbation operators $K_{\mu\nu}^{\mathrm{C,I}}$ and $K^{\mathrm{C,I}}$ by

$$K_{\mu\nu}^{\mathrm{C,I}}:=A_{\mu\nu}^{\mathrm{C,I}}-L_{\mu\nu}^{\mathrm{C,I}},\quad K^{\mathrm{C,I}}=(K_{\mu\nu}^{\mathrm{C,I}})=\begin{pmatrix}K_{11}^{\mathrm{C,I}} & K_{12}^{\mathrm{C,I}}\\ K_{21}^{\mathrm{C,I}} & K_{22}^{\mathrm{C,I}}\end{pmatrix}.$$

If $\varphi \in C(S^1)$, then we have

$$K^{\mathrm{C}}_{\mu\nu}\varphi(\tau) = \int_0^1 k_{\mu\nu}(\tau,\theta)\varphi(\theta)\,\mathrm{d}\theta,$$
$$K^{\mathrm{I}}_{\mu\nu}\varphi(\tau) = \int_0^1 k_{\mu\nu}(\tau,\theta)\left(\varphi(\theta) - \frac{1}{2}\hat{\varphi}(0)\right)\mathrm{d}\theta - \frac{1}{2}\int_0^1 k_{\mu,3-\nu}(\tau,\theta)\hat{\varphi}(0)\,\mathrm{d}\theta$$

for $\tau \in S^1$ and $\mu,\nu = 1,2$, where

$$\begin{aligned} k_{\mu\nu}(\tau,\theta) &= 2\pi R_\nu \left(E(\Psi_\mu(\rho_\mu \mathrm{e}^{2\pi\mathrm{i}\tau}) - \Psi_\nu(R_\nu \mathrm{e}^{2\pi\mathrm{i}\theta})) - E(\rho_\mu \mathrm{e}^{2\pi\mathrm{i}\tau} - R_\nu \mathrm{e}^{2\pi\mathrm{i}\theta})\right) \\ &= -R_\nu \log\left|\frac{\Psi_\mu(\rho_\mu \mathrm{e}^{2\pi\mathrm{i}\tau}) - \Psi_\nu(R_\nu \mathrm{e}^{2\pi\mathrm{i}\theta})}{\rho_\mu \mathrm{e}^{2\pi\mathrm{i}\tau} - R_\nu \mathrm{e}^{2\pi\mathrm{i}\theta}}\right|. \end{aligned}$$

Thus, the lth Fourier coefficients of $K^{\mathrm{C}}_{\mu\nu}\varphi$ and $K^{\mathrm{I}}_{\mu\nu}\varphi$ are given as follows:

$$\begin{aligned} (K^{\mathrm{C}}_{\mu\nu}\varphi)^\wedge(l) &= \int_0^1 K^{\mathrm{C}}_{\mu\nu}\varphi(\tau)\mathrm{e}^{-2\pi\mathrm{i}l\tau}\,\mathrm{d}\tau = \int_0^1\int_0^1 k_{\mu\nu}(\tau,\theta)\varphi(\theta)\,\mathrm{d}\theta\ \mathrm{e}^{-2\pi\mathrm{i}l\tau}\,\mathrm{d}\tau \\ &= \int_0^1\int_0^1 k_{\mu\nu}(\tau,\theta)\sum_{m\in\mathbb{Z}}\hat{\varphi}(-m)\mathrm{e}^{-2\pi\mathrm{i}\theta}\,\mathrm{d}\theta\ \mathrm{e}^{-2\pi\mathrm{i}l\tau}\,\mathrm{d}\tau \\ &= \sum_{m\in\mathbb{Z}}\hat{\varphi}(-m)\int_0^1\int_0^1 k_{\mu\nu}(\tau,\theta)\mathrm{e}^{-2\pi\mathrm{i}(l\tau+m\theta)}\,\mathrm{d}\tau\,\mathrm{d}\theta = \sum_{m\in\mathbb{Z}}\hat{k}_{\mu\nu}(l,m)\hat{\varphi}(-m), \\ (K^{\mathrm{I}}_{\mu\nu}\varphi)^\wedge(l) &= \int_0^1\int_0^1 k_{\mu\nu}(\tau,\theta)\left(\frac{1}{2}\hat{\varphi}(0) + \sum_{m\in\mathbb{Z}^*}\hat{\varphi}(-m)\mathrm{e}^{-2\pi\mathrm{i}m\theta}\right)\mathrm{d}\theta\ \mathrm{e}^{-2\pi\mathrm{i}l\tau}\,\mathrm{d}\tau \\ &\qquad - \frac{1}{2}\int_0^1\int_0^1 k_{\mu,3-\nu}(\tau,\theta)\hat{\varphi}(0)\,\mathrm{d}\theta\ \mathrm{e}^{-2\pi\mathrm{i}l\tau}\,\mathrm{d}\tau \\ &= \frac{1}{2}(\hat{k}_{\mu\nu}(l,0) - \hat{k}_{\mu,3-\nu}(l,0))\hat{\varphi}(0) + \sum_{m\in\mathbb{Z}^*}\hat{k}_{\mu\nu}(l,m)\hat{\varphi}(-m). \end{aligned}$$

We require the following estimates for $\hat{k}_{\mu\nu}(l,m)$ in order to extend $K^{\mathrm{C,I}}_{\mu\nu}$ and $K^{\mathrm{C,I}}$:

Lemma 2.4.1. *There exists some positive constant C such that*

$$|\hat{k}_{\mu\nu}(l,m)| \le C\kappa^{-|l|}(\kappa\xi(\nu,\nu))^{-|m|}$$

holds for all $l,m \in \mathbb{Z}$.

Proof. Define $\psi_{\mu\nu}\colon \overline{\mathcal{R}}_{\kappa^{-1}\rho_\mu,\kappa\rho_\mu} \times \overline{\mathcal{R}}_{\kappa^{-1}\rho_\nu,\kappa\rho_\nu} \to \mathbb{C}$ as

$$\psi_{\mu\nu}(z,w) = \begin{cases} \dfrac{\Psi_\mu(z) - \Psi_\nu(w)}{z-w}, & z \in \overline{\mathcal{R}}_{\kappa^{-1}\rho_\mu,\kappa\rho_\mu},\ w \in \overline{\mathcal{R}}_{\kappa^{-1}\rho_\nu,\kappa\rho_\nu},\ z \ne w, \\ \Psi'_\mu(w), & z \in \overline{\mathcal{R}}_{\kappa^{-1}\rho_\mu,\kappa\rho_\mu},\ w \in \overline{\mathcal{R}}_{\kappa^{-1}\rho_\nu,\kappa\rho_\nu},\ z = w. \end{cases}$$

Thus, $\psi_{\mu\nu}$ as defined is holomorphic in $\mathcal{R}_{\kappa^{-1}\rho_\mu,\kappa\rho_\mu} \times \mathcal{R}_{\kappa^{-1}\rho_\nu,\kappa\rho_\nu}$ and continuous on its closure. To verify the above statement, take any $w \in \mathcal{R}_{\kappa^{-1}\rho_\nu,\kappa\rho_\nu}$ and fix it. If $\mu \ne \nu$ and $\overline{\mathcal{R}}_{\kappa^{-1}\rho_1,\kappa\rho_1} \cap \overline{\mathcal{R}}_{\kappa^{-1}\rho_2,\rho_2} = \emptyset$, $\psi_{\mu\nu}$ is obviously a holomorphic function as a function of z. If not, considering the power series expansion of Ψ_μ around w as $\Psi_\mu(z) = \sum_{n=0}^\infty a_n(z-w)^n$, we have

$$\psi_{\mu\nu}(z,w) = \frac{\sum_{n=1}^\infty a_n(z-w)^n}{z-w} = \sum_{n=1}^\infty a_n(z-w)^{n-1} \longrightarrow a_1 = \Psi'_\mu(w) \quad \text{as } z \to w.$$

Here, note that we have used the relation $\Psi_\mu(w) = \Psi_\nu(w)$, which is the assumption (2.1.7). Therefore w is a removable singularity of $\psi_{\mu\nu}(z,w)$, that is, $\psi_{\mu\nu}(z,w)$ is a holomorphic function as a function of z for any fixed w. Similarly, for any fixed $z \in \mathcal{R}_{\kappa^{-1}\rho_\mu,\kappa\rho_\mu}$, $\psi_{\mu\nu}(z,w)$ is a holomorphic function as a function of w. Hence, Hartogs' theorem implies that $\psi_{\mu\nu}$ is a holomorphic function as a function of two variables z and w. The continuity of $\psi_{\mu\nu}$ is clear at this stage. Therefore, $\Re \log|\psi_{\mu\nu}|$ has the following double Fourier series expansion:

$$\begin{aligned}
&\Re \log|\psi_{\mu\nu}(\rho_\mu r_1 \mathrm{e}^{2\pi \mathrm{i}\tau}, \rho_\nu r_2 \mathrm{e}^{2\pi\mathrm{i}\theta})| \\
&\quad= \sum_{l,m\in\mathbb{Z}^*} \left(a_{lm} r_1^{|l|} r_2^{|m|} + b_{lm} r_1^{|l|} r_2^{-|m|} + c_{lm} r_1^{-|l|} r_2^{|m|} + d_{lm} r_1^{-|l|} r_2^{-|m|}\right) \mathrm{e}^{2\pi\mathrm{i}(l\tau+m\theta)} \\
&\qquad+ \sum_{m\in\mathbb{Z}^*} \left(a_{0m} r_2^{|m|} + b_{0m} r_2^{-|m|} + c_{0m} r_2^{|m|}\log r_1 + d_{0m} r_2^{-|m|}\log r_1\right) \mathrm{e}^{2\pi\mathrm{i}m\theta} \\
&\qquad+ \sum_{l\in\mathbb{Z}^*} \left(a_{l0} r_1^{|l|} + b_{l0} r_1^{|l|}\log r_2 + c_{l0} r_1^{-|l|} + d_{l0} r_1^{-|l|}\log r_2\right) \mathrm{e}^{2\pi\mathrm{i}l\tau} \\
&\qquad+ a_{00} + b_{00}\log r_2 + c_{00}\log r_1 + d_{00}\log r_1 \log r_2
\end{aligned}$$

for $r_1, r_2 \in [\kappa^{-1}, \kappa]$ and $\tau, \theta \in \mathbb{R}$. Then, by Proposition 1.6.1, there exists some positive constant M that depends on the supremum of $|\psi_{\mu\nu}|$ on $\partial\mathcal{R}_{\kappa^{-1}\rho_\mu,\kappa\rho_\mu} \times \partial\mathcal{R}_{\kappa^{-1}\rho_\nu,\kappa\rho_\nu}$ and κ such that a_{lm}, b_{lm}, c_{lm}, and d_{lm} can be estimated as follows:

$$|a_{lm}|, |b_{lm}|, |c_{lm}|, |d_{lm}| \le M\kappa^{-|l|-|m|} \quad (l, m \in \mathbb{Z}).$$

Because $k_{\mu\nu}(\tau,\theta) = -R_\nu \Re \log|\psi_{\mu\nu}(\rho_\mu \mathrm{e}^{2\pi\mathrm{i}\tau}, R_\nu \mathrm{e}^{2\pi\mathrm{i}\theta})|$, we obtain the desired estimates by applying those above. Indeed, we have

$$\begin{aligned}
|\hat{k}_{\mu\nu}(l,m)| &= R_\nu \left| a_{lm}\left(\frac{R_\nu}{\rho_\nu}\right)^{|m|} + b_{lm}\left(\frac{R_\nu}{\rho_\nu}\right)^{-|m|} + c_{lm}\left(\frac{R_\nu}{\rho_\nu}\right)^{|m|} + d_{lm}\left(\frac{R_\nu}{\rho_\nu}\right)^{-|m|} \right| \\
&\le 2MR_\nu\kappa^{-|l|}\left[\left(\frac{R_\nu}{\kappa\rho_\nu}\right)^{|m|} + \left(\frac{\rho_\nu}{\kappa R_\nu}\right)^{|m|}\right] \le 4MR_\nu\kappa^{-|l|}(\kappa\xi(\nu,\nu))^{-|m|} \quad (l, m \ne 0), \\
|\hat{k}_{\mu\nu}(0,m)| &\le 2MR_\nu(\kappa\xi(\nu,\nu))^{-|m|} \quad (m \ne 0), \quad |\hat{k}_{\mu\nu}(l,0)| \le 2MR_\nu\left(1 + \left|\log\frac{R_\nu}{\rho_\nu}\right|\right)\kappa^{-|l|} \quad (l \ne 0), \\
|\hat{k}_{\mu}(0,0)| &\le MR_\nu\left(1 + \left|\log\frac{R_\nu}{\rho_\nu}\right|\right).
\end{aligned}$$

□

Using this lemma, we can extend $K^{\mathrm{C,I}}_{\mu\nu}$ and $K^{\mathrm{C,I}} = (K^{\mathrm{C,I}}_{\mu\nu})$ as follows:

Lemma 2.4.2. *Suppose that* $(\epsilon_\nu, s_\nu) > ((\kappa\xi(\nu,\nu))^{-1}, 1/2)$ *for* $\nu = 1, 2$ *and* $(\delta, t) < (\kappa, -1/2)$.

(i) *Define an operator* $\mathscr{K}^{\mathrm{C}}_{\mu\nu} \colon \mathscr{X}_{\epsilon_\nu,s_\nu} \to \mathscr{X}_{\delta,t}$ *by*

$$(\mathscr{K}^{\mathrm{C}}_{\mu\nu}\varphi)^\wedge(l) = \sum_{m\in\mathbb{Z}} \hat{k}_{\mu\nu}(l,m)\hat{\varphi}(-m) \quad (m \in \mathbb{Z}).$$

Then, $\mathscr{K}^{\mathrm{C}}_{\mu\nu}$ *is a bounded linear extension of* $K^{\mathrm{C}}_{\mu\nu}$.

(ii) *Define an operator* $\mathscr{K}^{\mathrm{I}}_{\mu\nu} \colon \mathscr{X}_{\epsilon_\nu,s_\nu} \to \mathscr{X}_{\delta,t}$ *by*

$$(\mathscr{K}^{\mathrm{I}}_{\mu\nu}\varphi)^\wedge(l) = \frac{1}{2}(\hat{k}_{\mu\nu}(l,0) - \hat{k}_{\mu,3-\nu}(l,0))\hat{\varphi}(0) + \sum_{m\in\mathbb{Z}^*} \hat{k}_{\mu\nu}(l,m)\hat{\varphi}(-m).$$

Then, $\mathscr{K}^{\mathrm{I}}_{\mu\nu}$ *is a bounded linear extension of* $K^{\mathrm{I}}_{\mu\nu}$.

(iii) *Define an operator* $\mathscr{K}^{\mathrm{C}}\colon \mathscr{X}_{\epsilon_1,s_1}\times\mathscr{X}_{\epsilon_2,s_2}\to\mathbb{X}_{\delta,t}$ *by* $\mathscr{K}^{\mathrm{C}}=(\mathscr{K}^{\mathrm{C}}_{\mu\nu})$. *Then,* $\mathscr{K}^{\mathrm{C}}$ *is a bounded linear extension of* K^{C}*, and is compact.*

(iv) *Define an operator* $\mathscr{K}^{\mathrm{I}}\colon \mathscr{X}_{\epsilon_1,s_1}\times\mathscr{X}_{\epsilon_2,s_2}\to\mathbb{X}_{\delta,t}$ *by* $\mathscr{K}^{\mathrm{I}}=(\mathscr{K}^{\mathrm{I}}_{\mu\nu})$. *Then,* $\mathscr{K}^{\mathrm{I}}$ *is a bounded linear extension of* K^{I}*, and is compact.*

Proof. (i) For any $\varphi\in\mathscr{X}_{\epsilon_\nu,s_\nu}$, we have that

$$\begin{aligned}\|\mathscr{K}^{\mathrm{C}}_{\mu\nu}\varphi\|^2_{\delta,t}&=\sum_{l\in\mathbb{Z}}\left|\sum_{m\in\mathbb{Z}}\hat{k}_{\mu\nu}(l,m)\hat{\varphi}(-m)\right|^2\delta^{2|l|}\underline{l}^{2t}\\&\le\sum_{l\in\mathbb{Z}}\left(\sum_{m\in\mathbb{Z}}|\hat{k}_{\mu\nu}(l,m)|^2\epsilon_\nu^{-2|m|}\underline{m}^{-2s}\right)\left(\sum_{m\in\mathbb{Z}}|\hat{\varphi}(-m)|^2\epsilon_\nu^{2|m|}\underline{m}^{2s}\right)\delta^{2|l|}\underline{l}^{2t}\\&\le C\sum_{l\in\mathbb{Z}}\left(\frac{\delta}{\kappa}\right)^{2|l|}\underline{l}^{2t}\sum_{m\in\mathbb{Z}}(\epsilon_\nu\kappa\xi(\nu,\nu))^{-2|m|}\underline{m}^{-2s}\|\varphi\|^2_{\epsilon_\nu,s_\nu}.\end{aligned}$$

Note that, by assumption, the above infinite sums are convergent. Thus, $\mathscr{K}^{\mathrm{C}}_{\mu\nu}$ is a bounded linear extension of $\mathscr{K}^{\mathrm{C}}_{\mu\nu}$.
(ii) Because we can bound the lth Fourier coefficient $(\mathscr{K}^{\mathrm{I}}_{\mu\nu}\varphi)^\wedge(l)$ of $\mathscr{K}^{\mathrm{I}}_{\mu\nu}\varphi$ by

$$|(\mathscr{K}^{\mathrm{I}}_{\mu\nu}\varphi)^\wedge(l)|\le C\sum_{m\in\mathbb{Z}}\kappa^{-|l|}(\kappa\xi(\nu,\nu))^{-|m|}|\hat{\varphi}(-m)|,$$

we obtain the same estimate for $\mathscr{K}^{\mathrm{I}}_{\mu\nu}\varphi$. Namely, $\mathscr{K}^{\mathrm{I}}_{\mu\nu}$ is a bounded linear extension of $K^{\mathrm{I}}_{\mu\nu}$.
(iii) Because each $\mathscr{K}^{\mathrm{C}}_{\mu\nu}$ is a bounded linear extension of $K^{\mathrm{C}}_{\mu\nu}$, it immediately follows that $\mathscr{K}^{\mathrm{C}}$ is a bounded linear extension of K^{C}. In order to show the compactness of $\mathscr{K}^{\mathrm{C}}$, we choose (δ',t') arbitrarily such that it satisfies $(\delta,t)<(\delta',t')<(\kappa,-1/2)$, and we split $\mathscr{K}^{\mathrm{C}}$ as follows:

$$\begin{array}{ccc}\mathscr{K}^{\mathrm{C}}\colon\ \mathscr{X}_{\epsilon_1,s_1}\times\mathscr{X}_{\epsilon_2,s_2} & \longrightarrow & \mathbb{X}_{\delta,t}\\ & {\scriptstyle\tilde{\mathscr{K}}^{\mathrm{C}}}\searrow \quad \nearrow{\scriptstyle i\times i} & \\ & \mathbb{X}_{\delta',t'} & \end{array}$$

Here, $\tilde{\mathscr{K}}^{\mathrm{C}}\colon \mathscr{X}_{\epsilon_1,s_1}\times\mathscr{X}_{\epsilon_2,s_2}\to\mathbb{X}_{\delta',t'}$ is a bounded linear operator, defined in a similar manner to $\mathscr{K}^{\mathrm{C}}$, and $i\colon \mathscr{X}_{\delta',t'}\hookrightarrow\mathscr{X}_{\delta,t}$ is the natural inclusion, which is a compact operator by Proposition 1.1.1 (ii). It is clear that $i\times i$ is a compact operator, and $\mathscr{K}^{\mathrm{C}}=(i\times i)\circ\tilde{\mathscr{K}}^{\mathrm{C}}$ is also a compact operator.
(iv) It can be proved in a same manner to that in (iii), so we will omit the proof. □

Corollary 2.4.3. *If* (ϵ,s) *satisfies*

$$\left(\gamma,\frac{3}{2}\right)<(\epsilon,s)<\left(\kappa,-\frac{1}{2}\right),\tag{2.4.1}$$

then $\mathscr{K}^{\mathrm{C,I}}\colon\mathbb{Y}_{\epsilon,s}\to\mathbb{X}_{\epsilon,s}$ *is a compact operator, where* $\gamma=\kappa^{-1}\max\{\xi(\nu,\nu)^{-2}\mid\nu=1,2\}$.

Proof. Setting $\epsilon_1=\epsilon\rho_1/R_1$, $\epsilon_2=\epsilon R_2/\rho_2$, and $s_1=s_2=s-1$, the above corollary immediately follows from Lemma 2.4.2. □

When (ϵ,s) satisfies the condition (2.4.1), we define $\mathscr{A}^{\mathrm{C,I}}\colon\mathbb{Y}_{\epsilon,s}\to\mathbb{X}_{\epsilon,s}$ as $\mathscr{A}^{\mathrm{C,I}}=\mathscr{L}^{\mathrm{C,I}}+\mathscr{K}^{\mathrm{C,I}}$. These $\mathscr{A}^{\mathrm{C,I}}$ are extensions of $A^{\mathrm{C,I}}$.Thus, we are now in a position to state main results of this paper in their most general forms.

Theorem 2.4.4 (Unique existence and error estimate for C-MFS)**.** *Suppose that $R_1 \in]\rho_1, \kappa\rho_1[$ satisfies $R_1 \neq 1$ and $\mathrm{Cap}(\Gamma_{R_1}) \neq 1$, $R_2 \in]\kappa^{-1}\rho_2, \rho_2[$, $F \in \mathbb{X}_{\xi,\sigma}$ for some $(\xi,\sigma) > (1,1/2)$, (δ,t) satisfies $(1,1/2) < (\delta,t) < (\kappa,-1/2)$ and $(\delta,t) \leq (\xi,\sigma)$, and (ϵ,s) satisfies*

$$\max\left\{\delta r^2, \frac{1}{\delta}\right\} \leq \epsilon \leq \min\left\{\frac{1}{\delta r^2}, \delta\right\},$$
$$\text{if } \epsilon = \delta \text{ then } s < t; \quad \text{if } \epsilon = \frac{1}{r} \text{ then } s < \frac{1}{2},$$

and $\epsilon \geq \gamma$. Then, the following hold:

(i) *For a sufficiently large $N \in \mathbb{N}$, the equation*

$$\mathscr{A}^{\mathrm{C}} q^{(N)} = F \quad \text{on } \Delta_N$$

has a unique solution $q^{(N)} \in \mathscr{D}_{\mathrm{C}}^{(N)}$. Namely, an approximate solution $u_{\mathrm{C}}^{(N)}$ of the form (2.1.3) *satisfying the collocation equations* (2.1.4) *uniquely exists.*

(ii) *There exists some positive constant $C = C(\epsilon, s, \delta, t, \|\mathscr{A}^{\mathrm{C}}\|, \|(\mathscr{A}^{\mathrm{C}})^{-1}\|)$ such that the following error estimate holds:*

$$\|\mathscr{A}^{\mathrm{C}} q^{(N)} - F\|_{\mathbb{X}_{\epsilon,s}} \leq C N^{\tilde{P}(\epsilon,s,\delta,t)} \left(\frac{\epsilon}{\delta}\right)^{N/2} \|F\|_{\mathbb{X}_{\delta,t}},$$

where $\tilde{P}(\epsilon,s,\delta,t)$ is defined as

$$\tilde{P}(\epsilon,s,\delta,t) = \begin{cases} P(\epsilon,s,\delta,t) & \text{if } (\epsilon,s) \geq (\gamma,3/2), \\ P(\epsilon,3/2,\delta,t) & \text{if } \epsilon = \gamma \wedge s < 3/2. \end{cases}$$

Namely, the error decays exponentially when the boundary datum F is analytic, and it decays algebraically when F is not analytic but belongs to $\mathbb{X}_{1,\sigma}$ with $\sigma > 1/2$, which implies that F is at least Hölder continuous.

Theorem 2.4.5 (Unique existence and error estimate for I-MFS)**.** *Under the same conditions as in Theorem 2.4.4 where the assumptions $R_1 \neq 1$ and $\mathrm{Cap}(\Gamma_{R_1}) \neq 1$ are removed, the following hold:*

(i) *For a sufficiently large $N \in \mathbb{N}$, the equation*

$$\mathscr{A}^{\mathrm{I}} q^{(N)} = F \quad \text{on } \Delta_N$$

has a unique solution $q^{(N)} \in \mathscr{D}_{\mathrm{I}}^{(N)}$. Namely, an approximate solution $u_{\mathrm{I}}^{(N)}$ of the form (2.1.5) *satisfying the collocation equations* (2.1.6a) *and the constraint* (2.1.6b) *uniquely exists.*

(ii) *There exists some positive constant $C = C(\epsilon, s, \delta, t, \|\mathscr{A}^{\mathrm{I}}\|, \|(\mathscr{A}^{\mathrm{I}})^{-1}\|)$ such that the following error estimate holds:*

$$\|\mathscr{A}^{\mathrm{I}} q^{(N)} - F\|_{\mathbb{X}_{\epsilon,s}} \leq C N^{\tilde{P}(\epsilon,s,\delta,t)} \left(\frac{\epsilon}{\delta}\right)^{N/2} \|F\|_{\mathbb{X}_{\delta,t}}.$$

In order to prove the above theorems, we will require the following two lemmas.

Lemma 2.4.6. *Suppose that $R_1 \in]\rho_1, \kappa\rho_1[$, $R_2 \in]\kappa^{-1}\rho_2, \rho_2[$, and (ϵ,s) satisfies* (2.4.1)*. Then, the operators $\mathscr{A}^{\mathrm{C,I}}$ are bounded. Moreover, if it holds that $R_1 \neq 1$ and $\mathrm{Cap}(\Gamma_{R_1}) \neq 1$, then $\mathscr{A}^{\mathrm{C}}$ is a homeomorphism. Concerning $\mathscr{A}^{\mathrm{I}}$, without no additional assumption, it holds that $\mathscr{A}^{\mathrm{I}}$ is a homeomorphism.*

Proof. The boundedness of the operators $\mathscr{A}^{\mathrm{C,I}}$ are obvious.

Concerning the bijectivity of $\mathscr{A}^{\mathrm{C,I}}$, we only have to show that these are injective, because $\mathscr{A}^{\mathrm{C,I}}$ are Fredholm operators with indices 0, which can be justified by Lemma 2.3.1 (iii), (iv), from which $\mathscr{L}^{\mathrm{C,I}}$ are Fredholm operators with indices 0, and Corollary 2.4.3, from which $\mathscr{K}^{\mathrm{C,I}}$ are compact operators. Take $q = (q_1, q_2)^{\mathrm{T}} \in \operatorname{Ker} \mathscr{A}^{\mathrm{C,I}}$ arbitrarily, so $\mathscr{A}^{\mathrm{C,I}} q = 0$. Because each $\mathscr{L}^{\mathrm{C,I}}$ is a homeomorphism, we have that $\mathscr{A}^{\mathrm{C,I}} q = 0$ are equivalent to $q = -(\mathscr{L}^{\mathrm{C,I}})^{-1} \mathscr{K}^{\mathrm{C,I}} q$. Then, we have that $\mathscr{K}^{\mathrm{C,I}} q \in \mathbb{X}_{\kappa,t}$ for all $t < -1/2$, because $\mathscr{K}^{\mathrm{C,I}} \colon \mathbb{Y}_{\epsilon,s} \to \mathbb{X}_{\delta,t}$ define bounded linear operators when $(\epsilon, s) > (\gamma, 3/2)$ and $(\delta, t) < (\kappa, -1/2)$ are satisfied (Lemma 2.4.2). Therefore, we obtain that $q = -(\mathscr{L}^{\mathrm{C,I}})^{-1} \mathscr{K}^{\mathrm{C,I}} q \in \mathbb{Y}_{\kappa,t}$. Because it holds that $\kappa \xi(\nu, \nu) > 1$ for $\nu = 1, 2$, owing to the assumptions on R_ν, it follows that q_ν are Hölder continuous functions on S^1. Then, we have that

$$\mathscr{A}^{\mathrm{C,I}} q = 0 \iff u^{\mathrm{C,I}}(x) = 0 \quad \text{for all } x \in \Gamma^1 \cup \Gamma^2,$$

where

$$\begin{aligned} u^{\mathrm{C}}(x) &= \sum_{\nu=1}^{2} \int_0^1 2\pi R_\nu E(x - \Psi_\nu(R_\nu \mathrm{e}^{2\pi \mathrm{i}\theta})) q_\nu(\theta) \, \mathrm{d}\theta, \\ u^{\mathrm{I}}(x) &= \frac{\hat{q}_1(0) + \hat{q}_2(0)}{2} + \sum_{\nu=1}^{2} \int_0^1 2\pi R_\nu E(x - \Psi_\nu(R_\nu \mathrm{e}^{2\pi \mathrm{i}\theta})) \left(q_\nu(\theta) - \frac{\hat{q}_1(0) + \hat{q}_2(0)}{2} \right) \mathrm{d}\theta. \end{aligned}$$

The functions $u^{\mathrm{C,I}}$ are harmonic in $\mathbb{C} \setminus (\Gamma_{R_1} \cup \Gamma_{R_2})$, and continuous on $\mathbb{C}$. By the maximum principle for harmonic functions, it holds that $u^{\mathrm{C,I}} = 0$ in Ω. Denote by Ω' the interior doubly-connected region surrounded by Γ_{R_1} and Γ_{R_2}. Then, using the identity theorem for harmonic functions (see, for instance, [8, Theorem 1.27]), it holds that $u^{\mathrm{C,I}} = 0$ in Ω'. By the continuity of $u^{\mathrm{C,I}}$, we have that $u^{\mathrm{C,I}} = 0$ on $\Gamma_{R_1} \cup \Gamma_{R_2}$. Using the maximum principle for harmonic functions once again, we obtain that $u^{\mathrm{C,I}} = 0$ in K_2. Summarizing the above, we obtain $u = 0$ in $\overline{\Omega}_{R_1}$, where Ω_{R_1} denotes the interior simply-connected region surrounded by Γ_{R_1}. Thus, on Γ_{R_2} we have that $\partial_{\nu+} u = \partial_{\nu-} u = 0$, which yields that $q_2(\theta) = 0$ for $\theta \in S^1$ in the expression for u^{C}, and $q_2(\theta) - 2^{-1}(\hat{q}_1(0) + \hat{q}_2(0)) = 0$ for $\theta \in S^1$ in that for u^{I}, where $\partial_{\nu+}$ and $\partial_{\nu-}$ are the exterior and interior normal derivatives, respectively. Then, the functions $u^{\mathrm{C,I}}$ are reduced to the following forms:

$$\begin{aligned} u^{\mathrm{C}}(x) &= \int_0^1 2\pi R_1 E(x - \Psi_\nu(R_1 \mathrm{e}^{2\pi \mathrm{i}\theta})) q_1(\theta) \, \mathrm{d}\theta, \\ u^{\mathrm{I}}(x) &= \frac{\hat{q}_1(0) + \hat{q}_2(0)}{2} + \int_0^1 2\pi R_1 E(x - \Psi_1(R_1 \mathrm{e}^{2\pi \mathrm{i}\theta})) \left(q_1(\theta) - \frac{\hat{q}_1(0) + \hat{q}_2(0)}{2} \right) \mathrm{d}\theta. \end{aligned}$$

Then, we obtain that $q_1(\theta) = 0$ for $\theta \in S^1$ in the expression for u^{C}, by Proposition 1.3.1, and $2^{-1}(\hat{q}_1(0) + \hat{q}_2(0)) = 0$ and $q_1(\theta) - 2^{-1}(\hat{q}_1(0) + \hat{q}_2(0)) = 0$ for $\theta \in S^1$ in the expression for u^{I}, by Proposition 1.3.2. Hence, we obtain that $q \equiv \mathbf{0}$ for $u^{\mathrm{C,I}}$. Namely, $\mathscr{A}^{\mathrm{C,I}}$ are injective. □

Lemma 2.4.7. *Suppose that $R_1 \in]\rho_1, \kappa\rho_1[$ satisfies $R_1 \neq 1$ and $\operatorname{Cap}(\Gamma_{R_1}) \neq 1$, $R_2 \in]\kappa^{-1}\rho_2, \rho_2[$, $(1, 1/2) < (\delta, t) < (\kappa, -1/2)$, (ϵ, s) satisfies (2.3.10), (2.3.11), and $(\epsilon, s) > (\gamma, 3/2)$. When we consider I-MFS, the conditions that $R_1 \neq 1$ and $\operatorname{Cap}(\Gamma_{R_1}) \neq 1$ on R_1 are removed. Then, there exist some positive constants $C = C(\epsilon, s, \delta, t, \|\mathscr{A}^{\mathrm{C,I}}\|, \|(\mathscr{A}^{\mathrm{C,I}})^{-1}\|)$ such that for all $N \in \mathbb{N}$, with (2.3.7) when C-MFS is considered, all $q \in \mathbb{Y}_{\delta,t}$, and all $q^{(N)} \in \mathscr{D}^{(N)}_{\mathrm{C,I}}$ satisfying $\mathscr{A}^{\mathrm{C,I}} q = \mathscr{A}^{\mathrm{C,I}} q^{(N)}$ on Δ_N, the following estimates hold:*

$$\|q - q^{(N)}\|_{\mathbb{Y}_{\epsilon,s}} \leq C N^{P(\epsilon,s,\delta,t)} \left(\frac{\epsilon}{\delta} \right)^{N/2} \left(\|q\|_{\mathbb{Y}_{\delta,t}} + \|q - q^{(N)}\|_{\mathbb{Y}_{\epsilon,s}} \right).$$

Proof. Because the operators $\mathscr{A}^{\mathrm{C,I}}\colon \mathbb{Y}_{\epsilon,s} \to \mathbb{X}_{\epsilon,s}$ are homeomorphisms by Lemma 2.4.6, we have that

$$\|q - q^{(N)}\|_{\mathbb{Y}_{\epsilon,s}} \le C\|\mathscr{A}^{\mathrm{C,I}}q - \mathscr{A}^{\mathrm{C,I}}q^{(N)}\|_{\mathbb{X}_{\epsilon,s}}.$$

Define the following:

$$w_N := q^{(N)}, \quad w := q^{(N)} - (\mathscr{L}^{\mathrm{C,I}})^{-1}\mathscr{A}^{\mathrm{C,I}}(q^{(N)} - q).$$

Then, we can easily verify that

$$\mathscr{A}^{\mathrm{C,I}}(q^{(N)} - q) = \mathscr{L}^{\mathrm{C,I}}(w_N - w), \quad \mathscr{L}^{\mathrm{C,I}}w = \mathscr{L}^{\mathrm{C,I}}w_N \quad \text{on } \Delta_N.$$

Namely, w_N is an approximate solution given by C-/I-MFS in the annular region $\mathcal{R}_{\rho_2,\rho_1}$ with the boundary data $\mathscr{L}^{\mathrm{C,I}}w$. Therefore, we obtain the following estimates, by virtue of Theorems 2.3.7 and 2.3.8:

$$\|q - q^{(N)}\|_{\mathbb{Y}_{\epsilon,s}} \le \|\mathscr{L}^{\mathrm{C,I}}w - \mathscr{L}^{\mathrm{C,I}}w_N\|_{\mathbb{X}_{\epsilon,s}} \le CN^{P(\epsilon,s,\delta,t)}\left(\frac{\epsilon}{\delta}\right)^{N/2}\|\mathscr{L}^{\mathrm{C,I}}w\|_{\mathbb{X}_{\delta,t}}.$$

Moreover, using the relations $w = q + (\mathscr{L}^{\mathrm{C,I}})^{-1}(\mathscr{L}^{\mathrm{C,I}} - \mathscr{A}^{\mathrm{C,I}})(q^{(N)} - q)$, we obtain that

$$\begin{aligned}\|\mathscr{L}^{\mathrm{C,I}}w\|_{\mathbb{X}_{\delta,t}} &\le C\|w\|_{\mathbb{Y}_{\delta,t}} \le C\left[\|q\|_{\mathbb{Y}_{\delta,t}} + C'\| - \mathscr{K}^{\mathrm{C,I}}(q^{(N)} - q)\|_{\mathbb{X}_{\delta,t}}\right] \\ &\le C\left(\|q\|_{\mathbb{Y}_{\delta,t}} + \|q - q^{(N)}\|_{\mathbb{Y}_{\epsilon,s}}\right),\end{aligned}$$

where we have used the boundedness of $\mathscr{L}^{\mathrm{C,I}} - \mathscr{A}^{\mathrm{C,I}} = -\mathscr{K}^{\mathrm{C,I}}\colon \mathbb{Y}_{\epsilon,s} \to \mathbb{X}_{\delta,t}$ in the final inequality. Summarizing the above give us the desired estimates. □

Proof of Theorem 2.4.4. First, we note that

$$N^{P(\epsilon,s,\delta,t)}\left(\frac{\epsilon}{\delta}\right)^{N/2} = o(1) \quad \text{as } N \to \infty$$

holds, by considering the definition of $P(\epsilon, s, \delta, t)$ (Remark 2.3.10). Therefore, by Lemma 2.4.7 we obtain that

$$\|q - q^{(N)}\|_{\mathbb{Y}_{\epsilon,s}} \le CN^{P(\epsilon,s,\delta,t)}\left(\frac{\epsilon}{\delta}\right)^{N/2}\|q\|_{\mathbb{Y}_{\delta,t}}$$

for sufficiently large N, provided that $(\epsilon, s) > (\gamma, 3/2)$. By using the embedding relation $\mathscr{X}_{\gamma,s} \hookrightarrow \mathscr{X}_{\gamma,3/2}$ for $s > 3/2$, we obtain the above inequality for $(\epsilon, s) = (\gamma, 3/2)$. By using the embedding relation $\mathscr{X}_{\gamma,3/2} \hookrightarrow \mathscr{X}_{\gamma,s}$ for $s < 3/2$, we obtain that

$$\|q - q^{(N)}\|_{\mathbb{Y}_{\epsilon,s}} \le CN^{P(\epsilon,3/2,\delta,t)}\left(\frac{\epsilon}{\delta}\right)^{N/2}\|q\|_{\mathbb{Y}_{\delta,t}}$$

for $\epsilon = \gamma$ and $s < 3/2$. Therefore, the fact that $\mathscr{A}^{\mathrm{C}}q^{(N)} = 0$ on Δ_N yields that $q^{(N)} = 0$, because Lemma 2.4.6 gives that $\mathscr{A}^{\mathrm{C}}$ is a homeomorphism, which implies that $q = 0$ is the only possibility for $A^{\mathrm{C}}q = 0$, that is, $\|q^{(N)}\|_{\mathbb{Y}_{\epsilon,s}} = 0$. Because $A^{\mathrm{C}}q^{(N)} = F$ on Δ_N is equivalent to a system of linear equations, the above result indicates the unique existence of the solution $q^{(N)} \in \mathscr{D}_{\mathrm{C}}^{(N)}$ for the considered equation.

Because A^{C} is a homeomorphism of $\mathbb{Y}_{\xi,\sigma}$ onto $\mathbb{X}_{\xi,\sigma}$, it holds that for a given $F \in \mathbb{X}_{\xi,\sigma}$, there uniquely exists $q \in \mathbb{Y}_{\xi,\sigma}$ such that $A^{\mathrm{C}}q = F$. Therefore, we have that

$$\|F - \mathscr{A}^{\mathrm{C}}q^{(N)}\|_{\mathbb{X}_{\epsilon,s}} \le C\|q - q^{(N)}\|_{\mathbb{Y}_{\epsilon,s}} \le CN^{\tilde{P}(\epsilon,s,\delta,t)}\left(\frac{\epsilon}{\delta}\right)^{N/2}\|q\|_{\mathbb{Y}_{\delta,t}} \le CN^{\tilde{P}(\epsilon,s,\delta,t)}\left(\frac{\epsilon}{\delta}\right)^{N/2}\|F\|_{\mathbb{X}_{\delta,t}},$$

which gives the desired estimate. □

Proof of Theorem 2.4.5. This can be proved in a similar manner to Theorem 2.4.4, so we omit the details. □

2.5 Numerical experiments

In this section, we will present the results of some numerical experiments. We choose ρ_1 and ρ_2 as 2 and 1, respectively, throughout this section. In Figures 2.4–2.12, the horizontal and vertical axis represent N and the common logarithms of errors, respectively, except for in Figure 2.8.

2.5.1 Ω: annular region

In this subsection, we consider the case where Ω is an annular region $\mathcal{R}_{\rho_2,\rho_1}$. Then, we can take two peripheral conformal mappings Ψ_1 and Ψ_2 as the identity mappings.

2.5.1.1 Boundary data: harmonic polynomial

First, we consider the case that the boundary data f_μ are harmonic polynomials. Namely,

$$f_\mu(z) = \Re z^m, \quad \mu = 1, 2;\ m \in \{0, 1, \ldots, 5\}. \tag{2.5.1}$$

These can be extended analytically to the entire plane. Therefore, the errors can be estimated as

$$\|u - u^{(N)}_{\mathrm{C,I}}\|_{L^2(\Gamma^1)\times L^2(\Gamma^2)} = O(r^N), \quad \|u - u^{(N)}_{\mathrm{C,I}}\|_{L^\infty(\Gamma^1)\times L^\infty(\Gamma^2)} = O(N^{1/2} r^N),$$

where $r = \max\{\rho_1/R_1, R_2/\rho_2\}$. We choose $R_1 = 4$ and $R_2 = 1/2$, which yields that $r = 1/2$. That is,

$$\|u - u^{(N)}_{\mathrm{C,I}}\|_{L^2(\Gamma^1)\times L^2(\Gamma^2)} = O(2^{-N}), \quad \|u - u^{(N)}_{\mathrm{C,I}}\|_{L^\infty(\Gamma^1)\times L^\infty(\Gamma^2)} = O(N^{1/2} 2^{-N}).$$

The results of numerical experiments are presented in Figures 2.4 and 2.5. It can be observed that

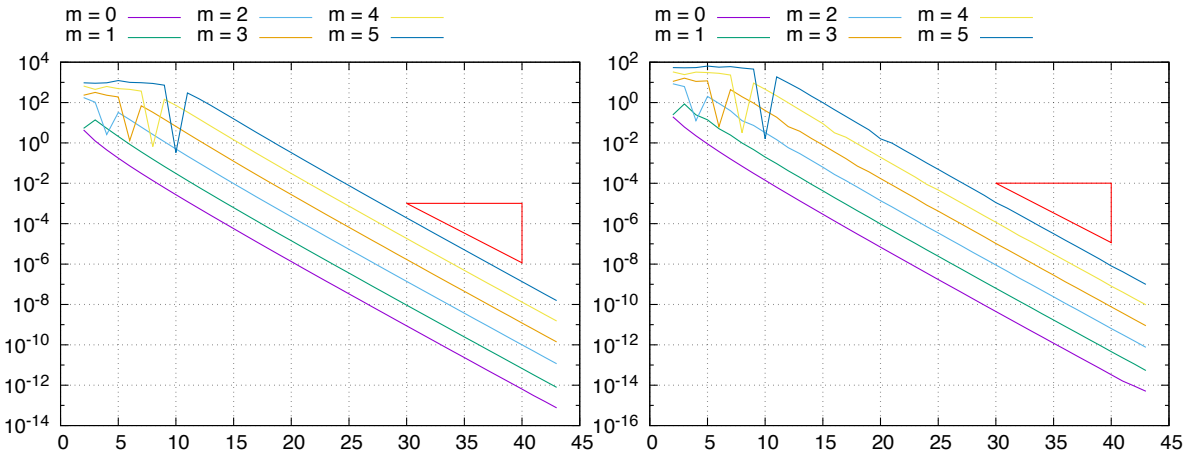

(a) L^2-error estimate (b) L^∞-error estimate

Figure 2.4: Numerical results of C-MFS in the annular region $\mathcal{R}_{1,2}$ with the boundary data being harmonic polynomials. The gradient of the hypotenuse of the triangle represents the theoretical order of convergence.

the theoretical order of convergence describes the behavior of the errors very accurately. However, it should be noted that the order $O(N^{1/2}r^N)$ for the L^∞ norm of the error is slightly overestimated, because of the appearance of the term $N^{1/2}$. Indeed, in [74, Theorems 2.2 and 2.4], it has been proved that the errors could be estimated as $O(r^N)$. We also note that there do not exist lines corresponding to the case $m = 0$ in Figure 2.5, while there does in Figure 2.4, which can be explained as follows.

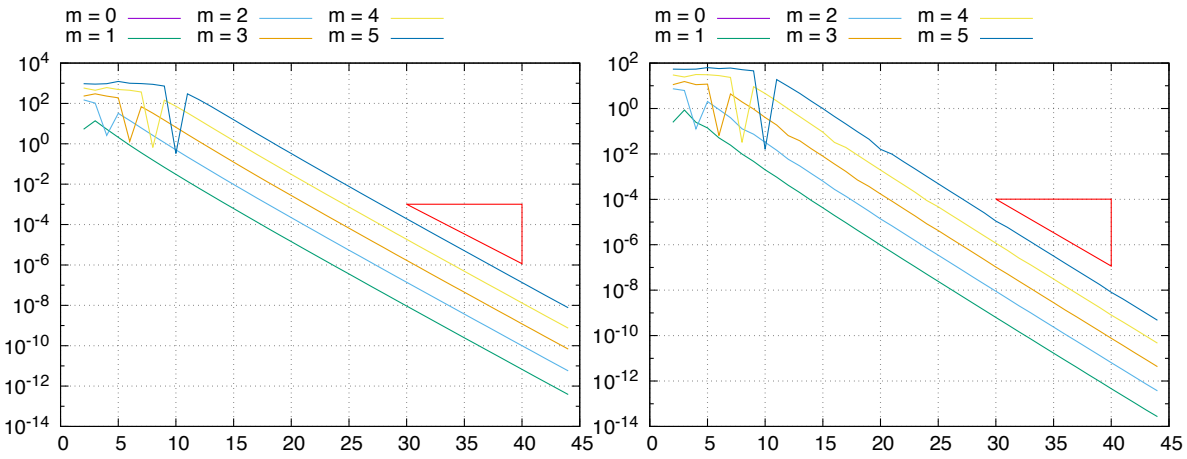

(a) L^2-error estimate (b) L^∞-error estimate

Figure 2.5: Numerical results of I-MFS in the annular region $\mathcal{R}_{1,2}$ with the boundary data being harmonic polynomials. The gradient of the hypotenuse of the triangle represents the theoretical order of convergence.

When $m = 0$, the boundary data f_μ are equal to 1, and therefore the exact solution u is the constant function 1. If we use C-MFS, then the constant function 1 is approximated by a linear combination of logarithmic functions, and therefore there should exist an approximation error. On the other hand, if we use I-MFS, then the approximate function is given by the linear combination of a constant and logarithmic functions, $u_{\mathrm{I}}^{(N)}(x) = Q_0 + \sum_{\nu=1}^{2}\sum_{k=1}^{N} Q_{\nu k} E(x - y_{\nu k})$. Moreover, a direct computation yields that $Q_0 = 1$ and $Q_{\nu k} = 0$ for $\nu = 1, 2$ and $k = 1, 2, \ldots, N$. That is, the approximate solution gives the exact solution in this case, which can be identified as the cause of such phenomena.

2.5.1.2 Boundary data: logarithmic potential

Next, we consider the case that the boundary data f_μ are logarithmic potentials. Namely,

$$f_\mu(z) = \log|z - z_0|, \quad \mu = 1, 2, \tag{2.5.2}$$

where $z_0 = 4\rho_1$. In this case, there exists a singularity at z_0, and therefore the error can be estimated as

$$\|u - u_{\mathrm{C,I}}^{(N)}\|_{L^2(\Gamma^1)\times L^2(\Gamma^2)} = O\left(\max\left\{\left(\frac{1}{2}\right)^N, r^N\right\}\right),$$

$$\|u - u_{\mathrm{C,I}}^{(N)}\|_{L^\infty(\Gamma^1)\times L^\infty(\Gamma^2)} = O\left(N^{1/2}\max\left\{\left(\frac{1}{2}\right)^N, r^N\right\}\right).$$

We take R_1 and R_2 as $R_1 = (1 + 0.2(m+1))\rho_1$ and $R_2 = 1/2$, respectively. Then, we have that

$$\|u - u_{\mathrm{C,I}}^{(N)}\|_{L^2(\Gamma^1)\times L^2(\Gamma^2)} = O\left(\max\left\{\left(\frac{1}{2}\right)^N, \left(\frac{1}{1 + 0.2(m+1)}\right)^N\right\}\right), \tag{2.5.3}$$

$$\|u - u_{\mathrm{C,I}}^{(N)}\|_{L^\infty(\Gamma^1)\times L^\infty(\Gamma^2)} = O\left(N^{1/2}\max\left\{\left(\frac{1}{2}\right)^N, \left(\frac{1}{1 + 0.2(m+1)}\right)^N\right\}\right). \tag{2.5.4}$$

The results of the numerical experiments are presented in Figures 2.6 and 2.7.

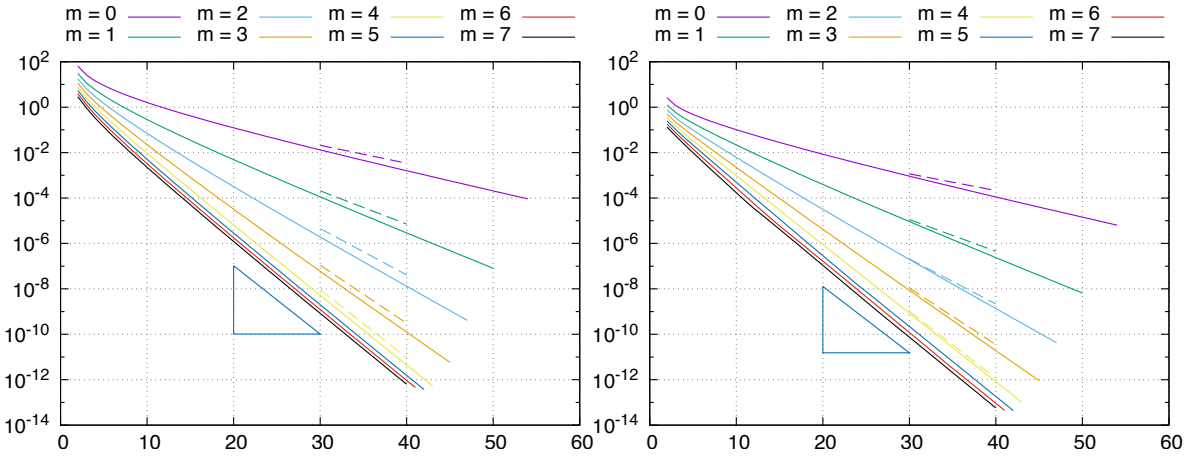

(a) L^2-error estimate (a) L^∞-error estimate

Figure 2.6: Numerical results of C-MFS in the annular region $\mathcal{R}_{1,2}$ with the boundary data being logarithmic potentials. The gradients of the broken lines represent the theoretical orders of convergence for the corresponding solid lines for $m = 0, 1, 2, 3, 4$, and the hypotenuse of the triangle is that for $m = 5, 6, 7$.

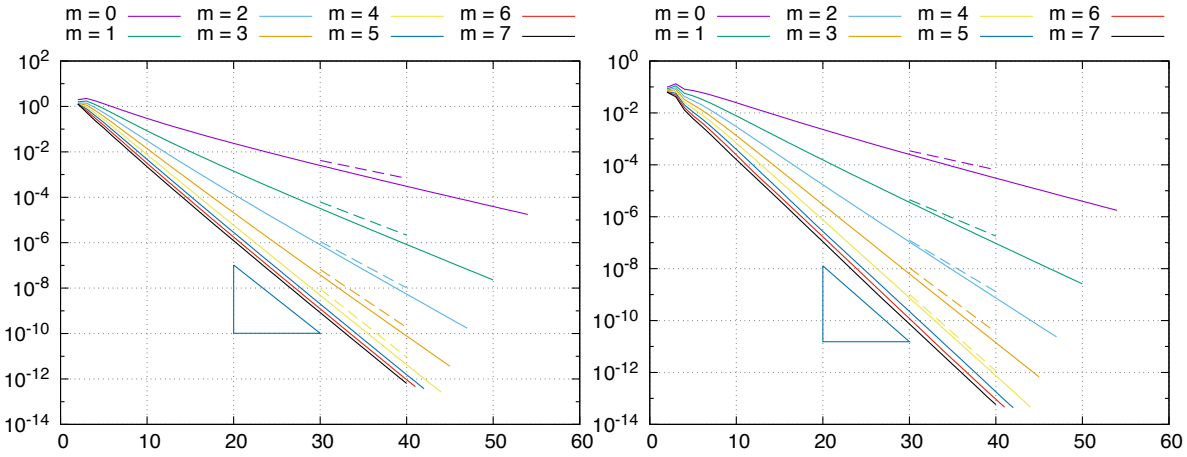

(a) L^2-error estimate (b) L^∞-error estimate

Figure 2.7: Numerical results of I-MFS in the annular region $\mathcal{R}_{1,2}$ with the boundary data being logarithmic potentials. The gradients of the broken lines represent the theoretical orders of convergence for the corresponding solid lines for $m = 0, 1, 2, 3, 4$, and the hypotenuse of the triangle is that for $m = 5, 6, 7$.

2.5.2 Ω: a doubly-connected region surrounded by polynomial curves

For positive real numbers α, β, l, and r, define a function $\Psi_{\alpha,\beta,l,r}$ as

$$\Psi_{\alpha,\beta,l,r}(z) = \beta\left(\frac{z}{\alpha} + \frac{(z/\alpha)^l}{r}\right).$$

Then, $\Psi_{\alpha,\beta,l,r}$ defines a conformal mapping of $D_{\alpha\, {}^{l-1}\sqrt{r/l}}$ to $\mathbb{C}$. Let Γ^1, and Γ^2 be defined as $\Gamma^1 = \Psi_{\rho_1,3,4,8}(\gamma_{\rho_1})$, and $\Gamma^2 = \Psi_{\rho_2,1,6,24}(\gamma_{\rho_2})$, respectively, and let Ω be the interior doubly-connected region surrounded by these polynomial curves. The configuration of Ω and the locations of the singular and collocation points are depicted in Figure 2.8. From Figure 2.8, we can easily check that $\mathrm{Cap}(\Gamma_{R_1}) >$

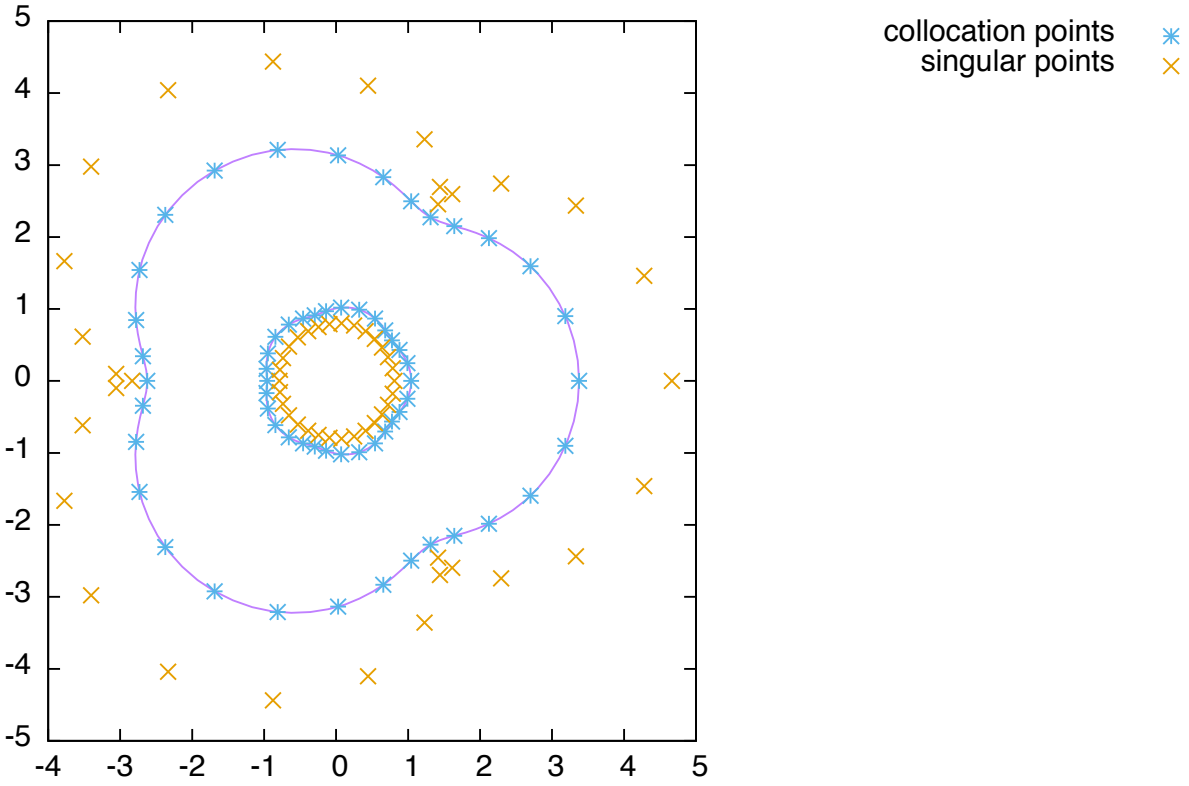

Figure 2.8: Configuration of the region Ω surrounded by two polynomial curves $\Gamma^1 = \Psi_{\rho_1,3,4,8}(\gamma_{\rho_1})$ and $\Gamma^2 = \Psi_{\rho_2,1,6,24}(\gamma_{\rho_2})$, and the locations of the singular and collocation points when $N = 30$, $R_1 = 1.25$, and $R_2 = \rho_1\rho_2/R_1$.

1, using Proposition 1.4.2. Therefore, Theorem 2.1.1 and Corollary 2.1.3 for C-MFS hold in this situation. Note that R_1 and R_2 can be chosen such that $R_1 \notin]\rho_1, \sqrt{\kappa}\rho_1]$ and $R_2 \notin [\sqrt{\kappa}^{-1}\rho_2, \rho_2[$, while $R_1 \in]\sqrt{\kappa\rho_1}, \kappa\rho_1[$ and $R_2 \in]\kappa^{-1}\rho_2, \sqrt{\kappa}^{-1}\rho_2[$. Nevertheless, the errors decay exponentially, and their convergence rates are what we can expect from Theorems 2.1.1 and 2.1.2, and Corollaries 2.1.3 and 2.1.4 (see Figures 2.9, 2.10, 2.11, and 2.12). Therefore, we can conjecture that these would hold for $R_1 \in]\rho_1, \kappa\rho_1[$ and $R_2 \in]\kappa^{-1}\rho_2, \rho_2[$.

2.5.2.1 Boundary data: harmonic potential

Here, we consider the harmonic polynomials (2.5.1) as the boundary data f_μ, and we define R_1 and R_2 as $R_1 = 1.25$ and $R_2 = \rho_1\rho_2/R_1$, so that $\rho_1/R_1 = R_2/\rho_2$. In this case, κ can be regarded as $\sqrt[3]{2} \approx 1.259921\cdots$, and the errors are estimated as follows:

$$\|u - u_{\mathrm{C,I}}^{(N)}\|_{L^2(\Gamma^1)\times L^2(\Gamma^2)} = O(r^N) = O\left(\left(\frac{4}{5}\right)^N\right),$$
$$\|u - u_{\mathrm{C,I}}^{(N)}\|_{L^\infty(\Gamma^1)\times L^\infty(\Gamma^2)} = O(N^{1/2}r^N) = O\left(N^{1/2}\left(\frac{4}{5}\right)^N\right).$$

The results of the numerical experiments are depicted in Figures 2.9 and 2.10, which imply that the above estimates accurately express the behaviar of errors.

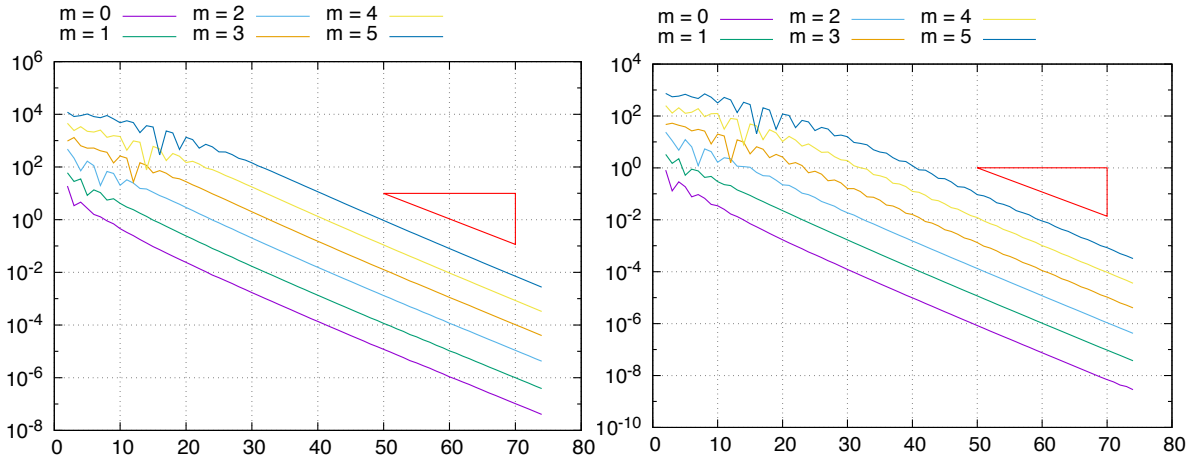

(a) L^2-error estimate (b) L^∞-error estimate

Figure 2.9: Numerical results of C-MFS in the region Ω surrounded by two polynomial curves with the boundary data being harmonic polynomials. The gradient of the hypotenuse of the triangle represents the theoretical order of convergence.

2.5.2.2 Boundary data: logarithmic potential

Now, the boundary data f_μ are given by logarithmic potentials as in (2.5.2), at which the singular point z_0 is replaced $\Psi_{\rho_1,3,4,8}(\rho_0)$, where $\rho_0 = 2.3$. Here, R_1 and R_2 are defined as $R_1 = (1+0.023(m+1))\rho_1$ for $m \in \{0,1,\ldots,7\}$ and $R_2 = \rho_1\rho_2/R_1$. Then, the errors can be estimated as

$$\|u - u^{(N)}\|_{L^2(\Gamma^1)\times L^2(\Gamma^2)} = O\left(\max\left\{\left(\frac{2}{2.3}\right)^{N/2}, \left(\frac{1}{1+0.023(m+1)}\right)^N\right\}\right),$$
$$\|u - u^{(N)}\|_{L^\infty(\Gamma^1)\times L^\infty(\Gamma^2)} = O\left(N^{1/2}\max\left\{\left(\frac{2}{2.3}\right)^{N/2}, \left(\frac{1}{1+0.023(m+1)}\right)^N\right\}\right).$$

The results are shown in Figures 2.11 and 2.12.

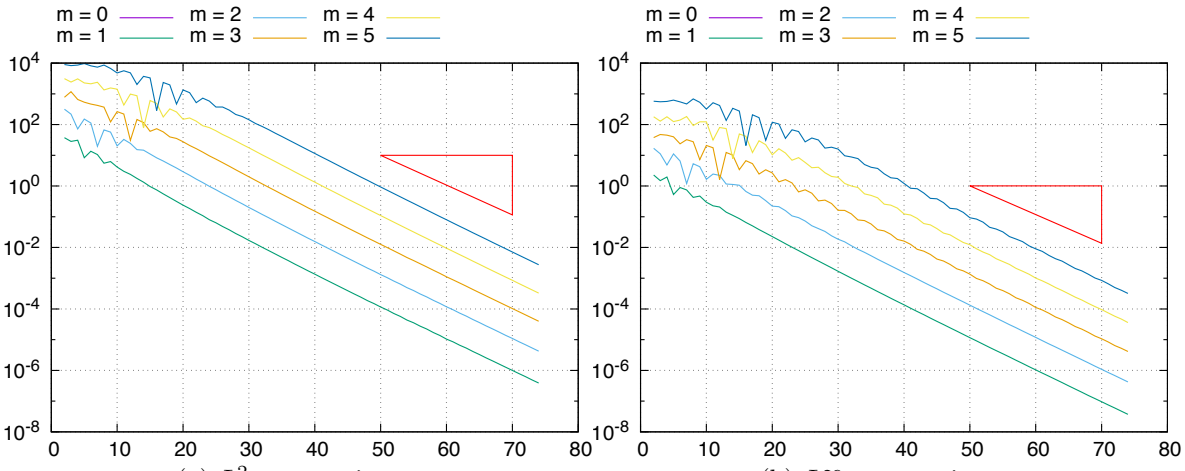

(a) L^2-error estimate (b) L^∞-error estimate

Figure 2.10: Numerical results of I-MFS in the region Ω surrounded by two polynomial curves with the boundary data being harmonic polynomials. The gradient of the hypotenuse of the triangle represents the theoretical order of convergence.

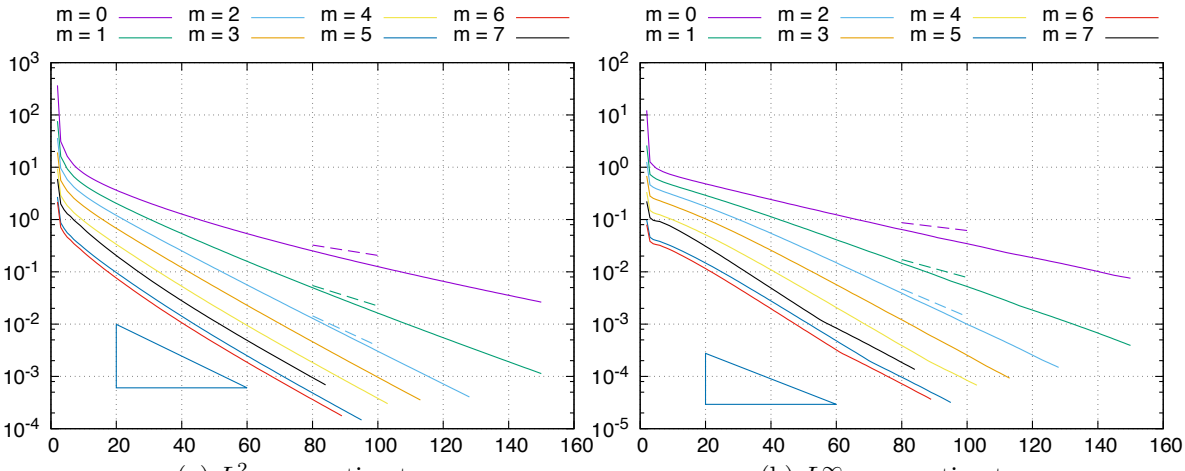

(a) L^2-error estimate (b) L^∞-error estimate

Figure 2.11: Numerical results of C-MFS in the region Ω surrounded by two polynomial curves with the boundary data being logarithmic potentials. The gradients of the broken lines represent the theoretical orders of convergence for the corresponding solid lines for $m = 0, 1, 2$, and the gradient of the hypotenuse of the triangle is that for $m = 3, 4, 5, 6, 7$.

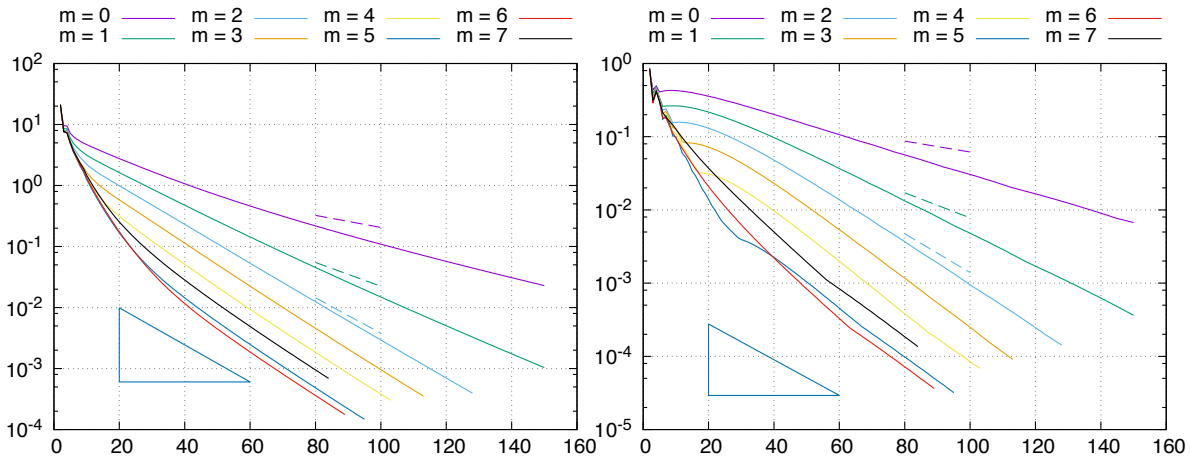

(a) L^2-error estimate (b) L^∞-error estimate

Figure 2.12: Numerical results of I-MFS in the region Ω surrounded by two polynomial curves with the boundary data being logarithmic potentials. The gradients of the broken lines represent the theoretical orders of convergence for the corresponding solid lines for $m = 0, 1, 2$, and the gradient of the hypotenuse of the triangle is that for $m = 3, 4, 5, 6, 7$.

2.6 Concluding remarks

In this chapter, we have built on the work of [48] by using two peripheral conformal mappings to arrange the singular and collocation points. Furthermore, we have established the stability and convergence of C-MFS and I-MFS for the potential problem in a nondegenerate doubly-connected region with boundary that is composed of two disjoint regular analytic Jordan curves. The work presented here could be regarded as the first step towards extending mathematical theory, unique existence and convergence, to cover multiply-connected regions.

Possible directions for future work are as follows. First, MFS should be considered for a potential problem in an n-ly connected region, where $n \geq 3$. To the author's knowledge, there currently exist no mathematical results concerning this problem. Second, MFS could be applied to a potential problem with a nonsmooth boundary; for instance, a polygonal curve. It can be extended that desirable positions for the singular and collocation points could be obtained using the Schwarz-Christoffel mapping. However, a mathematical theory regarding this does not exist so far.

2.7 Proof of Lemma 2.3.12

First, we bound the norm $\|q - q^{(N)}\|^2_{\mathbb{Y}_{\epsilon,s}}$ as follows:

$$\|q - q^{(N)}\|^2_{\mathbb{Y}_{\epsilon,s}} \leq \sum_{\nu=1}^{2} \left[T_1^{(\nu)} + (2\pi)^{s-1} \left(T_2^{(\nu)} + 2T_3^{(\nu)} + 2T_4^{(\nu)} \right) \right],$$

where

$$T_1^{(\nu)} = \left|\hat{q}_\nu(0) - \hat{q}_\nu^{(N)}(0)\right|^2, \quad T_2^{(\nu)} = \sum_{n\in\Lambda'_N\setminus\{0\}} \left|\hat{q}_\nu(n) - \hat{q}_\nu^{(N)}\right|^2 (\epsilon\xi(\nu,\nu))^{2|n|}|n|^{2(s-1)},$$
$$T_3^{(\nu)} = \sum_{\mathbb{Z}\setminus\Lambda'_N} \left|\hat{q}_\nu^{(N)}(n)\right|^2 (\epsilon\xi(\nu,\nu))^{2|n|}|n|^{2(s-1)}, \quad T_4^{(\nu)} = \sum_{\mathbb{Z}\setminus\Lambda'_N} |\hat{q}_\nu(n)|^2 (\epsilon\xi(\nu,\nu))^{2|n|}|n|^{2(s-1)}$$

for $\nu = 1, 2$. In the following, we provide estimates for $T_j^{(1)}$ for $j = 1, 2, 3, 4$.

Utilizing the relations (2.3.8), the Fourier coefficients $\hat{q}_\nu^{(N)}(n)$ can be obtained explicitly as follows:

$$\begin{aligned}\begin{pmatrix}\hat{q}_1^{(N)}(n)\\ \hat{q}_2^{(N)}(n)\end{pmatrix} &= \frac{1}{\det\Phi^{\mathrm{C}}(n)}\begin{pmatrix}\sum_{l\equiv n}\hat{G}_{22}(l) & -\sum_{l\equiv n}\hat{G}_{12}(l)\\ -\sum_{l\equiv n}\hat{G}_{21}(l) & \sum_{l\equiv n}\hat{G}_{11}(l)\end{pmatrix}\begin{pmatrix}\sum_{m\equiv n}\left(\hat{G}_{11}(m)\hat{q}_1(m)+\hat{G}_{12}(m)\hat{q}_2(m)\right)\\ \sum_{m\equiv n}\left(\hat{G}_{21}(m)\hat{q}_1(m)+\hat{G}_{22}(m)\hat{q}_2(m)\right)\end{pmatrix}\\ &= \frac{1}{\det\Phi^{\mathrm{C}}(n)}\sum_{m\equiv n}\sum_{l\equiv n}\begin{pmatrix}\Upsilon_1(m,l)\hat{q}_1(m)+\Upsilon_2(m,l)\hat{q}_2(m)\\ \Upsilon_3(m,l)\hat{q}_1(m)+\Upsilon_4(m,l)\hat{q}_2(m)\end{pmatrix},\end{aligned}$$

where

$$\Upsilon_1(m,l) = \hat{G}_{11}(m)\hat{G}_{22}(l) - \hat{G}_{21}(m)\hat{G}_{12}(l), \quad \Upsilon_2(m,l) = \hat{G}_{12}(m)\hat{G}_{22}(l) - \hat{G}_{22}(m)\hat{G}_{12}(l),$$
$$\Upsilon_3(m,l) = -\hat{G}_{11}(m)\hat{G}_{21}(l) + \hat{G}_{21}(m)\hat{G}_{11}(l), \quad \Upsilon_4(m,l) = -\hat{G}_{12}(m)\hat{G}_{21}(l) + \hat{G}_{22}(m)\hat{G}_{11}(l).$$

We will employ the following proposition without proof.

Proposition 2.7.1. (i) *There exists some positive constants C_j $(j = 1, 2, 3, 4)$ such that*

$$|\Upsilon_1(m,l)| \le \frac{C_1}{\underline{m}\cdot\underline{l}}\left(\frac{\rho_1}{R_1}\right)^{|m|}\left(\frac{R_2}{\rho_2}\right)^{|l|}, \quad |\Upsilon_2(m,l)| \le \frac{C_2}{\underline{m}\cdot\underline{l}}\left(\frac{R_2}{\rho_2}\right)^{|m|+|l|},$$
$$|\Upsilon_3(m,l)| \le \frac{C_3}{\underline{m}\cdot\underline{l}}\left(\frac{\rho_1}{R_1}\right)^{|m|+|l|}, \quad |\Upsilon_4(m,l)| \le \frac{C_4}{\underline{m}\cdot\underline{l}}\left(\frac{R_2}{\rho_2}\right)^{|m|}\left(\frac{\rho_1}{R_1}\right)^{|l|}.$$

(ii) *There exists some positive constant $C_{\rho_1,\rho_2,R_1,R_2}$ such that*

$$\frac{1}{(\det\Phi^{\mathrm{C}}(0))^2} \le C_{\rho_1,\rho_2,R_1,R_2}$$

holds for all $N \in \mathbb{N}$.

(iii) *There exists some positive constant $C_{\rho_1,\rho_2,R_1,R_2}$ such that*

$$\frac{1}{(\det\Phi^{\mathrm{C}}(n))^2} \le C_{\rho_1,\rho_2,R_1,R_2}|n|^4\left(\frac{R_1}{\rho_1}\right)^{2|n|}\left(\frac{\rho_2}{R_2}\right)^{2|n|}$$

holds for all $N \in \mathbb{N}$, and all $n \in \Lambda'_N \setminus \{0\}$.

(iv) *For all $(\epsilon, s) \in]0, +\infty[\times\mathbb{R}$ with $(\epsilon, s) < (1, -1)$, there exists some positive constant $C_{\epsilon,s}$ such that*

$$\sum_{m\in I(p)} |m|^s\epsilon^{|m|} \le C_{\epsilon,s}N^s\epsilon^{N-|p|}$$

holds for all $N \in \mathbb{N}$, and all $p \in \Lambda'_N$.

(v) *For all* $(\epsilon, s) \in]0, +\infty[\times\mathbb{R}$*, there exists some positive constant* $C_{\epsilon,s}$ *such that*

$$\max_{p\in\Lambda'_N\setminus\{0\}}\left[\left(\frac{N}{|p|}\right)^s \epsilon^{N-2|p|}\right] \le C_{\epsilon,s}$$

holds for all $N \in \mathbb{N}$.

$T_1^{(1)}$ can be bounded as follows:

$$\begin{aligned}
T_1^{(1)} &= \frac{1}{(\det\Phi^{\mathrm{C}}(0))^2}\left|\sum_{m\equiv 0}\sum_{l\equiv 0}\Upsilon_1(m,l)\hat{q}_1(0) - \sum_{m\equiv 0}\sum_{l\equiv 0}\Upsilon_1(m,l)\hat{q}_1(m) - \sum_{m\equiv 0}\sum_{l\equiv 0}\Upsilon_2(m,l)\hat{q}_2(m)\right|^2 \\
&= \frac{1}{(\det\Phi^{\mathrm{C}}(0))^2}\left|\sum_{m\in I(0)}\sum_{m\equiv 0}\Upsilon_1(m,l)\hat{q}_1(0) - \sum_{m\in I(0)}\sum_{m\equiv 0}\Upsilon_1(m,l)\hat{q}_1(m) - \sum_{m\equiv 0}\sum_{l\equiv 0}\Upsilon_2(m,l)\hat{q}_2(m)\right|^2 \\
&\le T_{11}^{(1)} + T_{12}^{(1)} + T_{13}^{(1)},
\end{aligned}$$

where

$$\begin{aligned}
T_{11}^{(1)} &= \frac{3}{(\det\Phi^{\mathrm{C}}(0))^2}\left(\sum_{m\in I(0)}\sum_{l\equiv 0}|\Upsilon_1(m,l)|\,|\hat{q}_1(0)|\right)^2, \\
T_{12}^{(1)} &= \frac{3}{(\det\Phi^{\mathrm{C}}(0))^2}\left(\sum_{m\in I(0)}\sum_{l\equiv 0}|\Upsilon_1(m,l)|\,|\hat{q}_1(m)|\right)^2, \\
T_{13}^{(1)} &= \frac{3}{(\det\Phi^{\mathrm{C}}(0))^2}\left(\sum_{m\equiv 0}\sum_{l\equiv 0}|\Upsilon_2(m,l)|\,|\hat{q}_2(m)|\right)^2.
\end{aligned}$$

By using Proposition 2.7.1 (i), (ii), and (iv), we have that

$$\begin{aligned}
T_{11}^{(1)} &\le 3C_{\rho_1,\rho_2,R_1,R_2}\left(\sum_{m\in I(0)}\sum_{l\equiv 0}\frac{C_1}{\underline{m}\cdot\underline{l}}\left(\frac{\rho_1}{R_1}\right)^{|m|}\left(\frac{R_2}{\rho_2}\right)^{|l|}|\hat{q}_1(0)|\right)^2 \\
&\le C_{11}^{(1)}N^{-2}\left(\frac{\rho_1}{R_1}\right)^{2N}\|q_1\|^2_{\delta\rho_1/R_1,t-1}.
\end{aligned}$$

By assumption, we have that $\delta r^2 \le \epsilon$. Therefore, the following inequalities can be obtained:

$$T_{11}^{(1)} \le C_{11}^{(1)}N^{-2}r^{2N}\|q_1\|^2_{\delta\rho_1/R_1,t-1} \le \begin{cases} C_{11}^{(1)}N^{-2}\left(\frac{\epsilon}{\delta}\right)^N\|q_1\|^2_{\delta\rho_1/R_1,t-1} & \text{if } \epsilon=\delta r^2 \text{ and } s-t\le -1, \\ C_{11}^{(1)}N^{2(s-t)}\left(\frac{\epsilon}{\delta}\right)^N\|q_1\|^2_{\delta\rho_1/R_1,t-1} & \text{otherwise.}\end{cases}$$

By using Proposition 2.7.1 (i), (ii), and (iv), we have that

$$\begin{aligned}
T_{12}^{(1)} &\le 3C_{\rho_1,\rho_2,R_1,R_2}\left(\sum_{m\in I(0)}\sum_{l\equiv 0}\frac{C_1}{\underline{m}\cdot\underline{l}}\left(\frac{\rho_1}{R_1}\right)^{|m|}\left(\frac{R_2}{\rho_2}\right)^{|l|}|\hat{q}_1(m)|\right)^2 \\
&\le C_{12}^{(1)}\sum_{m\in I(0)}\frac{1}{\delta^{2|m|}}\frac{1}{\underline{m}^{2t}}\sum_{m\in I(0)}|\hat{q}_1(m)|^2\left(\frac{\delta\rho_1}{R_1}\right)^{2|m|}\underline{m}^{2(t-1)} \le C_{12}^{(1)}N^{-2t}\frac{1}{\delta^{2N}}\|q_1\|^2_{\delta\rho_1/R_1,t-1}.
\end{aligned}$$

The assumption that $1/\delta \le \epsilon$ implies that

$$T_{12}^{(1)} \le \begin{cases} C_{12}^{(1)} N^{-2t} \left(\frac{\epsilon}{\delta}\right)^N \|q_1\|^2_{\delta\rho_1/R_1,t-1} & \text{if } \epsilon = 1/\delta \text{ and } s \le 0, \\ C_{12}^{(1)} N^{2(s-t)} \left(\frac{\epsilon}{\delta}\right)^N \|q_1\|^2_{\delta\rho_1/R_1,t-1} & \text{otherwise.} \end{cases}$$

Then, $T_{13}^{(1)}$ is bounded by splitting it into the following three terms:

$$T_{13}^{(1)} \le T_{131}^{(1)} + T_{132}^{(1)} + T_{133}^{(1)},$$

where

$$T_{131}^{(1)} = \frac{9}{(\det \Phi^{\mathrm{C}}(0))^2} \left(\sum_{l \in I(0)} |\Upsilon_2(0,l)|\, |\hat{q}_2(0)| \right)^2, \quad T_{132}^{(2)} = \frac{9}{(\det \Phi^{\mathrm{C}}(0))^2} \left(\sum_{m \in I(0)} |\Upsilon_2(m,0)|\, |\hat{q}_2(m)| \right)^2,$$

$$T_{133}^{(3)} = \frac{9}{(\det \Phi^{\mathrm{C}}(0))^2} \left(\sum_{m,l \in I(0)} |\Upsilon_2(m,l)|\, |\hat{q}_2(m)| \right)^2.$$

In the same manner as in deriving an estimate for $T_{11}^{(1)}$, $T_{131}^{(1)}$ can be bounded by Proposition 2.7.1 (i), (ii), and (iv) as follows:

$$T_{131}^{(1)} \le \begin{cases} C_{131}^{(1)} N^{-2} \left(\frac{\epsilon}{\delta}\right)^N \|q_2\|^2_{\delta R_2/\rho_2,t-1} & \text{if } \epsilon = \delta r^2 \text{ and } s - t \le -1, \\ C_{131}^{(1)} N^{2(s-t)} \left(\frac{\epsilon}{\delta}\right)^N \|q_2\|^2_{\delta R_2/\rho_2,t-1} & \text{otherwise.} \end{cases}$$

In a similar manner as for estimating $T_{12}^{(1)}$, a bound for $T_{132}^{(1)}$ can be given by

$$T_{132}^{(1)} \le \begin{cases} C_{132}^{(1)} N^{-2t} \left(\frac{\epsilon}{\delta}\right)^N \|q_2\|^2_{\delta R_2/\rho_2,t-1} & \text{if } \epsilon = 1/\delta \text{ and } s \le 0, \\ C_{132}^{(1)} N^{2(s-t)} \left(\frac{\epsilon}{\delta}\right)^N \|q_2\|^2_{\delta R_2/\rho_2,t-1} & \text{otherwise,} \end{cases}$$

by Proposition 2.7.1 (i), (ii), and (iv). Furthermore, $T_{133}^{(1)}$ can be estimated using Proposition 2.7.1 (i), (ii), and (iv) and the relation $\epsilon/\delta > (r/\delta)^2$, as follows:

$$T_{133}^{(1)} \le 9 C_{\rho_1,\rho_2,R_1,R_2} \left(\sum_{m,l \in I(0)} \frac{C_2}{\underline{m} \cdot \underline{l}} \left(\frac{R_2}{\rho_2}\right)^{|m|+|l|} |\hat{q}_2(m)| \right)^2 \le C_{133}^{(1)} N^{2(s-t)} \left(\frac{\epsilon}{\delta}\right)^N \|q_2\|^2_{\delta R_2/\rho_2,t-1}.$$

Summarizing the above, we can obtain the following bound for $T_1^{(1)}$:

$$T_1^{(1)} \le \begin{cases} C_1^{(1)} N^{-2} \left(\frac{\epsilon}{\delta}\right)^N \|q\|^2_{\mathbb{Y}_{\delta,t}} & \text{if } (\delta,\epsilon) \in L_1 \setminus \{C_1\} \text{ and } s - t \le -1, \\ C_1^{(1)} N^{-2t} \left(\frac{\epsilon}{\delta}\right)^N \|q\|^2_{\mathbb{Y}_{\delta,t}} & \text{if } (\delta,\epsilon) \in H_1 \setminus \{C_1\} \text{ and } s \le 0, \\ C_1^{(1)} N^{2\max\{s-t,-1,-t\}} \left(\frac{\epsilon}{\delta}\right)^N \|q\|^2_{\mathbb{Y}_{\delta,t}} & \text{if } (\delta,\epsilon) = C_1, \\ C_1^{(1)} N^{2(s-t)} \left(\frac{\epsilon}{\delta}\right)^N \|q_2\|^2_{\delta R_2/\rho_2,t-1} & \text{otherwise.} \end{cases}$$

Next, we estimate $T_2^{(1)}$. Because we can estimate $|\hat{q}_1(n) - \hat{q}_1^{(N)}(n)|^2$ as

$$
\begin{aligned}
&|\hat{q}_1(n) - \hat{q}_1^{(N)}(n)|^2 \\
&\quad = \frac{1}{(\det \Phi^{\mathrm{C}}(n))^2} \left| \sum_{m\equiv n} \sum_{l\equiv n} \Upsilon_1(m,l)\hat{q}_1(n) - \sum_{m\equiv n} \sum_{l\equiv n} \Upsilon_1(m,l)\hat{q}_1(m) - \sum_{m\equiv n} \sum_{l\equiv n} \Upsilon_2(m,l)\hat{q}_2(m) \right|^2 \\
&\quad = \frac{1}{(\det \Phi^{\mathrm{C}}(n))^2} \left| \sum_{m\in I(n)} \sum_{l\equiv n} \Upsilon_1(m,l)\hat{q}_1(n) - \sum_{m\in I(n)} \sum_{l\equiv n} \Upsilon_1(m,l)\hat{q}_1(m) - \sum_{\substack{m,l\equiv n \\ m\neq l}} \Upsilon_2(m,l)\hat{q}_2(m) \right|^2 \\
&\quad \leq \frac{3}{(\det \Phi^{\mathrm{C}}(n))^2} \left[\left(\sum_{m\in I(n)} \sum_{l\equiv n} |\Upsilon_1(m,l)|\,|\hat{q}_1(n)| \right)^2 + \left(\sum_{m\in I(n)} \sum_{l\equiv n} |\Upsilon_1(m,l)|\,|\hat{q}_1(m)| \right)^2 \right. \\
&\qquad\qquad \left. + \left(\sum_{\substack{m,l\equiv n \\ m\neq l}} |\Upsilon_2(m,l)|\,|\hat{q}_2(m)| \right)^2 \right],
\end{aligned}
$$

we have that

$$
T_2^{(1)} \leq T_{21}^{(1)} + T_{22}^{(1)} + T_{23}^{(1)},
$$

where

$$
\begin{aligned}
T_{21}^{(1)} &= \sum_{n\in\Lambda_N'\setminus\{0\}} \frac{3}{(\det \Phi^{\mathrm{C}}(n))^2} \left(\sum_{m\in I(n)} \sum_{l\equiv n} |\Upsilon_1(m,l)|\,|\hat{q}_1(n)| \right)^2 \left(\frac{\epsilon\rho_1}{R_1} \right)^{2|n|} |n|^{2(s-1)}, \\
T_{22}^{(1)} &= \sum_{n\in\Lambda_N'\setminus\{0\}} \frac{3}{(\det \Phi^{\mathrm{C}}(n))^2} \left(\sum_{m\in I(n)} \sum_{l\equiv n} |\Upsilon_1(m,l)|\,|\hat{q}_1(m)| \right)^2 \left(\frac{\epsilon\rho_1}{R_1} \right)^{2|n|} |n|^{2(s-1)}, \\
T_{23}^{(1)} &= \sum_{n\in\Lambda_N'\setminus\{0\}} \frac{3}{(\det \Phi^{\mathrm{C}}(n))^2} \left(\sum_{\substack{m,l\equiv n \\ m\neq l}} |\Upsilon_2(m,l)|\,|\hat{q}_2(m)| \right)^2 \left(\frac{\epsilon\rho_1}{R_1} \right)^{2|n|} |n|^{2(s-1)}.
\end{aligned}
$$

Using Proposition 2.7.1 (i), (iii), and (iv), for $n \in \Lambda_N' \setminus \{0\}$, we have that

$$
\begin{aligned}
&\frac{1}{(\det \Phi^{\mathrm{C}}(n))^2} \left(\sum_{m\in I(n)} \sum_{l\equiv n} |\Upsilon_1(m,l)|\,|\hat{q}_1(n)| \right)^2 \\
&\qquad \leq C_{\rho_1,\rho_2,R_1,R_2} |n|^4 \left(\frac{R_1}{\rho_1} \right)^{2|n|} \left(\frac{\rho_2}{R_2} \right)^{2|n|} \left(\sum_{m\in I(n)} \sum_{l\equiv n} \frac{C_1}{\underline{m}\cdot\underline{l}} \left(\frac{\rho_1}{R_1} \right)^{|m|} \left(\frac{R_2}{\rho_2} \right)^{|l|} \right)^2 |\hat{q}_1(n)|^2 \\
&\qquad \leq \tilde{C}_{21}^{(1)} |n|^2 N^{-2} \left(\frac{\rho_1}{R_1} \right)^{2(N-2|n|)} |\hat{q}_1(n)|^2,
\end{aligned}
$$

which yields that

$$\begin{aligned}
T_{21}^{(1)} &\le 3\tilde{C}_{21}^{(1)} N^{-2} \sum_{n\in\Lambda_N'\setminus\{0\}} |n|^2 \left(\frac{\rho_1}{R_1}\right)^{2(N-2|n|)} |\hat{q}_1(n)|^2 \left(\frac{\epsilon\rho_1}{R_1}\right)^{2|n|} |n|^{2(s-1)} \\
&\le C_{21}^{(1)} N^{2[-1+\max\{s-t+1,0\}]} \left(\frac{\epsilon}{\delta}\right)^N \\
&\qquad \times \sum_{n\in\Lambda_N'\setminus\{0\}} |\hat{q}_1(n)|^2 \left(\frac{\delta\rho_1}{R_1}\right)^{2|n|} \underline{n}^{2(t-1)} \left(\frac{\delta r^2}{\epsilon}\right)^{N-2|n|} |n|^{2(s-t+1)} N^{-2\max\{s-t+1,0\}} \\
&\le C_{21}^{(1)} N^{2[-1+\max\{s-t+1,0\}]} \left(\frac{\epsilon}{\delta}\right)^N \|q_1\|^2_{\delta\rho_1/R_1,t-1} A_{21}^{(1)},
\end{aligned}$$

where

$$A_{21}^{(1)} = \sup_{\Lambda_N'\setminus\{0\}} \left[\left(\frac{\delta r^2}{\epsilon}\right)^{N-2|n|} |n|^{2(s-t+1)} N^{-2\max\{s-t+1,0\}} \right].$$

Because this constant can be evaluated using Proposition 2.7.1 (v) as

$$A_{21}^{(1)} \le \begin{cases} 1 & \text{if } \epsilon = \delta r^2 \text{ and } s-t \le -1, \\ 4^{-s+t-1} & \text{if } \epsilon = \delta r^2 \text{ and } s-t > -1, \\ C_{\delta r^2/\epsilon,-2(s-t+1)} N^{2(s-t+1)} & \text{if } \epsilon > \delta r^2 \text{ and } s-t \le -1, \\ C_{\delta r^2/\epsilon,-2(s-t+1)} & \text{if } \epsilon > \delta r^2 \text{ and } s-t > -1, \end{cases}$$

we obtain that

$$T_{21}^{(1)} \le \begin{cases} C_{21}^{(1)} N^{-2} \left(\frac{\epsilon}{\delta}\right)^N \|q_1\|^2_{\delta\rho_1/R_1,t-1} & \text{if } \epsilon = \delta r^2 \text{ and } s-t \le -1, \\ C_{21}^{(1)} N^{2(s-t)} \left(\frac{\epsilon}{\delta}\right)^N \|q_1\|^2_{\delta\rho_1/R_1,t-1} & \text{otherwise.} \end{cases}$$

By Proposition 2.7.1 (i), (iii), and (iv), we have that

$$\begin{aligned}
&\frac{1}{(\det\Phi^{\mathrm{C}}(n))^2} \left(\sum_{m\in I(n)} \sum_{l\equiv n} |\Upsilon_1(m,l)|\, |\hat{q}_1(m)| \right)^2 \\
&\qquad \le C_{\rho_1,\rho_2,R_1,R_2} |n|^4 \left(\frac{R_1}{\rho_1}\right)^{2|n|} \left(\frac{\rho_2}{R_2}\right)^{2|n|} \left(\sum_{m\in I(n)} \sum_{l\equiv n} \frac{C_1}{\underline{m}\cdot\underline{l}} \left(\frac{\rho_1}{R_1}\right)^{|m|} \left(\frac{R_2}{\rho_2}\right)^{|l|} |\hat{q}_1(m)| \right)^2 \\
&\qquad \le \tilde{C}_{21}^{(2)} |n|^2 N^{-2t} \frac{1}{\delta^{2(N-|n|)}} \left(\frac{R_1}{\rho_1}\right)^{2|n|} \sum_{m\in I(n)} |\hat{q}_1(m)|^2 \left(\frac{\delta\rho_1}{R_1}\right)^{2|m|} \underline{m}^{2(t-1)}
\end{aligned}$$

for $n \in \Lambda'_N \setminus \{0\}$. Therefore, $T_{22}^{(1)}$ can be bounded as follows:

$$\begin{aligned}
T_{22}^{(1)} &\le 3\tilde{C}_{22}^{(1)} N^{-2t} \sum_{n\in\Lambda'_N\setminus\{0\}} |n|^2 \frac{1}{\delta^{2(N-|n|)}} \left(\frac{R_1}{\rho_1}\right)^{2|n|} \left(\frac{\epsilon\rho_1}{R_1}\right)^{2|n|} |n|^{2(s-1)} \\
&\qquad\qquad \times \sum_{m\in I(n)} |\hat{q}_1(m)|^2 \left(\frac{\delta\rho_1}{R_1}\right)^{2|m|} \underline{m}^{2(t-1)} \\
&\le C_{22}^{(1)} N^{2[-t+\max\{s,0\}]} \left(\frac{\epsilon}{\delta}\right)^N \sum_{n\in\Lambda'_N\setminus\{0\}} \left(\frac{1}{\epsilon\delta}\right)^{N-2|n|} |n|^{2s} N^{-2\max\{s,0\}} \\
&\qquad\qquad \times \sum_{m\in I(n)} |\hat{q}_1(m)|^2 \left(\frac{\delta\rho_1}{R_1}\right)^{2|m|} \underline{m}^{2(t-1)} \\
&\le C_{22}^{(1)} N^{2[-t+\max\{s,0\}]} \left(\frac{\epsilon}{\delta}\right)^N A_{22}^{(1)} \|q_1\|^2_{\delta\rho_1/R_1},
\end{aligned}$$

where

$$A_{22}^{(1)} = \sup_{n\in\Lambda'_N\setminus\{0\}} \left[\left(\frac{1}{\epsilon\delta}\right)^{N-2|n|} |n|^{2s} N^{-2\max\{s,0\}}\right],$$

which can be bounded as

$$A_{22}^{(1)} \le \begin{cases} 1 & \text{if } \epsilon = 1/\delta \text{ and } s \le 0, \\ 4^{-s} & \text{if } \epsilon = 1/\delta \text{ and } s > 0, \\ C_{1/(\epsilon\delta),-2s} N^{2s} & \text{if } \epsilon > 1/\delta \text{ and } s \le 0, \\ C_{1/(\epsilon\delta),-2s} & \text{if } \epsilon > 1/\delta \text{ and } s > 0 \end{cases}$$

by Proposition 2.7.1 (v). Then, we obtain the following estimate for $T_{22}^{(1)}$:

$$T_{22}^{(1)} \le \begin{cases} C_{22}^{(1)} N^{-2t} \left(\frac{\epsilon}{\delta}\right)^N \|q_1\|^2_{\delta\rho_1/R_1,t-1} & \text{if } \epsilon = 1/\delta \text{ and } s \le 0, \\ C_{22}^{1} N^{2(s-t)} \left(\frac{\epsilon}{\delta}\right)^N \|q_1|^2_{\delta\rho_1/R_1,t-1} & \text{otherwise.} \end{cases}$$

Concerning the estimation of $T_{23}^{(1)}$, we use Proposition 2.7.1 (i), (iii), and (iv) to yield that

$$\begin{aligned}
&\frac{1}{(\det\Phi^{\mathrm{C}}(n))^2} \left(\sum_{\substack{m,l\equiv n \\ m\neq l}} |\Upsilon_2(m,l)|\,|\hat{q}_2(m)|\right)^2 \\
&\le C_{\rho_1,\rho_2,R_1,R_2} |n|^4 \left(\frac{R_1}{\rho_1}\right)^{2|n|} \left(\frac{\rho_2}{R_2}\right)^{2|n|} \left(\sum_{\substack{m,l\equiv n \\ m\neq l}} \frac{C_2}{\underline{m}\cdot\underline{l}} \left(\frac{R_2}{\rho_2}\right)^{|m|+|l|} |\hat{q}_2(m)|\right)^2 \\
&\le \tilde{C}_{231}^{(1)} |n|^2 N^{-2} \left(\frac{R_1}{\rho_1}\right)^{2|n|} \left(\frac{R_2}{\rho_2}\right)^{2(N-|n|)} |\hat{q}_2(n)|^2 \\
&\qquad + \tilde{C}_{232}^{(1)} |n|^2 \left(\frac{R_1}{\rho_1}\right)^{2|n|} \frac{1}{\delta^{2(N-|n|)}} N^{-2t} \sum_{m\in I(n)} |\hat{q}_2(m)|^2 \left(\frac{\delta R_2}{\rho_2}\right)^{2|m|} \underline{m}^{2(t-1)}
\end{aligned}$$

$$+ \tilde{C}^{(1)}_{233}|n|^4 N^{-2(t+1)} \left(\frac{R_1}{\rho_1}\right)^{2|n|} \left(\frac{R_2}{\rho_2}\right)^{2(N-2|n|)} \frac{1}{\delta^{2(N-|n|)}} \sum_{m\in I(n)} |\hat{q}_2(m)|^2 \left(\frac{\delta R_2}{\rho_2}\right)^{2|m|} \underline{m}^{2(t-1)},$$

which implies that

$$T^{(1)}_{23} \le T^{(1)}_{231} + T^{(1)}_{232} + T^{(1)}_{233},$$

where

$$T^{(1)}_{231} = C^{(1)}_{231} \sum_{n\in\Lambda'_N\setminus\{0\}} \epsilon^{2|n|}|n|^{2s} N^{-2} \left(\frac{R_2}{\rho_2}\right)^{2(N-|n|)} |\hat{q}_2(n)|^2,$$

$$T^{(1)}_{232} = C^{(1)}_{232} \sum_{n\in\Lambda'_N\setminus\{0\}} \epsilon^{2|n|}|n|^{2s} \frac{1}{\delta^{2(N-|n|)}} N^{-2t} \sum_{m\in I(n)} |\hat{q}_2(m)|^2 \left(\frac{\delta R_2}{\rho_2}\right)^{2|m|} \underline{m}^{2(t-1)},$$

$$T^{(1)}_{233} = C^{(1)}_{233} \sum_{n\in\Lambda'_N\setminus\{0\}} \epsilon^{2|n|}|n|^{2(s+1)} \frac{1}{\delta^{2(N-|n|)}} N^{-2(t+1)} \left(\frac{R_2}{\rho_2}\right)^{2(N-2|n|)} \times \sum_{m\in I(n)} |\hat{q}_2(m)|^2 \left(\frac{\delta R_2}{\rho_2}\right)^{2|m|} \underline{m}^{2(t-1)}.$$

We estimate each of these quantities below. Concerning $T^{(1)}_{231}$, we have that

$$T^{(1)}_{231} \le C^{(1)}_{231} N^{2[-1+\max\{s-t+1,0\}]} \left(\frac{\epsilon}{\delta}\right)^N \|q_2\|^2_{\delta R_2/\rho_2,t-1} A^{(1)}_{231},$$

where

$$A^{(1)}_{231} = \sup_{n\in\Lambda'_N\setminus\{0\}} \left[|n|^{2(s-t+1)} N^{-2\max\{s-t+1,0\}} \left(\frac{\delta r^2}{\epsilon}\right)^{N-2|n|} \right].$$

This can be bounded by virtue of Proposition 2.7.1 (v) as follows:

$$A^{(1)}_{231} \le \begin{cases} 1 & \text{if } \epsilon = \delta r^2 \text{ and } s-t \le -1, \\ 4^{-s+t-1} & \text{if } \epsilon = \delta r^2 \text{ and } s-t > -1, \\ C_{\delta r^2/\epsilon,-2(s-t+1)} N^{2(s-t+1)} & \text{if } \epsilon > \delta r^2 \text{ and } s-t \le -1, \\ C_{\delta r^2/\epsilon,-2(s-t+1)} & \text{if } \epsilon > \delta r^2 \text{ and } s-t > -1. \end{cases}$$

Therefore, we can determine an estimate for $T^{(1)}_{231}$ as

$$T^{(1)}_{231} \le \begin{cases} C^{(1)}_{231} N^{-2} \left(\frac{\epsilon}{\delta}\right)^N \|q_2\|^2_{\delta R_2/\rho_2,t-1} & \text{if } \epsilon = \delta r^2 \text{ and } s-t \le -1, \\ C^{(1)}_{231} N^{2(s-t)} \left(\frac{\epsilon}{\delta}\right)^N \|q_2\|^2_{\delta R_2/\rho_2,t-1} & \text{otherwise.} \end{cases}$$

Concerning $T^{(1)}_{232}$, we have that

$$T^{(1)}_{232} \le C^{(1)}_{232} N^{2[-t+\max\{s,0\}]} \left(\frac{\epsilon}{\delta}\right)^N \|q_2\|^2_{\delta R_2/\rho_2,t-1} A^{(1)}_{232},$$

where

$$A^{(1)}_{232} = \sup_{n\in\Lambda'_N\setminus\{0\}} \left[|n|^{2s} N^{-2\max\{s,0\}} \left(\frac{1}{\delta\epsilon}\right)^{N-2|n|} \right].$$

The constant $A^{(1)}_{232}$ can be bounded by using Proposition 2.7.1 (v), as follows:

$$A^{(1)}_{232} \leq \begin{cases} 1 & \text{if } \epsilon = 1/\delta \text{ and } s \leq 0, \\ 4^{-s} & \text{if } \epsilon = 1/\delta \text{ and } s > 0, \\ C_{1/(\delta\epsilon),-2s} N^{2s} & \text{if } \epsilon > 1/\delta \text{ and } s \leq 0, \\ C_{1/(\delta\epsilon),-2s} & \text{if } \epsilon > 1/\delta \text{ and } s > 0. \end{cases}$$

Then, we obtain the following estimate for $T^{(1)}_{232}$:

$$T^{(1)}_{232} \leq \begin{cases} C^{(1)}_{232} N^{-2t} \left(\frac{\epsilon}{\delta}\right)^N \|q_2\|^2_{\delta R_2/\rho_2, t-1} & \text{if } \epsilon = 1/\delta \text{ and } s \leq 0, \\ C^{(1)}_{232} N^{2(s-t)} \left(\frac{\epsilon}{\delta}\right)^N \|q_2\|^2_{\delta R_2/\rho_2, t-1} & \text{otherwise.} \end{cases}$$

Finally, for $T^{(1)}_{233}$ we have that

$$T^{(1)}_{233} \leq C^{(1)}_{233} N^{2(s-t)} \left(\frac{\epsilon}{\delta}\right)^N \|q_2\|^2_{\delta R_2/\rho_2, t-1} \sup_{n \in \Lambda'_N \setminus \{0\}} \left[\left(\frac{N}{|n|}\right)^{-2(s+1)} \left\{ \frac{1}{\delta\epsilon} \left(\frac{R_2}{\rho_2}\right)^2 \right\}^{N-2|n|} \right].$$

The above supremum can be bounded by some constant, because $(\delta\epsilon)^{-1}(R_2/\rho_2)^2 < 1$, and so we obtain that

$$T^{(1)}_{233} \leq C^{(1)}_{233} N^{2(s-t)} \left(\frac{\epsilon}{\delta}\right)^N \|q_2\|^2_{\epsilon R_2/\rho_2, t-1}.$$

Summarizing the above, we obtain the following estimate for $T^{(1)}_2$:

$$T^{(1)}_2 \leq \begin{cases} C^{(1)}_2 N^{-2} \left(\frac{\epsilon}{\delta}\right)^N \|q\|^2_{\mathbb{Y}_{\delta,t}} & \text{if } (\delta,\epsilon) \in L_1 \setminus \{C_1\} \text{ and } s - t \leq -1, \\ C^{(1)}_2 N^{-2t} \left(\frac{\epsilon}{\delta}\right)^N \|q\|^2_{\mathbb{Y}_{\delta,t}} & \text{if } (\delta,\epsilon) \in H_1 \setminus \{C_1\} \text{ and } s \leq 0, \\ C^{(1)}_2 N^{2\max\{s-t,-1,-t\}} \left(\frac{\epsilon}{\delta}\right)^N \|q\|^2_{\mathbb{Y}_{\delta,t}} & \text{if } (\delta,\epsilon) = C_1, \\ C^{(1)}_2 N^{2(s-t)} \left(\frac{\epsilon}{\delta}\right)^N \|q\|^2_{\mathbb{Y}_{\delta,t}} & \text{otherwise.} \end{cases}$$

Next, we give the estimate for $T^{(1)}_3$. We divide $T^{(1)}_3$ into two parts, as follows:

$$T^{(1)}_3 = T^{(1)}_{31} + T^{(1)}_{32},$$

where

$$T^{(1)}_{31} = \sum_{l \in \mathbb{Z}\setminus\{0\}} |lN|^{2(s-1)} \left(\frac{\epsilon\rho_1}{R_1}\right)^{2|lN|} \left|\hat{q}^{(N)}_1(0)\right|^2,$$

$$T^{(1)}_{32} = \sum_{p \in \Lambda'_N \setminus \{0\}} \left(\sum_{l \in \mathbb{Z}\setminus\{0\}} |p + lN|^{2(s-1)} \left(\frac{\epsilon\rho_1}{R_1}\right)^{2|p+lN|} \right) |\hat{q}^{(N)}_1(p)|^2.$$

First, we consider $T^{(1)}_{31}$. By Proposition 2.7.1 (iv), we have that

$$\sum_{l \in \mathbb{Z}\setminus\{0\}} |lN|^{2(s-1)} \left(\frac{\epsilon\rho_1}{R_1}\right)^{2|lN|} = \sum_{m \in I(0)} |m|^{2(s-1)} \left(\frac{\epsilon\rho_1}{R_1}\right)^{2|m|} \leq C_{(\epsilon r)^2, 2(s-1)} N^{2(s-1)} (\epsilon r)^{2N}$$

and by Proposition 2.7.1 (i) and (ii) we have that

$$\begin{aligned}
|\hat{q}_1^{(N)}(0)|^2 &\le \frac{2}{(\det \Phi^{\mathrm{C}}(0))^2}\left[\left(\sum_{m\equiv 0}\sum_{l\equiv 0}|\Upsilon_1(m,l)|\,|\hat{q}_1(m)|\right)^2+\left(\sum_{m\equiv 0}\sum_{l\equiv 0}|\Upsilon_2(m,l)|\,|\hat{q}_2(m)|\right)^2\right]\\
&\le 2C_{\rho_1,\rho_2,R_1,R_2}\left[\left(\sum_{m\equiv 0}\sum_{l\equiv 0}\frac{C_1}{\underline{m}\cdot\underline{l}}\left(\frac{\rho_1}{R_1}\right)^{|m|}\left(\frac{R_2}{\rho_2}\right)^{|l|}|\hat{q}_1(m)|\right)^2\right.\\
&\qquad\left.+\left(\sum_{m\equiv 0}\sum_{l\equiv 0}\frac{C_2}{\underline{m}\cdot\underline{l}}\left(\frac{R_2}{\rho_2}\right)^{|m|+|l|}|\hat{q}_2(m)|\right)^2\right]\\
&\le C\|q\|^2_{\mathbb{Y}_{\delta,t}}.
\end{aligned}$$

Because it holds by definition that $\epsilon \le 1/(\delta r^2)$, we obtain that

$$T_{31}^{(1)} \le \begin{cases} C_{31}^{(1)} N^{2(s-1)}\left(\dfrac{\epsilon}{\delta}\right)^N \|q\|^2_{\mathbb{Y}_{\delta,t}} & \text{if } \epsilon = 1/(\delta r^2) \text{ and } t \ge 1,\\ C_{31}^{(1)} N^{2(s-t)}\left(\dfrac{\epsilon}{\delta}\right)^N \|q\|^2_{\mathbb{Y}_{\delta,t}} & \text{otherwise.}\end{cases}$$

Concerning $T_{32}^{(1)}$, we have by virtue of Proposition 2.7.1 (iv) that

$$\begin{aligned}
\sum_{l\in\mathbb{Z}\setminus\{0\}}|p+lN|^{2(s-1)}\left(\frac{\epsilon\rho_1}{R_1}\right)^{2|p+lN|} &= \sum_{m\in I(p)}|m|^{2(s-1)}\left(\frac{\epsilon\rho_1}{R_1}\right)^{2|m|}\\
&\le C_{(\epsilon\rho_1/R_1)^2,2(s-1)}N^{2(s-1)}\left(\frac{\epsilon\rho_1}{R_1}\right)^{2(N-|p|)}
\end{aligned}$$

for all $p \in \Lambda'_N \setminus \{0\}$. Furthermore, it follows from Proposition 2.7.1 (i) and (iii) that

$$\begin{aligned}
|\hat{q}_1^{(N)}(p)|^2 &\le \frac{2}{(\det \Phi^{\mathrm{C}}(p))^2}\left[\left(\sum_{m\equiv p}\sum_{l\equiv p}|\Upsilon_1(m,l)|\,|\hat{q}_1(m)|\right)^2\right.\\
&\quad\left.+\left(\sum_{m\in I(p)}|\Upsilon_2(m,p)|\,|\hat{q}_2(m)|+\sum_{l\in I(p)}|\Upsilon_2(p,l)|\,|\hat{q}_2(p)|+\sum_{m,l\in I(p)}|\Upsilon_2(m,l)|\,|\hat{q}_2(m)|\right)^2\right]\\
&\le 2C_{\rho_1,\rho_2,R_1,R_2}|p|^4\left(\frac{R_1}{\rho_1}\right)^{2|p|}\left(\frac{\rho_2}{R_2}\right)^{2|p|}\left[\left(\sum_{m\equiv p}\sum_{l\equiv p}\frac{C_1}{\underline{m}\cdot\underline{l}}\left(\frac{\rho_1}{R_1}\right)^{2|m|}\left(\frac{R_2}{\rho_2}\right)^{|l|}|\hat{q}_1(m)|\right)^2\right.\\
&\quad+\left(\sum_{m\in I(p)}\frac{C_2}{\underline{m}\cdot\underline{p}}\left(\frac{R_2}{\rho_2}\right)^{|m|+|p|}|\hat{q}_2(m)|+\sum_{l\in I(p)}\frac{C_2}{\underline{p}\cdot\underline{l}}\left(\frac{R_2}{\rho_2}\right)^{|p|+|l|}|\hat{q}_2(p)|\right.\\
&\qquad\left.\left.+\sum_{m,l\in I(p)}\frac{C_2}{\underline{m}\cdot\underline{l}}\left(\frac{R_2}{\rho_2}\right)^{|m|+|l|}|\hat{q}_2(m)|\right)^2\right]\\
&\le C|p|^4\left(\frac{R_1}{\rho_1}\right)^{2|p|}\left(\frac{\rho_2}{R_2}\right)^{2|p|}\left[\left(\frac{R_2}{\rho_2}\right)^{2|p|}\frac{1}{|p|^{2(t+1)}}\frac{1}{\delta^{2|p|}}\sum_{m\equiv p}|\hat{q}_1(m)|^2\left(\frac{\delta\rho_1}{R_1}\right)^{2|m|}\underline{m}^{2(t-1)}\right.
\end{aligned}$$

$$
\begin{aligned}
&+\left(\frac{R_2}{\rho_2}\right)^{2|p|}\frac{1}{|p|^2}\frac{1}{N^{2t}}\frac{1}{\delta^{2(N-|p|)}}\sum_{m\in I(p)}|\hat{q}_2(m)|^2\left(\frac{\delta R_2}{\rho_2}\right)^{2|m|}\underline{m}^{2(t-1)}\\
&+\left(\frac{R_2}{\rho_2}\right)^{2|p|}\frac{1}{|p|^{2t}}\frac{1}{N^2}\frac{1}{\delta^{2|p|}}|\hat{q}_2(p)|^2\left(\frac{\delta R_2}{\rho_2}\right)^{2|p|}\underline{p}^{2(t-1)}\left(\frac{R_2}{\rho_2}\right)^{2(N-2|p|)}\\
&+\left(\frac{R_2}{\rho_2}\right)^{2(N-|p|)}\frac{1}{N^{2(t+1)}}\frac{1}{\delta^{2(N-|p|)}}\sum_{m\in I(p)}|\hat{q}_2(m)|^2\left(\frac{\delta R_2}{\rho_2}\right)^{2|m|}\underline{m}^{2(t-1)}\Bigg]\\
&\le C|p|^2\left(\frac{R_1}{\rho_1}\right)^{2|p|}\left(\frac{1}{|p|^{2t}}\frac{1}{\delta^{2|p|}}+\frac{1}{N^{2t}}\frac{1}{\delta^{2(N-|p|)}}\right)\\
&\qquad\times\left[\sum_{m\equiv p}|\hat{q}_1(m)|^2\left(\frac{\delta\rho_1}{R_1}\right)^{2|m|}\underline{m}^{2(t-1)}+\sum_{m\equiv p}|\hat{q}_2(m)|^2\left(\frac{\delta R_2}{\rho_2}\right)^{2|m|}\underline{m}^{2(t-1)}\right].
\end{aligned}
$$

Therefore, we obtain that

$$
\begin{aligned}
T_{32}^{(1)}&\le C_{32}^{(1)}N^{2(s-1)}\sum_{p\in\Lambda_N'\setminus\{0\}}\left(\frac{\epsilon\rho_1}{R_1}\right)^{2(N-|p|)}|p|^2\left(\frac{R_1}{\rho_1}\right)^{2|p|}\left(\frac{1}{|p|^{2t}}\frac{1}{\delta^{2|p|}}+\frac{1}{N^{2t}}\frac{1}{\delta^{2(N-|p|)}}\right)\\
&\qquad\times\left[\sum_{m\equiv p}|\hat{q}_1(m)|^2\left(\frac{\delta\rho_1}{R_1}\right)^{2|m|}\underline{m}^{2(t-1)}+\sum_{m\equiv p}|\hat{q}_2(m)|^2\left(\frac{\delta R_2}{\rho_2}\right)^{2|m|}\underline{m}^{2(t-1)}\right]\\
&\le CN^{2[s-1+\max\{-t+1,0\}]}\left(\frac{\epsilon}{\delta}\right)^N\|q\|^2_{\mathbb{Y}_{\delta,t}}A_{32}^{(1)},
\end{aligned}
$$

where

$$
A_{32}^{(1)}=\sup_{p\in\Lambda_N'\setminus\{0\}}\left\{\frac{N^{-2\max\{-t+1,0\}}}{|p|^{2(t-1)}}(\epsilon\delta r^2)^{N-2|p|}+|p|^2N^{-2[t+\max\{-t+1,0\}]}\left(\frac{\epsilon r^2}{\delta}\right)^{N-2|p|}\right\}.
$$

This supremum can be bounded as follows:

$$
A_{32}^{(1)}\le\begin{cases}C'N^{2(-t+1)} & \text{if } \epsilon=1/(\delta r^2) \text{ and } t\ge 1,\\ C' & \text{otherwise.}\end{cases}
$$

Then, we obtain the following estimate for $T_{32}^{(1)}$:

$$
T_{32}^{(1)}\le\begin{cases}C_{32}^{(1)}N^{2(s-1)}\left(\frac{\epsilon}{\delta}\right)^N\|q\|^2_{\mathbb{Y}_{\delta,t}} & \text{if } \epsilon=1/(\delta r^2) \text{ and } t\ge 1,\\ C_{32}^{(1)}N^{2(s-t)}\left(\frac{\epsilon}{\delta}\right)^N\|q\|^2_{\mathbb{Y}_{\delta,t}} & \text{otherwise.}\end{cases}
$$

Summarizing the above, we have that

$$
T_3^{(1)}\le\begin{cases}C_3^{(1)}N^{2(s-1)}\left(\frac{\epsilon}{\delta}\right)^N\|q\|^2_{\mathbb{Y}_{\delta,t}} & \text{if } (\delta,\epsilon)\in H_2 \text{ and } t\ge 1,\\ C_3^{(1)}N^{2(s-t)}\left(\frac{\epsilon}{\delta}\right)^N\|q\|^2_{\mathbb{Y}_{\delta,t}} & \text{otherwise.}\end{cases}
$$

Finally, we will establish the estimate for $T_4^{(1)}$, which can be obtained by straightforward arguments

as follows:

$$\begin{aligned}
T_4^{(1)} &= \sum_{n\in\mathbb{Z}\setminus\Lambda_N'} |\hat{q}_1(n)|^2 \left(\frac{\delta\rho_1}{R_1}\right)^{2|n|} \underline{n}^{2(t-1)} \cdot \frac{|n|^{2(s-1)}}{\underline{n}^{2(t-1)}} \left(\frac{\epsilon}{\delta}\right)^{2|n|} \\
&\le C_4^{(1)} N^{2(s-t)} \left(\frac{\epsilon}{\delta}\right)^N \|q\|^2_{\delta\rho_1/R_1,t-1} \sup_{n\in\mathbb{Z}\setminus\Lambda_N'} \left\{ \left(\frac{N}{|n|}\right)^{-2(s-t)} \left(\frac{\epsilon}{\delta}\right)^{2|n|-N} \right\} \\
&\le C_4^{(1)} N^{2(s-t)} \left(\frac{\epsilon}{\delta}\right)^N \|q_1\|^2_{\delta\rho_1/R_1,t-1}.
\end{aligned}$$

Hence, we obtain the following estimate for $\|q_1 - q_1^{(N)}\|^2_{\epsilon\rho_1/R_1,s-1}$:

$$\begin{aligned}
\|q_1 - q_1^{(N)}\|^2_{\epsilon\rho_1/R_1,s-1} &\le T_1^{(1)} + (2\pi)^{2(s-1)}(T_2^{(1)} + 2T_3^{(1)} + 2T_4^{(1)}) \\
&\le \begin{cases}
C_1^{(1)} N^{2\max\{s-t,-1,-t\}} \left(\frac{\epsilon}{\delta}\right)^N \|q\|^2_{\mathbb{Y}_{\delta,t}} & \text{if } (\delta,\epsilon) = C_1, \\
C_1^{(1)} N^{2\max\{s-t,-1,s-1\}} \left(\frac{\epsilon}{\delta}\right)^N \|q\|^2_{\mathbb{Y}_{\delta,t}} & \text{if } (\delta,\epsilon) = C_2, \\
C_1^{(1)} N^{2\max\{s-t,-t\}} \left(\frac{\epsilon}{\delta}\right)^N \|q\|^2_{\mathbb{Y}_{\delta,t}} & \text{if } (\delta,\epsilon) \in H_1 \setminus \{C_1\}, \\
C_1^{(1)} N^{2\max\{s-t,s-1\}} \left(\frac{\epsilon}{\delta}\right)^N \|q\|^2_{\mathbb{Y}_{\delta,t}} & \text{if } (\delta,\epsilon) \in H_2 \setminus \{C_2\}, \\
C_1^{(1)} N^{2\max\{s-t,-1\}} \left(\frac{\epsilon}{\delta}\right)^N \|q\|^2_{\mathbb{Y}_{\delta,t}} & \text{if } (\delta,\epsilon) \in L_1 \setminus \{C_1, C_2\}, \\
C_1^{(1)} N^{2(s-t)} \left(\frac{\epsilon}{\delta}\right)^N \|q\|^2_{\mathbb{Y}_{\delta,t}} & \text{otherwise.}
\end{cases}
\end{aligned}$$

2.8 Proof of Lemma 2.3.13

We require one additional proposition as to the upper bound for $(\det \Phi^{\mathrm{I}}(0))^{-2}$, which will be used without proof.

Proposition 2.8.1. *There exists some positive constant $C_{\rho_1,\,\rho_2,\,R_1,\,R_2}$ such that*

$$\frac{1}{(\det \Phi^{\mathrm{I}}(0))^2} \le C_{\rho_1,\,\rho_2,\,R_1,\,R_2}$$

holds for all $N \in \mathbb{N}$.

We can represent $\hat{q}_1^{(N)}(0)$ explicitly from (2.3.9), which yields that

$$\hat{q}_1(0) - \hat{q}_1^{(N)}(0) = \frac{1}{\det \Phi^{\mathrm{I}}(0)} \left[B_1\hat{q}_1(0) - B_1\hat{q}_2(0) + \sum_{l\in I(0)} (B_3(l)\hat{q}_1(l) + B_4(l)\hat{q}_2(l)) \right],$$

where

$$\begin{aligned}
B_1 &= \frac{1}{2} \sum_{m\in I(0)} (-\hat{G}_{11}(m) + \hat{G}_{12}(m) + \hat{G}_{21}(m) - \hat{G}_{22}(m) \\
&\qquad\qquad - \Upsilon_1(m,0) + \Upsilon_2(m,0) - \Upsilon_3(m,0) + \Upsilon_4(m,0)), \\
B_3(l) &= \hat{G}_{11}(l) - \hat{G}_{21}(l) + \Upsilon_4(0,l) - \Upsilon_3(0,l) - \sum_{m\in I(0)} (\Upsilon_3(m,l) - \Upsilon_4(m,l)),
\end{aligned}$$

$$B_4(l) = \hat{G}_{12}(l) - \hat{G}_{22}(l) - \Upsilon_2(0,l) + \Upsilon_1(0,l) - \sum_{m\in I(0)} (-\Upsilon_1(m,l) + \Upsilon_2(m,l)).$$

Each term can be evaluated as follows, by Proposition 2.7.1 (i) and (iv):

$$|B_1\hat{q}_1(0)|^2 \le C_{11}^{(1)} N^{-2} r^{2N} \|q_1\|^2_{\delta\rho_1/R_1,t-1}, \quad |B_1\hat{q}_2(0)|^2 \le C_{12}^{(1)} N^{-2} r^{2N} \|q_2\|^2_{\delta R_2/\rho_2,t-1},$$

$$\left|\sum_{l\in I(0)} B_3(l)\hat{q}_1(l)\right|^2 \le C_{13}^{(1)} \sum_{l\in I(0)} \frac{1}{\delta^{2|l|}} \frac{1}{\underline{l}^{2t}} \sum_{l\in I(0)} |\hat{q}_1(l)|^2 \left(\frac{\delta\rho_1}{R_1}\right)^{2|l|} \underline{l}^{2t} \le C_{13}^{(1)} N^{-2t}\delta^{-2N} \|q_1\|^2_{\delta\rho_1/R_1,t-1},$$

$$\left|\sum_{l\in I(0)} B_4(l)\hat{q}_2(l)\right|^2 \le C_{14}^{(1)} \sum_{l\in I(0)} \frac{1}{\delta^{2|l|}} \frac{1}{\underline{l}^{2t}} \sum_{l\in I(0)} |\hat{q}_2(l)|^2 \left(\frac{\delta R_2}{\rho_2}\right)^{2|l|} \underline{l}^{2t} \le C_{14}^{(1)} N^{-2t}\delta^{-2N} \|q_2\|^2_{\delta R_2/\rho_2,t-1}.$$

Therefore, using Proposition 2.8.1 (i), we obtain that

$$T_1^{(1)} \le \begin{cases} C_1^{(1)} N^{-2} \left(\frac{\epsilon}{\delta}\right)^N \|q_1\|^2_{\delta\rho_1/R_1,t-1} & \text{if } (\delta,\epsilon) \in L_1 \setminus \{C_1\} \text{ and } s-t \le -1, \\ C_1^{(1)} N^{-2t} \left(\frac{\epsilon}{\delta}\right)^N \|q_2\|^2_{\delta R_2/\rho_2,t-1} & \text{if } (\delta,\epsilon) \in H_1 \setminus \{C_1\} \text{ and } s \le 0, \\ C_1^{(1)} N^{2\max\{s-t,-1,-t\}} \left(\frac{\epsilon}{\delta}\right)^N \|q\|^2_{\mathbb{Y}_{\delta,t}} & \text{if } (\delta,\epsilon) = C_1, \\ C_1^{(1)} N^{2(s-t)} \left(\frac{\epsilon}{\delta}\right)^N \|q\|^2_{\mathbb{Y}_{\delta,t}} & \text{otherwise.} \end{cases}$$

Because $\hat{q}_1^{(N)}(n)$ ($n \in \Lambda'_N \setminus \{0\}$) are the same as for C-MFS, we immediately obtain the estimate

$$T_2^{(1)} \le \begin{cases} C_2^{(1)} N^{-2} \left(\frac{\epsilon}{\delta}\right)^N \|q\|^2_{\mathbb{Y}_{\delta,t}} & \text{if } (\delta,\epsilon) \in L_1 \setminus \{C_1\} \text{ and } s-t \le -1, \\ C_2^{(1)} N^{-2t} \left(\frac{\epsilon}{\delta}\right)^N \|q\|^2_{\mathbb{Y}_{\delta,t}} & \text{if } (\delta,\epsilon) \in H_1 \setminus \{C_1\} \text{ and } s \le 0, \\ C_2^{(1)} N^{2\max\{s-t,-1,-t\}} \left(\frac{\epsilon}{\delta}\right)^N \|q\|^2_{\mathbb{Y}_{\delta,t}} & \text{if } (\delta,\epsilon) = C_1, \\ C_2^{(1)} N^{2(s-t)} \left(\frac{\epsilon}{\delta}\right)^N \|q\|^2_{\mathbb{Y}_{\delta,t}} & \text{otherwise.} \end{cases}$$

Now we consider $T_3^{(1)}$, which we decompose as follows:

$$T_3^{(1)} = T_{31}^{(1)} + T_{32}^{(1)},$$

where

$$T_{31}^{(1)} = \sum_{l\in\mathbb{Z}\setminus\{0\}} |lN|^{2(s-1)} \left(\frac{\epsilon\rho_1}{R_1}\right)^{2|lN|} |\hat{q}_1^{(N)}(N)|^2,$$

$$T_{32}^{(2)} = \sum_{p\in\Lambda'_N\setminus\{0\}} \left(\sum_{l\in\mathbb{Z}\setminus\{0\}} |p+lN|^{2(s-t)} \left(\frac{\epsilon\rho_1}{R_1}\right)^{2|p+lN|} \right) |\hat{q}_1^{(N)}(p)|^2.$$

The definition of $T_{31}^{(1)}$ is slightly different from that for C-MFS, while that of $T_{32}^{(1)}$ is the same as for C-MFS. Therefore, we only have to consider the estimate of $T_{31}^{(1)}$. From (2.3.9), we have that

$$\hat{q}_1^{(N)}(N) = \frac{1}{\det \Phi^{\mathrm{I}}(0)} \left[\frac{1}{2}(\hat{G}_{12}(0) - \hat{G}_{22}(0))\hat{q}_1(0) + \frac{1}{2}(\hat{G}_{22}(0) - \hat{G}_{12}(0))\hat{q}_2(0) \right.$$
$$\left. + \sum_{l \in I(0)} \Big((\hat{G}_{21}(l) - \hat{G}_{11}(l))\hat{q}_1(l) + (\hat{G}_{22}(l) - \hat{G}_{12}(l))\hat{q}_2(l) \Big) \right],$$

from which we can easily obtain by Proposition 2.7.1 (ii) and Proposition 2.8.1 that

$$|\hat{q}_1^{(N)}(N)|^2 \le C \|q\|^2_{\mathbb{Y}_{\delta,t}}.$$

By using the results in Section 2.7, we have that

$$T_3^{(1)} \le \begin{cases} C_3^{(1)} N^{2(s-1)} \left(\frac{\epsilon}{\delta}\right)^N \|q\|^2_{\mathbb{Y}_{\delta,t}} & \text{if } \epsilon = 1/(\delta r^2) \text{ and } t \ge 1, \\ C_3^{(1)} N^{2(s-t)} \left(\frac{\epsilon}{\delta}\right)^N \|q\|^2_{\mathbb{Y}_{\delta,t}} & \text{otherwise.} \end{cases}$$

The estimate of $T_4^{(1)}$ is the same as for C-MFS. That is,

$$T_4^{(1)} \le C_4^{(1)} N^{2(s-t)} \left(\frac{\epsilon}{\delta}\right)^N \|q_1\|^2_{\delta\rho_1/R_1,t-1}.$$

Summarizing the above, we obtain the following estimate for $\|q_1 - q_1^{(N)}\|^2_{\epsilon\rho_1/R_1,s-1}$:

$$\|q_1 - q_1^{(N)}\|^2_{\epsilon\rho_1/R_1,s-1} \le \begin{cases} C_1^{(1)} N^{2\max\{s-t,-1,-t\}} \left(\frac{\epsilon}{\delta}\right)^N \|q\|^2_{\mathbb{Y}_{\delta,t}} & \text{if } (\delta,\epsilon) = C_1, \\ C_1^{(1)} N^{2\max\{s-t,-1,s-1\}} \left(\frac{\epsilon}{\delta}\right)^N \|q\|^2_{\mathbb{Y}_{\delta,t}} & \text{if } (\delta,\epsilon) = C_2, \\ C_1^{(1)} N^{2\max\{s-t,-t\}} \left(\frac{\epsilon}{\delta}\right)^N \|q\|^2_{\mathbb{Y}_{\delta,t}} & \text{if } (\delta,\epsilon) \in H_1 \setminus \{C_1\}, \\ C_1^{(1)} N^{2\max\{s-t,s-1\}} \left(\frac{\epsilon}{\delta}\right)^N \|q\|^2_{\mathbb{Y}_{\delta,t}} & \text{if } (\delta,\epsilon) \in H_2 \setminus \{C_2\}, \\ C_1^{(1)} N^{2\max\{s-t,-1\}} \left(\frac{\epsilon}{\delta}\right)^N \|q\|^2_{\mathbb{Y}_{\delta,t}} & \text{if } (\delta,\epsilon) \in L_1 \setminus \{C_1, C_2\}, \\ C_1^{(1)} N^{2(s-t)} \left(\frac{\epsilon}{\delta}\right)^N \|q\|^2_{\mathbb{Y}_{\delta,t}} & \text{otherwise.} \end{cases}$$

Then $\|q_2 - q_2^{(N)}\|^2_{\epsilon R_2/\rho_2,s-1}$ can be estimated in a similar manner, and we obtain the desired estimate.

Chapter 3

Analysis of the dipole simulation method for two-dimensional Dirichlet problems in Jordan regions with analytic boundaries

Abstract

This chapter presents a unique solvability and error estimate of the dipole simulation method applied to Dirichlet problems in Jordan regions. Specifically, it is proved that the error decays exponentially when the boundary data is analytic, and it decays algebraically when the boundary data is not analytic but belongs to some Sobolev space. Moreover, some numerical results and conjectures are presented. This chapter is based on the following published paper:

- K. Sakakibara, *Analysis of the dipole simulation method for two-dimensional Dirichlet problems in Jordan regions with analytic boundaries*, BIT Numer. Math. **56** (2016), no. 4, 1369–1400.

3.1 Introduction and main results

Let Ω be a Jordan region in the two-dimensional Euclidean space $\mathbb{R}^2$. Consider the following Dirichlet problem for the Laplace equation:

$$\begin{cases} \triangle u = 0 & \text{in } \Omega, \\ u = f & \text{on } \Gamma, \end{cases} \tag{3.1.1}$$

where Γ denotes the boundary $\partial\Omega$ of Ω, and $\triangle$ the Laplace operator. Throughout this chapter, suppose that Γ is regular analytic and f satisfies the following regularity condition:

$$f \text{ is analytic or belongs to } H^{\sigma}(\Gamma) \text{ for some } \sigma > 1/2, \tag{3.1.2}$$

and we identify $\mathbb{R}^2$ with the complex plane $\mathbb{C}$.

As is well known, the Dirichlet problem (3.1.1) appears in many fields in mathematical physics and engineering. Therefore numerous numerical methods have been developed and studied for (3.1.1) such

as the boundary integral method (BIM) [104, 75, 30], multipole method (MM) [9, 29, 23], method of fundamental solutions (MFS) [49, 43, 27], and singular boundary method (SBM) [15, 24, 51]. A remarkable feature of them is that the error decays exponentially with respect to the number of degrees of freedom used under some suitable conditions. In the following, we focus on MFS and BIM especially.

MFS is applied to homogeneous linear partial differential equations (PDEs), and offers an approximate solution by using a linear combination of the fundamental solutions of the considered problem. Especially, an approximate solution for the potential problem (3.1.1) could be found by using a linear combination of logarithmic potentials in which case the MFS would also be known as the charge simulation method (CSM). The MFS requires us to choose singular points exterior to the region under consideration and collocation points on the boundary of this region, to enable us to determine the coefficients of the approximate solution by using an approach that would provide approximate boundary conditions, for instance, collocation or least-squares methods. This approach would allow us to avoid having to address problems caused by the existence of singularities and would also obviate the need for numerical integrations, as opposed to using BIM. This enables us to apply the MFS to various PDEs, with the advantage that the implementation of the MFS and its extension to 3D problems are much easier compared to the use of BIM. However, in general, because MFS reduces an ill-conditioned linear system, the system is hard to solve (cf. Kitagawa [57, 58], Tsai et al. [100], and Barnett and Betcke [10]). On the other hand, when using BIM, the resulting system is usually well-conditioned; thus, in this respect BIM has many advantages over MFS. Nonetheless, in view of the simplicity and extendability of MFS, we adopt MFS in this paper and provide a mathematical analysis.

On account of its simplicity, MFS has been used to solve various problems. However, obtaining a mathematical result is rather difficult, especially in terms of ensuring unique existence and convergence of approximate solution. Restricting ourselves to the potential problem, the CSM was first mathematically analyzed by Katsurada and Okamoto [49]. They considered (3.1.1) for the case where Ω is a disk D_ρ with radius ρ having the origin as its center, and showed its unique solvability (cf. [49, Theorem 1]) and exponential convergence (cf. [49, Theorem 2]). Unlike the finite difference or finite element methods, the unique existence of approximate solution is not as obvious. In fact, when we select the singular points in a slightly different manner, an approximate solution cannot exist (cf. [45, Theorem 8.2]). After this pioneering work, the unique solvability and exponential convergence of CSM were well established for a Jordan region with an analytic boundary [46, 47, 50, 48], an annular region [45, 74], and an elliptic region [76]. Furthermore, CSM was also applied to compute numerical conformal mappings in various regions, and offers a high-precision and simple numerical scheme (cf. Amano et.al [3] and references therein). Besides the above result, several mathematical and numerical results have been established. See for instance [13, 43, 20, 95, 100, 10, 107, 38, 102, 44, 108] and references therein.

Note that an approximate solution of CSM can be regarded as a discretization of the single-layer potential representation of the exact solution. On the other hand, in the usual potential theory, the exact solution for the potential problem is represented by the double-layer potential. Therefore, it is natural to consider that the logarithmic potential, which is the basis function of CSM, should be replaced with the dipole potential. Based on this consideration, Katsurada [45] concentrated on the case of disk $\Omega = D_\rho$ and proposed the dipole simulation method (DSM), in which the basis function E is given as follows:

$$E(\boldsymbol{x}, \boldsymbol{y}) = -\frac{1}{2\pi} \frac{(\boldsymbol{n_y} \mid \boldsymbol{x} - \boldsymbol{y})}{\|\boldsymbol{x} - \boldsymbol{y}\|^2},$$

where $\boldsymbol{n_y} = \boldsymbol{y}/\|\boldsymbol{y}\|$, and $(\cdot \mid \cdot)$ denotes the Euclidean inner product on $\mathbb{R}^2$. It has been shown that there exists an approximate solution for DSM uniquely (cf. [45, Theorem 5.1]) and that exponential convergence occurs (cf. comments before [45, Theorem 5.2]). Note that the multiple multipole method was developed by Ballisti and Hafner [9], and has been commonly used in the field of engineering (see for instance Hafner [29]). Therefore, the idea of using DSM also seems natural from the viewpoint of

engineering. Recently, Ogata [77] generalized Katsurada's DSM and examined its effectiveness through numerical experiments. Thus, he treated (3.1.1) in the case where Ω is a Jordan region in $\mathbb{R}^2$ and considered an approximate solution of the form

$$u^{(N)}(\boldsymbol{x}) = \sum_{k=1}^{N} Q_k D(\boldsymbol{x}, \boldsymbol{y}_k; \boldsymbol{n}_k), \tag{3.1.3}$$

where $\{\boldsymbol{y}_k\}_{k=1}^N \subset \mathbb{R}^2 \setminus \overline{\Omega}$ are the dipole points, $\{\boldsymbol{n}_k\}_{k=1}^N$ are the unit vectors, which are known as dipole moments, and $\boldsymbol{n}_k$ represents the direction of the dipole located at $\boldsymbol{y}_k$, and D is defined as

$$D(\boldsymbol{x}, \boldsymbol{y}_k; \boldsymbol{n}_k) = -\frac{1}{2\pi} \frac{(\boldsymbol{n}_k \mid \boldsymbol{x} - \boldsymbol{y}_k)}{\|\boldsymbol{x} - \boldsymbol{y}_k\|^2}.$$

The coefficients $\{Q_k\}_{k=1}^N$ are determined by the collocation method, that is, take the collocation points $\{\boldsymbol{x}_j\}_{j=1}^N \subset \Gamma$ and impose the following boundary conditions:

$$u^{(N)}(\boldsymbol{x}_j) = f(\boldsymbol{x}_j) \quad (j = 1, 2, \ldots, N). \tag{3.1.4}$$

In fact, the approximate solution of DSM can be represented as the real part of a holomorphic function:

$$u^{(N)}(\boldsymbol{x}) = u^{(N)}(z) = \Re\left[-\frac{1}{2\pi} \sum_{k=1}^{N} Q_k \frac{n_k}{z - \zeta_k}\right],$$

where $z = x + \mathrm{i}y$, $\zeta_k = \xi_k + \mathrm{i}\eta_k$, and $n_k = n_k^{(1)} + \mathrm{i}n_k^{(2)}$ in which $\boldsymbol{x} = (x, y)^{\mathrm{T}}$, $\boldsymbol{y}_k = (\xi_k, \eta_k)^{\mathrm{T}}$, and $\boldsymbol{n}_k = (n_k^{(1)}, n_k^{(2)})^{\mathrm{T}}$. Inspired by the above expression, the complex dipole simulation method, which is an approximation technique for holomorphic functions, was proposed in our previous paper [87] (see also Chapter 8 in this thesis).

Moreover, in [77], Ogata applied DSM to compute numerical conformal mappings, which permits us to remove the difficulty of computing complex arguments; therefore, his method offers a much easier and simpler scheme for numerical conformal mappings than that obtained by CSM (see also Chapter 7 in this thesis). However, this work of his did not include a mathematical result.

The purpose of this chapter is to suggest ways in which to arrange the dipole points $\{\boldsymbol{y}_k\}_{k=1}^N$ and collocation points $\{\boldsymbol{x}_j\}_{j=1}^N$, and to define the dipole moments $\{\boldsymbol{n}_k\}_{k=1}^N$ that guarantee the unique solvability and exponential convergence of DSM composed of (3.1.3) and (3.1.4). As a preliminary step to this end, we first consider the case where Γ is a circle $\gamma_\rho = \{z \in \mathbb{C} \mid |z| = \rho\}$ with $\rho > 0$. Introducing the dipole points, collocation points, and dipole moments as $y_k = R\omega^{k-1}$, $x_j = \rho\omega^{j-1}$, and $n_k = y_k/|y_k|$, respectively, we establish the unique solvability (cf. Theorem 3.3.3) and exponential convergence (cf. Theorem 3.3.4), where $\omega = \exp(2\pi\mathrm{i}/N)$ and $R > \rho$. We then extend the results to more general regions by following the approach of Katsurada [48].

Let Ψ be a peripheral conformal mapping of Γ with a reference radius ρ. Then, the regularity condition (3.1.2) on f is equivalent to $F \in \mathscr{X}_{\xi,\sigma}$ for some $(\xi, \sigma) > (1, 1/2)$, where F is defined as $F(\tau) = f(\Psi(\rho \mathrm{e}^{2\pi\mathrm{i}\tau}))$ $(\tau \in S^1)$. Letting $R \in]\rho, \kappa\rho[$, we propose an arrangement of the dipole and collocation points and a definition of the dipole moments as

$$y_j = \Psi(R\omega^{j-1}), \quad x_j = \Psi(\rho\omega^{j-1}), \quad n_j = \frac{\omega^{j-1}\Psi'(R\omega^{j-1})}{|\Psi'(R\omega^{j-1})|} \quad (j = 1, 2, \ldots, N). \tag{3.1.5}$$

We are now in a position to state the main result of this chapter, where the unique solvability and exponential convergence of DSM under the arrangement and definition (3.1.5) are established by applying the results for a circle.

Theorem 3.1.1. *Assume that there exists a peripheral conformal mapping Ψ of Γ with reference radius ρ. Let $R \in]\rho, \kappa\rho[$ and suppose that $F \in \mathscr{X}_{\xi,\sigma}$ for some $(\xi,\sigma) > (1,1/2)$, (δ,t) satisfies*

$$1 \le \delta \le \min\left\{\mu, \left(\frac{R}{\rho}\right)^2, \kappa\right\},$$

$$\text{if } \delta = 1 \text{ then } t > \frac{1}{2} \text{ and } s < t; \quad \text{if } \delta = \kappa \text{ then } t < -\frac{1}{2}; \qquad \text{if } \delta = \xi \text{ then } t \le \sigma,$$

and that the dipole, collocation points, and dipole moments are deifned as (3.1.5)*, where $F(\tau) = f(\Psi(\rho e^{2\pi i\tau}))$ for $\tau \in S^1$.*

(i) *For a sufficiently large $N \in \mathbb{N}$, there exists a unique $\{Q_k\}_{k=1}^N$ satisfying* (3.1.3) *and* (3.1.4)*. Thus, an approximate solution of DSM actually exists uniquely.*

(ii) *There exists a constant C such that the error estimate*

$$\|u - u^{(N)}\|_{H^s(\Gamma)} \le C N^{\tilde{P}(s,\delta,t)} \frac{1}{\delta^{N/2}} \|F\|_{\delta,t}$$

holds true for a sufficiently large $N \in \mathbb{N}$, where C is independent of N, and

$$\tilde{P}(s,\delta,t) = \begin{cases} \max\{s-t, 0, s\} & \text{if } \delta = (R/\rho)^2 \wedge (\sqrt{\kappa}\rho, s) \ge (R, 1/2), \\ \max\{s-t, -t\} & \text{if } \delta = 1 \wedge (\sqrt{\kappa}\rho, s) \ge (R, 1/2), \\ s-t & \text{if } \delta \in]1, (R/\rho)^2[\wedge (\sqrt{\kappa}\rho, s) \ge (R, 1/2), \\ \max\{1/2 - t, 1/2\} & \text{if } \delta = (R/\rho)^2 \wedge R = \sqrt{\kappa}\rho \wedge s < 1/2, \\ 1/2 - t & \text{if } \delta \in [1, (R/\rho)^2[\wedge R = \sqrt{\kappa}\rho \wedge s < 1/2. \end{cases}$$

This error estimate shows that the error of the approximate solution $u_{\mathrm{D}}^{(N)}$ decays exponentially with respect to N when the boundary data f is analytic, but it decays algebraically with respect to N when f is not analytic but in $H^\sigma(\Gamma)$ with $\sigma > 1/2$ (especially, f is Hölder continuous).

In Theorem 3.1.1 and in the following, (ξ,σ) denotes the regularity of the datum f, ρ the reference radius of the peripheral conformal mapping Ψ of Γ, κ the parameter for Ψ appearing in Definition 1.2.1, s the index of the Hilbert space H^s in which the norm of the error is measured, (δ,t) the index of the Hilbert space $\mathscr{X}_{\delta,t}$ in which the norm of the boundary datum is measured, and R the parameter concerning the locations of the dipole points. This theorem is a readily obtainable corollary of Theorem 3.4.4 below. Indeed, putting $\epsilon = 1$ in Theorem 3.4.4 and considering the conditions for R and (δ,t), we reach Theorem 3.1.1. Therefore, hereafter we aim to prove Theorem 3.4.4 instead of Theorem 3.1.1 itself. From the viewpoint of real computations, it is important to measure the error by using L^∞ norm. If $v \in H^s(\Gamma)$ with $s > 1/2$, then $v \in C(\Gamma)$ (see the comments after Proposition 1.1.1) and there exists some positive constant C such that $\|v\|_\infty \le C\|v\|_{H^s(\Gamma)}$. Therefore, we immediately obtain the following corollary from Theorem 3.1.1.

Corollary 3.1.2. *Under the hypothesis in Theorem 3.1.1, we have the following error estimate:*

$$\|u - u^{(N)}\|_{L^\infty(\Gamma)} \le C N^{\tilde{P}(s,\delta,t)} \frac{1}{\delta^{N/2}} \|F\|_{\delta,t}$$

for any $s > 1/2$, where C is a constant independent of N.

The contents of this paper are as follows. In Section 3.2, we introduce integral operators and approximate function spaces which are used in the analysis below. Section 3.3 is devoted to the

case where Γ is a circle for which we prove the unique solvability (cf. Theorem 3.3.3) and exponential convergence (cf. Theorem 3.3.4). The general case is studied in Section 3.4, where the proof of Theorem 3.4.4 is described. In Section 3.5, results of several numerical experiments are shown. We conclude this paper with a summary of the results, and some concluding remarks and conjectures in Section 3.6.

3.2 Integral operator and approximate function space

3.2.1 Integral operator

Specify $R \in]\rho, \kappa\rho[$ and suppose that there exists some function Q defined on $\Gamma_R = \Psi(\gamma_R)$ such that the boundary data f of (3.1.1) can be written as a double-layer potential:

$$f(\boldsymbol{x}) = \int_{\Gamma_R} \frac{-1}{2\pi} \frac{(\boldsymbol{n_y} \mid \boldsymbol{x}-\boldsymbol{y})}{\|\boldsymbol{x}-\boldsymbol{y}\|^2} Q(\boldsymbol{y})\, \mathrm{d}s_{\boldsymbol{y}}, \quad \boldsymbol{x} \in \Gamma, \tag{3.2.1}$$

where $\boldsymbol{n_y}$ denotes the unit outward normal vector of Γ_R at $\boldsymbol{y} \in \Gamma_R$ and $\mathrm{d}s_y$ the line element of Γ_R. Then, the exact solution u of (3.1.1) is as follows:

$$u(\boldsymbol{x}) = \int_{\Gamma_R} \frac{-1}{2\pi} \frac{(\boldsymbol{n_y} \mid \boldsymbol{x}-\boldsymbol{y})}{\|\boldsymbol{x}-\boldsymbol{y}\|^2} Q(\boldsymbol{y})\, \mathrm{d}s_{\boldsymbol{y}}, \quad \boldsymbol{x} \in \Omega.$$

At this moment, our problem is reduced to finding an approximation of Q. If f is not sufficiently smooth then it cannot be written as in (3.2.1); thus, f must be taken in one of the Hilbert spaces $\mathscr{X}_{\epsilon,s}$ described in Section 1.1.

We introduce an integral operator by providing S^1-parameterizations of Γ, Γ_R, and Q as follows:

$$\begin{aligned}
&\Gamma\colon S^1 \ni \tau \longmapsto \Psi(\rho \mathrm{e}^{2\pi \mathrm{i}\tau}) \in \mathbb{C},\\
&\Gamma_R\colon S^1 \ni \theta \longmapsto \Psi(R \mathrm{e}^{2\pi \mathrm{i}\theta}) \in \mathbb{C},\\
&q(\theta) := Q(\Psi(R\mathrm{e}^{2\pi\mathrm{i}\theta})), \quad \theta \in S^1.
\end{aligned}$$

Then, we can represent (3.2.1) as

$$\begin{aligned}
F(\tau) &= \int_0^1 \frac{-1}{2\pi} \Re \left\{ \frac{-\mathrm{i}\cdot 2\pi \mathrm{i} R \mathrm{e}^{2\pi\mathrm{i}\theta} \Psi'(R\mathrm{e}^{2\pi\mathrm{i}\theta})}{|2\pi\mathrm{i} R \mathrm{e}^{2\pi\mathrm{i}\theta} \Psi'(R\mathrm{e}^{2\pi\mathrm{i}\theta})|} \cdot \frac{1}{\Psi(\rho\mathrm{e}^{2\pi\mathrm{i}\tau}) - \Psi(R\mathrm{e}^{2\pi\mathrm{i}\theta})} \right\} \\
&\qquad \times Q(\Psi(R\mathrm{e}^{2\pi\mathrm{i}\theta}))|2\pi\mathrm{i}R\Psi'(R\mathrm{e}^{2\pi\mathrm{i}\theta})|\, \mathrm{d}\theta \\
&= \int_0^1 \Re \left(\frac{-R\mathrm{e}^{2\pi\mathrm{i}\theta}\Psi'(R\mathrm{e}^{2\pi\mathrm{i}\theta})}{\Psi(\rho\mathrm{e}^{2\pi\mathrm{i}\tau}) - \Psi(R\mathrm{e}^{2\pi\mathrm{i}\theta})} \right) q(\theta)\, \mathrm{d}\theta, \quad \tau \in S^1.
\end{aligned}$$

Thus if we define an integral operator A as

$$\begin{aligned}
A\varphi(\tau) &= \int_0^1 a(\tau,\theta)\varphi(\theta)\, \mathrm{d}\theta \quad (\tau \in S^1), \\
a(\tau,\theta) &= \Re \left(\frac{-R\mathrm{e}^{2\pi\mathrm{i}\theta}\Psi'(R\mathrm{e}^{2\pi\mathrm{i}\theta})}{\Psi(\rho\mathrm{e}^{2\pi\mathrm{i}\tau}) - \Psi(R\mathrm{e}^{2\pi\mathrm{i}\theta})} \right) \quad (\tau, \theta \in S^1)
\end{aligned} \tag{3.2.2}$$

for $\varphi \in C(S^1)$, then the boundary condition in (3.1.1) is equivalent to $F = Aq$. Eventually, our problem is reduced to finding an approximation of the above q.

3.2.2 Approximate function space

We introduce an approximate function space defined on S^1 for q as follows:

$$\mathscr{D}^{(N)} = \left\{ \sum_{k=1}^{N} Q_k \delta\left(\cdot - \frac{k-1}{N}\right) \;\middle|\; Q_k \in \mathbb{C}\ (k = 1, 2, \ldots, N) \right\},$$

where δ is the Dirac delta function on S^1. Concerning $\mathscr{D}^{(N)}$, the following proposition, which is described in [48, Lemma 4.3], [79, Lemma 2] for example, is well known.

Proposition 3.2.1. (i) *For all $v \in \mathscr{D}^{(N)}$, the sequence $\{\hat{v}(n)\}_{n\in\mathbb{Z}}$ is periodic with respect to n with period N, that is, $\hat{v}(n) = \hat{v}(m)$ $(n \equiv m)$.*

(ii) *If $(\epsilon, s) < (1, -1/2)$, then $\mathscr{D}^{(N)} \subset \mathscr{X}_{\epsilon,s}$.*

For any $q^{(N)} \in \mathscr{D}^{(N)}$, formal computation yields that

$$\begin{aligned} Aq^{(N)}(\tau) &= \sum_{k=1}^{N} Q_k A\delta\left(\cdot - \frac{k-1}{N}\right)(\tau) = \sum_{k=1}^{N} Q_k \Re\left(\frac{-R\mathrm{e}^{2\pi\mathrm{i}(k-1)/N}\Psi'(R\mathrm{e}^{2\pi\mathrm{i}(k-1)/N})}{\Psi(\rho\mathrm{e}^{2\pi\mathrm{i}\tau}) - \Psi(R\mathrm{e}^{2\pi\mathrm{i}(k-1)/N})}\right) \\ &= \sum_{k=1}^{N} 2\pi R|\Psi'(R\mathrm{e}^{2\pi\mathrm{i}(k-1)/N})| Q_k \frac{-1}{2\pi} \Re\left(\frac{\mathrm{e}^{2\pi\mathrm{i}(k-1)/N}\Psi'(R\mathrm{e}^{2\pi\mathrm{i}(k-1)/N})/|\Psi'(R\mathrm{e}^{2\pi\mathrm{i}(k-1)/N})|}{\Psi(\rho\mathrm{e}^{2\pi\mathrm{i}\tau}) - \Psi(R\mathrm{e}^{2\pi\mathrm{i}(k-1)/N})}\right) \\ &= \sum_{k=1}^{N} 2\pi R|\Psi'(R\omega^{k-1})| Q_k \frac{-1}{2\pi} \Re\left(\frac{n_k}{\Psi(\rho\mathrm{e}^{2\pi\mathrm{i}\tau}) - y_k}\right), \end{aligned}$$

which is nothing but an approximate solution by DSM. Therefore, it is natural to consider that the integral operator A and the approximate solution $\mathscr{D}^{(N)}$ are appropriate for the analysis of DSM.

3.3 DSM in a disk

The unique solvability and exponential convergence of DSM were studied in [45] for the case where Γ is a circle. However, the settings in this chapter differ from those of [45], which does not seem to contain the complete proof. Therefore, we state the results and proofs for DSM for the case where Γ is a circle in this section.

Let Ω be a disk with radius ρ with the origin as its center: $\Omega = D_\rho$. In this case, we can take the peripheral conformal mapping Ψ as the identity mapping, and the integral operator A is reduced to an integral operator L defined as

$$Lq(\tau) = \int_0^1 \Re\left(\frac{-R\mathrm{e}^{2\pi\mathrm{i}\theta}}{\rho\mathrm{e}^{2\pi\mathrm{i}\tau} - R\mathrm{e}^{2\pi\mathrm{i}\theta}}\right) q(\theta)\,\mathrm{d}\theta \quad (\tau \in S^1)$$

for $q \in C(S^1)$. If we define a function G as

$$G(\tau) := \Re\left(\frac{-R}{\rho\mathrm{e}^{2\pi\mathrm{i}\tau} - R}\right) \quad (\tau \in S^1),$$

then Lq can be represented as the convolution of L and q:

$$Lq = G * q. \tag{3.3.1}$$

By direct calculation, the Fourier series expansion of G is

$$G(\tau) = 1 + \frac{1}{2} \sum_{n \in \mathbb{Z} \setminus \{0\}} \left(\frac{\rho}{R}\right)^{|n|} \mathrm{e}^{2\pi i n \tau} \quad (\tau \in S^1). \tag{3.3.2}$$

Then, the nth Fourier coefficient of Lq can be calculated as

$$(Lq)^\wedge(n) = \hat{G}(n)\hat{q}(n) \quad (n \in \mathbb{Z}), \quad \hat{G}(n) = \begin{cases} 1 & (n = 0) \\ \dfrac{1}{2}\left(\dfrac{\rho}{R}\right)^{|n|} & (n \neq 0) \end{cases}$$

according to (3.3.1) and (3.3.2).

Addressing the problem under consideration on the Hilbert space $\mathscr{X}_{\epsilon,s}$ requires us to extend L to $\mathscr{X}_{\epsilon,s}$.

Lemma 3.3.1. *For each $(\epsilon, s) \in]0, +\infty[\times\mathbb{R}$, we define an operator $\mathscr{L}\colon \mathscr{X}_{\epsilon,s} \to \mathscr{X}_{\epsilon R/\rho,s}$ as $\mathscr{L}q = G*q$. Then, $\mathscr{L}$ is an extension of L to $\mathscr{X}_{\epsilon,s}$ and a homeomorphism, that is, $\mathscr{L}$ is continuous, bijective, and has a bounded inverse.*

Proof. For all $q \in \mathscr{X}_{\epsilon,s}$, we have

$$\|\mathscr{L}q\|_{\epsilon R/\rho,s}^2 = \sum_{n\in\mathbb{Z}} |(\mathscr{L}q)^\wedge(n)|^2 \left(\frac{\epsilon R}{\rho}\right)^{2|n|} \underline{n}^{2s} = |\hat{q}(0)|^2 + \frac{1}{4} \sum_{n \in \mathbb{Z}\setminus\{0\}} |\hat{q}(n)|^2 \epsilon^{2|n|} \underline{n}^{2s}.$$

Therefore, we obtain

$$\frac{1}{4}\|q\|_{\epsilon,s}^2 \leq \|\mathscr{L}q\|_{\epsilon R/\rho,s}^2 \leq \|q\|_{\epsilon,s}^2. \tag{3.3.3}$$

The linearity of $\mathscr{L}$ is clear, and its continuity follows from the right inequality of (3.3.3). The injectivity of $\mathscr{L}$ follows from the left inequality of (3.3.3). Concerning the surjectivity of $\mathscr{L}$, take $\psi \in \mathscr{X}_{\epsilon R/\rho,s}$ arbitrarily and define a function φ as

$$\varphi(\tau) = \sum_{n\in\mathbb{Z}} \hat{\varphi}(n)\mathrm{e}^{2\pi i n\tau} \quad (\tau \in S^1), \quad \hat{\varphi}(n) = \frac{1}{\hat{G}(n)}\hat{\psi}(n) \quad (n \in \mathbb{Z}).$$

Then, we have that

$$\|\varphi\|_{\epsilon,s}^2 = |\hat{\psi}(0)|^2 + 4 \sum_{n\in\mathbb{Z}\setminus\{0\}} |\hat{\psi}(n)|^2 \left(\frac{\epsilon R}{\rho}\right)^{2|n|} \underline{n}^{2s} \leq 4\|\psi\|_{\epsilon R/\rho,s}^2,$$

which implies that $\varphi \in \mathscr{X}_{\epsilon,s}$, and by definition that $\mathscr{L}\varphi = \psi$ holds. Therefore $\mathscr{L}$ is surjective. The continuity of $\mathscr{L}^{-1}$ follows from the left inequality of (3.3.3). □

Remark 3.3.2. Let X and Y be two Banach spaces, and $\mathscr{B}(X,Y)$ be the set of all bounded linear operators from X into Y. We can compute the operator norms $\|\mathscr{L}\| = \|\mathscr{L}\|_{\mathscr{B}(\mathscr{X}_{\epsilon,s},\mathscr{X}_{\epsilon R/\rho,s})}$ and $\|\mathscr{L}^{-1}\| = \|\mathscr{L}^{-1}\|_{\mathscr{B}(\mathscr{X}_{\epsilon R/\rho,s},\mathscr{X}_{\epsilon,s})}$ explicitly. From the inequalities (3.3.3), we have $\|\mathscr{L}\| \leq 1$ and $\|\mathscr{L}^{-1}\| \leq 2$. If we take $q \equiv 1$ then $\|\mathscr{L}q\|_{\epsilon R/\rho,s} = \|q\|_{\epsilon,s}$ holds, and if we take $q(\tau) = \sin(2\pi\tau)$ then $\|\mathscr{L}^{-1}q\|_{\epsilon,s} = 2\|q\|_{\epsilon R/\rho,s}$ holds. Therefore, $\|\mathscr{L}\| = 1$ and $\|\mathscr{L}^{-1}\| = 2$ follow.

Here, we can rewrite the collocation equations (3.1.4) by the extended operator $\mathscr{L}$. We take $q^{(N)} \in \mathscr{D}^{(N)}$ arbitrarily and write it as

$$q^{(N)} = \sum_{k=1}^{N} Q_k \delta\left(\cdot - \frac{k-1}{N}\right).$$

Then, we have

$$\begin{aligned}\mathscr{L}q^{(N)}(\tau) &= \sum_{k=1}^{N} Q_k \left(G * \delta\left(\cdot - \frac{k-1}{N}\right)\right)(\tau) = \sum_{k=1}^{N} Q_k \Re\left(\frac{-R}{\rho \mathrm{e}^{2\pi \mathrm{i}(\tau-(k-1)/N)} - R}\right) \\ &= \sum_{k=1}^{N} 2\pi R Q_k \frac{-1}{2\pi} \Re\left(\frac{n_k}{\rho \mathrm{e}^{2\pi \mathrm{i}\tau} - y_k}\right).\end{aligned}$$

Therefore, the unique solvability of (3.1.4) is equivalent to that of

$$\mathscr{L}q^{(N)} = F \quad \text{on } \Delta_N. \tag{3.3.4}$$

As to the unique solvability of (3.3.4), the following theorem holds, which assures the unique solvability of DSM when Ω is a disk.

Theorem 3.3.3. *Let $0 < \rho < R$ and $F \in \mathscr{X}_{\xi,\sigma}$ with some $(\xi, \sigma) > (1, 1/2)$. Then, there exists a unique $q^{(N)} \in \mathscr{D}^{(N)}$ which satisfies* (3.3.4)*, and its Fourier coefficients are given by*

$$\hat{q}^{(N)}(p) = \left(\sum_{m \equiv p} \hat{F}(m)\right) / \varphi_p^{(N)}(\rho) \quad (p \in \Lambda_N), \tag{3.3.5}$$

where

$$\varphi_p^{(N)}(\rho) = \sum_{m \equiv p} \hat{G}(m).$$

Proof. Note that $\mathscr{L}q^{(N)} \in L^1(S^1)$ and it is Hölder continuous in some neighborhood of Δ_N. By Proposition 1.5.1, (3.3.4) is equivalent to

$$\sum_{m \equiv p} \hat{G}(m)\hat{q}(m) = \sum_{m \equiv p} \hat{F}(m) \quad (\forall p \in \Lambda_N).$$

Since $q^{(N)}$ is periodic with respect to m with period N because of Proposition 3.2.1 (i), the above system is equivalent to

$$\varphi_p^{(N)}(\rho)\hat{q}^{(N)}(p) = \sum_{m \equiv p} \hat{F}(m) \quad (\forall p \in \Lambda_N). \tag{3.3.6}$$

Since $\varphi_p^{(N)}(\rho) \neq 0$ for all $p \in \mathbb{Z}$, (3.3.6) is uniquely solvable and its Fourier coefficients are given by (3.3.5). □

We next give the error estimate of DSM, which asserts the exponential convergence of DSM for analytic boundary data.

Theorem 3.3.4. *Let $0 < \rho < R$ and $F \in \mathscr{X}_{\xi,\sigma}$ with some $(\xi, \sigma) > (1, 1/2)$. Take any (δ, t) satisfying $(1, 1/2) < (\delta, t) \le (\xi, \sigma)$ and suppose that (ϵ, s) satisfies the following conditions:*

$$\max\left\{\delta\left(\frac{\rho}{R}\right)^2, \frac{1}{\delta}\right\} \le \epsilon \le \min\left\{\frac{1}{\delta}\left(\frac{R}{\rho}\right)^2, \delta\right\};$$

$$\text{if } \epsilon = \delta \text{ then } s \le t; \text{ if } \epsilon = \frac{R}{\rho} \text{ then } s < -\frac{1}{2}. \tag{3.3.7}$$

Then, there exist some positive constant $C = C(\epsilon, s, \delta, t, \rho, R)$ and real constant $P = P(\epsilon, s, \delta, t)$ such that the following error estimate holds:

$$\|F - \mathscr{L}q^{(N)}\|_{\epsilon,s} \le CN^P\left(\frac{\epsilon}{\delta}\right)^{N/2}\|F\|_{\delta,t},$$

where $q^{(N)} \in \mathscr{D}^{(N)}$ is the unique solution of $\mathscr{L}q^{(N)} = F$ on Δ_N, of which the existence is assured by Theorem 3.3.3.

Remark 3.3.5. The same as in Remark 2.3.9, we use a graph to understand the conditions on δ and ϵ in Theorem 3.3.3. We set

$$L_1 = \left\{(\delta,\epsilon) \;\middle|\; \frac{R}{\rho} \le \delta \le \left(\frac{R}{\rho}\right)^2,\ \epsilon = \delta\left(\frac{\rho}{R}\right)^2\right\}, \quad L_2 = \left\{(\delta,\epsilon) \;\middle|\; 1 \le \delta \le \frac{R}{\rho},\ \epsilon = \delta\right\},$$
$$H_1 = \left\{(\delta,\epsilon) \;\middle|\; 1 \le \delta \le \frac{R}{\rho},\ \epsilon = \frac{1}{\delta}\right\}, \quad H_2 = \left\{(\delta,\epsilon) \;\middle|\; \frac{R}{\rho} \le \delta \le \left(\frac{R}{\rho}\right)^2,\ \epsilon = \left(\frac{R}{\rho}\right)^2\frac{1}{\delta}\right\},$$
$$C_1 = \left(\frac{R}{\rho}, \frac{\rho}{R}\right), \quad C_2 = \left(\left(\frac{R}{\rho}\right)^2, 1\right),$$

$\mathcal{J}$ as a closed region surrounded by $H_1 \cup L_1 \cup H_2 \cup L_2$ and $\mathcal{I} := \mathcal{J}|_{\delta\le\xi}$. Then δ and ϵ satisfy the conditions in Theorem 3.3.4 if and only if $(\delta, \epsilon) \in \mathcal{I}$ (see Figure 3.1)

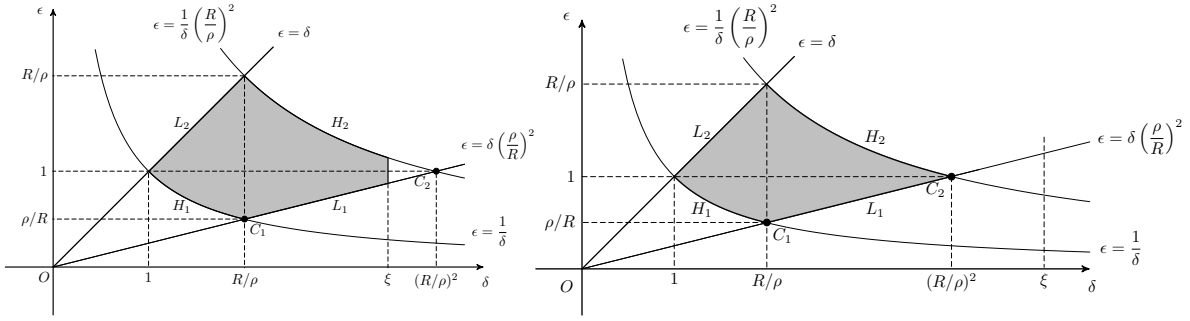

Figure 3.1: Graphic representation showing the boundaries of $\mathcal{I}$ of (δ, ϵ). **a** $\xi < (R/\rho)^2$. **b** $\xi \ge (R/\rho)^2$

Remark 3.3.6. Exponent P in Theorem 3.3.4 can be defined as follows:

$$P = P(\epsilon, s, \delta, t) = \begin{cases} \max\{s-t, 0, -t\} & ((\delta,\epsilon) = C_1), \\ \max\{s-t, 0, s\} & ((\delta,\epsilon) = C_2), \\ \max\{s-t, -t\} & ((\delta,\epsilon) \in H_1 \setminus \{C_1\}), \\ \max\{s-t, s\} & ((\delta,\epsilon) \in H_2 \setminus \{C_2\}), \\ \max\{s-t, 0\} & ((\delta,\epsilon) \in L_1 \setminus \{C_1, C_2\}), \\ s-t & (\text{otherwise}). \end{cases}$$

The appearance of explicit representation of P is similar to that for MFS (see Remark 2.3.10).

Remark 3.3.7. s and t could take any real values if (δ, ϵ) were in the interior of the region $\mathcal{I}$, whereas they would have to satisfy some constraints if they were on the boundary. Especially, if we consider the case where $\epsilon = 1$, the exponent P becomes the following:

$$P = P(s, \delta, t) = \begin{cases} \max\{s-t, 0, s\} & (\delta = (R/\rho)^2), \\ \max\{s-t, -t\} & (\delta = 1), \\ s-t & (1 < \delta < (R/\rho)^2). \end{cases}$$

If $\xi = 1$ (then $\sigma > 1/2$), that is, the boundary data f is not analytic but in $H^\sigma(\Gamma)$ (expecially Hölder continuous), in which case the exponentially decaying term $(\epsilon/\delta)^N$ is omitted, and the order of convergence becomes "algebraical".

Proving Theorem 3.3.4 requires the following lemma.

Lemma 3.3.8. *Under the same hypothesis in Theorem 3.3.4, there exists some positive constant $C = C(\epsilon, s, \delta, t, \rho, R)$ such that the following estimate holds for $q \in \mathscr{X}_{\xi\rho/R,\sigma}$ with $\mathscr{L}q = F$ and $q^{(N)} \in \mathscr{D}^{(N)}$ with $\mathscr{L}q^{(N)} = F$ on Δ_N, of which the unique existence is assured by Theorem 3.3.3:*

$$\|q - q^{(N)}\|_{\epsilon\rho/R,s} \le C N^{P(\epsilon,s,\delta,t)} \left(\frac{\epsilon}{\delta}\right)^{N/2} \|q\|_{\delta\rho/R,t}.$$

We include the proof of Lemma 3.3.8 in Section 3.7, and provide the proof of Theorem 3.3.4 by virtue of Lemma 3.3.8.

Proof of Theorem 3.3.4. Since $\mathscr{L}$ is a homeomorphism according to Lemma 3.3.1, there exists a unique $q \in \mathscr{X}_{\xi\rho/R,\sigma}$ such that $F = \mathscr{L}q$ holds. Moreover, we know that $\|\mathscr{L}\| = 1$ and $\|\mathscr{L}^{-1}\| = 2$ by Remark 3.3.2. Therefore we obtain

$$\begin{aligned} \|F - \mathscr{L}q^{(N)}\|_{\epsilon,s} = \|\mathscr{L}q - \mathscr{L}q^{(N)}\|_{\epsilon,s} &\le \|q - q^{(N)}\|_{\epsilon\rho/R,s} \le C N^{P(\epsilon,s,\delta,t)} \left(\frac{\epsilon}{\delta}\right)^{N/2} \|q\|_{\delta\rho/R,t} \\ &\le 2C N^{P(\epsilon,s,\delta,t)} \left(\frac{\epsilon}{\delta}\right)^{N/2} \|\mathscr{L}q\|_{\delta,t} = 2C N^{P(\epsilon,s,\delta,t)} \left(\frac{\epsilon}{\delta}\right)^{N/2} \|F\|_{\delta,t}, \end{aligned}$$

which is the desired estimate. □

3.4 DSM in a Jordan region

At first, we extend the integral operator A defined by (3.2.2) to $\mathscr{X}_{\epsilon,s}$. To this end, we define a perturbation operator K as

$$K = A - L.$$

If q is a continuous function on S^1, then we have

$$Kq(\tau) = \int_0^1 k(\tau,\theta)q(\theta)\,\mathrm{d}\theta,$$

where

$$k(\tau,\theta) = \Re\left(-\frac{R\mathrm{e}^{2\pi\mathrm{i}\theta}\Psi'(R\mathrm{e}^{2\pi\mathrm{i}\theta})}{\Psi(\rho\mathrm{e}^{2\pi\mathrm{i}\tau})-\Psi(R\mathrm{e}^{2\pi\mathrm{i}\theta})}+\frac{R\mathrm{e}^{2\pi\mathrm{i}\theta}}{\rho\mathrm{e}^{2\pi\mathrm{i}\tau}-R\mathrm{e}^{2\pi\mathrm{i}\theta}}\right) \quad (\tau,\theta\in S^1).$$

Thus, the lth Fourier coefficient of Kq can be calculated as

$$(Kq)^\wedge(l) = \sum_{m\in\mathbb{Z}} \hat{k}(l,m)\hat{q}(-m),$$

where $\hat{k}(l,m)$ is the double Fourier coefficient defined as

$$\hat{k}(l,m) = \int_0^1\int_0^1 k(\tau,\theta)\mathrm{e}^{-2\pi\mathrm{i}(l\tau+m\theta)}\,\mathrm{d}\tau\,\mathrm{d}\theta.$$

We require estimates on $\hat{k}(l,m)$ to extend K to $\mathscr{X}_{\epsilon,s}$.

Lemma 3.4.1. *There exists some positive constant C such that*

$$|\hat{k}(l,m)| \le C\kappa^{-|l|}\left(\frac{R}{\kappa\rho}\right)^{|m|}$$

holds for all $l,m\in\mathbb{Z}$, where κ is the parameter introduced in Definition 1.2.1.

Proof. Define a function ψ on $\overline{\mathcal{R}}_{\kappa^{-1}\rho,\kappa\rho}\times\overline{\mathcal{R}}_{\kappa^{-1}\rho,\kappa\rho}$ as

$$\psi(z,w) = \begin{cases} \dfrac{-w\Psi'(w)}{\Psi(z)-\Psi(w)}+\dfrac{w}{z-w}, & z,w\in\overline{\mathcal{R}}_{\kappa^{-1}\rho,\kappa\rho},\ z\ne w,\\ \dfrac{w\Psi''(w)}{2\Psi'(w)}, & z=w\in\overline{\mathcal{R}}_{\kappa^{-1}\rho,\kappa\rho}.\end{cases}$$

Then, ψ is holomorphic in $\mathcal{R}_{\kappa^{-1}\rho,\kappa\rho}\times\mathcal{R}_{\kappa^{-1}\rho,\kappa\rho}$ and continuous on its closure. Since $\Re\psi$ is harmonic in $\mathcal{R}_{\kappa^{-1}\rho,\kappa\rho}\times\mathcal{R}_{\kappa^{-1}\rho,\kappa\rho}$ and continuous on its closure, it has the following Fourier series expansion:

$$\begin{aligned}
&\Re\psi(\rho r_1\mathrm{e}^{2\pi\mathrm{i}\tau},\rho r_2\mathrm{e}^{2\pi\mathrm{i}\theta})\\
&\quad=\sum_{l,m\in\mathbb{Z}^*}\left(a_{lm}r_1^{|l|}r_2^{|m|}+b_{lm}r_1^{|l|}r_2^{-|m|}+c_{lm}r_1^{-|l|}r_2^{|m|}+d_{lm}r_1^{-|l|}r_2^{-|m|}\right)\mathrm{e}^{2\pi\mathrm{i}(l\tau+m\theta)}\\
&\qquad+\sum_{m\in\mathbb{Z}^*}\left(a_{0m}r_2^{|m|}+b_{0m}r_2^{-|m|}+c_{0m}r_2^{|m|}\log r_1+d_{0m}r_2^{-|m|}\log r_1\right)\mathrm{e}^{2\pi\mathrm{i}m\theta}\\
&\qquad+\sum_{l\in\mathbb{Z}^*}\left(a_{l0}r_1^{|l|}+b_{l0}r_1^{|l|}\log r_2+c_{l0}r_1^{-|l|}+d_{l0}r_1^{-|l|}\log r_2\right)\mathrm{e}^{2\pi\mathrm{i}l\tau}\\
&\qquad+a_{00}+b_{00}\log r_2+c_{00}\log r_1+d_{00}\log r_1\log r_2
\end{aligned}$$

for $r_1,r_2\in[\kappa^{-1},\kappa]$ and $\tau,\theta\in\mathbb{R}$. Then, we can evaluate the Fourier coefficients a_{lm}, b_{lm}, c_{lm}, and d_{lm} as follows:

$$|a_{lm}|,|b_{lm}|,|c_{lm}|,|d_{lm}| \le M\kappa^{-|l|-|m|} \quad (l,m\in\mathbb{Z}),$$

where M is some positive constant depending on κ and the supremum of $|\Re\psi|$ on $\partial\mathcal{R}_{\kappa^{-1}\rho,\kappa\rho}\times\partial\mathcal{R}_{\kappa^{-1}\rho,\kappa\rho}$. Since $k(\tau,\theta)=\Re\psi(\rho\mathrm{e}^{2\pi\mathrm{i}\tau},R\mathrm{e}^{2\pi\mathrm{i}\theta})$, substituting this into the definition of $\hat{k}(l,m)$ and evaluating it by using the above estimates for a_{lm}, b_{lm}, c_{lm}, and d_{lm}, we obtain the desired estimates. □

The above estimates enable us to extend K as follows:

Lemma 3.4.2. *Suppose that $(\epsilon, s) > (R/(\kappa\rho), 1/2)$ and $(\delta, t) < (\kappa, -1/2)$. If we define $\mathscr{K}\colon \mathscr{X}_{\epsilon,s} \to \mathscr{X}_{\delta,t}$ as*

$$(\mathscr{K}q)^\wedge(l) = \sum_{m\in\mathbb{Z}} \hat{k}(l,m)\hat{q}(-m), \quad l \in \mathbb{Z},$$

then $\mathscr{K}$ is a bounded linear extension of K and is compact.

Proof. For all $q \in \mathscr{X}_{\epsilon,s}$ we have

$$\begin{aligned}
\|\mathscr{K}q\|_{\delta,t}^2 &= \sum_{l\in\mathbb{Z}} |(\mathscr{K}q)^\wedge(l)|^2 \delta^{2|l|}\underline{l}^{2t} = \sum_{l\in\mathbb{Z}} \left|\sum_{m\in\mathbb{Z}} \hat{k}(l,m)\hat{q}(-m)\right|^2 \delta^{2|l|}\underline{l}^{2t} \\
&\le \sum_{l\in\mathbb{Z}} \left(\sum_{m\in\mathbb{Z}} |\hat{k}(l,m)|^2 \epsilon^{-2|m|}\underline{m}^{-2s}\right)\left(\sum_{m\in\mathbb{Z}} |\hat{q}(-m)|^2\epsilon^{2|m|}\underline{m}^{2s}\right)\delta^{2|l|}\underline{l}^{2t} \\
&\le C\sum_{l\in\mathbb{Z}} \left(\frac{\delta}{\kappa}\right)^{2|l|} \underline{l}^{2t} \sum_{m\in\mathbb{Z}} \left(\frac{1}{\epsilon}\frac{R}{\kappa\rho}\right)^{2|m|} \underline{m}^{-2s}\|q\|_{\epsilon,s}^2 \le C\|q\|_{\epsilon,s}^2.
\end{aligned}$$

This implies that $\mathscr{K}$ is a bounded linear operator.

We then verify the compactness of $\mathscr{K}$ by taking $(\delta', t') \in]0, +\infty[\times\mathbb{R}$ to satisfy $(\delta, t) < (\delta', t') < (\kappa, -1/2)$, and decomposing it as follows:

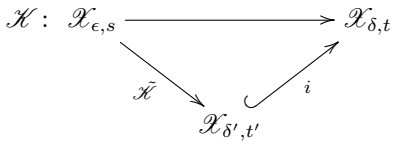

Here, $\tilde{\mathscr{K}}\colon \mathscr{X}_{\epsilon,s} \to \mathscr{X}_{\delta',t'}$ is a bounded linear operator defined similarly to $\mathscr{K}$ and i is a natural inclusion, which is compact operator by Proposition 1.1.1 (ii). Since $\mathscr{K} = i \circ \tilde{\mathscr{K}}$, $\mathscr{K}$ is compact. □

The following corollary immediately follows from the above lemma.

Corollary 3.4.3. *If (ϵ, s) satisfies*

$$\left(\frac{R}{\kappa\rho}, \frac{1}{2}\right) < (\epsilon, s) < \left(\frac{\kappa\rho}{R}, -\frac{1}{2}\right), \tag{3.4.1}$$

then the operator $\mathscr{K}\colon \mathscr{X}_{\epsilon,s} \to \mathscr{X}_{\epsilon R/\rho,s}$ is compact.

When (ϵ, s) satisfies the condition (3.4.1), we define $\mathscr{A}\colon \mathscr{X}_{\epsilon,s} \to \mathscr{X}_{\epsilon R/\rho,s}$ as $\mathscr{A} = \mathscr{K} + \mathscr{L}$. Then, $\mathscr{A}$ is an extension of A. We can now state the most general version of Theorem 3.1.1.

Theorem 3.4.4. *Suppose that $R \in]\rho, \kappa\rho[$, $F \in \mathscr{X}_{\xi,\sigma}$ with some $(\xi, \sigma) > (1, 1/2)$, (δ, t) satisfies $(1, 1/2) < (\delta, t) < (\kappa, -1/2)$ and $(\delta, t) \le (\xi, \sigma)$, and (ϵ, s) satisfies the conditions*

$$\max\left\{\delta\left(\frac{\rho}{R}\right)^2, \frac{1}{\delta}\right\} \le \epsilon \le \min\left\{\frac{1}{\delta}\left(\frac{R}{\rho}\right)^2, \delta\right\};$$

$$\text{if } \epsilon = \delta \text{ then } s \le t; \quad \text{if } \epsilon = \frac{R}{\rho} \text{ then } s < -\frac{1}{2},$$

and $\epsilon \ge (R/\rho)^2\kappa^{-1}$. Then the following hold true:

(i) *For sufficiently large $N \in \mathbb{N}$, there exists a unique $q^{(N)} \in \mathscr{D}^{(N)}$ such that*

$$\mathscr{A}q^{(N)}(\tau) = F(\tau), \quad \tau \in \Delta_N.$$

(ii) *There exists some positive constant C which depends on ϵ, s, δ, t, ρ, R, $\|\mathscr{A}\|$, and $\|\mathscr{A}^{-1}\|$ such that*

$$\|F - \mathscr{A}q^{(N)}\|_{\epsilon,s} \le CN^{\tilde{P}(\epsilon,s,\delta,t)} \left(\frac{\epsilon}{\delta}\right)^{N/2} \|F\|_{\delta,t},$$

where

$$\tilde{P}(\epsilon,s,\delta,t) = \begin{cases} P(\epsilon,s,\delta,t) & \text{if } (\epsilon,s) \ge ((R/\rho)^2\kappa^{-1}, 1/2), \\ P((R/\rho)^2\kappa^{-1}, 1/2, \delta, t) & \text{if } \epsilon = (R/\rho)^2\kappa^{-1} \wedge s < 1/2. \end{cases}$$

Note that all the operator norms $\|\mathscr{A}\|$ and $\|\mathscr{A}^{-1}\|$ are the abbreviated forms of $\|\mathscr{A}\|_{\mathscr{B}(\mathscr{X}_{\epsilon,s}, \mathscr{X}_{\epsilon R/\rho,s})}$ and $\|\mathscr{A}^{-1}\|_{\mathscr{B}(\mathscr{X}_{\epsilon R/\rho,s}, \mathscr{X}_{\epsilon,s})}$ for some $(\epsilon, s) \in]0, +\infty[\times\mathbb{R}$, respectively. We need the following two lemmas to prove the above theorem.

Lemma 3.4.5. *Suppose that $R \in]\rho, \kappa\rho[$ and that (ϵ, s) satisfies* (3.4.1)*. Then, $\mathscr{A}$ is a homeomorphism.*

Proof. The boundedness of $\mathscr{A}$ is clear. Considering that $\mathscr{A}$ is bijective, we only have to show that $\mathscr{A}$ is injective, because $\mathscr{A}$ is a Fredholm operator with index 0. We take $q \in \operatorname{Ker}\mathscr{A}$ arbitrarily. Since $\mathscr{L}$ is a homeomorphism, $\mathscr{A}q = 0$ is equivalent to $q = -\mathscr{L}^{-1}\mathscr{K}q$. Then, we have $\mathscr{K}q \in \mathscr{X}_{\kappa,t}$ for all $t < -1/2$ since $\mathscr{K}\colon \mathscr{X}_{\epsilon,s} \to \mathscr{X}_{\delta,t}$ defines a bounded linear operator when $(\epsilon, s) > (R/(\kappa\rho), 1/2)$ and $(\delta, t) < (\kappa, -1/2)$ are satisfied due to Lemma 3.4.2. Therefore, $q = -\mathscr{L}^{-1}\mathscr{K}q \in \mathscr{X}_{\kappa\rho/R,t}$. Note that $\kappa\rho/R > 1$. Defining a function Q on Γ_R as

$$Q(\Psi(R\mathrm{e}^{2\pi\mathrm{i}\tau})) = q(\tau) \quad (\tau \in S^1),$$

$Q\colon \Gamma_R \to \mathbb{C}$ is continuous. Then we have

$$\begin{aligned} \mathscr{A}q = 0 &\iff \int_0^1 \Re\left\{\frac{-R\mathrm{e}^{2\pi\mathrm{i}\theta}\Psi'(R\mathrm{e}^{2\pi\mathrm{i}\theta})}{\Psi(\rho\mathrm{e}^{2\pi\mathrm{i}\tau}) - \Psi(R\mathrm{e}^{2\pi\mathrm{i}\theta})}\right\} q(\theta)\,\mathrm{d}\theta = 0 \quad (\forall \tau \in S^1) \\ &\iff \underbrace{\int_{\Gamma_R} \frac{-1}{2\pi} \frac{(\boldsymbol{n}_{\boldsymbol{y}} \mid \boldsymbol{x} - \boldsymbol{y})}{\|\boldsymbol{x} - \boldsymbol{y}\|^2} Q(\boldsymbol{y})\,\mathrm{d}s_{\boldsymbol{y}}}_{=:u(\boldsymbol{x})} = 0 \quad (\forall \boldsymbol{x} \in \Gamma). \end{aligned}$$

The function u is harmonic in the interior simply-connected region Ω_R of Γ_R, and especially continuous on $\overline{\Omega}$. Thus, we have $u = 0$ in Ω because of the maximum principle for harmonic functions. Furthermore, we have $u = 0$ in Ω_R because of the identity theorem for real analytic functions. Hence, $Q \equiv 0$ follows from Proposition 1.3.4, and this yields $q \equiv 0$. The open mapping theorem determines that $\mathscr{A}^{-1}$ is bounded. □

Lemma 3.4.6. *Suppose that $R \in]\rho, \kappa\rho[$, (δ, t) satisfies $(1, 1/2) < (\delta, t) < (\kappa, -1/2)$ and $(\delta, t) \le (\xi, \sigma)$, and that (ϵ, s) satisfies* (3.3.7) *and $(\epsilon, s) > ((R/\rho)^2\kappa^{-1}, 1/2)$. Then, there exists some positive constant C which depends on ϵ, s, δ, t, ρ, R, $\|\mathscr{A}\|$, and $\|\mathscr{A}^{-1}\|$ such that for all $N \in \mathbb{N}$, all $q \in \mathscr{X}_{\delta\rho/R,t}$ and all $q^{(N)} \in \mathscr{D}^{(N)}$ satisfying $\mathscr{A}q = \mathscr{A}q^{(N)}$ on Δ_N, the following estimate holds:*

$$\|q - q^{(N)}\|_{\epsilon\rho/R,s} \le CN^{P(\epsilon,s,\delta,t)} \left(\frac{\epsilon}{\delta}\right)^{N/2} (\|q\|_{\delta\rho/R,t} + \|q - q^{(N)}\|_{\epsilon\rho/R,s}).$$

Proof. Since $\mathscr{A}$ is a homeomorphism by Lemma 3.4.5, the following estimate holds:

$$\|q - q^{(N)}\|_{\epsilon\rho/R,s} \le C\|\mathscr{A}(q^{(N)} - q)\|_{\epsilon,s}.$$

Here we put

$$w_N = q^{(N)}, \quad w = q^{(N)} - \mathscr{L}^{-1}\mathscr{A}(q^{(N)} - q).$$

Then, we have

$$\begin{aligned} &w_N \in \mathscr{D}^{(N)}, \quad \mathscr{L}^{-1}\mathscr{A}(q^{(N)} - q) = w_N - w, \quad \mathscr{L}w = \mathscr{L}w_N \quad \text{on } \Delta_N, \\ &w = q + \mathscr{L}^{-1}(\mathscr{L} - \mathscr{A})(q^{(N)} - q). \end{aligned}$$

Therefore, by Theorem 3.3.4, which gives the error estimate of DSM when Ω is a disk, we have

$$\begin{aligned} \|q^{(N)} - q\|_{\epsilon\rho/R,s} &\le C\|\mathscr{L}w_N - \mathscr{L}w\|_{\epsilon,s} \le CN^{P(\epsilon,s,\delta,t)} \left(\frac{\epsilon}{\delta}\right)^{N/2} \|\mathscr{L}w\|_{\delta,t} \\ &\le CN^{P(\epsilon,s,\delta,t)} \left(\frac{\epsilon}{\delta}\right)^{N/2} \|w\|_{\delta\rho/R,t}. \end{aligned} \tag{3.4.2}$$

Moreover, we have

$$\begin{aligned} \|w\|_{\delta\rho/R,t} &= \|q + \mathscr{L}^{-1}(\mathscr{L} - \mathscr{A})(q^{(N)} - q)\|_{\delta\rho/R,t} \le \|q\|_{\delta\rho/R,t} + C\|(\mathscr{L} - \mathscr{A})(q^{(N)} - q)\|_{\delta,t} \\ &\le \|q\|_{\delta\rho/R,t} + C\|q^{(N)} - q\|_{\epsilon\rho/R,s} \le C\left(\|q\|_{\delta\rho/R,t} + \|q^{(N)} - q\|_{\epsilon\rho/R,s}\right), \end{aligned} \tag{3.4.3}$$

where we use the boundedness of $\mathscr{L} - \mathscr{A} = -\mathscr{K} \colon \mathscr{X}_{\epsilon\rho/R,s} \to \mathscr{X}_{\delta,t}$. Combining (3.4.2) with (3.4.3), we obtain the desired estimate. □

Proof of Theorem 3.4.4. At first, we remark that

$$N^{P(\epsilon,s,\delta,t)} \left(\frac{\epsilon}{\delta}\right)^{N/2} = o(1) \quad \text{as } N \to \infty$$

follows from $(\epsilon, s) < (\delta, t)$ and the value of P in Remark 3.3.6. Therefore, by Lemma 3.4.6, for a sufficiently large $N \in \mathbb{N}$ and all $q^{(N)} \in \mathscr{D}^{(N)}$ with $\mathscr{A}q^{(N)} = \mathscr{A}q$ on Δ_N, we have

$$\|q - q^{(N)}\|_{\epsilon\rho/R,s} \le CN^{P(\epsilon,s,\delta,t)} \left(\frac{\epsilon}{\delta}\right)^{N/2} \|q\|_{\delta\rho/R,t} \tag{3.4.4}$$

provided that $(\epsilon, s) > ((R/\rho)^2\kappa^{-1}, 1/2)$. Since this relation holds for $\epsilon = (R/\rho)^2\kappa^{-1}$ with any $s > 1/2$, using the embedding relation $\mathscr{X}_{(R/\rho)^2\kappa^{-1},s} \hookrightarrow \mathscr{X}_{(R/\rho)^2\kappa^{-1},1/2}$, we obtain the inequality (3.4.4) when $(\epsilon, s) = ((R/\rho)^2\kappa^{-1}, 1/2)$. Using the embedding relation $\mathscr{X}_{(R/\rho)^2\kappa^{-1},1/2} \hookrightarrow \mathscr{X}_{(R/\rho)^2\kappa^{-1},s}$ for $s < 1/2$ once more, we obtain

$$\|q - q^{(N)}\|_{\epsilon\rho/R,s} \le CN^{P(\epsilon,1/2,\delta,t)} \left(\frac{\epsilon}{\delta}\right)^{N/2} \|q\|_{\delta\rho/R,t} \tag{3.4.5}$$

for $\epsilon = (R/\rho)^2\kappa^{-1}$ and $s < 1/2$. Therefore, using the fact that $\mathscr{A}$ is a homeomorphism, which follows from Lemma 3.4.5, $\mathscr{A}q^{(N)} = 0$ on Δ_N yields $q^{(N)} = 0$. Since $\mathscr{A}q^{(N)} = F$ on Δ_N is equivalent to a finite system of linear equations, this shows the unique solvability of the considered functional equation.

Finally, we prove the second statement. For $F \in \mathscr{X}_{\xi,\sigma}$, there exists a unique $q \in \mathscr{X}_{\xi\rho/R,\sigma}$ that satisfies $\mathscr{A}q = F$ because $\mathscr{A}$ is a homeomorphism. Then, we have

$$\|F - \mathscr{A}q^{(N)}\|_{\epsilon,s} = \|\mathscr{A}q - \mathscr{A}q^{(N)}\|_{\epsilon,s} \le C\|q - q^{(N)}\|_{\epsilon\rho/R,s}$$

and

$$\|q\|_{\delta\rho/R,t} \le C\|F\|_{\delta,t}.$$

Hence, we obtain the desired error estimate by the above two inequalities, (3.4.4), and (3.4.5). □

3.5 Numerical experiments

In this section, we present the results of two numerical experiments. The first considers the case where Ω is a disk D_ρ, that is, Ψ is the identity mapping. The other involves the case where Ω is the interior simply-connected region surrounded by the curve defined by a polynomial. In each numerical experiment, we consider two types of boundary conditions: the harmonic polynomial and the logarithmic potential. The error is measured by the L^2 norm ($s = 0$ in Theorem 3.1.1) and the L^∞ norm (Corollary 3.1.2). In each Figures 3.2, 3.3, 3.5, and 3.6, the horizontal and vertical axes represent N and the common logarithm of the errors, respectively.

3.5.1 The case of the disk D_ρ

Since Ω is a disk D_ρ, the peripheral conformal mapping Ψ can be taken as the identity mapping. Therefore, κ can be regarded as $+\infty$. In this case, the values of ρ and R are selected as 1 and 2, respectively.

3.5.1.1 Boundary data f: a harmonic polynomial

Let the boundary data f be a harmonic polynomial. Namely, f is defined as

$$f(\rho e^{2\pi i\tau}) = \rho^m \cos(m\tau) \quad (\tau \in S^1;\ m \in \{0, 1, \ldots, 5\}).$$

Obviously, f can be continued to the whole plane $\mathbb{C}$ complex analytically. Hence, the errors can be estimated as follows:

$$\|u - u^{(N)}\|_{L^2(\Gamma)} = O\left(\left(\frac{\rho}{R}\right)^N\right), \quad \|u - u^{(N)}\|_{L^\infty(\Gamma)} = O\left(N^{1/2}\left(\frac{\rho}{R}\right)^N\right). \tag{3.5.1}$$

The numerical results are depicted in Figure 3.2. The errors are investigated by a Monte-Carlo method,

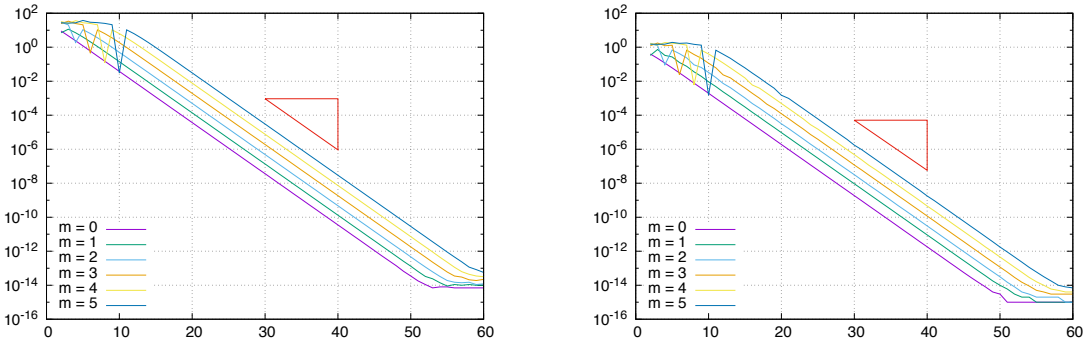

Figure 3.2: Numerical results of DSM with the boundary data $f(\rho e^{2\pi i\tau}) = \rho^m \cos(m\tau)$ ($\tau \in S^1$; $m = 0, 1, \ldots, 5$). The gradient of the hypotenuse of the red colored triangle is the theoretical order of convergence. **a** L^2-norm estimate. **b** L^∞-error estimate

that is, we take a sufficiently large number of points, i.e., a number greater than $10 \max N$, on the boundary Γ and compute the error on them. We found the behavior of the errors to be estimated well by (3.5.1). In this experiment, the estimation of the L^2 norm is optimal; however, the estimation of the L^∞ error is "not" optimal because $N^{1/2}$ appears in the error estimate. Indeed, in the case of a disk, the power of N does not appear in the error estimate (see for instance [45, Theorem 5.2] and the comments before it).

3.5.2 Boundary data f: logarithmic potential

We next consider the following boundary condition:

$$f(\rho e^{2\pi i\tau}) = \log|\rho e^{2\pi i\tau} - p(m)|, \quad p(m) = \rho + 0.2(m+1) \quad (\tau \in S^1;\ m \in \{0, 1, \dots, 10\}).$$

There exists a singularity at $p(m)$; therefore, f can be continued complex analytically to the disk $D_{p(m)}$. This means the error can be estimated as

$$\|u - u^{(N)}\|_{L^2(\Gamma)} = O\left(\max\left\{\left(\frac{\rho}{p(m)}\right)^{N/2}, \left(\frac{\rho}{R}\right)^{N}\right\}\right),$$

$$\|u - u^{(N)}\|_{L^\infty(\Gamma)} = O\left(N^{1/2}\max\left\{\left(\frac{\rho}{p(m)}\right)^{N/2}, \left(\frac{\rho}{R}\right)^{N}\right\}\right).$$

The results of the numerical experiments can be found in Figure 3.3.

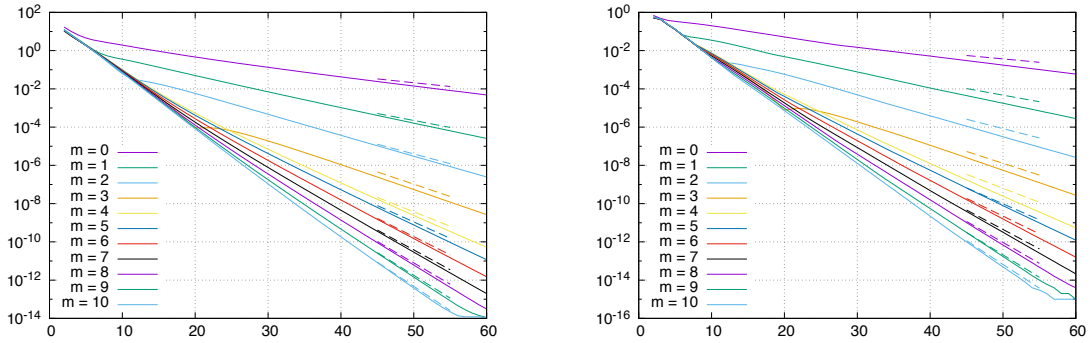

(a) **(b)**

Figure 3.3: Numerical results of DSM with the boundary data $f(\rho e^{2\pi i\tau}) = \log|\rho e^{2\pi i\tau} - p(m)|$ ($\tau \in S^1$; $m = 0, 1, \dots, 10$). The gradients of the broken lines are the theoretical orders of convergence for the corresponding solid lines. **a** L^2-error estimate. **b** L^∞-error estimate

3.5.3 The case of a curve defined by a polynomial

The second example considers the case where Ω is the region surrounded by the following closed curve:

$$\Gamma = \Psi_{l,r}(\gamma_1), \quad \Psi_{l,r}(z) = z + \frac{z^l}{r} \tag{3.5.2}$$

with $r > 0$ and $l > 0$. $\Psi_{l,r}$ is a conformal mapping in $D_{\sqrt[l-1]{r/l}}$, therefore κ could take any value between 1 and $\sqrt[l-1]{r/l}$, which enables us to think κ to be equal to $\sqrt[l-1]{r/l}$. In the following numerical experiments, we take $r = 8$ and $l = 4$. The collocation points $\{x_j\}_{j=1}^N$, the dipole points $\{y_k\}_{k=1}^N$, and dipole moments $\{n_k\}_{k=1}^N$ are defined as in (3.1.5) under $\rho = 1$ and $R = 1.2$, in which Ψ is replaced with $\Psi_{l,r}$. Note that $R \in]\sqrt{\kappa}\rho, \kappa\rho[$. Therefore, although the definitions of the dipole points and dipole moments in (3.1.5) make sense, the unique existence and covergence are not assured. However, as we shall see in each Figures 3.5 and 3.6, the exponential convergence is achieved, and the order of convergence is what we can expect from Theorem 3.1.1 and Corollary 3.1.2. Hence we can conjecture that the unique existence and convergence hold for $R \in]\rho, \kappa\rho[$. The shape of the region Ω, the arrangements of the dipole, and collocation points, and the directions of the dipole moments are depicted in Figure 3.4.

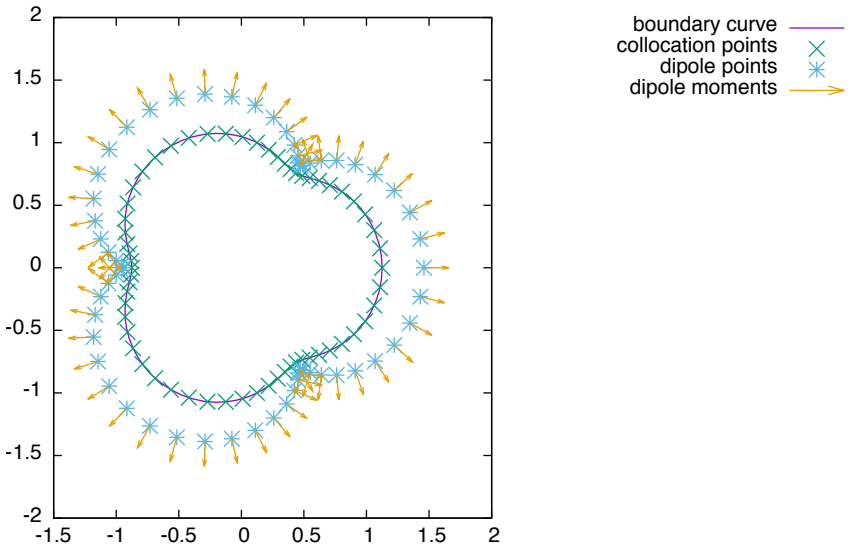

Figure 3.4: Graphic representation showing the shape of Ω, the arrangements of the dipole, and collocation points, and the directions of the dipole moments when $N = 60$, $\rho = 1$, and $R = 1.2$.

3.5.3.1 Boundary data f: a harmonic polynomial

Since f can be extended complex analytically to the whole plane $\mathbb{C}$, the errors could be estimated in a similar way as in (3.5.1). The results are found in Figure 3.5.

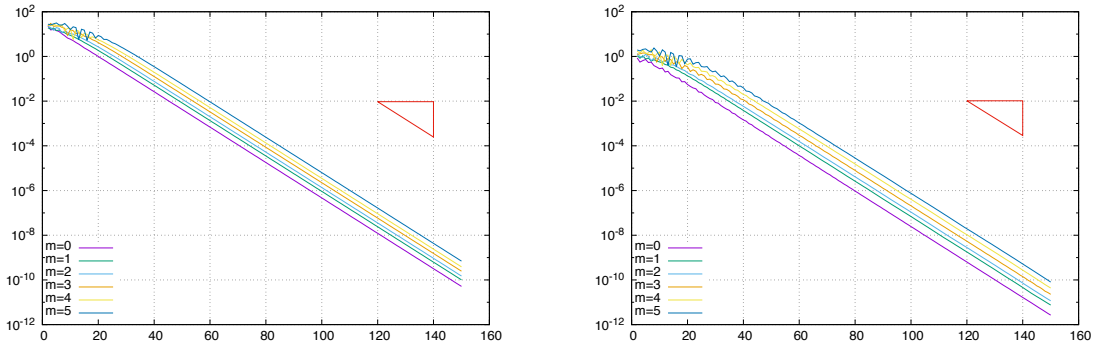

(a) **(b)**

Figure 3.5: Numerical results of DSM with the boundary data $f(z) = f(\Psi(\rho e^{2\pi i\tau})) = \Re(\Psi(\rho e^{2\pi i\tau})^m)$ ($z = \Psi(\rho e^{2\pi i\tau}) \in \Gamma$, $\tau \in [0,1]$; $m = 0, 1, \ldots, 5$). The gradient of the hypotenuse of the red colored triangle is the prospected order of convergence. **a** L^2-error estimate. **b** L^∞-error estimate.

3.5.3.2 Boundary data f: logarithmic potential

Since f can be continued complex analytically to the disk $D_{\tilde{p}(m)}$, this results in the following error estimate:

$$\|u - u^{(N)}\|_{L^2(\Gamma)} = O\left(\max\left\{\left(\frac{\rho}{\tilde{p}(m)}\right)^{N/2}, \left(\frac{\rho}{R}\right)^{N}\right\}\right),$$
$$\|u - u^{(N)}\|_{L^\infty(\Gamma)} = O\left(N^{1/2}\max\left\{\left(\frac{\rho}{\tilde{p}(m)}\right)^{N/2}, \left(\frac{\rho}{R}\right)^{N}\right\}\right),$$

where $\tilde{p}(m)$ is the positive real number satisfying $\Psi(\tilde{p}(m)) = p(m)$, and $p(m) = 1.0 + 0.05(m+3)$ $(m \in \{0, 1, \ldots, 10\})$ in this experiment. The numerical results are shown in Figure 3.6.

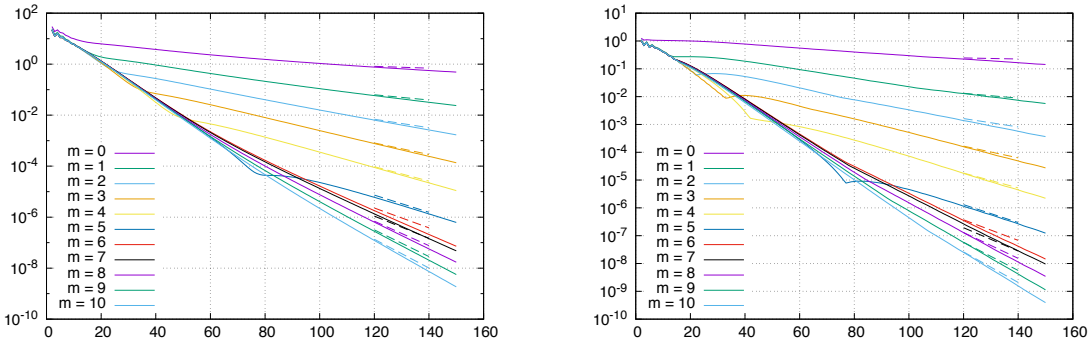

(a) **(b)**

Figure 3.6: Numerical results of DSM with the boundary data $f(z) = f(\Psi(\rho e^{2\pi i\tau})) = \log|\Psi(\rho e^{2\pi i\tau}) - p(m)|$ $(z = \Psi(\rho e^{2\pi i\tau}) \in \Gamma,\ \tau \in [0,1];\ m = 0, 1, \ldots, 10)$. The gradients of the broken lines are the prospected orders of convergence for the corresponding solid lines. **a** L^2-error estimate. **b** L^∞-error estimate.

3.6 Concluding remarks

In this chapter, we introduced the concept of peripheral conformal mapping following Katsurada [48], and used it to arrange the dipole and collocation points and to define the dipole moments. For this situation, we proved the stability and exponential convergence of DSM. The numerical results in Section 3.5 show that our error estimate provides a good bound but that there is a slight overestimation, and that our convergence theorem could hold even if $R > \sqrt{\kappa}\rho$.

This presents an opportunity for further research, namely to extend this result to a multiply-connected region. However, it should be considered that it would not be possible to apply the original DSM to potential problems in a multiply-connected region, which may require some modifications. Furthermore, the reason for the overestimate needs to be clarified. Finally, the approach in this paper may be applied to the multipole method; therefore, the mathematical analysis of the multipole method using the proposed method would be expected to be possible.

3.7 Proof of Lemma 3.3.8

We here prove Lemma 3.3.8. The basic concept is the same as that in [48].

Firstly, note that $\hat{q}^{(N)}(p)$ can be represented as

$$\hat{q}^{(N)}(p) = \left(\sum_{m \equiv p} \hat{G}(m)\hat{q}(m) \right) / \varphi_p^{(N)}(\rho).$$

We decompose and estimate $\|q - q^{(N)}\|_{\epsilon\rho/R,s}$ as follows:

$$\begin{aligned} \|q - q^{(N)}\|_{\epsilon\rho/R,s}^2 &= |\hat{q}(0) - \hat{q}^{(N)}(0)|^2 + \sum_{n \in \mathbb{Z}\setminus\{0\}} |\hat{q}(n) - \hat{q}^{(N)}(n)|^2 \left(\frac{\epsilon\rho}{R}\right)^2 \underline{n}^{2s} \\ &\leq T_1 + (2\pi)^{2s}\{T_2 + 2T_3 + 2T_4\}, \end{aligned}$$

where

$$T_1 = |\hat{q}(0) - \hat{q}^{(N)}(0)|^2, \quad T_2 = \sum_{n \in \Lambda_N' \setminus \{0\}} |\hat{q}(n) - \hat{q}^{(N)}(n)|^2 \left(\frac{\epsilon\rho}{R}\right)^{2|n|} |n|^{2s},$$

$$T_3 = \sum_{n \in \mathbb{Z}\setminus\Lambda_N'} |\hat{q}(n)|^2 \left(\frac{\epsilon\rho}{R}\right)^{2|n|} |n|^{2s}, \quad T_4 = \sum_{n \in \mathbb{Z}\setminus\Lambda_N'} |\hat{q}^{(N)}(n)|^2 \left(\frac{\epsilon\rho}{R}\right)^{2|n|} |n|^{2s}.$$

We frequently use the following proposition without providing proof.

Proposition 3.7.1. (i) *For arbitrary $N \in \mathbb{N}$ we have $|\varphi_0^{(N)}(\rho)| \geq 1$.*
(ii) *For each $n \in \Lambda_N' \setminus \{0\}$ we have $|\varphi_n^{(N)}(\rho)| \geq 2^{-1}(\rho/R)^{|n|}$.*
(iii) *For all $\epsilon \in]0,1[$ and all $t \in \mathbb{R}$ there exists some positive constant $C_{\epsilon,t}$ such that*

$$\max_{p \in \Lambda_N' \setminus \{0\}} \left\{ \left(\frac{N}{|p|}\right)^t \epsilon^{N-2|p|} \right\} \leq C_{\epsilon,t}$$

holds for all $N \in \mathbb{N}$.
(iv) *For all $(\epsilon, s) < (1, -1)$ there exists some positive constant $C_{\epsilon,s}$ such that*

$$\sum_{m \in I(p)} |m|^s \epsilon^{|m|} \leq C_{\epsilon,s} N^s \epsilon^{N-|p|}$$

holds for all $N \in \mathbb{N}$ and all $p \in \Lambda_N'$.

In the remainder of this section we estimate each T_j $(j = 1, 2, 3, 4)$. Since

$$\hat{q}(0) - \hat{q}^{(N)}(0) = \left[\sum_{m \in I(0)} \hat{G}(m)\hat{q}(0) - \sum_{m \in I(0)} \hat{G}(m)\hat{q}(m) \right] / \varphi_0^{(N)}(\rho)$$

we have

$$T_1 = |\hat{q}(0) - \hat{q}^{(N)}(0)|^2 \leq T_{11} + T_{12},$$

where

$$T_{11} = \frac{2}{|\varphi_0^{(N)}(\rho)|^2} \left| \sum_{m \in I(0)} \hat{G}(m)\hat{q}(0) \right|^2, \quad T_{12} = \frac{2}{|\varphi_0^{(N)}(\rho)|^2} \left| \sum_{m \in I(0)} \hat{G}(m)\hat{q}(m) \right|^2.$$

From Proposition 3.7.1 (i) and the assumption $\delta(\rho/R)^2 \le \epsilon$ we obtain

$$T_{11} \le 2\left(\sum_{l=1}^{\infty}\left(\frac{\rho}{R}\right)^{lN}\right)^2 |\hat{q}(0)|^2 \le C_{11}\left(\frac{\rho}{R}\right)^{2N}\|q\|^2_{\delta\rho/R,t}$$
$$\le \begin{cases} C_{11}\left(\frac{\epsilon}{\delta}\right)^N \|q\|^2_{\delta\rho/R,t} & \text{if } \epsilon = \delta(\rho/R)^2 \wedge s - t \le 0, \\ C_{11}N^{2(s-t)}\left(\frac{\epsilon}{\delta}\right)^N \|q\|^2_{\delta\rho/R,t} & \text{otherwise.} \end{cases}$$

Here and hereafter $C^{\text{superscript}}_{\text{subscript}}$ denotes some constant independent of N and each symbol may represent a different constant. By Proposition 3.7.1 (i) and (iv), we have

$$T_{12} \le 2\left(\sum_{m\in I(0)}\frac{1}{2}\left(\frac{\rho}{R}\right)^{|m|}|\hat{q}(m)|\right)^2$$
$$\le \frac{1}{2}\left(\sum_{m\in I(0)}|\hat{q}(m)|^2\left(\frac{\delta\rho}{R}\right)^{2|m|}\underline{m}^{2t}\right)\left(\sum_{m\in I(0)}\frac{1}{\delta^{2|m|}}\frac{1}{\underline{m}^{2t}}\right)$$
$$\le C_{12}\delta^{-2N}N^{-2t}\|q\|^2_{\delta\rho/R,t} \le \begin{cases} C_{12}N^{-2t}\left(\frac{\epsilon}{\delta}\right)^N \|q\|^2_{\delta\rho/R,t} & \text{if } \delta^{-1} = \epsilon \wedge s \le 0, \\ C_{12}N^{2(s-t)}\left(\frac{\epsilon}{\delta}\right)^N \|q\|^2_{\delta\rho/R,t} & \text{otherwise.} \end{cases}$$

Here, we use the assumption $\delta^{-1} \le \epsilon$.

Next, we estimate T_2. For $n \in \Lambda'_N \setminus \{0\}$ we have

$$\hat{q}(n) - \hat{q}^{(N)}(n) = \left[\sum_{m\in I(n)}\hat{G}(m)\hat{q}(n) - \sum_{m\in I(n)}\hat{G}(m)\hat{q}(m)\right]/\varphi_n^{(N)}(\rho);$$

therefore,

$$|\hat{q}(n) - \hat{q}^{(N)}(n)|^2 \le \frac{2}{|\varphi_n^{(N)}(\rho)|^2}\left[\left|\sum_{m\in I(n)}\hat{G}(m)\hat{q}(n)\right|^2 + \left|\sum_{m\in I(n)}\hat{G}(m)\hat{q}(m)\right|^2\right]$$

holds. Thus, we obtain $T_2 \le T_{21} + T_{22}$, where

$$T_{21} = \sum_{n\in\Lambda'_N\setminus\{0\}}\frac{2}{|\varphi_n^{(N)}(\rho)|^2}\left|\sum_{m\in I(n)}\hat{G}(m)\hat{q}(n)\right|^2\left(\frac{\epsilon\rho}{R}\right)^{2|n|}|n|^{2s},$$
$$T_{22} = \sum_{n\in\Lambda'_N\setminus\{0\}}\frac{2}{|\varphi_n^{(N)}(\rho)|^2}\left|\sum_{m\in I(n)}\hat{G}(m)\hat{q}(m)\right|^2\left(\frac{\epsilon\rho}{R}\right)^{2|n|}|n|^{2s}.$$

As to T_{21}, from Proposition 3.7.1 (ii), we have

$$\frac{1}{|\varphi_n^{(N)}(\rho)|^2}\left|\sum_{m\in I(n)}\hat{G}(m)\right|^2 \le 4\left(\frac{R}{\rho}\right)^{2|n|}\left|\sum_{m\in I(n)}\frac{1}{2}\left(\frac{\rho}{R}\right)^{|m|}\right|^2 \le C_{21}\left(\frac{\rho}{R}\right)^{2(N-2|n|)}$$

for $n \in \Lambda'_N \setminus \{0\}$; therefore,

$$\begin{aligned} T_{21} &\le C_{21} \sum_{n\in\Lambda'_N\setminus\{0\}} |\hat{q}(n)|^2 \left(\frac{\rho}{R}\right)^{2(N-2|n|)} \left(\frac{\epsilon\rho}{R}\right)^{2|n|} |n|^{2s} \\ &\le C_{21} N^{2\max\{s-t,0\}} \left(\frac{\epsilon}{\delta}\right)^N \|q\|^2_{\delta\rho/R,t} A_{21}, \end{aligned}$$

where

$$A_{21} = \sup_{n\in\Lambda'_N\setminus\{0\}} \left\{ |n|^{2(s-t)} N^{-2\max\{s-t,0\}} \left\{ \frac{\delta}{\epsilon} \left(\frac{\rho}{R}\right)^2 \right\}^{N-2|n|} \right\}.$$

By ensuring that $\epsilon \ge \delta(\rho/R)^2$, the above supremum A_{21} is bounded as follows according to Proposition 3.7.1 (iii):

$$A_{21} \le \begin{cases} 1 & \text{if } \epsilon = \delta(\rho/R)^2 \wedge s \le t, \\ 4^{-(s-t)} & \text{if } \epsilon = \delta(\rho/R)^2 \wedge s > t, \\ C_{\delta\epsilon^{-1}(\rho/R)^2,-2(s-t)} N^{2(s-t)} & \text{if } \epsilon > \delta(\rho/R)^2 \wedge s \le t, \\ C_{\delta\epsilon^{-1}(\rho/R)^2,-2(s-t)} & \text{if } \epsilon > \delta(\rho/R)^2 \wedge s > t. \end{cases}$$

Therefore, we obtain

$$T_{21} \le \begin{cases} C_{21} \left(\frac{\epsilon}{\delta}\right)^N \|q\|^2_{\delta\rho/R,t} & \text{if } \epsilon = \delta(\rho/R)^2 \wedge s \le t, \\ C_{21} N^{2(s-t)} \left(\frac{\epsilon}{\delta}\right)^N \|q\|^2_{\delta\rho/R,t} & \text{otherwise.} \end{cases}$$

For $n \in \Lambda'_N \setminus \{0\}$ we have

$$\begin{aligned} &\frac{1}{|\varphi_n^{(N)}(\rho)|^2} \left| \sum_{m\in I(n)} \hat{G}(m)\hat{q}(m) \right|^2 \\ &\qquad \le \left(\frac{R}{\rho}\right)^{2|n|} \sum_{m\in I(n)} |\hat{q}(m)|^2 \left(\frac{\delta\rho}{R}\right)^{2|m|} \underline{m}^{2t} \sum_{m\in I(n)} \frac{1}{\delta^{2|m|}} \frac{1}{\underline{m}^{2t}} \\ &\qquad \le C_{22} \left(\frac{R}{\rho}\right)^{2|n|} \frac{1}{\delta^{2(N-|n|)}} N^{-2t} \sum_{m\in I(n)} |\hat{q}(m)|^2 \left(\frac{\delta\rho}{R}\right)^{2|m|} \underline{m}^{2t} \end{aligned}$$

by Proposition 3.7.1 (ii) and (iv). Thus, we have

$$\begin{aligned} T_{22} &\le C_{22} \sum_{n\in\Lambda'_N\setminus\{0\}} \left(\frac{R}{\rho}\right)^{2|n|} \frac{1}{\delta^{2(N-|n|)}} N^{-2t} \sum_{m\in I(n)} |\hat{q}(m)|^2 \left(\frac{\delta\rho}{R}\right)^{2|m|} \underline{m}^{2t} \left(\frac{\epsilon\rho}{R}\right)^{2|n|} |n|^{2s} \\ &\le C_{22} \|q\|^2_{\delta\rho/R,t} N^{2[-t+\max\{s,0\}]} \left(\frac{\epsilon}{\delta}\right)^N \underbrace{\sup_{n\in\Lambda'_N\setminus\{0\}} \left\{ \left(\frac{1}{\epsilon\delta}\right)^{N-2|n|} |n|^{2s} N^{-2\max\{s,0\}} \right\}}_{=:A_{22}}. \end{aligned}$$

Because $\epsilon \ge \delta^{-1}$ we have the following estimate on A_{22} as a consequence of Proposition 3.7.1 (iii):

$$A_{22} \le \begin{cases} 1 & \text{if } \epsilon = \delta^{-1} \wedge s \le 0, \\ 4^{-s} & \text{if } \epsilon = \delta^{-1} \wedge s > 0, \\ C_{(\epsilon\delta)^{-1},-2s} N^{2s} & \text{if } \epsilon > \delta^{-1} \wedge s \le 0, \\ C_{(\epsilon\delta)^{-1},-2s} & \text{if } \epsilon > \delta^{-1} \wedge s > 0. \end{cases}$$

Therefore, we obtain

$$T_{22} \leq \begin{cases} C_{22} N^{-2s} \left(\frac{\epsilon}{\delta}\right)^N \|q\|^2_{\delta\rho/R,t} & \text{if } \epsilon = \delta^{-1} \wedge s \leq 0, \\ C_{22} N^{2(s-t)} \left(\frac{\epsilon}{\delta}\right)^N \|q\|^2_{\delta\rho/R,t} & \text{otherwise.} \end{cases}$$

Concerning T_3 we have

$$\begin{aligned} T_3 &\leq \sum_{n \in \mathbb{Z}\setminus\Lambda'_N} |\hat{q}(n)|^2 \left(\frac{\delta\rho}{R}\right)^{2|n|} |n|^{2t} \sup_{n\in\mathbb{Z}\setminus\Lambda'_N} \left\{ \left(\frac{\epsilon}{\delta}\right)^{2|n|} |n|^{2(s-t)} \right\} \\ &\leq C_3 \|q\|^2_{\delta\rho/R,t} N^{2(s-t)} \left(\frac{\epsilon}{\delta}\right)^N \underbrace{\sup_{n\in\mathbb{Z}\setminus\Lambda'_N} \left\{ \left(\frac{\epsilon}{\delta}\right)^{2|n|-N} \left(\frac{|n|}{N}\right)^{2(s-t)} \right\}}_{=:A_3}. \end{aligned}$$

Remarking that $(\epsilon, s) \leq (\delta, t)$, A_3 can be bounded by some positive constant. Thus, we obtain

$$T_3 \leq C_3 N^{2(s-t)} \left(\frac{\epsilon}{\delta}\right)^N \|q\|^2_{\delta\rho/R,t}.$$

Finally, as to T_4 we have

$$T_4 = \sum_{p\in\Lambda'_N} \sum_{l\in\mathbb{Z}\setminus\{0\}} |\hat{q}^{(N)}(p+lN)|^2 \left(\frac{\epsilon\rho}{R}\right)^{2|p+lN|} |p+lN|^{2s} = T_{41} + T_{42},$$

where

$$\begin{aligned} T_{41} &= \sum_{l\in\mathbb{Z}\setminus\{0\}} |lN|^{2s} \left(\frac{\epsilon\rho}{R}\right)^{2|lN|} |\hat{q}^{(N)}(0)|^2, \\ T_{42} &= \sum_{p\in\Lambda'_N\setminus\{0\}} \left\{ \sum_{l\in\mathbb{Z}\setminus\{0\}} |p+lN|^{2s} \left(\frac{\epsilon\rho}{R}\right)^{2|p+lN|} |\hat{q}^{(N)}(p)|^2 \right\}. \end{aligned}$$

Here, note that the infinite series

$$\sum_{l\in\mathbb{Z}\setminus\{0\}} |p+lN|^{2s} \left(\frac{\epsilon\rho}{R}\right)^{2|p+lN|} \quad (\forall p \in \Lambda'_N)$$

is absolutely convergent because of the assumption $(\epsilon, s) < (R/\rho, -1/2)$. By implementing Proposition 3.7.1 (i) we have $|\hat{q}^{(N)}(0)|^2 \leq C\|q\|^2_{\delta\rho/R,t}$ and from Proposition 3.7.1 (iv) this yields an estimate

$$\begin{aligned} T_{41} &\leq C_{\epsilon\rho/R,2s} N^{2s} \left(\frac{\epsilon\rho}{R}\right)^{2N} \cdot C\|q\|^2_{\delta\rho/R,t} \\ &\leq \begin{cases} C_{41} N^{2s} \left(\frac{\epsilon}{\delta}\right)^N \|q\|^2_{\delta\rho/R,t} & \text{if } \epsilon = \delta^{-1}(R/\rho)^2 \wedge t \geq 0, \\ C_{41} N^{2(s-t)} \left(\frac{\epsilon}{\delta}\right)^N \|q\|^2_{\delta\rho/R,t} & \text{otherwise.} \end{cases} \end{aligned}$$

Concerning T_{42} we first have an estimate of $\hat{q}^{(N)}(p)$ for $p \in \Lambda'_N \setminus \{0\}$

$$\begin{aligned} |\hat{q}^{(N)}(p)|^2 \leq \frac{1}{(2\pi)^{2t}} \sum_{m\equiv p} |\hat{q}(m)|^2 \left(\frac{\delta\rho}{R}\right)^{2|m|} \underline{m}^{2t} \left(\frac{R}{\rho}\right)^{2|p|} \\ \times \left[\frac{1}{\delta^{2|p|}} \frac{1}{|p|^{2t}} + C_{\delta^{-2},-2t} N^{-2t} \left(\frac{1}{\delta}\right)^{2(N-|p|)} \right]. \end{aligned}$$

Then, we have

$$\begin{aligned}
T_{42} \leq \sum_{p\in\Lambda'_N\setminus\{0\}} \Bigg[& \left(\sum_{l\in\mathbb{Z}\setminus\{0\}} |p+lN|^{2s} \left(\frac{\epsilon\rho}{R}\right)^{2|p+lN|} \right) \\
& \times \frac{1}{(2\pi)^{2t}} \left(\sum_{m\equiv p} |\hat{q}(m)|^2 \left(\frac{\delta\rho}{R}\right)^{2|m|} \underline{m}^{2t} \left(\frac{R}{\rho}\right)^{2|p|} \right) \\
& \times \left[\frac{1}{\delta^{2|p|}} \frac{1}{|p|^{2t}} + C_{\delta^{-2},-2t} N^{-2t} \left(\frac{1}{\delta}\right)^{2(N-|p|)} \right] \\
\leq C_{\epsilon\rho/R,2s} N^{2[s+\max\{-t,0\}]} & \left(\frac{\epsilon}{\delta}\right)^N \|q\|^2_{\delta\rho/R,t} A_{42},
\end{aligned}$$

where

$$\begin{aligned}
A_{42} = \sup_{p\in\Lambda'_N\setminus\{0\}} \Bigg[& \frac{N^{-2\max\{-t,0\}}}{|p|^{2t}} \left\{ \epsilon\delta \left(\frac{\rho}{R}\right)^2 \right\}^{N-2|p|} \\
& + C_{\delta^{-2},-2t} N^{-2[t+\max\{-t,0\}]} \left\{ \frac{\epsilon}{\delta} \left(\frac{\rho}{R}\right)^2 \right\}^{N-2|p|} \Bigg].
\end{aligned}$$

Noting that $\epsilon \leq \delta^{-1}(R/\rho)^2$ we have

$$A_{42} \leq \begin{cases} C' N^{-2t} & \text{if } \epsilon = \delta^{-1}(R/\rho)^2 \wedge t \geq 0, \\ C' & \text{otherwise} \end{cases}$$

due to Proposition 3.7.1 (iii). Therefore, we obtain

$$T_{42} \leq \begin{cases} C_{42} N^{2s} \left(\frac{\epsilon}{\delta}\right)^N \|q\|^2_{\delta\rho/R,t} & \text{if } \epsilon = \delta^{-1}(R/\rho)^2 \wedge t \geq 0, \\ C_{42} N^{2(s-t)} \left(\frac{\epsilon}{\delta}\right)^N \|q\|^2_{\delta\rho/R,t} & \text{otherwise.} \end{cases}$$

Combining the above estimates we obtain

$$\|q - q^{(N)}\|^2_{\epsilon\rho/R,s} \leq C N^{2P(\epsilon,s,\delta,t)} \left(\frac{\epsilon}{\delta}\right)^N \|q\|^2_{\delta\rho/R,t}$$

as desired.

Chapter 4

Method of fundamental solutions for biharmonic equation in disk based on Almansi-type decomposition

Abstract

The aim of this chapter is to analyze mathematically the method of fundamental solutions applied to biharmonic problem. The key idea is to use Almansi-type decomposition of biharmonic function, which enables us to represent the biharmonic function in terms of two harmonic functions. Based on this decomposition, we prove that an approximate solution exists uniquely and that an approximation error decays exponentially with respect to the number of the singular points. We finally present results of numerical experiments, which verify that our error estimate is almost optimal. This chapter is based on the following submitted paper:

- K. Sakakibara *Method of fundamental solutions for biharmonic equation based on Almansi-type decomposition*, submitted.

4.1 Introduction and main results

Let Ω be a simply-connected region in the plane. We then consider the following boundary value problem for biharmonic equation:

$$\begin{cases} \triangle^2 u = 0 & \text{in } \Omega, \\ u = f & \text{on } \partial\Omega, \\ \dfrac{\partial u}{\partial \nu} = g & \text{on } \partial\Omega, \end{cases} \tag{4.1.1}$$

where $\triangle^2 = \dfrac{\partial^2}{\partial x^4} + \dfrac{\partial^4}{\partial x^2 \partial y^2} + \dfrac{\partial^4}{\partial y^4}$ is the biharmonic operator in the plane, $\partial u/\partial \nu$ denotes the outward normal derivative of u on $\partial\Omega$, and f and g are given functions defined on $\partial\Omega$.

Goursat [28] proved that for a given biharmonic function u, there exist two holomorphic function φ and ψ in Ω such that the following relation holds:

$$u(x,y) = \varphi(z) + \overline{\varphi}(z) + \overline{z}\psi(z) + z\overline{\psi}(z) = 2\Re(\varphi(z) + \overline{z}\psi(z)).$$

Especially, defining $\gamma(x,y) = 2\Re\varphi(z)$, $\alpha(x,y) = 2\Re\psi(z)$, and $\beta(x,y) = 2\Im\psi(z)$, we have

$$u(x,y) = \gamma(x,y) + x\alpha(x,y) + y\beta(x,y).$$

Namely, the above implies that any biharmonic function can be decomposed into three harmonic functions, two of which are conjugate harmonic. Moreover, Krakowski and Charnes [61] and Bock and Gürlebeck [12] showed that the number of harmonic functions are indeed equal to 2, that is, for a given biharmonic function u in Ω, there exist harmonic functions p, q, $\overline{p}$, $\overline{q}$, $\overline{\overline{p}}$, $\overline{\overline{q}}$ such that the following hold:

$$\begin{aligned} u(x,y) &= p(x,y) + (x^2+y^2)q(x,y), \\ u(x,y) &= \overline{p}(x,y) + x\overline{q}(x,y), \\ u(x,y) &= \overline{\overline{p}}(x,y) + y\overline{\overline{q}}(x,y). \end{aligned} \tag{4.1.2}$$

Especially, (4.1.2) is a decomposition of Almansi type. Therefore we only have to find suitable approximations of two harmonic functions. We hereafter consider the case of (4.1.2) restricted to the case where Ω is a disk D_ρ with radius ρ having the origin as its center.

Based on the Almansi-type decomposition of biharmonic function, the following scheme for MFS can be obtained [42]. Choose the singular points $\{y_k\}_{k=1}^n$ as $y_k = R\omega^{k-1}$, $1 \le k \le N$, and construct approximations for p and q as follows:

$$p^{(N)}(x) = \sum_{k=1}^{N} Q_k^p E(x-y_k), \quad q^{(N)}(x) = \sum_{k=1}^{N} Q_k^q E(x-y_k),$$

where $E(x) = (2\pi)^{-1}\log|x|$ is the fundamental solution of the Laplace operator $\triangle$, $R > \rho$, and $\omega = \exp(2\pi\mathrm{i}/N)$. Namely, an approximation $u^{(N)}$ for the solution u of (4.1.1) is given by

$$u^{(N)}(x) = \sum_{k=1}^{N} (Q_k^p + |x|^2 Q_k^q) E(x-y_k). \tag{4.1.3}$$

Remark 4.1.1. In the usual formulation of MFS, the approximate solution is given by

$$u^{(N)}(x) = \sum_{k=1}^{N} (Q_k^p + |x-y_k|^2 Q_k^q) E(x-y_k) \tag{4.1.4}$$

since the function $(8\pi)^{-2}|x|^2E(x)$ is the fundamental solution for the biharmonic operator $\triangle^2$. MFS of the form (4.1.4) has been proposed firstly in Karageorghis and Fairweather [41], but there does not exist any mathematical result so far.

The coefficients $\{Q_k^{p,q}\}_{k=1}^N$ are determined by the collocation method, that is, take the collocation points $\{x_j\}_{j=1}^N$ as $x_j = \rho\omega^{j-1}$, and impose the following boundary conditions:

$$u^{(N)}(x_j) = f(x_j), \quad \frac{\partial u^{(N)}}{\partial \nu}(x_j) = g(x_j), \quad j = 1,2,\dots,N. \tag{4.1.5}$$

This type of MFS based on Almansi-type decomposition has been investigated in Li et al. [67] and some mathematical analysis has been done. However, they consider the Trefftz method rather than the collocation method. Thus, the aim of this chapter is to establish mathematical theory of MFS based on Almansi-type decomposition (4.1.3) together with the collocation method when Ω is a disk as a first step for developing mathematical theory in arbitrary region.

We are now in a position to state the main theorems of this chapter.

Theorem 4.1.2. *An approximate solution $u^{(N)}$ for (4.1.1) satisfying (4.1.5) exists uniquely if and only if $R^N - \rho^N \neq 1$.*

Theorem 4.1.3. *Suppose that $R^N - \rho^N \neq 1$ and $R \neq 1$ holds. Also suppose that the Fourier coefficients $\{f_n\}_{n\in\mathbb{Z}}$ and $\{g_n\}_{n\in\mathbb{Z}}$ of f and g can be estimated as follows:*

$$|f_n|,\ |g_n| = O\left(\left(\frac{\rho}{r_0}\right)^{|n|}\right) \quad (\forall n \in \mathbb{Z}),$$

where $r_0 > \rho$. Then we have

$$\|u - u^{(N)}\|_{L^\infty(\Omega)} = \begin{cases} O\left(N\left(\dfrac{\rho}{r_0}\right)^{N/2}\right) & (R^2/(\rho r_0) > 1), \\ O\left(N^2\left(\dfrac{\rho}{R}\right)^{N}\right) & (R^2/(\rho r_0) = 1), \\ O\left(N\left(\dfrac{\rho}{R}\right)^{N}\right) & (R^2/(\rho r_0) < 1). \end{cases}$$

The contents of this chapter are as follows. In Section 4.2, we prove Theorem 4.1.2, which assures the unqiue existence of approximate solution. In Section 4.3, the exponential decay of approximation error, that is, Theorem 4.3 is proved. In Section 4.4, we present several results of numerical experiments, which exemplify the sharpness of our error estimate. We also compare the conventional scheme (4.1.4) with the present scheme (4.1.3) based on Almansi-type decomposition. In Section 4.5, we summarize this chapter and give some concluding remarks.

4.2 Unique existence

In this section, we establish the unique existence of approximate solution $u^{(N)}$ for (4.1.1) of the form (4.1.3) satisfying (4.1.5) provided that the singular points $\{y_k\}_{k=1}^N$ and the collocation points $\{x_j\}_{j=1}^N$ are given as in the previous section.

Since we have

$$\frac{\partial}{\partial x_{1,2}} E(x - y_k) = \frac{1}{2\pi} \frac{x_{1,2} - y_{k1,k2}}{|x - y_k|^2},$$
$$\frac{\partial}{\partial x_{1,2}} (|x|^2 E(x - y_k)) = 2x_{1,2} E(x - y_k) + |x|^2 \frac{1}{2\pi} \frac{x_{1,2} - y_{k1,k2}}{|x - y_k|^2},$$

the normal derivative of $u^{(N)}$ at $x = (x_1, x_2)^{\mathrm{T}} \in \partial\Omega$ can be computed as

$$\begin{aligned} \frac{\partial u^{(N)}}{\partial \nu}(x) &= \sum_{k=1}^N \left[\frac{Q_k^p}{2\pi|x - y_k|^2} \begin{pmatrix} x_1 - y_{k1} \\ x_2 - y_{k2} \end{pmatrix} \cdot \frac{1}{|x|} \begin{pmatrix} x_1 \\ x_2 \end{pmatrix} \right. \\ &\qquad \left. + Q_k^q \left\{ 2E(x - y_k) \begin{pmatrix} x_1 \\ x_2 \end{pmatrix} \cdot \frac{1}{|x|} \begin{pmatrix} x_1 \\ x_2 \end{pmatrix} + \frac{|x|^2}{2\pi|x - y_k|^2} \begin{pmatrix} x_1 - y_{k1} \\ x_2 - y_{k2} \end{pmatrix} \cdot \frac{1}{|x|} \begin{pmatrix} x_1 \\ x_2 \end{pmatrix} \right\} \right] \\ &= \sum_{k=1}^N \left[\frac{Q_k^p}{2\pi} \frac{(x/|x| \mid x - y_k)}{|x - y_k|^2} + Q_k^q \left\{ 2|x| E(x - y_k) + \frac{|x|^2}{2\pi} \frac{(x/|x| \mid x - y_k)}{|x - y_k|^2} \right\} \right] \\ &= \sum_{k=1}^N \left[\frac{Q_k^p}{2\pi} \Re\left(\frac{x/|x|}{x - y_k}\right) + Q_k^q \left\{ 2|x| E(x - y_k) + \frac{|x|^2}{2\pi} \Re\left(\frac{x/|x|}{x - y_k}\right) \right\} \right]. \end{aligned}$$

Especially, on the collocation point $x_j = \rho\omega^{j-1}$, we have

$$\frac{\partial u^{(N)}}{\partial \nu}(x_j) = \sum_{k=1}^{N} \left[\frac{Q_k^p}{2\pi} \Re\left(\frac{\omega^{j-1}}{x_j - y_k} \right) + Q_k^q \left\{ 2\rho E(x_j - y_k) + \frac{\rho^2}{2\pi} \Re\left(\frac{\omega^{j-1}}{x_j - y_k} \right) \right\} \right].$$

Therefore the collocation equations (4.1.5) are equivalent to the following system of $2N$ linear equations:

$$G\boldsymbol{Q} = \boldsymbol{b},$$

where

$$\begin{aligned}
&G = \begin{pmatrix} G_{11} & G_{12} \\ G_{21} & G_{22} \end{pmatrix} \in \mathbb{R}^{2N\times 2N}, \\
&G_{11} = (E(x_j - y_k) \mid \ j,k = 1,2,\dots,N) \in \mathbb{R}^{N\times N}, \\
&G_{12} = \left(\rho^2 E(x_j - y_k) \ \middle|\ j,k = 1,2,\dots,N\right) = \rho^2 G_{11} \in \mathbb{R}^{N\times N}, \\
&G_{21} = \left(\frac{1}{2\pi} \Re\left(\frac{\omega^{j-1}}{x_j - y_k} \right) \ \middle|\ j,k = 1,2,\dots,N \right) \in \mathbb{R}^{N\times N}, \\
&G_{22} = \left(2\rho E(x_j - y_k) + \frac{\rho^2}{2\pi} \Re\left(\frac{\omega^{j-1}}{x_j - y_k} \right) \ \middle|\ j,k = 1,2,\dots,N \right) \\
&\qquad = 2\rho G_{11} + \rho^2 G_{21} \in \mathbb{R}^{N\times N}, \\
&\boldsymbol{Q} = \begin{pmatrix} \boldsymbol{Q}^p \\ \boldsymbol{Q}^q \end{pmatrix} \in \mathbb{R}^{2N}, \quad \boldsymbol{Q}^{p,q} = (Q_1^{p,q}, Q_2^{p,q}, \dots, Q_N^{p,q})^{\mathrm{T}} \in \mathbb{R}^N, \\
&\boldsymbol{b} = \begin{pmatrix} \boldsymbol{f} \\ \boldsymbol{g} \end{pmatrix} \in \mathbb{R}^{2N}, \quad \boldsymbol{f} = (f(x_1), f(x_2), \dots, f(x_N))^{\mathrm{T}} \in \mathbb{R}^N, \\
&\qquad\qquad\qquad\qquad \boldsymbol{g} = (g(x_1), g(x_2), \dots, g(x_N))^{\mathrm{T}} \in \mathbb{R}^N.
\end{aligned}$$

We here note that each matrix $G_{\mu\nu}$ is circulant. Indeed, we have

$$\begin{aligned}
(G_{11})_{jk} &= E(x_j - y_k) = \frac{1}{2\pi} \log|\rho\omega^{j-1} - R\omega^{k-1}| = \frac{1}{2\pi} \log|\rho - R\omega^{k-j}|, \\
(G_{12})_{jk} &= \rho^2 (G_{11})_{jk} = \frac{\rho^2}{2\pi} \log|\rho - R\omega^{k-j}|, \\
(G_{21})_{jk} &= \frac{1}{2\pi} \Re\left(\frac{\omega^{j-1}}{x_j - y_k} \right) = \frac{1}{2\pi} \Re\left(\frac{1}{\rho - R\omega^{k-j}} \right), \\
(G_{22})_{jk} &= 2\rho (G_{11})_{jk} + \rho^2 (G_{21})_{jk} = \frac{\rho}{\pi} \log|\rho - R\omega^{k-j}| + \frac{\rho^2}{2\pi} \Re\left(\frac{1}{\rho - R\omega^{k-j}} \right).
\end{aligned}$$

Therefore, using the discrete Fourier transform, these matrices can be diagonalized as follows:

$$W^{-1} G_{jk} W = \operatorname{diag}\left[\gamma_{jk0}, \gamma_{jk1}, \dots, \gamma_{jk,N-1}\right],$$

where $W = \left(\frac{1}{\sqrt{N}} \omega^{(j-1)(k-1)} \ \middle|\ j,k = 1,2,\dots,N \right)$ denotes the discrete Fourier transform, and

$$\begin{aligned}
\gamma_{11l} &= \sum_{m=0}^{N-1} \omega^{ml} \frac{1}{2\pi} \log|\rho - R\omega^m|, \quad \gamma_{12l} = \rho^2 \gamma_{11l} = \rho^2 \sum_{m=0}^{N-1} \omega^{ml} \frac{1}{2\pi} \log|\rho - R\omega^m|, \\
\gamma_{21l} &= \sum_{m=0}^{N-1} \omega^{ml} \frac{1}{2\pi} \Re\left(\frac{1}{\rho - R\omega^m} \right),
\end{aligned}$$

$$\gamma_{22l} = 2\rho\gamma_{11l} + \rho^2\gamma_{21l} = 2\rho \sum_{m=0}^{N-1} \omega^{ml} \frac{1}{2\pi} \log|\rho - R\omega^m| + \rho^2 \sum_{m=0}^{N-1} \omega^{ml} \frac{1}{2\pi} \Re\left(\frac{1}{\rho - R\omega^m}\right).$$

Defining two auxiliary functions φ_l and ψ_l as

$$\varphi_l(z) = \sum_{m=0}^{N-1} \omega^{ml} E(z - R\omega^m), \quad \psi_l(z) = \sum_{m=0}^{N-1} \frac{\omega^{ml}}{2\pi} \Re\left(\frac{z/|z|}{z - R\omega^m}\right)$$

for each $l = 1, 2, \ldots, N$, we have

$$\gamma_{11l} = \varphi_l(\rho), \quad \gamma_{12l} = \rho^2\varphi_l(\rho), \quad \gamma_{21l} = \psi_l(\rho), \quad \gamma_{22l} = 2\rho\varphi_l(\rho) + \rho^2\psi_l(\rho). \tag{4.2.1}$$

Consequently, we obtain

$$\tilde{W}^{-1}G\tilde{W} = \begin{pmatrix} \gamma_{110} & & & & \gamma_{120} & & & \\ & \gamma_{111} & & & & \gamma_{121} & & \\ & & \ddots & & & & \ddots & \\ & & & \gamma_{11,N-1} & & & & \gamma_{12,N-1} \\ \gamma_{210} & & & & \gamma_{220} & & & \\ & \gamma_{211} & & & & \gamma_{221} & & \\ & & \ddots & & & & \ddots & \\ & & & \gamma_{21,N-1} & & & & \gamma_{22,N-1} \end{pmatrix},$$

where

$$\tilde{W} = \begin{pmatrix} W & O \\ O & W \end{pmatrix}.$$

Using the permutation matrix

$$P = \begin{pmatrix} \boldsymbol{e}_1 & \boldsymbol{e}_{N+1} & \boldsymbol{e}_2 & \boldsymbol{e}_{N+2} & \cdots & \boldsymbol{e}_N & \boldsymbol{e}_{2N} \end{pmatrix},$$

we have

$$P^{-1}\tilde{W}^{-1}G\tilde{W}P = \operatorname{diag}(\Phi_0, \Phi_1, \cdots, \Phi_{N-1}), \quad \Phi_l = \begin{pmatrix} \gamma_{11l} & \gamma_{12l} \\ \gamma_{21l} & \gamma_{22l} \end{pmatrix},$$

thus

$$\det G = \prod_{l=0}^{N-1} \det \Phi_l.$$

Therefore G is nonsingular if and only if all Φ_l's are nonsingular. The determinant of Φ_l can be computed as

$$\det \Phi_l = \gamma_{11l}\gamma_{22l} - \gamma_{12l}\gamma_{21l} = \varphi_l(\rho)(2\rho\varphi_l(\rho) + \rho^2\psi_l(\rho)) - \rho^2\varphi_l(\rho)\psi_l(\rho) = 2\rho\varphi_l(\rho)^2.$$

Therefore G is nonsingular if and only if all $\varphi_l(\rho)$ are not equal to 0.

In order to see the precise nature of φ_l and ψ_l, the following lemma is useful.

Lemma 4.2.1. *For all $z = re^{i\theta}$ ($r \in [0, R[$, $\theta \in \mathbb{R}$), we have*

$$\varphi_l(z) = \begin{cases} \dfrac{1}{2\pi} \log|z^N - R^N| & (l = 0), \\ -\dfrac{N}{4\pi} \displaystyle\sum_{n \equiv l} \frac{1}{|n|} \left(\frac{r}{R}\right)^{|n|} e^{in\theta} & (l = 1, \ldots, N-1). \end{cases}$$

Also, for all $z = re^{i\theta}$ $(r \in]0, R[\,,\ \theta \in \mathbb{R})$, *we have*

$$\psi_l(z) = -\frac{N}{4\pi r} \sum_{\substack{n \equiv l \\ n \in \mathbb{Z}\setminus\{0\}}} \left(\frac{r}{R}\right)^{|n|} e^{in\theta}.$$

Proof. We first prove formulae for φ_l. When $l \neq 0$, we have

$$\begin{aligned}\varphi_l(z) &= \sum_{m=0}^{N-1} E(z - R\omega^m) = \frac{1}{2\pi} \sum_{m=0}^{N-1} \log|z - R\omega^m| = \frac{1}{2\pi} \log\left|\prod_{m=0}^{N-1} (z - R\omega^m)\right| \\ &= \frac{1}{2\pi} \log|z^N - R^N|.\end{aligned}$$

When $l = 1, \ldots, N-1$, using the expansion

$$\begin{aligned}\log|z - R\omega^m| &= \log\left|-R\omega^m \left(1 - \frac{z}{R\omega^m}\right)\right| = \log R + \log\left|1 - \frac{z}{R\omega^m}\right| \\ &= \log R + \Re \log\left(1 - \frac{z}{R\omega^m}\right) = \log R - \Re \sum_{n=1}^{\infty} \frac{1}{n} \left(\frac{z}{R\omega^m}\right)^n \\ &= \log R - \Re \sum_{n=1}^{\infty} \frac{1}{n} \left(\frac{r}{R}\right)^n e^{in\theta} \omega^{-mn} \\ &= \log R - \sum_{n=1}^{\infty} \frac{1}{n} \left(\frac{r}{R}\right)^n \frac{e^{in\theta}\omega^{-mn} + e^{-in\theta}\omega^{mn}}{2} \\ &= \log R - \sum_{n \in \mathbb{Z}\setminus\{0\}} \frac{1}{2|n|} \left(\frac{r}{R}\right)^{|n|} e^{in\theta} \omega^{-mn}\end{aligned}$$

for $z = re^{i\theta}$, we have

$$\begin{aligned}\varphi_l(z) &= \sum_{m=0}^{N-1} \omega^{ml} \frac{1}{2\pi} \log|z - R\omega^m| \\ &= \frac{1}{2\pi} \sum_{m=0}^{N-1} \omega^{ml} \left[\log R - \sum_{n \in \mathbb{Z}\setminus\{0\}} \frac{1}{2|n|} \left(\frac{r}{R}\right)^{|n|} e^{in\theta} \omega^{-mn}\right] \\ &= -\frac{1}{4\pi} \sum_{n \in \mathbb{Z}\setminus\{0\}} \frac{1}{|n|} \left(\frac{r}{R}\right)^{|n|} e^{in\theta} \sum_{m=0}^{N-1} \omega^{m(l-n)} = -\frac{N}{4\pi} \sum_{n \equiv l} \frac{1}{|n|} \left(\frac{r}{R}\right)^{|n|} e^{in\theta}.\end{aligned}$$

Next we prove a formula for ψ_l. We can expand the kernel function as

$$\begin{aligned}\Re\left(\frac{z/|z|}{z - R\omega^m}\right) &= \Re\left(\frac{e^{i\theta}}{re^{i\theta} - R\omega^m}\right) = \Re\left(-\frac{1}{R\omega^m} \frac{e^{i\theta}}{1 - re^{i\theta}/R\omega^m}\right) \\ &= \Re\left(-\frac{e^{i\theta}}{R\omega^m} \sum_{n=0}^{\infty} \left(\frac{re^{i\theta}}{R\omega^m}\right)^n\right) = \Re\left(-\frac{1}{r} \sum_{n=1}^{\infty} \left(\frac{r}{R}\right)^n e^{in\theta} \omega^{-mn}\right) \\ &= -\frac{1}{2r} \sum_{n \in \mathbb{Z}\setminus\{0\}} \left(\frac{r}{R}\right)^{|n|} e^{in\theta} \omega^{-mn}.\end{aligned}$$

Therefore, we obtain

$$\psi_l(z) = \sum_{m=0}^{N-1} \frac{\omega^{ml}}{2\pi} \left[-\frac{1}{2r} \sum_{n\in\mathbb{Z}\setminus\{0\}} \left(\frac{r}{R}\right)^{|n|} \mathrm{e}^{\mathrm{i}n\theta} \omega^{-mn} \right]$$
$$= -\frac{1}{4\pi r} \sum_{n\in\mathbb{Z}\setminus\{0\}} \left(\frac{r}{R}\right)^{|n|} \mathrm{e}^{\mathrm{i}n\theta} \sum_{m=0}^{N-1} \omega^{m(l-n)} = -\frac{N}{4\pi r} \sum_{\substack{n\equiv l \\ n\in\mathbb{Z}\setminus\{0\}}} \left(\frac{r}{R}\right)^{|n|} \mathrm{e}^{\mathrm{i}n\theta}. \qquad \square$$

From this lemma, we have

$$\varphi_0(\rho) = \frac{1}{2\pi} \log|\rho^N - R^N|, \quad \varphi_l(\rho) = -\frac{N}{4\pi} \sum_{n\equiv l} \frac{1}{|n|} \left(\frac{\rho}{R}\right)^{|n|} < 0 \quad (l = 1, \ldots, N-1).$$

Hence, we can conclude that G is nonsingular if and only if $R^N - \rho^N \neq 1$ holds, which proves Theorem 4.1.2.

4.3 Error analysis

In this section, we give estimate for approximation error, which shows that the approximation error decays exponentially with respect to N when the boundary data f and g are analytic.

4.3.1 Exact solution for (4.1.1)

We here write down the exact solution u for (4.1.1) by virtue of Fourier expansion. Since p and q are harmonic in the disk D_ρ, they have the following complex Fourier expansions:

$$p(r,\theta) = \sum_{n\in\mathbb{Z}} a_n \left(\frac{r}{\rho}\right)^{|n|} \mathrm{e}^{\mathrm{i}n\theta}, \quad q(r,\theta) = \sum_{n\in\mathbb{Z}} b_n \left(\frac{r}{\rho}\right)^{|n|} \mathrm{e}^{\mathrm{i}n\theta}$$

for $0 \le r \le \rho$ and $\theta \in \mathbb{R}$. Then the exact solution have the following form:

$$u(r,\theta) = p(r,\theta) + r^2 q(r,\theta) = \sum_{n\in\mathbb{Z}} (a_n + r^2 b_n) \left(\frac{r}{\rho}\right)^{|n|} \mathrm{e}^{\mathrm{i}n\theta}$$

for $0 \le r \le \rho$ and $\theta \in \mathbb{R}$. The coefficients $\{a_n\}_{n\in\mathbb{Z}}$ and $\{b_n\}_{n\in\mathbb{Z}}$ are determined by the boundary conditions. From the Dirichlet boundary condition, we have

$$f(\theta) = \sum_{n\in\mathbb{Z}} a_n \mathrm{e}^{\mathrm{i}n\theta} + \sum_{n\in\mathbb{Z}} \rho^2 b_n \mathrm{e}^{\mathrm{i}n\theta},$$

that is,

$$a_n + \rho^2 b_n = \frac{1}{2\pi} \int_0^{2\pi} f(\theta) \mathrm{e}^{-\mathrm{i}n\theta} \,\mathrm{d}\theta = f_n.$$

Concerning the Neumann boundary condition, since the normal derivative of u can be computed as

$$\begin{aligned}\frac{\partial u}{\partial \nu} &= \frac{\partial u}{\partial r}\Big|_{r=\rho} = \frac{\partial}{\partial r}\left[a_0 + \sum_{n\in\mathbb{Z}\setminus\{0\}} \frac{a_n}{\rho^{|n|}} r^{|n|}\mathrm{e}^{\mathrm{i}n\theta} + \sum_{n\in\mathbb{Z}} \frac{b_n}{\rho^{|n|}} r^{|n|+2}\mathrm{e}^{\mathrm{i}n\theta}\right]\Bigg|_{r=\rho} \\ &= \frac{1}{\rho}\sum_{n\in\mathbb{Z}\setminus\{0\}} a_n|n|\mathrm{e}^{\mathrm{i}n\theta} + \rho\sum_{n\in\mathbb{Z}} b_n(|n|+2)\mathrm{e}^{\mathrm{i}n\theta} \\ &= \frac{1}{\rho}\sum_{n\in\mathbb{Z}} a_n|n|\mathrm{e}^{\mathrm{i}n\theta} + \rho\sum_{n\in\mathbb{Z}} b_n(|n|+2)\mathrm{e}^{\mathrm{i}n\theta},\end{aligned}$$

we obtain

$$\frac{a_n|n|}{\rho} + \rho b_n(|n|+2) = \frac{1}{2\pi}\int_0^{2\pi} g(\theta)\mathrm{e}^{-\mathrm{i}n\theta}\,\mathrm{d}\theta = g_n \quad (n\in\mathbb{Z}\setminus\{0\}).$$

Using the above relations, we can write down $\{a_n\}_{n\in\mathbb{Z}}$ and $\{b_n\}_{n\in\mathbb{Z}}$ explicitly in terms of the Fourier coefficients of f and g as follows:

$$a_n = \left(1+\frac{|n|}{2}\right)f_n - \frac{\rho}{2}g_n, \quad b_n = \frac{1}{2\rho^2}(\rho g_n - |n|f_n) \quad (n\in\mathbb{Z}).$$

4.3.2 Explicit form of the approximate solution

Let $G' = P^{-1}GP$ and $W' = P^{-1}\tilde{W}P$, that is,

$$W' = \begin{pmatrix} I & I & I & \cdots & I \\ I & \omega I & \omega^2 I & \cdots & \omega^{N-1} I \\ I & \omega^2 I & \omega^4 I & \cdots & \omega^{2(N-1)} I \\ \vdots & \vdots & \vdots & & \vdots \\ I & \omega^{(N-1)} I & \omega^{2(N-1)} I & \cdots & \omega^{(N-1)(N-1)} I \end{pmatrix},$$

where I denotes the 2×2 identity matrix. Then we have

$$P^{-1}\tilde{W}^{-1}G\tilde{W}P = (W')^{-1}G'W',$$

therefore we have

$$(W')^{-1}G'W' = \operatorname{diag}\left(\Phi_0, \Phi_1, \ldots, \Phi_{N-1}\right). \tag{4.3.1}$$

Using these matrices, the linear system $G\boldsymbol{Q} = \boldsymbol{b}$ could be transformed into the following one:

$$G'\boldsymbol{Q}' = \boldsymbol{b}',$$

where

$$\begin{aligned}\boldsymbol{Q}' &= P^{-1}\boldsymbol{Q} = \left(Q_1^p, Q_1^q, Q_2^p, Q_2^q, \ldots, Q_N^p, Q_N^q\right)^{\mathrm{T}}, \\ \boldsymbol{b}' &= P^{-1}\boldsymbol{f} = \left(f(x_1), g(x_1), f(x_2), g(x_2), \ldots, f(x_N), g(x_N)\right)^{\mathrm{T}}.\end{aligned}$$

We can represent $(G')^{-1}$ explicitly from (4.3.1) as follows:

$$(G')^{-1} = \left([(G')^{-1}]_{kj} \;\middle|\; k,j = 1,2,\ldots,N\right), \quad [(G')^{-1}]_{kj} = \frac{1}{N}\sum_{l=1}^{N}\omega^{(k-j)(l-1)}\Phi_{l-1}^{-1} \in \mathbb{R}^{2\times 2}.$$

If we write the boundary data f and g in the form of Fourier series expansion

$$f(\theta) = \sum_{n\in\mathbb{Z}} f_n \mathrm{e}^{\mathrm{i}n\theta}, \quad g(\theta) = \sum_{n\in\mathbb{Z}} g_n \mathrm{e}^{\mathrm{i}n\theta},$$

then the coefficients $\{Q_k^{p,q}\}_{k=1}^N$ are given as follows:

$$\begin{aligned}\begin{pmatrix} Q_k^p \\ Q_k^q \end{pmatrix} &= \sum_{j=1}^N \left(\frac{1}{N} \sum_{l=1}^N \omega^{(k-j)(l-1)} \Phi_{l-1}^{-1} \right) \sum_{n\in\mathbb{Z}} \begin{pmatrix} f_n \\ g_n \end{pmatrix} \omega^{(j-1)n} \\ &= \sum_{n\in\mathbb{Z}} \omega^{(k-1)n} \Phi_n^{-1} \begin{pmatrix} f_n \\ g_n \end{pmatrix}.\end{aligned}$$

Therefore the approximate solution can be written as

$$\begin{aligned} u^{(N)}(x) &= \sum_{k=1}^N \left(Q_k^p + |x|^2 Q_k^q\right) E(x-y_k) = \sum_{k=1}^N E(x-y_k) \begin{pmatrix} 1 & |x|^2 \end{pmatrix} \begin{pmatrix} Q_k^p \\ Q_k^q \end{pmatrix} \\ &= \sum_{k=1}^N E(x-y_k) \begin{pmatrix} 1 & |x|^2 \end{pmatrix} \sum_{n\in\mathbb{Z}} \omega^{(k-1)n} \Phi_n^{-1} \begin{pmatrix} f_n \\ g_n \end{pmatrix} \\ &= \sum_{n\in\mathbb{Z}} \varphi_n(x) \begin{pmatrix} 1 & |x|^2 \end{pmatrix} \Phi_n^{-1} \begin{pmatrix} f_n \\ g_n \end{pmatrix} \\ &= \sum_{n\in\mathbb{Z}} \frac{\varphi_n(x)}{\det \Phi_n} \left[\gamma_{22,n} f_n - \gamma_{12,n} g_n + |x|^2 \left(-\gamma_{21,n} f_n + \gamma_{11,n} g_n\right)\right]. \end{aligned}$$

Therefore we can evaluate the error $\|u - u^{(N)}\|_{L^\infty(\Omega)}$ as

$$\begin{aligned} \|u - u^{(N)}\|_{L^\infty(\Omega)} &= \sup_{\substack{0\le r<\rho \\ \theta\in\mathbb{R}}} |u(r\mathrm{e}^{\mathrm{i}\theta}) - u^{(N)}(r\mathrm{e}^{\mathrm{i}\theta})| \\ &= \sup_{\substack{0\le r<\rho \\ \theta\in\mathbb{R}}} \left| \sum_{n\in\mathbb{Z}} \left(a_n \left(\frac{r}{\rho}\right)^{|n|} \mathrm{e}^{\mathrm{i}n\theta} - (\gamma_{22,n} f_n - \gamma_{12,n} g_n) \frac{\varphi_n(r\mathrm{e}^{\mathrm{i}\theta})}{\det \Phi_n} \right) \right. \\ &\qquad \left. + r^2 \sum_{n\in\mathbb{Z}} \left(b_n \left(\frac{r}{\rho}\right)^{|n|} \mathrm{e}^{\mathrm{i}n\theta} - (-\gamma_{21,n} f_n + \gamma_{11,n} g_n) \frac{\varphi_n(r\mathrm{e}^{\mathrm{i}\theta})}{\det \Phi_n} \right) \right| \\ &= \sup_{\substack{0\le r<\rho \\ \theta\in\mathbb{R}}} \left| \sum_{n\in\mathbb{Z}} f_n \left(\left(1 + \frac{|n|}{2}\right) \left(\frac{r}{\rho}\right)^{|n|} \mathrm{e}^{\mathrm{i}n\theta} - \gamma_{22,n} \frac{\varphi_n(r\mathrm{e}^{\mathrm{i}\theta})}{\det \Phi_n} \right) \right. \\ &\qquad + \sum_{n\in\mathbb{Z}} g_n \left(-\frac{\rho}{2} \left(\frac{r}{\rho}\right)^{|n|} \mathrm{e}^{\mathrm{i}n\theta} + \gamma_{12,n} \frac{\varphi_n(r\mathrm{e}^{\mathrm{i}\theta})}{\det \Phi_n} \right) \\ &\qquad + r^2 \sum_{n\in\mathbb{Z}} f_n \left(-\frac{|n|}{2\rho^2} \left(\frac{r}{\rho}\right)^{|n|} \mathrm{e}^{\mathrm{i}n\theta} + \gamma_{21,n} \frac{\varphi_n(r\mathrm{e}^{\mathrm{i}\theta})}{\det \Phi_n} \right) \\ &\qquad \left. + r^2 \sum_{n\in\mathbb{Z}} g_n \left(\frac{1}{2\rho} \left(\frac{r}{\rho}\right)^{|n|} \mathrm{e}^{\mathrm{i}n\theta} - \gamma_{11,n} \frac{\varphi_n(r\mathrm{e}^{\mathrm{i}\theta})}{\det \Phi_n} \right) \right|. \end{aligned}$$

Since the 1st and 2nd terms are harmonic, and the 3rd and 4th terms are of the form $r^2 \times$ harmonic, the above can be bounded by

$$\sum_{n\in\mathbb{Z}} \left(|f_n| g_{1n} + |g_n| g_{2n} + \rho^2 |f_n| g_{3n} + \rho^2 |g_n| g_{4n} \right), \tag{4.3.2}$$

where $g_{jn} = \sup_{\theta\in\mathbb{R}} \alpha_{jn}(\theta)$ and

$$\alpha_{1n}(\theta) = \left| \left(1 + \frac{|n|}{2}\right) \mathrm{e}^{\mathrm{i}n\theta} - \gamma_{22,n} \frac{\varphi_n(\rho \mathrm{e}^{\mathrm{i}\theta})}{\det \Phi_n} \right|, \quad \alpha_{2n}(\theta) = \left| -\frac{\rho}{2} \mathrm{e}^{\mathrm{i}n\theta} + \gamma_{12,n} \frac{\varphi_n(\rho \mathrm{e}^{\mathrm{i}\theta})}{\det \Phi_n} \right|,$$
$$\alpha_{3n}(\theta) = \left| -\frac{|n|}{2\rho^2} \mathrm{e}^{\mathrm{i}n\theta} + \gamma_{21,n} \frac{\varphi_n(\rho \mathrm{e}^{\mathrm{i}\theta})}{\det \Phi_n} \right|, \quad \alpha_{4n}(\theta) = \left| \frac{1}{2\rho} \mathrm{e}^{\mathrm{i}n\theta} - \gamma_{11,n} \frac{\varphi_n(\rho \mathrm{e}^{\mathrm{i}\theta})}{\det \Phi_n} \right|$$

Firstly, we give global estimates on g_{jn}.

Lemma 4.3.1. *There exists some positive constant $C = C(\rho, R)$ such that*

$$g_{1n}, g_{3n} \le C(1 + |n|), \quad g_{2n}, g_{4n} \le C$$

hold for all $n \in \mathbb{Z}$.

Proof. Note that $g_{jn} = g_{jm}$ holds if $n \equiv m$. Therefore we only have to show that the desired inequalities hold for $n \in \Lambda'_N$.

We first show the estimate on g_{1n}. By definition we have

$$|\alpha_{1n}(\theta)| \le 1 + \frac{|n|}{2} + \left| \gamma_{22n} \frac{\varphi_n(\rho \mathrm{e}^{\mathrm{i}\theta})}{\det \Phi_n} v \right|$$

for all $\theta \in \mathbb{R}$. Since $\gamma_{22n} = 2\rho\varphi_n(\rho) + \rho^2 \psi_n(\rho)$ and $\det \Phi_n = 2\rho\varphi_n(\rho)^2$, the 3rd term is bounded as

$$\left| \gamma_{22n} \frac{\varphi_n(\rho \mathrm{e}^{\mathrm{i}\theta})}{\det \Phi_n} \right| \le \left(1 + \frac{\rho}{2} \frac{|\psi_n(\rho)|}{|\varphi_n(\rho)|} \right) \frac{|\varphi_n(\rho \mathrm{e}^{\mathrm{i}\theta})|}{|\varphi_n(\rho)|}.$$

When $n = 0$, we evaluate $|\varphi_0(\rho)|$, $|\psi_0(\rho)|$, $|\varphi_0(\rho \mathrm{e}^{\mathrm{i}\theta})|$ as in the following. As to $|\varphi_0(\rho)|$, we know that $|\varphi_0(\rho)| \neq 0$ and

$$|\varphi_0(\rho)| = \left| \frac{1}{2\pi} \log(\rho^N - R^N) \right| = \frac{1}{2\pi} \left| N \log R + \log \left(1 - \left(\frac{\rho}{R} \right) \right)^N \right| \longrightarrow \infty \quad \text{as } N \to \infty,$$

which implies that there exists some positive constant C' such that $|\varphi_0(\rho)| \ge C'$ holds. Next, $|\psi_0(\rho)|$ can be bounded straightforwardly as

$$|\psi_0(\rho)| = \left| -\frac{N}{4\pi\rho} \cdot 2 \sum_{l=1}^{\infty} \left(\frac{\rho}{R} \right)^{lN} \right| = \left| -\frac{N}{2\pi\rho} \frac{(\rho/R)^N}{1 - (\rho/R)^N} \right| \le CN \left(\frac{\rho}{R} \right)^N.$$

Finally, concerning $|\varphi_0(\rho \mathrm{e}^{\mathrm{i}\theta})|$, we have

$$|\varphi_0(\rho \mathrm{e}^{\mathrm{i}\theta})| = \left| \frac{1}{2\pi} \log |(\rho \mathrm{e}^{\mathrm{i}\theta})^N - R^N| \right| \le \frac{1}{2\pi} \max \left\{ |\log(R^N - \rho^N)|, |\log(R^N + \rho^N)| \right\}.$$

These estimates lead us to

$$|\alpha_{10}(\theta)| \le 1 + \left(1 + CN \left(\frac{\rho}{R} \right)^N \right) \max \left\{ 1, \frac{|\log(R^N + \rho^N)|}{|\log(R^N - \rho^N)|} \right\} \le C.$$

When $n \in \Lambda'_N \setminus \{0\}$, we have

$$|\psi_n(\rho)| = \left| -\frac{N}{4\pi\rho} \sum_{m\equiv n} \left(\frac{\rho}{R}\right)^{|m|} \right| \le CN \left(\frac{\rho}{R}\right)^{|n|},$$
$$|\varphi_n(\rho)| = \left| -\frac{N}{4\pi} \sum_{m\equiv n} \frac{1}{|m|} \left(\frac{\rho}{R}\right)^{|m|} \right| \ge \frac{N}{4\pi|n|} \left(\frac{\rho}{R}\right)^{|n|},$$
$$|\varphi_n(\rho \mathrm{e}^{\mathrm{i}\theta})| = \left| -\frac{N}{4\pi} \sum_{m\equiv n} \frac{1}{|m|} \left(\frac{\rho}{R}\right)^{|m|} \mathrm{e}^{\mathrm{i}m\theta} \right| \le \frac{N}{4\pi} \sum_{m\equiv n} \frac{1}{|m|} \left(\frac{\rho}{r}\right)^{|m|} = |\varphi_n(\rho)|.$$

Therefore we obtain

$$|\alpha_{1n}(\theta)| \le 1 + \frac{|n|}{2} + (1 + C|n|) \le C(1 + |n|).$$

Using the estimate on g_{1n} and the relations (4.2.1), we have

$$|\alpha_{2n}(\theta)| \le \frac{\rho}{2} + \frac{\rho}{2} \frac{|\varphi_n(\rho \mathrm{e}^{\mathrm{i}\theta})|}{|\varphi_n(\rho)|}, \quad |\alpha_{3n}(\theta)| \le \frac{|n|}{2\rho^2} + \frac{1}{2\rho} \frac{|\psi_n(\rho)|}{|\varphi_n(\rho)|} \frac{|\varphi_n(\rho \mathrm{e}^{\mathrm{i}\theta})|}{|\varphi_n(\rho)|},$$
$$|\alpha_{4n}(\theta)| \le \frac{1}{2\rho} + \frac{1}{2\rho} \frac{|\varphi_0(\rho \mathrm{e}^{\mathrm{i}\theta})|}{|\varphi_n(\rho)|}.$$

Hence we have the desired global bounds. □

We next give more precise estimates on g_{jn} for $0 \le n \le N/2$.

Lemma 4.3.2. *There exists some positive constant $C = C(\rho, R)$ such that*

$$g_{10}, g_{30} \le C \left(\frac{\rho}{R}\right)^N, \quad g_{20}, g_{40} \le CN^{-1} \left(\frac{\rho}{R}\right)^N,$$

and

$$g_{1n}, g_{3n} \le Cn \left(\frac{\rho}{R}\right)^{N-2n}, \quad g_{2n}, g_{4n} \le \frac{Cn}{N-n} \left(\frac{\rho}{R}\right)^{N-2n}$$

hold for $1 \le n \le N/2$ with sufficiently large N.

Proof. We first note that if N is sufficiently large then $|\varphi_0(\rho)|^{-1} \le C/(N|\log R|)$ holds.

Firstly, we show estimates on g_{1n}. When $n = 0$, we have

$$|\alpha_{10}(\theta)| = \left| 1 - \gamma_{220} \frac{\varphi_0(\rho \mathrm{e}^{\mathrm{i}\theta})}{\det \Phi_0} \right| = \frac{|2\rho\varphi_0(\rho)^2 - (2\rho\varphi_0(\rho) + \rho^2\psi_0(\rho))\varphi_0(\rho \mathrm{e}^{\mathrm{i}\theta})|}{2\rho\varphi_0(\rho)^2}$$
$$= \frac{|2\rho\varphi_0(\rho)(\varphi_0(\rho) - \varphi_0(\rho \mathrm{e}^{\mathrm{i}\theta})) - \rho^2\psi_0(\rho)\varphi_0(\rho \mathrm{e}^{\mathrm{i}\theta})|}{2\rho\varphi_0(\rho)^2}$$
$$\le \frac{|\varphi_0(\rho) - \varphi_0(\rho \mathrm{e}^{\mathrm{i}\theta})|}{|\varphi_0(\rho)|} + \frac{\rho}{2} \frac{|\psi_0(\rho)|}{|\varphi_0(\rho)|} \frac{|\varphi_0(\rho \mathrm{e}^{\mathrm{i}\theta})|}{|\varphi_0(\rho)|}.$$

The previous estimates yields the following bound for the 2nd term:

$$\frac{\rho}{2} \frac{|\psi_0(\rho)|}{|\varphi_0(\rho)|} \frac{|\varphi_0(\rho \mathrm{e}^{\mathrm{i}\theta})|}{|\varphi_0(\rho)|} \le C \left(\frac{\rho}{R}\right)^N.$$

As to the 1st term, we have

$$\begin{aligned}|\varphi_0(\rho)-\varphi_0(\rho\mathrm{e}^{\mathrm{i}\theta})| &= \left|\frac{1}{2\pi}\log|\rho^N-R^N|-\frac{1}{2\pi}\log|(\rho\mathrm{e}^{\mathrm{i}\theta})^N-R^N|\right| \\ &= \frac{1}{2\pi}\left|-\sum_{l=1}^{\infty}\frac{1}{l}\left(\frac{\rho}{R}\right)^{lN}+\sum_{l=1}^{\infty}\frac{1}{l}\left(\frac{\rho}{R}\right)^{lN}\Re\left(\mathrm{e}^{\mathrm{i}lN\theta}\right)\right| \\ &\le \frac{1}{\pi}\sum_{l=1}^{\infty}\frac{1}{l}\left(\frac{\rho}{R}\right)^{lN}\le C\left(\frac{\rho}{R}\right)^{N}.\end{aligned}$$

Therefore we obtain

$$|\alpha_{10}(\theta)|\le C\left(\frac{\rho}{R}\right)^{N},\quad \text{or}\quad g_{10}\le C\left(\frac{\rho}{R}\right)^{N}.$$

When $1\le n\le N/2$, since $\gamma_{22n}=2\rho\varphi_n(\rho)+\rho^2\psi_n(\rho)$ and $\det\Phi_n=2\rho\varphi_n(\rho)^2$, we have

$$\begin{aligned}&\left(1+\frac{|n|}{2}\right)\mathrm{e}^{\mathrm{i}n\theta}-\gamma_{22n}\frac{\varphi_n(\rho\mathrm{e}^{\mathrm{i}\theta})}{\det\Phi_n} \\ &\quad=\frac{1}{2\rho\varphi_n(\rho)^2}\left[2\rho\varphi_n(\rho)^2\left(1+\frac{|n|}{2}\right)\mathrm{e}^{\mathrm{i}n\theta}-(2\rho\varphi_n(\rho)+\rho^2\psi_n(\rho))\varphi_n(\rho\mathrm{e}^{\mathrm{i}\theta})\right] \\ &\quad=\frac{1}{2\rho\varphi_n(\rho)^2}\underbrace{\left[2\rho\varphi_n(\rho)\left(\varphi_n(\rho)\left(1+\frac{|n|}{2}\right)\mathrm{e}^{\mathrm{i}n\theta}-\varphi_n(\rho\mathrm{e}^{\mathrm{i}\theta})\right)-\rho^2\psi_n(\rho)\varphi_n(\rho\mathrm{e}^{\mathrm{i}\theta})\right]}_{=:(*)}\end{aligned}$$

The equation $(*)$ within the brackets can be computed as follows:

$$\begin{aligned}(*) &= 2\rho\cdot\underbrace{\frac{-N}{4\pi}\sum_{l\equiv n}\frac{1}{|l|}\left(\frac{\rho}{R}\right)^{|l|}}_{=\varphi_n(\rho)} \\ &\quad\times\Bigg[\underbrace{-\frac{N}{4\pi}\sum_{m\equiv n}\frac{1}{|m|}\left(\frac{\rho}{R}\right)^{|m|}}_{=\varphi_n(\rho)}\left(1+\frac{|n|}{2}\right)\mathrm{e}^{\mathrm{i}n\theta}-\underbrace{\frac{-N}{4\pi}\sum_{m\equiv n}\frac{1}{|m|}\left(\frac{\rho}{R}\right)^{|m|}\mathrm{e}^{\mathrm{i}m\theta}}_{=\varphi_n(\rho\mathrm{e}^{\mathrm{i}\theta})}\Bigg] \\ &\qquad-\rho^2\underbrace{\frac{-N}{4\pi\rho}\sum_{l\equiv n}\left(\frac{\rho}{R}\right)^{|l|}}_{=\psi_n(\rho)}\underbrace{\frac{-N}{4\pi}\sum_{m\equiv n}\frac{1}{|m|}\left(\frac{\rho}{R}\right)^{|m|}\mathrm{e}^{\mathrm{i}m\theta}}_{=\varphi_n(\rho\mathrm{e}^{\mathrm{i}\theta})} \\ &=\frac{\rho N^2}{8\pi^2}\sum_{l\equiv n}\frac{1}{|l|}\left(\frac{\rho}{R}\right)^{|l|}\sum_{m\equiv n}\frac{1}{|m|}\left(\frac{\rho}{R}\right)^{|m|}(\mathrm{e}^{\mathrm{i}n\theta}-\mathrm{e}^{\mathrm{i}m\theta}) \\ &\qquad+\frac{\rho N^2}{16\pi^2}\sum_{l\equiv n}\frac{1}{|l|}\left(\frac{\rho}{R}\right)^{|l|}\sum_{m\equiv n}\frac{|n|}{|m|}\left(\frac{\rho}{R}\right)^{|m|}\mathrm{e}^{\mathrm{i}n\theta}-\frac{\rho N^2}{16\pi^2}\sum_{l\equiv n}\left(\frac{\rho}{R}\right)^{|l|}\sum_{m\equiv n}\frac{1}{|m|}\left(\frac{\rho}{R}\right)^{|m|}\mathrm{e}^{\mathrm{i}m\theta} \\ &=\frac{\rho N^2}{8\pi^2}\sum_{l\equiv n}\frac{1}{|l|}\left(\frac{\rho}{R}\right)^{|l|}\sum_{m\equiv n}\frac{1}{|m|}\left(\frac{\rho}{R}\right)^{|m|}(\mathrm{e}^{\mathrm{i}n\theta}-\mathrm{e}^{\mathrm{i}m\theta})\quad\cdots\cdots\quad①\\ &\qquad+\frac{\rho N^2}{16\pi^2}\sum_{\substack{l,m\equiv n\\(l,m)\neq(n,n)}}\frac{1}{|m|}\left(\frac{\rho}{R}\right)^{|l|+|m|}\left[\frac{|n|}{|l|}\mathrm{e}^{\mathrm{i}n\theta}-\mathrm{e}^{\mathrm{i}m\theta}\right].\quad\cdots\cdots\quad②\end{aligned}$$

① can be bounded as follows:

$$
\begin{aligned}
|①| &\le \frac{\rho N^2}{8\pi^2}\sum_{l\equiv n}\frac{1}{|l|}\left(\frac{\rho}{R}\right)^{|l|}\left|\sum_{\substack{m\equiv n\\ m\neq n}}\frac{1}{|m|}\left(\frac{\rho}{R}\right)^{|m|}(\mathrm{e}^{\mathrm{i}n\theta}-\mathrm{e}^{\mathrm{i}m\theta})\right| \\
&= C\frac{N^2}{n}\left(\frac{\rho}{R}\right)^{n}\left|\sum_{t=1}^{\infty}\left\{\frac{1}{tN+n}\left(\frac{\rho}{R}\right)^{tN+n}(\mathrm{e}^{\mathrm{i}n\theta}-\mathrm{e}^{\mathrm{i}(tN+n)\theta})\right.\right. \\
&\qquad\left.\left.+\frac{1}{tN-n}\left(\frac{\rho}{R}\right)^{tN-n}(\mathrm{e}^{\mathrm{i}n\theta}-\mathrm{e}^{\mathrm{i}(tN-n)\theta})\right\}\right| \\
&\le C\frac{N^2}{n}\left(\frac{\rho}{R}\right)^{n}\sum_{t=1}^{\infty}\left\{\frac{1}{tN+n}\left(\frac{\rho}{R}\right)^{tN+n}+\frac{1}{tN-n}\left(\frac{\rho}{R}\right)^{tN-n}\right\} \\
&\le C\frac{N^2}{n(N-n)}\left(\frac{\rho}{R}\right)^{N}\left(1+\left(\frac{\rho}{R}\right)^{2n}\right)\sum_{t=0}^{\infty}\left(\frac{\rho}{R}\right)^{tN} \le C\frac{N^2}{n(N-n)}\left(\frac{\rho}{R}\right)^{N}.
\end{aligned}
$$

② is decomposed into 3 parts as follows:

$$
\begin{aligned}
② = \frac{\rho N^2}{16\pi^2}\Bigg[&\left(\frac{\rho}{R}\right)^{n}\sum_{m\in I(n)}\frac{1}{|m|}\left(\frac{\rho}{R}\right)^{|m|}(\mathrm{e}^{\mathrm{i}n\theta}-\mathrm{e}^{\mathrm{i}m\theta}) \quad \cdots\cdots \quad ③ \\
&\frac{1}{|n|}\left(\frac{\rho}{R}\right)^{|n|}\sum_{l\in I(n)}\left(\frac{|n|}{|l|}-1\right)\left(\frac{\rho}{R}\right)^{|l|}\mathrm{e}^{\mathrm{i}n\theta} \quad \cdots\cdots \quad ④ \\
&\sum_{l\in I(n)}\left(\frac{\rho}{R}\right)^{|l|}\sum_{m\in I(n)}\frac{1}{|m|}\left(\frac{\rho}{R}\right)^{|m|}\left[\frac{|n|}{|l|}\mathrm{e}^{\mathrm{i}n\theta}-\mathrm{e}^{\mathrm{i}m\theta}\right]\Bigg]. \quad \cdots\cdots \quad ⑤
\end{aligned}
$$

Each term could be estimated as in the following:

$$
\begin{aligned}
|③| &= \left(\frac{\rho}{R}\right)^{n}\left|\sum_{t=1}^{\infty}\left\{\frac{1}{tN+n}\left(\frac{\rho}{R}\right)^{tN+n}(\mathrm{e}^{\mathrm{i}n\theta}-\mathrm{e}^{\mathrm{i}(tN+n)\theta})\right.\right. \\
&\qquad\left.\left.+\frac{1}{tN-n}\left(\frac{\rho}{R}\right)^{tN-n}(\mathrm{e}^{\mathrm{i}n\theta}-\mathrm{e}^{\mathrm{i}(tN-n)\theta})\right\}\right| \\
&\le 2\left(\frac{\rho}{R}\right)^{n}\sum_{t=1}^{\infty}\left[\frac{1}{tN+n}\left(\frac{\rho}{R}\right)^{tN+n}+\frac{1}{tN-n}\left(\frac{\rho}{R}\right)^{tN-n}\right] \\
&= \frac{2}{N-n}\left(\frac{\rho}{R}\right)^{n}\sum_{t=1}^{\infty}\left[\frac{N-n}{tN+n}\left(\frac{\rho}{R}\right)^{tN+n}+\frac{N-n}{tN-n}\left(\frac{\rho}{R}\right)^{tN-n}\right] \\
&\le \frac{2}{N-n}\left(\frac{\rho}{R}\right)^{N}\left(1+\left(\frac{\rho}{R}\right)^{2n}\right)\sum_{t=1}^{\infty}\left(\frac{\rho}{R}\right)^{(t-1)N} \le \frac{C_1}{N-n}\left(\frac{\rho}{R}\right)^{N}, \\
|④| &= \frac{1}{n}\left(\frac{\rho}{R}\right)^{n}\left|\sum_{s=1}^{\infty}\left\{\left(\frac{n}{sN+n}-1\right)\left(\frac{\rho}{R}\right)^{sN+n}+\left(\frac{n}{sN-n}-1\right)\left(\frac{\rho}{R}\right)^{sN-n}\right\}\right| \\
&\le \frac{1}{n}\left(\frac{\rho}{R}\right)^{n}\sum_{s=1}^{\infty}\left[\left(\frac{\rho}{R}\right)^{sN+n}+\left(\frac{\rho}{R}\right)^{sN-n}\right] \le \frac{C_2}{n}\left(\frac{\rho}{R}\right)^{N},
\end{aligned}
$$

$$
\begin{aligned}
|⑤| &= \left| \sum_{l\in I(n)} \left(\frac{\rho}{R}\right)^{|l|} \left[\sum_{t=1}^{\infty} \left\{ \frac{1}{tN+n} \left(\frac{\rho}{R}\right)^{tN+n} \left(\frac{|n|}{|l|} \mathrm{e}^{\mathrm{i}n\theta} - \mathrm{e}^{\mathrm{i}(tN+n)\theta} \right) \right.\right.\right. \\
&\qquad \left.\left.\left. + \frac{1}{tN-n} \left(\frac{\rho}{R}\right)^{tN-n} \left(\frac{|n|}{|l|} \mathrm{e}^{\mathrm{i}n\theta} - \mathrm{e}^{\mathrm{i}(tN-n)\theta} \right) \right\} \right] \right| \\
&\le \frac{1}{N-n} \left(\frac{\rho}{R}\right)^{N-n} \sum_{l\in I(n)} \left(\frac{\rho}{R}\right)^{|l|} \left(\frac{|n|}{|l|} + 1 \right) \left\{ \left(\frac{\rho}{R}\right)^{2n} + 1 \right\} \sum_{t=1}^{\infty} \left(\frac{\rho}{R}\right)^{(t-1)N} \\
&\le \frac{C_3}{N-n} \left(\frac{\rho}{R}\right)^{N-n} \sum_{l\in I(n)} \left(\frac{\rho}{R}\right)^{|l|} \le \frac{C_3}{N-n} \left(\frac{\rho}{R}\right)^{2(N-n)}.
\end{aligned}
$$

Combining the estimates on ③, ④, and ⑤, we have

$$
\begin{aligned}
② &\le \frac{\rho N^2}{16\pi^2} \left[\frac{C_1}{N-n} \left(\frac{\rho}{R}\right)^{N} + \frac{C_2}{n} \left(\frac{\rho}{R}\right)^{N} + \frac{C_3}{N-n} \left(\frac{\rho}{R}\right)^{2(N-n)} \right] \\
&\le C \left[\frac{N^2}{N-n} \left(\frac{\rho}{R}\right)^{N} + \frac{N^2}{n} \left(\frac{\rho}{R}\right)^{N} + \frac{N^2}{N-n} \left(\frac{\rho}{R}\right)^{2(N-n)} \right].
\end{aligned}
$$

Therefore we have

$$
\begin{aligned}
&|①| + |②| \\
&\quad \le C \left[\frac{N^2}{n(N-n)} \left(\frac{\rho}{R}\right)^{N} + \frac{N^2}{N-n} \left(\frac{\rho}{R}\right)^{N} + \frac{N^2}{n} \left(\frac{\rho}{R}\right)^{N} + \frac{N^2}{N-n} \left(\frac{\rho}{R}\right)^{2(N-n)} \right].
\end{aligned}
$$

Hence we obtain

$$
\begin{aligned}
\alpha_{1n}(\theta) &\le \frac{C \left[\frac{N^2}{n(N-n)} \left(\frac{\rho}{R}\right)^{N} + \frac{N^2}{N-n} \left(\frac{\rho}{R}\right)^{N} + \frac{N^2}{n} \left(\frac{\rho}{R}\right)^{N} + \frac{N^2}{N-n} \left(\frac{\rho}{R}\right)^{2(N-n)} \right]}{\frac{N^2}{16n^2\pi^2} \left(\frac{\rho}{R}\right)^{2n}} \\
&\le C \left[\frac{n^2}{n(N-n)} \left(\frac{\rho}{R}\right)^{N-2n} + \frac{n^2}{N-n} \left(\frac{\rho}{R}\right)^{N-2n} + n \left(\frac{\rho}{R}\right)^{N-2n} + \frac{n^2}{N-n} \left(\frac{\rho}{R}\right)^{2(N-2n)} \right] \\
&= C \left[\frac{n^2}{n(N-n)} + \frac{n^2}{N-n} + n + \frac{n^2}{N-n} \left(\frac{\rho}{R}\right)^{N-2n} \right] \left(\frac{\rho}{R}\right)^{N-2n} \\
&\le Cn \left(\frac{\rho}{R}\right)^{N-2n},
\end{aligned}
$$

that is, we have shown that

$$
g_{1n} = \sup_{\theta\in\mathbb{R}} \alpha_{1n}(\theta) \le Cn \left(\frac{\rho}{R}\right)^{N-2n}.
$$

We next show the estimate on g_{2n}. By definition, we have

$$
|\alpha_{2n}(\theta)| = \left| -\frac{\rho}{2} \mathrm{e}^{\mathrm{i}n\theta} + \rho^2 \varphi_n(\rho) \frac{\varphi_n(\rho\mathrm{e}^{\mathrm{i}\theta})}{2\rho\varphi_n(\rho)^2} \right| = \frac{\rho}{2} \left| \mathrm{e}^{\mathrm{i}n\theta} - \frac{\varphi_n(\rho\mathrm{e}^{\mathrm{i}\theta})}{\varphi_n(\rho)} \right| = \frac{\rho}{2} \frac{|\varphi_n(\rho)\mathrm{e}^{\mathrm{i}n\theta} - \varphi_n(\rho\mathrm{e}^{\mathrm{i}\theta})|}{|\varphi_n(\rho)|}.
$$

Therefore we find the following estimate from [49, Lemma 2]:

$$
g_{20} \le CN^{-1} \left(\frac{\rho}{R}\right)^{N}, \quad g_{2n} \le \frac{Cn}{N-n} \left(\frac{\rho}{R}\right)^{N-2n} \quad \left(1 \le n \le \frac{N}{2}\right).
$$

By definition, we have

$$\alpha_{3n}(\theta) = \left| -\frac{|n|}{2\rho^2}\mathrm{e}^{\mathrm{i}n\theta} + \psi_n(\rho)\frac{\varphi_n(\rho\mathrm{e}^{\mathrm{i}\theta})}{2\rho\varphi_n(\rho)^2} \right| = \frac{1}{2\rho^2\varphi_n(\rho)^2}\left| |n|\varphi_n(\rho)^2\mathrm{e}^{\mathrm{i}n\theta} - \rho\psi_n(\rho)\varphi_n(\rho\mathrm{e}^{\mathrm{i}\theta}) \right|.$$

When $n = 0$, we have

$$\alpha_{30}(\theta) = \frac{1}{2\rho^2\varphi_0(\rho)^2}\cdot\rho|\psi_0(\rho)||\varphi_0(\rho\mathrm{e}^{\mathrm{i}\theta})| \le C\left(\frac{\rho}{R}\right)^N.$$

When $1 \le n \le N/2$, we have

$$\begin{aligned}
&|n|\varphi_n(\rho)^2\mathrm{e}^{\mathrm{i}n\theta} - \rho\psi_n(\rho)\varphi_n(\rho\mathrm{e}^{\mathrm{i}\theta}) \\
&\quad= |n|\frac{-N}{4\pi}\sum_{l\equiv n}\frac{1}{|l|}\left(\frac{\rho}{R}\right)^{|l|}\frac{-N}{4\pi}\sum_{m\equiv n}\frac{1}{|m|}\left(\frac{\rho}{R}\right)^{|m|}\mathrm{e}^{\mathrm{i}n\theta} - \rho\frac{-N}{4\pi\rho}\sum_{l\equiv n}\left(\frac{\rho}{R}\right)^{|l|}\frac{-N}{4\pi}\sum_{m\equiv n}\frac{1}{|m|}\left(\frac{\rho}{R}\right)^{|m|}\mathrm{e}^{\mathrm{i}m\theta} \\
&\quad= \frac{N^2}{16\pi^2}\sum_{l,m\equiv n}\frac{1}{|m|}\left(\frac{\rho}{R}\right)^{|l|+|m|}\left[\frac{|n|}{|l|}\mathrm{e}^{\mathrm{i}n\theta} - \mathrm{e}^{\mathrm{i}m\theta}\right] \\
&\quad= \frac{N^2}{16\pi^2}\sum_{\substack{l,m\equiv n\\(l,m)\neq(n,n)}}\frac{1}{|m|}\left(\frac{\rho}{R}\right)^{|l|+|m|}\left[\frac{|n|}{|l|}\mathrm{e}^{\mathrm{i}n\theta} - \mathrm{e}^{\mathrm{i}m\theta}\right].
\end{aligned}$$

Therefore, we can estimate $\alpha_{3n}(\theta)$ in the same say for $\alpha_{1n}(\theta)$ as follows:

$$\alpha_{3n}(\theta) \le Cn\left(\frac{\rho}{R}\right)^{N-2n}, \quad \text{or} \quad g_{3n} \le Cn\left(\frac{\rho}{R}\right)^{N-2n}.$$

We finally show the estimate on g_{4n}. By definition, we have

$$\alpha_{4n}(\theta) = \left|\frac{1}{2\rho}\mathrm{e}^{\mathrm{i}n\theta} - \varphi_n(\rho)\frac{\varphi_n(\rho\mathrm{e}^{\mathrm{i}\theta})}{2\rho\varphi_n(\rho)^2}\right| = \frac{1}{2\rho}\left|\mathrm{e}^{\mathrm{i}n\theta} - \frac{\varphi_n(\rho\mathrm{e}^{\mathrm{i}\theta})}{\varphi_n(\rho)}\right|,$$

which can be bounded as $\alpha_{2n}(\theta)$, that is,

$$\alpha_{40}(\theta) \le CN^{-1}\left(\frac{\rho}{R}\right)^N, \quad \alpha_{4n}(\theta) \le \frac{Cn}{N-n}\left(\frac{\rho}{R}\right)^{N-2n} \quad \left(1 \le n \le \frac{N}{2}\right). \qquad \square$$

We then give the error estimate here. Using the symmetricity $g_{jn} = g_{j,-n}$, we have by (4.3.2) that

$$\begin{aligned}
\|u - u^{(N)}\|_{L^\infty} &\le \sum_{n\in\mathbb{Z}}\left(|f_n|g_{1n} + |g_n|g_{2n} + \rho^2|f_n|g_{3n} + \rho^2|g_n|g_{4n}\right) \\
&= 2(|f_0|g_{10} + |g_0|g_{20} + \rho^2|f_0|g_{30} + \rho^2|g_0|g_{40}) \quad \cdots \quad \langle 1\rangle \\
&\quad + 2\sum_{n=1}^{[N/2]}\left(|f_n|g_{1n} + |g_n|g_{2n} + \rho^2|f_n|g_{3n} + \rho^2|g_n|g_{4n}\right) \quad \cdots \quad \langle 2\rangle \\
&\quad + 2\sum_{n=[N/2]+1}^{\infty}\left(|f_n|g_{1n} + |g_n|g_{2n} + \rho^2|f_n|g_{3n} + \rho^2|g_n|g_{4n}\right). \quad \cdots \quad \langle 3\rangle
\end{aligned}$$

$\langle 1\rangle$ can be estimated as

$$\langle 1\rangle \le C\left(\frac{\rho}{R}\right)^N.$$

$\langle 2 \rangle$ is estimated as in the following way:

$$\langle 2 \rangle \leq C \sum_{n=1}^{[N/2]} \left(\frac{\rho}{r_0} \right)^n n \left(\frac{\rho}{R} \right)^{N-2n} \leq CN \left(\frac{\rho}{R} \right)^N \sum_{n=1}^{[N/2]} \left(\frac{R^2}{\rho r_0} \right)^n.$$

Using

$$\sum_{n=1}^{m} \tau^m \leq \begin{cases} \dfrac{\tau^m}{\tau - 1} & (\text{if } \tau > 1), \\ m & (\text{if } \tau = 1), \\ \dfrac{1}{1-\tau} & (\text{if } 0 < \tau < 1), \end{cases}$$

for $\tau = R^2/(\rho r_0)$, we have

$$\langle 2 \rangle \leq \begin{cases} CN \left(\dfrac{\rho}{r_0} \right)^{N/2} & (R^2/\rho r_0 > 1), \\ CN^2 \left(\dfrac{\rho}{R} \right)^N & (R^2/\rho r_0 = 1), \\ CN \left(\dfrac{\rho}{R} \right)^N & (R^2/\rho r_0 < 1). \end{cases}$$

Finally, the last term $\langle 3 \rangle$ can be estimated as

$$\langle 3 \rangle = C \sum_{n=[N/2]+1}^{\infty} \left(\frac{\rho}{r_0} \right)^n \leq C \left(\frac{\rho}{r_0} \right)^{N/2}.$$

Hence we have shown Theorem 4.1.3.

4.4 Numerical experiments

We here present some results of numerical experiments.

4.4.1 Ω: disk

We first consider the case where Ω is a disk D_ρ, where $\rho = 1$. We adopt the following polynomials as the boundary conditions:

$$f(x) = x_1^4 - x_2^4 \ (x = (x_1, x_2)^{\mathrm{T}}), \quad g(x) = 4(x_1^3, -x_2^3)^{\mathrm{T}} \cdot \nu. \tag{4.4.1}$$

Then, it can be easily checked that $u(x) = x_1^4 - x_2^4$ is the exact solution for (4.1.1). We define R equal to 2, and the result is depicted in Figure 4.1. It can be observed that our error estimate grasps the behavior of approximation error very well. Moreover, it can be found that the order of convergence for the present scheme is higher than that for the conventional scheme, which yields the difference in accuracy. In order to investigate the reason for such a phenomenon, it would be expected that backward error analysis should be done in future work.

4.4.2 Ω: interior simply-connected region surrounded by polynomial curve

We next consider the case where the boundary Γ is given by a polynomial curve $\Psi_{l,r}$, where $r = 8$, $l = 4$, and $\Psi_{l,r}$ is defined in (3.5.2). It is natural to expect that theoretical error analysis could be done

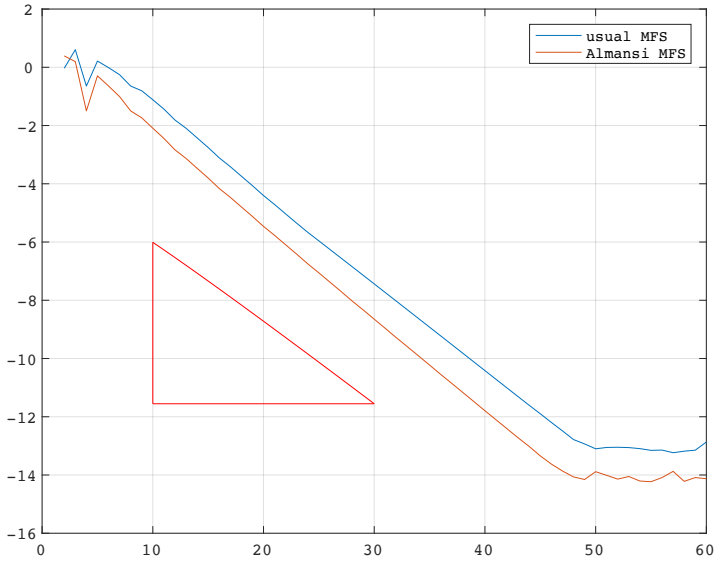

Figure 4.1: Numerical experiment with boundary data f and g are given by (4.4.1), and the parameter $R = 2$. The blue colored line and the orange colored one represent numerical solutions obtained by the conventional scheme (4.1.4) and the present scheme (4.1.3), respectively, and the gradient of the hypotenuse of the *red colored triangle* is the theoretical order of convergence.

for the present scheme as we have shown in Chapters 2 and 3. Therefore, we here present numerical experiment for the case where Ω is the interior simply-connected region surrounded by polynomial curve, and verify numerically that the same error estimate could be obtained. The parameter R is taken to be equal to 1.2, and the boundary conditions are given by (4.4.1). The result of numerical experiment is depicted in Figure 4.2. We can also observe in this situation that the accuracy of approximate solution by present scheme is better than that by conventional scheme. Moreover, its convergence rate is what we can expect from theoretical analysis of MFS and DSM in Chapters 2 and 3. Therefore, it should be expected that theoretical convergence analysis could be done in the case where Ω is bounded by an regular analytic Jordan curve.

4.5 Concluding remarks

In this chapter, we have considered a typical boundary value problem for the biharmonic equation, and its approximate solution by MFS based on the Almansi-type decomposition of biharmonic function. As a result, we have proved that an approximate solution actually exists uniquely except for at most one value of N, and an approximation error decays exponentially with respect to N. Numerical results have supported our error analysis.

We here note that Almansi-type decomposition can also hold for polyharmonic function, therefore, our approach in this chapter can be applied to boundary value problems for the polyharmonic equations. Possible direction of the future research can be listed as in the following. The first topic is to extend the results in this chapter to general Jordan regions. Numerical results in section 4.4 strongly imply that theoretical error estimate such as in Chapters 2 and 3 also hold for present scheme. The second topic is to compute numerically the stream function for Stokes flow. Since the stream function for Stokes flow satisfies the biharmonic equation, there exists possibility to apply the present scheme to Stokes flow, which enables us to understand the aspect in the Stokes fluid.

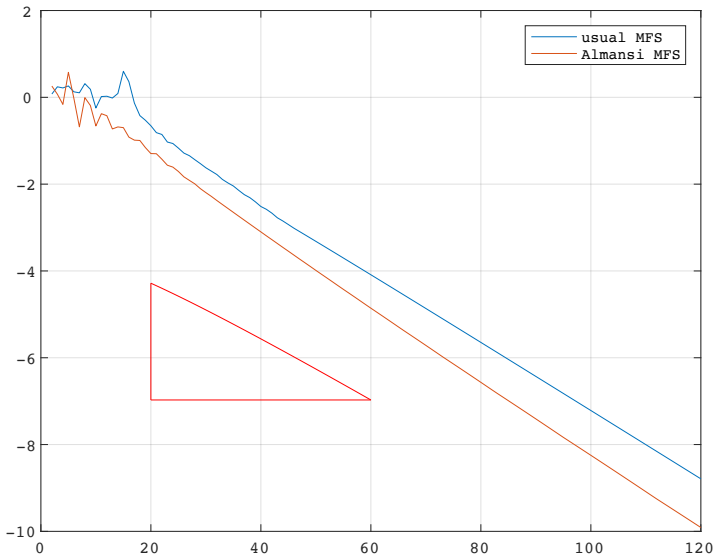

Figure 4.2: Numerical experiment with boundary data f and g are given by (4.4.1), and the parameter $R = 1.2$. The blue colored line and the orange colored one represent numerical solutions obtained by the conventional scheme (4.1.4) and the present scheme (4.1.3), respectively, and the gradient of the hypotenuse of the *red colored triangle* is the expected order of convergence.

Chapter 5

Method of fundamental solutions with weighted average condition and dummy points

Abstract

The aim of this chapter is to develop the method of fundamental solutions using weighted average condition and dummy points. We accomplish mathematical analysis, a unique existence of an approximate solution and an exponential decay of the approximation error, for potential problem in disk, and show some numerical experiments which exemplify sharpness of our error estimate. This chapter is based on the following submitted paper:

- K. Sakakibara and S. Yazaki, *Method of fundamental solutions with weighted average condition and dummy points*, submitted revised vertion to JSIAM Lett.

5.1 Introduction and main result

Let Ω be a Jordan region with smooth boundary $\partial\Omega$. Then we consider the following potential problem:

$$\begin{cases} \triangle u = 0 & \text{in } \Omega, \\ u = f & \text{on } \partial\Omega, \end{cases} \tag{5.1.1}$$

where f is a given datum. In this chapter, we develop new formultation of the method of fundamental solutions (MFS), which is numerical solver for linear homogeneous partial differential equations, by introducing dummy points and weighted average condition. Namely, we seek an approximate solution $u^{(N)}$ for the problem (5.1.1) of the form

$$u^{(N)}(x) = Q_0 + \sum_{j=1}^{N} Q_j E_j(x), \quad E_j(x) = E(x-y_j) - E(x-z_j), \quad E(x) = \frac{1}{2\pi}\log|x|, \tag{5.1.2}$$

where $\{y_j\}_{j=1}^N$ and $\{z_j\}_{j=1}^N$ are the singular and dummy points, which are taken in $\mathbb{C}\setminus\overline{\Omega}$, respectively, and E is the fundamental solution of the Laplace operator $\triangle$. The coefficients $\{Q_0\}_{j=0}^N$ are determined by the collocation method and weighted average condition, that is, choosing the collocation points $\{x_j\}_{j=1}^N$, we solve the following linear system:

$$u^{(N)}(x_j) = f(x_j), \quad j = 1, 2, \ldots, N \tag{5.1.3a}$$

with the weighted average condition:

$$\sum_{j=1}^{N} Q_j H_j = 0, \quad H_j \in \mathbb{R} \ \ (j = 1, 2, \ldots, N). \tag{5.1.3b}$$

In this chapter, we consider the case where Ω is a disk D_ρ with radius ρ having the origin as its center, and choose the collocation, singular and dummy points as follows:

$$x_j = \rho\omega^{j-1}, \quad y_j = R\omega^{j-1}, \quad z_j = R\sigma\omega^{j-1}, \quad j = 1, 2, \ldots, N, \tag{5.1.4}$$

where $R > \rho$, $\sigma > 1$ and $\omega = \exp(2\pi \mathrm{i}/N)$. The following are main results of this chapter.

Theorem 5.1.1. *Suppose that the collocation, singular and dummy points are chosen as in* (5.1.4)*. Then, an approximate solution of the form* (5.1.2) *satisfying the collocation equations* (5.1.3a) *and the weighted average condition* (5.1.3b) *actually exists uniquely if and only if the average* $\sum_{j=1}^{N} H_j$ *of weights* $\{H_j\}_{j=1}^{N}$ *is not equal to* 0*.*

Theorem 5.1.2. *In addition to the hypothesis in Theorem 5.1.1, suppose that the boundary* f *is real analytic. Namely, there exists some constant* $b \in]0, 1[$ *such that the Fourier coefficients* $\{f_n\}$ *of the boundary data* f *can be estimated as follows:*

$$|f_n| = O(b^{|n|}) \quad (n \in \mathbb{Z}).$$

Then there exists some positive constant C*, which depends on* $\left|\sum_{i=1}^{N} H_i\right|$*, such that the following error estimate holds:*

$$\sup_{x\in\Omega} \left|u(x) - u^{(N)}(x)\right| \leq \begin{cases} C\left(\dfrac{\rho}{R}\right)^N & \text{if } bR^2/\rho^2 < 1, \\ CN\left(\dfrac{\rho}{R}\right)^N & \text{if } bR^2/\rho^2 = 1, \\ Cb^{N/2} & \text{if } bR^2/\rho^2 > 1. \end{cases}$$

The contents of this chapter are as follows. We prove the unique existence (Theorem 5.1.1) and exponential decay of an approximate solution (Theorem 5.1.2) in Sections 5.2 and 5.3, respectively. In Section 5.4, we show results of numerical experiments together with that of condition numbers, which imply that we should place the dummy points not so far from the boundary $\partial\Omega$ of Ω. We finally conclude this chapter in Section 5.5 by giving some concluding remarks.

5.2 Unique existence

The collocation equations (5.1.3a) and the weighted average condition (5.1.3b) are equivalent to the following linear system:

$$G\boldsymbol{Q} = \boldsymbol{f}, \tag{5.2.1}$$

where

$$\begin{aligned} &G = \begin{pmatrix} 0 & \boldsymbol{H}^{\mathrm{T}} \\ \mathbf{1} & \tilde{G} \end{pmatrix}, \quad \tilde{G} = (E_j(x_i)) \in \mathbb{R}^{N\times N}, \\ &\boldsymbol{H} = (H_1, H_2, \ldots, H_N)^{\mathrm{T}} \in \mathbb{R}^N, \quad \mathbf{1} = (1, 1, \ldots, 1)^{\mathrm{T}} \in \mathbb{R}^N, \\ &\boldsymbol{Q} = (Q_0, Q_1, \ldots, Q_N)^{\mathrm{T}} \in \mathbb{R}^{N+1}, \quad \boldsymbol{f} = (0, f(x_1), \ldots, f(x_N))^{\mathrm{T}} \in \mathbb{R}^{N+1}. \end{aligned}$$

The (i,j)-element of $\tilde{G}$ can be rewritten as

$$E_j(x_i) = \frac{1}{2\pi}\log|\rho - R\omega^{j-i}| - \frac{1}{2\pi}\log|\rho - R\sigma\omega^{j-i}|.$$

Thus $\tilde{G}$ is a circulant matrix, that is, $\tilde{G}$ can be diagonalized by discrete Fourier transform. Indeed, putting

$$\tilde{W} = \left(\frac{1}{\sqrt{N}}\omega^{(i-1)(j-1)} \;\middle|\; i,j = 1,2,\dots,N\right) \in \mathbb{C}^{N\times N},$$

we have

$$\tilde{W}^{-1}\tilde{G}\tilde{W} = \operatorname{diag}\left(\varphi_0^{(N)}(\rho), \varphi_1^{(N)}(\rho), \dots, \varphi_{N-1}^{(N)}(\rho)\right),$$

where

$$\varphi_p^{(N)}(z) = \sum_{k=1}^{N} \omega^{p(k-1)} E_k(z).$$

Therefore, defining

$$W = \begin{pmatrix} 1 & \mathbf{0}^{\mathrm{T}} \\ \mathbf{0} & \tilde{G} \end{pmatrix},$$

we obtain

$$W^{-1}GW = \begin{pmatrix} 0 & \boldsymbol{H}^{\mathrm{T}}W \\ W^{-1}\mathbf{1} & W^{-1}GW \end{pmatrix}$$

$$= \begin{pmatrix} 0 & N^{-1/2}\sum_{i=1}^{N} H_i & N^{-1/2}\sum_{i=1}^{N} H_i\omega^{i-1} & \cdots & N^{-1/2}\sum_{i=1}^{N} H_i\omega^{(i-1)(N-1)} \\ N^{1/2} & \varphi_0^{(N)}(\rho) & 0 & \cdots & 0 \\ 0 & 0 & \varphi_1^{(N)}(\rho) & & 0 \\ \vdots & \vdots & & \ddots & \vdots \\ 0 & 0 & 0 & \cdots & \varphi_{N-1}^{(N)}(\rho) \end{pmatrix}. \tag{5.2.2}$$

Therefore $\det G$, the determinant of G, can be explicitly computed as

$$\det G = -\sum_{i=1}^{N} H_i \prod_{p=1}^{N-1} \varphi_p^{(N)}(\rho).$$

The following lemma represents more precise nature of the function $\varphi_p^{(N)}$.

Lemma 5.2.1. *For any $z = re^{i\theta}$, $r < R$, $\theta \in \mathbb{R}$, we have*

$$\varphi_p^{(N)}(z) = \begin{cases} \dfrac{1}{2\pi}\log\left|\dfrac{z^N - R^N}{z^N - (\sigma R)^N}\right|, & \text{if } p \equiv 0 \pmod N, \\ -\dfrac{N}{4\pi}\displaystyle\sum_{m\equiv p \pmod N} \frac{1}{|m|}\left(\frac{r}{R}\right)^{|m|}\left[1 - \frac{1}{\sigma^{|m|}}\right]e^{im\theta}, & \text{otherwise.} \end{cases}$$

The above lemma is a direct consequence of [49, Lemma 1]. Then we can easily verify that

$$\varphi_p^{(N)}(\rho) < 0, \quad p = 1,2,\dots,N-1,$$

which implies that the coefficient matrix G in (5.2.1) is nonsingular if and only if $\sum_{j=1}^{N} H_j \neq 0$. Thus Theorem 5.1.1 has been shown.

5.3 Error estimate

We compute G^{-1}, the inverse matrix of G, explicitly from (5.2.2). Defining

$$A = \begin{pmatrix} 0 & N^{-1/2}\sum_{i=1}^{N} H_i \\ N^{1/2} & \varphi_0^{(N)}(\rho) \end{pmatrix},$$
$$B = \begin{pmatrix} N^{-1/2}\sum_{i=1}^{N} \omega^{i-1} H_i & \cdots & N^{-1/2}\sum_{i=1}^{N} \omega^{(N-1)(i-1)} H_i \\ 0 & \cdots & 0 \end{pmatrix},$$
$$D = \mathrm{diag}(\varphi_1^{(N)}(\rho), \ldots, \varphi_{N-1}^{(N)}(\rho)),$$

we have

$$W^{-1} G W = \begin{pmatrix} A & B \\ O & D \end{pmatrix},$$

which yields that

$$W^{-1} G^{-1} W = (W^{-1} G W)^{-1} = \begin{pmatrix} A^{-1} & -A^{-1} B D^{-1} \\ O & D^{-1} \end{pmatrix} =: M.$$

Each component can be easily computed as follows:

$$A^{-1} = -\frac{1}{\sum_{i=1}^{N} H_i} \begin{pmatrix} \varphi_0^{(N)}(\rho) & -N^{-1/2}\sum_{i=1}^{N} H_i \\ -N^{-1/2} & 0 \end{pmatrix} = \begin{pmatrix} -\frac{\varphi_0^{(N)}(\rho)}{\sum_{i=1}^{N} H_i} & N^{-1/2}\frac{\varphi_0^{(N)}(\rho)}{\varphi_0^{(N)}(\rho)}\frac{\sum_{i=1}^{N} \omega^{0(i-1)} H_i}{\sum_{i=1}^{N} H_i} \\ \frac{N^{1/2}}{\sum_{i=1}^{N} H_i} & 0 \end{pmatrix},$$
$$D^{-1} = \mathrm{diag}\left(\frac{1}{\varphi_1^{(N)}(\rho)}, \ldots, \frac{1}{\varphi_{N-1}^{(N)}(\rho)} \right),$$
$$-A^{-1} B D^{-1} = \begin{pmatrix} N^{-1/2}\frac{\varphi_0^{(N)}(\rho)}{\varphi_1^{(N)}(\rho)}\frac{\sum_{i=1}^{N} \omega^{i-1} H_i}{\sum_{i=1}^{N} H_i} & \cdots & N^{-1/2}\frac{\varphi_0^{(N)}(\rho)}{\varphi_{N-1}^{(N)}(\rho)}\frac{\sum_{i=1}^{N} \omega^{(N-1)(i-1)} H_i}{\sum_{i=1}^{N} H_i} \\ -\frac{\sum_i \omega^{i-1} H_i}{\sum_{i=1}^{N} H_i}\frac{1}{\varphi_1^{(N)}(\rho)} & \cdots & -\frac{\sum_{i=1}^{N} \omega^{(N-1)(i-1)} H_i}{\sum_{i=1}^{N} H_i}\frac{1}{\varphi_{N-1}^{(N)}(\rho)} \end{pmatrix}.$$

From these expressions, we obtain the explicit formulae for coefficients $\{Q_j\}_{j=0}^{N}$ as follows:

$$Q_0 = \sum_{k=0}^{N} [G^{-1}]_{0,k} [\boldsymbol{f}]_k = \sum_{k=1}^{N} \frac{1}{N} \sum_{l=1}^{N} \omega^{-(k-1)(l-1)} \frac{\varphi_0^{(N)}(\rho)}{\varphi_{l-1}^{(N)}(\rho)} \frac{\sum_{i=1}^{N} \omega^{(l-1)(i-1)} H_i}{\sum_{i=1}^{N} H_i} f(x_k)$$
$$= \sum_{n \equiv 0} f_n + \frac{1}{\sum_{j=1}^{N} H_j} \sum_{n \not\equiv 0} \frac{\varphi_0^{(N)}(\rho)}{\varphi_n^{(N)}(\rho)} f_n \sum_{i=1}^{N} \omega^{n(i-1)} H_i$$

and

$$\begin{aligned}
Q_j &= \sum_{k=0}^{N} [G^{-1}]_{jk} [\boldsymbol{f}]_k \\
&= \sum_{k=1}^{N} \left[-\frac{1}{N} \sum_{l=2}^{N} \omega^{-(k-1)(l-1)} \frac{\sum\limits_{i=1}^{N} \omega^{(i-1)(l-1)} H_i}{\sum\limits_{i=1}^{N} H_i} \frac{1}{\varphi_{l-1}^{(N)}(\rho)} + \frac{1}{N} \sum_{p=2}^{N} \omega^{(j-k)(p-1)} \frac{1}{\varphi_{p-1}^{(N)}(\rho)} \right] f(x_k) \\
&= \frac{1}{\sum\limits_{i=1}^{N} H_i} \sum_{n \not\equiv 0} f_n \left[-\frac{1}{\varphi_n^{(N)}(\rho)} \sum_{i=1}^{N} \omega^{n(i-1)} H_i + \frac{\omega^{n(j-1)}}{\varphi_n^{(N)}(\rho)} \sum_{k=1}^{N} H_k \right]
\end{aligned}$$

for $j = 1, \ldots, N$. Therefore we can write down the approximate solution $u^{(N)}$ as follows:

$$\begin{aligned}
u^{(N)}(x) &= Q_0 + \sum_{j=1}^{N} Q_j E_j(x) \\
&= \sum_{n \equiv 0} f_n + \frac{1}{\sum\limits_{i=1}^{N} H_i} \sum_{n \not\equiv 0} \frac{\varphi_0^{(N)}(\rho)}{\varphi_n^{(N)}(\rho)} f_n \sum_{i=1}^{N} \omega^{n(i-1)} H_i \\
&\qquad + \sum_{j=1}^{N} \left[\frac{1}{\sum\limits_{i=1}^{N} H_i} \sum_{n \not\equiv 0} f_n \left[-\frac{1}{\varphi_n^{(N)}(\rho)} \sum_{i=1}^{N} \omega^{n(i-1)} H_i + \frac{\omega^{n(j-1)}}{\varphi_n^{(N)}(\rho)} \sum_{k=1}^{N} H_k \right] \right] E_j(x) \\
&= \sum_{n \equiv 0} f_n + \frac{1}{\sum\limits_{i=1}^{N} H_i} \sum_{n \not\equiv 0} f_n \left[\frac{\varphi_0^{(N)}(\rho)}{\varphi_n^{(N)}(\rho)} \sum_{i=1}^{N} \omega^{n(i-1)} H_i \right. \\
&\qquad \left. - \frac{1}{\varphi_n^{(N)}(\rho)} \sum_{i=1}^{N} \omega^{n(i-1)} H_i \sum_{j=1}^{N} E_j(x) + \frac{1}{\varphi_n^{(N)}(\rho)} \sum_{k=1}^{N} H_k \sum_{j=1}^{N} \omega^{n(j-1)} E_j(x) \right] \\
&= \sum_{n \equiv 0} f_n + \frac{1}{\sum\limits_{i=1}^{N} H_i} \sum_{n \not\equiv 0} f_n \left[\frac{\varphi_0^{(N)}(\rho) - \varphi_0^{(N)}(x)}{\varphi_n^{(N)}(\rho)} + \sum_{k=1}^{N} H_k \frac{\varphi_n^{(N)}(x)}{\varphi_n^{(N)}(\rho)} \right].
\end{aligned}$$

Since the exact solution u for the problem (5.1.1) is written by the Fourier series as

$$u(x) = u(r\mathrm{e}^{\mathrm{i}\theta}) = \sum_{n \in \mathbb{Z}} f_n \left(\frac{r}{\rho} \right)^{|n|} \mathrm{e}^{\mathrm{i}n\theta},$$

owing to the maximum principle for harmonic functions, we have

$$\begin{aligned}
&\sup_{x \in \Omega} |u(x) - u^{(N)}(x)| = \sup_{x \in \partial\Omega} |u(x) - u^{(N)}(x)| \\
&= \sup_{\theta \in \mathbb{R}} \left| \sum_{n \in \mathbb{Z}} f_n \mathrm{e}^{\mathrm{i}n\theta} - \left[\sum_{n \equiv 0} f_n + \frac{1}{\sum\limits_{i=1}^{N} H_i} \sum_{n \not\equiv 0} f_n \left(\frac{\varphi_0^{(N)}(\rho) - \varphi_0^{(N)}(\rho \mathrm{e}^{\mathrm{i}\theta})}{\varphi_n^{(N)}(\rho)} + \sum_{k=1}^{N} H_k \frac{\varphi_n^{(N)}(\rho \mathrm{e}^{\mathrm{i}\theta})}{\varphi_n^{(N)}(\rho)} \right) \right] \right|
\end{aligned}$$

$$\leq \sum_{n\equiv 0} |f_n| \sup_{\theta\in\mathbb{R}} |\mathrm{e}^{\mathrm{i}n\theta} - 1|$$

$$+ \sum_{n\not\equiv 0} |f_n| \sup_{\theta\in\mathbb{R}} \left| \mathrm{e}^{\mathrm{i}n\theta} - \frac{1}{\sum_{k=1}^{N} H_k} \left(\frac{\varphi_0^{(N)}(\rho) - \varphi_0^{(N)}(\rho\mathrm{e}^{\mathrm{i}\theta})}{\varphi_n^{(N)}(\rho)} + \sum_{k=1}^{N} H_k \frac{\varphi_n^{(N)}(\rho\mathrm{e}^{\mathrm{i}\theta})}{\varphi_n^{(N)}(\rho)} \right) \right|$$

$$= \sum_{n\in\mathbb{Z}} |f_n| g_n^{(N)}, \tag{5.3.1}$$

where

$$g_n^{(N)} = \begin{cases} \sup_{\theta\in\mathbb{R}} |\mathrm{e}^{\mathrm{i}n\theta} - 1| & \text{if } n \equiv 0, \\ \sup_{\theta\in\mathbb{R}} \left| \mathrm{e}^{\mathrm{i}n\theta} - \frac{1}{\sum_{i=1}^{N} H_i} \left(\frac{\varphi_0^{(N)}(\rho) - \varphi_0^{(N)}(\rho\mathrm{e}^{\mathrm{i}\theta})}{\varphi_n^{(N)}(\rho)} + \sum_{k=1}^{N} H_k \frac{\varphi_n^{(N)}(\rho\mathrm{e}^{\mathrm{i}\theta})}{\varphi_n^{(N)}(\rho)} \right) \right| & \text{if } n \not\equiv 0. \end{cases}$$

We split the error bound (5.3.1) into three parts as

$$\sum_{n\in\mathbb{Z}} |f_n| g_n^{(N)} = |f_0| g_0^{(N)} + \sum_{n=1}^{[N/2]} (|f_n| + |f_{-n}|) g_n^{(N)} + \sum_{n=[N/2]+1}^{\infty} (|f_n| + |f_{-n}|) g_n^{(N)},$$

and estimate them. We immediately obtain from the definition that $g_0^{(N)} = 0$. In order to estimate the second term we prepare the following lemma.

Lemma 5.3.1. *For sufficiently large N so that $(\rho/R)^N \leq 1/2$ is satisfied, there exists some positive constant C, which depends on $\left|\sum_{i=1}^{N} H_i\right|$ such that*

$$g_n^{(N)} \leq C \left(\frac{\rho}{R}\right)^{N-2n}$$

holds for $1 \leq n \leq N/2$.

Proof. We estimate the following equation for θ:

$$\frac{1}{\sum_{i=1}^{N} H_i \varphi_n^{(N)}(\rho)} \left(\sum_{k=1}^{N} H_k \left(\mathrm{e}^{\mathrm{i}n\theta} \varphi_n^{(N)}(\rho) - \varphi_n^{(N)}(\rho\mathrm{e}^{\mathrm{i}\theta}) \right) - (\varphi_0^{(N)}(\rho) - \varphi_0^{(N)}(\rho\mathrm{e}^{\mathrm{i}\theta})) \right).$$

We obtain from Lemma 5.2.1 and [49, Proof of Lemma 2] that

$$|\mathrm{e}^{\mathrm{i}n\theta} \varphi_n^{(N)}(\rho) - \varphi_n^{(N)}(\rho\mathrm{e}^{\mathrm{i}\theta})| \leq \frac{2N}{\pi(N-n)} \left(\frac{\rho}{R}\right)^{N-n} + \frac{2N}{\pi(N-n)} \left(\frac{\rho}{R\sigma}\right)^{N-n} \leq \frac{4N}{\pi(N-n)} \left(\frac{\rho}{R}\right)^{N-n}.$$

We also have from Lemma 5.2.1 that

$$|\varphi_n^{(N)}(\rho)| = \left| -\frac{N}{4\pi} \sum_{\substack{m\equiv n \pmod N \\ m\in\mathbb{Z}}} \frac{1}{|m|} \left(\frac{\rho}{R}\right)^{|m|} \left(1 - \frac{1}{\sigma^{|m|}}\right) \right|$$

$$\geq \frac{N}{4\pi} \cdot \frac{1}{n} \left(\frac{\rho}{R}\right)^{n} \left(1 - \frac{1}{\sigma^{n}}\right) \geq \frac{N}{4\pi n} \left(\frac{\rho}{R}\right)^{n} \left(1 - \frac{1}{\sigma}\right).$$

Concerning the term $\varphi_0^{(N)}(\rho) - \varphi_0^{(N)}(\rho e^{i\theta})$, we have

$$\begin{aligned}
&\left| \frac{1}{2\pi} \log |\rho^N - R^N| - \frac{1}{2\pi} \log |(\rho e^{i\theta})^N - R^N| \right| \\
&\qquad = \left| \frac{1}{2\pi} \left[\log \left| R^N \left(1 - \left(\frac{\rho}{R} \right)^N \right) \right| - \log \left| R^N \left(1 - \left(\frac{\rho e^{i\theta}}{R} \right)^N \right) \right| \right] \right| \\
&\qquad = \frac{1}{2\pi} \left| -\sum_{n=1}^{\infty} \frac{1}{n} \left(\frac{\rho}{R} \right)^{nN} + \Re \sum_{n=1}^{\infty} \frac{1}{n} \left(\frac{\rho e^{i\theta}}{R} \right)^{nN} \right| \\
&\qquad = \frac{1}{4\pi} \left| \sum_{\substack{n \in \mathbb{Z} \\ n \neq 0}} \frac{1}{|n|} \left(\frac{\rho}{R} \right)^{|n|N} (e^{inN\theta} - 1) \right| \leq \frac{1}{2\pi} \sum_{\substack{n \in \mathbb{Z} \\ n \neq 0}} \frac{1}{|n|} \left(\frac{\rho}{R} \right)^{|n|N} \leq \frac{1}{\pi} \sum_{n=1}^{\infty} \frac{1}{n} \left(\frac{\rho}{R} \right)^{nN} \\
&\qquad \leq \frac{1}{\pi} \cdot \frac{(\rho/R)^N}{1 - (\rho/R)^N} \leq \frac{2}{\pi} \left(\frac{\rho}{R} \right)^N,
\end{aligned}$$

which yields that

$$|\varphi_0^{(N)}(\rho) - \varphi_0^{(N)}(\rho e^{i\theta})| \leq \frac{2}{\pi} \left(\frac{\rho}{R} \right)^N \left(1 + \frac{1}{\sigma^N} \right) \leq \frac{4}{\pi} \left(\frac{\rho}{R} \right)^N.$$

Summarizing the above, we obtain

$$\begin{aligned}
g_n^{(N)} &\leq \frac{1}{\left| \sum_{i=1}^{N} H_i \right|} \frac{4\pi n}{N(1 - \sigma^{-1})} \left(\frac{R}{\rho} \right)^n \left(\left| \sum_{k=1}^{N} H_k \right| \cdot \frac{4N}{\pi(N-n)} \left(\frac{\rho}{R} \right)^{N-n} + \frac{4}{\pi} \left(\frac{\rho}{R} \right)^N \right) \\
&\leq \frac{8}{\left| \sum_{i=1}^{N} H_i \right| (1 - \sigma^{-1})} \left(2 \left| \sum_{k=1}^{N} H_k \right| + 1 \right) \left(\frac{\rho}{R} \right)^{N-2n},
\end{aligned}$$

which is the desired estimate. □

Concerning the third term we need the following lemma.

Lemma 5.3.2. *Suppose that N is taken large enough to satisfy $(\rho/R)^N \leq 1/2$. Then there exists some positive constant C, which depends on $\left| \sum_{i=1}^{N} H_i \right|$, such that the following estimate holds for all $n \in \mathbb{Z}$:*

$$g_n^{(N)} \leq C.$$

Proof. Note firstly that the function $\varphi_n^{(N)}$ satisfies the following relations:

$$\varphi_n^{(N)} = \varphi_m^{(N)} \quad (n \equiv m \pmod N), \quad \varphi_n^{(N)}(\rho) = \varphi_{N-n}^{(N)}(\rho) \quad (n = 1, 2, \ldots, N-1). \tag{5.3.2}$$

When $n = 0$, it is clear that $g_0^{(N)} = 0$. When $n \in I(0)$, using the periodicity of $\varphi_n^{(N)}$ with respect to

n, we have

$$
\begin{aligned}
g_n^{(N)} &= \sup_{\theta\in\mathbb{R}} \left| \mathrm{e}^{\mathrm{i}n\theta} - \frac{1}{\sum_{i=1}^{N} H_i} \left(\frac{\varphi_0^{(N)}(\rho) - \varphi_0^{(N)}(\rho\mathrm{e}^{\mathrm{i}\theta})}{\varphi_0^{(N)}(\rho)} + \sum_{k=1}^{N} H_k \frac{\varphi_0^{(N)}(\rho\mathrm{e}^{\mathrm{i}\theta})}{\varphi_0^{(N)}(\rho)} \right) \right| \\
&\le 1 + \frac{1}{\left| \sum_{i=1}^{N} H_i \right|} \left(1 + \frac{\sup_{\theta\in\mathbb{R}} |\varphi_0^{(N)}(\rho\mathrm{e}^{\mathrm{i}\theta})|}{|\varphi_0^{(N)}(\rho)|} + \left| \sum_{k=1}^{N} H_k \right| \frac{\sup_{\theta\in\mathbb{R}} |\varphi_0^{(N)}(\rho\mathrm{e}^{\mathrm{i}\theta})|}{|\varphi_0^{(N)}(\rho)|} \right) \\
&\le 1 + \frac{1}{\left| \sum_{i=1}^{N} H_i \right|} \left(2 + \left| \sum_{k=1}^{N} H_k \right| \right),
\end{aligned}
$$

where we have used an inequality $\sup_{\theta\in\mathbb{R}} |\varphi_0^{(N)}(\rho\mathrm{e}^{\mathrm{i}\theta})| \le |\varphi_0^{(N)}(\rho)|$, which can be proved as follows:

$$
\begin{aligned}
|\varphi_0^{(N)}(\rho\mathrm{e}^{\mathrm{i}\theta})| &= \left| \frac{1}{2\pi} \log \left| \frac{(\rho\mathrm{e}^{\mathrm{i}\theta})^N - R^N}{(\rho\mathrm{e}^{\mathrm{i}\theta})^N - (\sigma R)^N} \right| \right| = \frac{1}{2\pi} \left| \log |(\rho\mathrm{e}^{\mathrm{i}\theta}))^N - R^N| - \log |(\rho\mathrm{e}^{\mathrm{i}\theta}))^N - (R\sigma)^N| \right| \\
&= \frac{1}{2\pi} \left| \log \left| R^N \left(1 - \left(\frac{\rho\mathrm{e}^{\mathrm{i}\theta}}{R} \right)^N \right) \right| - \log \left| (R\sigma)^N \left(1 - \left(\frac{\rho\mathrm{e}^{\mathrm{i}\theta}}{R\sigma} \right)^N \right) \right| \right| \\
&= \frac{1}{2\pi} \left| -N \log \sigma - \Re \sum_{n=1}^{\infty} \frac{1}{n} \left(\frac{\rho}{R} \right)^{nN} \mathrm{e}^{\mathrm{i}nN\theta} + \Re \sum_{n=1}^{\infty} \frac{1}{n} \left(\frac{\rho}{R\sigma} \right)^{nN} \mathrm{e}^{\mathrm{i}nN\theta} \right| \\
&= \frac{1}{2\pi} \left| -N \log \sigma + \sum_{\substack{n\in\mathbb{Z} \\ n\neq 0}} \frac{1}{2|n|} \left(\frac{\rho}{R} \right)^{|n|N} \left(\frac{1}{\sigma^{|n|N}} - 1 \right) \mathrm{e}^{\mathrm{i}nN\theta} \right| \\
&\le \frac{1}{2\pi} \left(N \log \sigma + \sum_{\substack{n\in\mathbb{Z} \\ n\neq 0}} \frac{1}{2|n|} \left(\frac{\rho}{R} \right)^{|n|N} \left(1 - \frac{1}{\sigma^{|n|N}} \right) \right) \\
&= \frac{1}{2\pi} \left(N \log \sigma - \log \left| 1 - \left(\frac{\rho}{R} \right)^N \right| + \log \left| 1 - \left(\frac{\rho}{R\sigma} \right)^N \right| \right) \\
&= \frac{1}{2\pi} \left(N \log \sigma + N \log R - \log |R^N - \rho^N| - N \log(R\sigma) + \log |(R\sigma)^N - \rho^N| \right) \\
&= \frac{1}{2\pi} \log \frac{(R\sigma)^N - \rho^N}{R^N - \rho^N} = \left| \frac{1}{2\pi} \log \left| \frac{\rho^N - R^N}{\rho^N - (R\sigma)^N} \right| \right| = |\varphi_0^{(N)}(\rho)|.
\end{aligned}
$$

When $n \not\equiv 0$, we only need to consider the case where $1 \le n \le N/2$ owing to the periodicity (5.3.2). As we have already written in the proof of Lemma 5.3.1, we have

$$
\frac{|\varphi_0^{(N)}(\rho) - \varphi_0^{(N)}(\rho\mathrm{e}^{\mathrm{i}\theta})|}{|\varphi_n^{(N)}(\rho)|} \le \frac{4/\pi(\rho/R)^N}{N/(4\pi n)(\rho/R)^n} = \frac{16n}{N} \left(\frac{\rho}{R} \right)^{N-n} \le 8.
$$

Since $\sup_{\theta\in\mathbb{R}} |\varphi_n^{(N)}(\rho\mathrm{e}^{\mathrm{i}\theta})| \le |\varphi_n^{(N)}(\rho)|$ holds, which can be proved in similar way that for $\varphi_0^{(N)}$, we

obtain

$$g_n^{(N)} \le 1 + \frac{1}{\left|\sum_{i=1}^{N} H_i\right|}\left(8 + \left|\sum_{k=1}^{N} H_k\right|\right).$$

Hence, defining a constant C as right hand side in the above inequality, we obtain the desired estimate. □

Proof of Theorem 5.1.2. Using the estimate (5.3.1), Lemmas 5.3.1 and 5.3.2, and the assumption on the decay of Fourier coefficients of f, we have

$$\begin{aligned}\sup_{x\in\Omega}\left|u(x) - u^{(N)}(x)\right| &\le 2C\sum_{n=1}^{[N/2]} b^n \cdot \left(\frac{\rho}{R}\right)^{N-2n} + 2C\sum_{n=[N/2]+1}^{\infty} b^n \\ &= 2C\left(\frac{\rho}{R}\right)^N \sum_{n=1}^{[N/2]}\left(\frac{bR^2}{\rho^2}\right)^n + 2C\sum_{n=[N/2]+1}^{\infty} b^n.\end{aligned}$$

The summation part in the first term in the right hand side can be estimated as follows:

- When $bR^2/\rho^2 < 1$, we have

$$(\text{1st term}) = 2C\left(\frac{\rho}{R}\right)^N \cdot \frac{bR^2}{\rho^2}\frac{1-(bR^2/\rho^2)^{[N/2]}}{1-bR^2/\rho^2} \le 2C\left(\frac{\rho}{R}\right)^N \cdot \frac{1}{\rho^2/(bR^2)-1};$$

- When $bR^2/\rho^2 = 1$, we have

$$(\text{1st term}) = 2C\left(\frac{\rho}{R}\right)^N \cdot \left[\frac{N}{2}\right] \le CN\left(\frac{\rho}{R}\right)^N;$$

- When $bR^2/\rho^2 > 1$, we have

$$\begin{aligned}(\text{1st term}) &= 2C\left(\frac{\rho}{R}\right)^N \cdot \frac{bR^2}{\rho^2}\frac{(bR^2/\rho^2)^{[N/2]}-1}{bR^2/\rho^2-1} \le 2C\left(\frac{\rho}{R}\right)^N \left(\frac{bR^2}{\rho^2}\right)^{N/2}\frac{bR^2}{\rho^2}\frac{1}{bR^2/\rho^2-1} \\ &\le 2Cb^{N/2}\cdot\frac{1}{1-\rho^2/(bR^2)}.\end{aligned}$$

The second term can be estimated by straightforward computation as follows:

$$(\text{2nd term}) = 2Cb^{[N/2]+1}\cdot\frac{1}{1-b} \le \frac{2C}{1-b}b^{N/2}.$$

Summarizing the above, we obtain

$$\sup_{x\in\Omega}\left|u(x) - u^{(N)}(x)\right| \le \begin{cases} C\left(\frac{\rho}{R}\right)^N & \text{if } bR^2/\rho^2 < 1, \\ CN\left(\frac{\rho}{R}\right)^N & \text{if } bR^2/\rho^2 = 1, \\ Cb^{N/2} & \text{if } bR^2/\rho^2 > 1, \end{cases}$$

which concludes the proof of Theorem 5.1.2. □

5.4 Numerical experiments

In this section, we present some results of numerical experiments in order to examine the sharpness of our error estimate. Throughout these experiments, we only consider the case where $\rho = 1$, which is the radius of the problem region Ω.

Example 5.4.1. We first adopt harmonic polynomials as the boundary data, that is,

$$f(x) = \Re x^m \quad (x \in \partial\Omega), \quad m = 0, 1, \ldots, 5.$$

Parameters are taken as follows:

- $R = 2$ (the parameter for singular points);
- $\sigma = 2$ (the parameter for dummy points);
- $H_j = 1 + \epsilon \cos(2\pi j/N)$ for $j = 1, 2, \ldots, N$ (the weights), where $\epsilon = 0, 1$.

The result is depicted in Figure 5.1, in which the horizontal and vertical axes represent N and common logarithms of errors, respectively, here and hereafter. We can observe that the errors decay exponen-

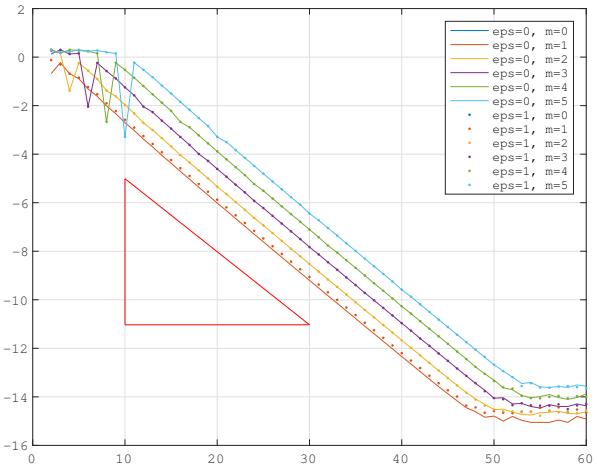

Figure 5.1: Numerical experiment with boundary data being harmonic polynomials, and the parameters $R = 2$ and $\sigma = 2$. The solid lines and dots represent numerical solutions where $\epsilon = 0$ and $\epsilon = 1$, respectively, and the gradient of the hypotenuse of the *red colored triangle* is the theoretical order of convergence.

tially with respect to N, and their convergence rates agree well with the theoretical error estimate Theorem 5.1.2, which tells us that $\|u - u^{(N)}\|_{L^\infty(\Omega)} = O((1/2)^N)$. We can also see that differences of weights affect very little behavior of errors. Note that lines corresponding to the case $m = 0$ do not appear in Figure 5.1, since the numerical solution coincides with the exact solution in this case.

Example 5.4.2. We next consider the case where the boundary data are logarithmic potentials:

$$f(x) = \log|x - x_0| \quad (x \in \partial\Omega),$$

where x_0 is the singularity of f, which is located outside Ω. In this case, the approximation error is estimated by Theorem 5.1.2 as follows:

$$\|u - u^{(N)}\|_{L^\infty(\Omega)} = O\left(\max\left\{\left(\frac{\rho}{R}\right)^N, \left(\frac{\rho}{|x_0|}\right)^{N/2}\right\}\right).$$

The parameters R and x_0 are taken as $R = (1 + 0.1m)\rho$ $(m = 1, 2, \ldots, 7)$ and $x_0 = 2\rho$, respectively, which yields for $m = 1, 2, \ldots, 7$ that

$$\|u - u^{(N)}\|_{L^\infty(\Omega)} = O\left(\max\left\{\left(\frac{1}{1+0.1m}\right)^N, \left(\frac{1}{2}\right)^N\right\}\right).$$

The results are depicted in Figure 5.2, which represents the sharpness of our error estimate.

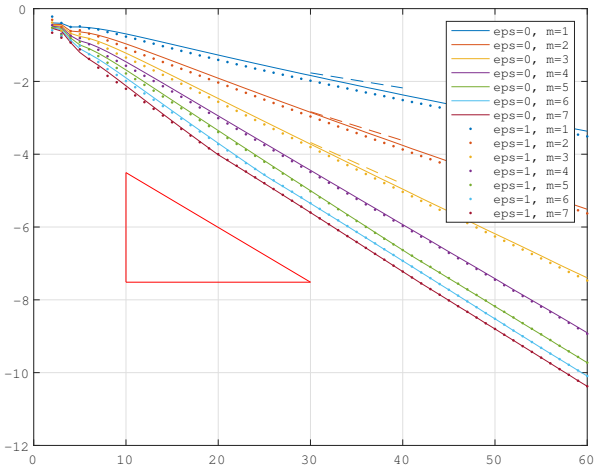

Figure 5.2: Numerical experiment with boundary data being logarithmic potentials, and the parameters $R = (1 + 0.1m)\rho$ $(m = 1, 2, \ldots, 7)$ and $\sigma = 2$. The solid lines and dots represent numerical solutions where $\epsilon = 0$ and $\epsilon = 1$, respectively, and the gradients of broken lines and that of the hypotenuse of the *red colored triangle* are the theoretical order of convergence for $m = 1, 2, 3$ and $m = 4, 5, 6, 7$, respectively.

Example 5.4.3. We also compute condition number of coefficient matrix numerically. Results in Figure

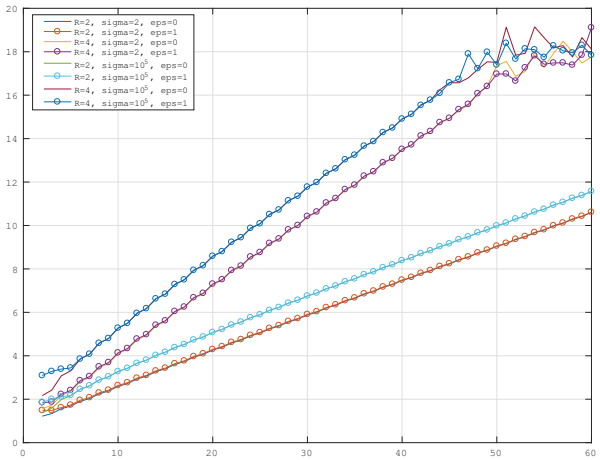

Figure 5.3: Numerical computation of condition numbers of coefficient matrices

5.3 imply that the linear system (5.2.1) would be ill-conditioned, and the condition number of coefficient

matrix becomes large if σ is large, that is, the parameter σ should not be taken large in vain. Note also in this case that the weights $\{H_j\}_{j=1}^N$ do not affect condition numbers.

5.5 Concluding remarks

In this chapter, we studied MFS with weighted average condition and dummy points for potential problem in disk, and established that an approximate solution actually exists uniquely if and only if the average of weights is not equal to 0, and that the error decays exponentially with respect to N when the boundary datum is real analytic. We showed numerical results with boundary data being harmonic polynomials and logarithmic potentials, which exemplified the sharpness of our error estimate. We also computed the condition number of coefficient matrix numerically, which told us that the parameter σ for dummy points should not be taken so large.

Part II

Application of the method of fundamental solutions to the complex analysis and fluid mechanics

Chapter 6

Structure-preserving numerical scheme for the one-phase Hele-Shaw problems by the method of fundamental solutions

Abstract

The solutions to the one-phase interior or the classical Hele-Shaw problem are discretized in space by means of the method of fundamental solutions combined with the uniform distribution method, and then a system of ordinary differential equations is obtained, which is solved by the usual fourth order Runge-Kutta method. The one-phase interior Hele-Shaw problem has curve-shortening (CS), area-preserving (AP), and barycenter-fixed (BF) properties. Under our numerical scheme, discrete versions of CS-, AP-, and BF-properties hold, while simple boundary element method does not satisfy these properties in general. The one-phase exterior Hele-Shaw problem and the one-phase interior Hele-Shaw problem with sink/source points can also be treated. In each problem, a non-trivial exact solution is constructed and an experimental order of convergence is shown. This chapter is based on the following submitted paper:

- K. Sakakibara and S. Yazaki, *Structure-preserving numerical scheme for the one-phase Hele-Shaw problems by the method of fundamental solutions*, submitted revised version to Numer. Math.

6.1 Introduction

The classical Hele-Shaw problems is description of a motion of viscous fluid in a quasi two-dimensional space, which was starting from a short paper [32] in 1898 by Henry Selby Hele-Shaw (1854–1941). In his experiment, viscous fluid is sandwiched between two parallel plates with a narrow gap, and the apparatus is called Hele-Shaw cell. He succeeded to visualize stream lines by means of colored water in the cell. The classical or the *one-phase interior Hele-Shaw problem* is stated as follows (see Lamb

[62] or Gustafsson and Vasil'ev [26] in detail):

$$\begin{cases} \triangle p(\cdot,t) = 0 & \text{in } \mathscr{D}(t),\ t \in [0,T), \\ p(\cdot,t) = \gamma k(\cdot,t) & \text{on } \mathscr{C}(t),\ t \in [0,T), \\ V(\cdot,t) = -\nabla p(\cdot,t)\cdot \boldsymbol{N}(\cdot,t) & \text{on } \mathscr{C}(t),\ t \in [0,T), \end{cases} \tag{6.1.1}$$

where $\triangle = \partial^2/\partial x^2 + \partial^2/\partial y^2$ is the Laplace operator and $\nabla = (\partial/\partial x, \partial/\partial y)^{\mathrm{T}}$ is the gradient in $\mathbb{R}^2$, $\mathscr{D}(t) \subset \mathbb{R}^2$ is a bounded region occupied by fluid, $\mathscr{C}(t)$ is the boundary of $\mathscr{D}(t)$ (positively oriented closed curve), $p(\cdot,t)$ is the pressure function in $\mathscr{D}(t)$, γ is the surface tension coefficient, $k(\boldsymbol{x},t)$ is the curvature (sing convention is the way that $k = 1$ if $\mathscr{D}(t)$ is a unit disk), $\boldsymbol{N}(\boldsymbol{x},t)$ is the unit outward normal vector defined by $\boldsymbol{N}(\boldsymbol{x},t) = -\boldsymbol{T}(\boldsymbol{x},t)^{\perp}$, and $V(\boldsymbol{x},t)$ is the normal velocity, of $\mathscr{C}(t)$ at $\boldsymbol{x} \in \mathscr{C}(t)$. See Figure 6.1(a) (in the figure, $\boldsymbol{x}$ is the position vector and $\boldsymbol{T}$ is the unit tangent vector). Here

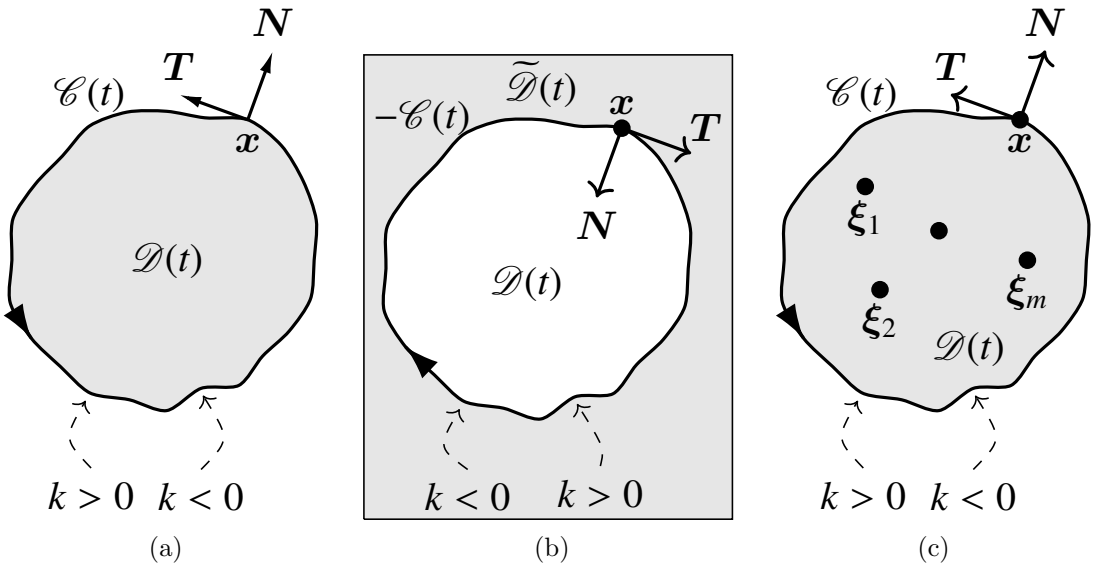

Figure 6.1: One-phase interior Hele-Shaw problem (a) and its variations: (b) one-phase exterior Hele-Shaw problem and (c) one-phase interior Hele-Shaw problem with sink/source points $\{\boldsymbol{\xi}_i\}_{i=1}^m$.

and hereafter, $\boldsymbol{a}\cdot\boldsymbol{b}$ represents the usual two-dimensional Euclidean inner product for $\boldsymbol{a},\boldsymbol{b} \in \mathbb{R}^2$ and $\boldsymbol{a}^{\perp} = (-b,a)^{\perp}$ for $\boldsymbol{a} = (a,b)^{\mathrm{T}}$.

We have three marked properties of the one-phase interior Hele-Shaw problem (6.1.1): the total length of $\mathscr{C}(t)$ is decreasing in time, the enclosed area of $\mathscr{D}(t)$ is preserving and the barycenter of $\mathscr{D}(t)$ is being fixed. These properties are called curve-shortening (CS), area-preserving (AP) and barycenter-fixed (BF), respectively. See Proposition 6.2.2.

The purpose of this chapter is that for (6.1.1) we propose a simple numerical scheme by means of the method of fundamental solutions combined with the uniform distribution method. Our scheme can be applied for two variations: the one-phase exterior problem (see Figure 6.1(b) and the problem (6.2.1) below) and the one-phase interior problem with sink/source points (see Figure 6.1(b) and the problem (6.2.2) below).

This chapter is organized as follows. In Section 6.2, two variations of one-phase interior Hele-Shaw problem (6.1.1) will be stated and variational structures and several properties of Hele-Shaw problems such as CS-, AP- and BF-properties will be given. In Sections 6.3, 6.4 and 6.5, we will propose numerical schemes for the problems (6.1.1), (6.2.1) and (6.2.2), respectively. In Section 6.6, numerical

experiments will be shown with the results of numerical CS- and AP-properties and an experimental order of convergence (EOC) compared with a non-trivial exact solution, and we will remark some future works in the final Section 6.7.

A feature of our scheme is to realize the CS-, AP- and BF-properties asymptotically in a discrete sense by means of the normal velocity determined by a modified invariant scheme of MFS, so-called Murota's invariant scheme [73, 74], and the tangential velocity determined by MFS and the uniform distribution method (UDM) [93]. Note that under UDM, we have stable numerical computation. Of course, there are many ways to solve the Hele-Shaw problem numerically (see selected just a few papers or a monograph [53, 94, 26, 106]). However, many of known schemes did not focus on making schemes which preserve a variational structure of the Hele-Shaw problems such as CS-, AP- and BF-properties. Note that one can find polygonal Hele-Shaw flow [56] which satisfies discrete CS-, AP- and BF-properties, and can be regarded as semi-discretization scheme from a numerical point of view.

6.2 Variational structures

6.2.1 Two variations of the one-phase interior Hele-Shaw problem (6.1.1)

Besides the interior problem, an exterior problem is also interested. The first variation is the *one-phase exterior Hele-Shaw problem* which is stated as follows:

$$\begin{cases} \triangle p(\cdot,t) = 0 & \text{in } \widetilde{\mathscr{D}}(t),\ t\in[0,T), \\ p(\cdot,t) = \gamma k(\cdot,t) & \text{on } -\mathscr{C}(t),\ t\in[0,T), \\ p(\boldsymbol{x},t) = qE(\boldsymbol{x}) + O(1) & \text{as } |\boldsymbol{x}|\to\infty,\ t\in[0,T), \\ V(\cdot,t) = -\nabla p(\cdot,t)\cdot \boldsymbol{N}(\cdot,t) & \text{on } -\mathscr{C}(t),\ t\in[0,T), \end{cases} \tag{6.2.1}$$

where $\widetilde{\mathscr{D}}(t) := \mathbb{R}^2 \setminus \overline{\mathscr{D}}(t)$ is an unbounded region occupied by fluid with a bounded region $\mathscr{D}(t)$, q is a given real number, $|\boldsymbol{x}| = \sqrt{\boldsymbol{x}\cdot\boldsymbol{x}}$ for $\boldsymbol{x}\in\mathbb{R}^2$ and

$$E(\boldsymbol{x}) = \frac{1}{2\pi}\log|\boldsymbol{x}|$$

is a fundamental solution of the Laplace operator $\triangle$. Here and hereafter we use the notations that k and $\boldsymbol{N}$ denote the curvature and the unit outward normal vector of $-\mathscr{C}(t)$, respectively, when the exterior problem is considered, where $-\mathscr{C}(t)$ is the boundary of $\mathscr{D}(t)$ (negatively oriented closed curve). See Figure 6.1(b).

If q is positive, then changing speed of the enclosed area of $\mathscr{D}(t)$ is negative $-q$, which corresponds to existence of source at the infinity $|\boldsymbol{x}| = \infty$. Conversely, the case $q < 0$ corresponds to existence of sink at the infinity. See Proposition 6.2.3.

The second variation is referred as the *one-phase interior Hele-Shaw problem with sink/source points*, which is stated as follows.

$$\begin{cases} \triangle p(\cdot,t) = \displaystyle\sum_{i=1}^{m} q_i\delta(\cdot-\boldsymbol{\xi}_i) & \text{in } \mathscr{D}(t),\ t\in[0,T), \\ p(\cdot,t) = \gamma k(\cdot,t) & \text{on } \mathscr{C}(t),\ t\in[0,T), \\ V(\cdot,t) = -\nabla p(\cdot,t)\cdot\boldsymbol{N}(\cdot,t) & \text{on } \mathscr{C}(t),\ t\in[0,T), \end{cases} \tag{6.2.2}$$

where $\delta(\cdot)$ denotes the Dirac delta function with the singularity at the origin, $\{q_i\}_{i=1}^m$ are given real numbers, and $\{\boldsymbol{\xi}_i\}_{i=1}^m$ denote the positions of sink or source points located in a bounded fluid region $\mathscr{D}(t)\subset\mathbb{R}^2$. See Figure 6.1(c).

If $q_i > 0$ (resp. $q_i < 0$), then $\boldsymbol{\xi}_i$ is a sink (resp. source) point. Hence we have area-decreasing or area-increasing property depending on sign of sum of all q_i's. See Proposition 6.2.4.

6.2.2 Moving boundary problem

Let $\{\mathscr{C}(t)\}_{t\geq 0}$ be a family of closed embedded $C^{2,1}$-curves, parameterized as $[0,1] \ni u \mapsto \boldsymbol{x}(u,t) \in \mathbb{R}^2$ for each time t, governed its motion by the evolution law:

$$\partial_t \boldsymbol{x}(u,t) = \alpha(u,t)\boldsymbol{T}(u,t) + V(u,t)\boldsymbol{N}(u,t) \tag{6.2.3}$$

for $u \in [0,1]$ and $t \geq 0$, where $\partial_t = \partial/\partial t$ is the time derivative, and $\boldsymbol{T}(u,t)$ and $\boldsymbol{N}(u,t) = -\boldsymbol{T}(u,t)^{\perp}$ denote the unit tangent and the unit outward normal vectors of $\mathscr{C}(t)$ at $\boldsymbol{x}(u,t) \in \mathscr{C}(t)$, respectively. Then $\alpha(u,t)$ and $V(u,t)$ denote the tangential and normal velocities of $\mathscr{C}(t)$ at $\boldsymbol{x}(u,t) \in \mathscr{C}(t)$, respectively. In general, it is known that the shape of $\mathscr{C}(t)$ does not depend on the tangential velocity $\alpha(\cdot,t)$ [18, Proposition 2.4]. Then one can take $\alpha = 0$, but it causes numerical instability in general. Therefore a nontrivial α has been utilized from a numerical point of view [34, 52, 53, 70, 71, 72, 92, 93]. See Section 6.3.5 for our choice α. On the other hand, the normal velocity $V(\cdot,t)$ determines the shape of $\mathscr{C}(t)$, and in this chapter, V is given by the one-phase Hele-Shaw problems (6.1.1), (6.2.1) or (6.2.2). Here and hereafter we abbreviate a notation for function $\mathsf{F}(u,t)$ as F unless there is confusion.

Let $\mathscr{D}(t)$ be a bounded region surrounded by $\mathscr{C}(t)$. The total length $\mathcal{L}(t)$ of $\mathscr{C}(t)$, the enclosed area $\mathcal{A}(t)$ of $\mathscr{D}(t)$ and the barycenter $\boldsymbol{\mathcal{G}}(t)$ of $\mathscr{D}(t)$ are respectively defined as follows:

$$\mathcal{L}(t) = \int_{\mathscr{C}(t)} \mathrm{d}s, \quad \mathcal{A}(t) = \int_{\mathscr{D}(t)} \mathrm{d}S, \quad \boldsymbol{\mathcal{G}}(t) = \frac{1}{A(t)} \int_{\mathscr{D}(t)} \boldsymbol{x}\, \mathrm{d}S.$$

Here $\mathrm{d}s$ is the line element of $\mathscr{C}(t)$ and $\mathrm{d}S$ the area element of $\mathscr{D}(t)$. Note that $\mathscr{D}(t)$ is a bounded region surrounded by an unbounded fluid region for Problem (6.2.1), and so $\mathcal{A}(t)$ and $\boldsymbol{\mathcal{G}}(t)$ are respectively the area and the barycenter of $\mathscr{D}(t)$ in the geometric sense. Their time evolution under the evolution law (6.2.3) can be computed as follows (see e.g. Gurtin [25, (2E) Transport theorem for area and total length] and Kimura [54, Theorem 6.4]).

Theorem 6.2.1. *Let $\{\mathscr{C}(t)\}_{t\geq 0}$ be a family of closed embedded $C^{2,1}$-curves, governed its motion by the evolution law* (6.2.3)*. Then we have*

$$\dot{\mathcal{L}}(t) = \int_{\mathscr{C}(t)} kV\, \mathrm{d}s, \quad \dot{\mathcal{A}}(t) = \int_{\mathscr{C}(t)} V\, \mathrm{d}s, \quad \dot{\boldsymbol{\mathcal{G}}}(t) = -\frac{\dot{\mathcal{A}}(t)}{\mathcal{A}(t)}\boldsymbol{\mathcal{G}}(t) + \frac{1}{\mathcal{A}(t)} \int_{\mathscr{C}(t)} \boldsymbol{x} V\, \mathrm{d}s.$$

Here and hereafter, $\dot{\mathsf{F}}$ denotes the time derivative $\mathrm{d}\mathsf{F}/\mathrm{d}t$.

Using this theorem, we can derive the variational structures for the one-phase Hele-Shaw problems as follows.

Proposition 6.2.2 (One-phase interior Hele-Shaw problem (6.1.1))**.** *In addition to the hypothesis in Theorem 6.2.1, suppose that the normal velocity V is computed by* (6.1.1)*. Then we have*

$$\dot{\mathcal{L}}(t) \leq 0, \quad \dot{\mathcal{A}}(t) = 0, \quad \dot{\boldsymbol{\mathcal{G}}}(t) = \boldsymbol{0}.$$

Namely, CS-, AP- and BF-properties hold.

Proposition 6.2.3 (One-phase exterior Hele-Shaw problem (6.2.1))**.** *In addition to the hypothesis in Theorem 6.2.1, suppose that the normal velocity V is computed by* (6.2.1)*. Then we have*

$$\dot{\mathcal{A}}(t) = -q.$$

Namely, $\mathscr{D}(t)$ shrinks if $q > 0$ and enlarges if $q < 0$.

Proposition 6.2.4 (One-phase interior Hele-Shaw problems with sink/source points (6.2.2))**.** *In addition to the hypothesis in Theorem 6.2.1, suppose that the normal velocity V is computed by* (6.2.2)*. Then we have*

$$\dot{\mathcal{A}}(t) = -\sum_{i=1}^{m} q_i.$$

Namely, $\boldsymbol{\xi}_i$ is a sink point if $q_i > 0$ and a source point if $q_i < 0$.

Proof of Proposition 6.2.2. Let p be the solution for the one-phase interior Hele-Shaw problem (6.1.1). Then the time derivative of the total length can be estimated using Theorem 6.2.1, (6.1.1) and the divergence theorem as follows:

$$\begin{aligned}\dot{\mathcal{L}}(t) &= -\frac{1}{\gamma}\int_{\mathscr{C}(t)} p\nabla p\cdot\boldsymbol{N}\,\mathrm{d}s = -\frac{1}{\gamma}\int_{\mathscr{D}(t)} \operatorname{div}(p\nabla p)\,\mathrm{d}S = -\frac{1}{\gamma}\int_{\mathscr{D}(t)} (|\nabla p|^2 + p\triangle p)\,\mathrm{d}S\\ &= -\frac{1}{\gamma}\int_{\mathscr{D}(t)} |\nabla p|^2\,\mathrm{d}S \le 0.\end{aligned}$$

Especially, the length decreases strictly monotonically unless $\mathscr{D}(t)$ is a disk. In similar way, the time derivative of the enclosed area can be computed as

$$\dot{\mathcal{A}}(t) = -\int_{\mathscr{C}(t)} \nabla p\cdot\boldsymbol{N}\,\mathrm{d}s = -\int_{\mathscr{D}(t)} \operatorname{div}(\nabla p)\,\mathrm{d}S = -\int_{\mathscr{D}(t)} \triangle p\,\mathrm{d}S = 0.$$

Finally, using the divergence theorem repeatedly, the time derivative of the barycenter can be computed as follows:

$$\begin{aligned}\dot{\boldsymbol{\mathcal{G}}}(t) &= -\frac{1}{\mathcal{A}(t)}\int_{\mathscr{C}(t)} \boldsymbol{x}\nabla p\cdot\boldsymbol{N}\,\mathrm{d}s = -\frac{1}{\mathcal{A}(t)}\int_{\mathscr{D}(t)} \begin{pmatrix}\operatorname{div}(x\nabla p)\\ \operatorname{div}(y\nabla p)\end{pmatrix}\mathrm{d}S = -\frac{1}{\mathcal{A}(t)}\int_{\mathscr{D}(t)} (\nabla p + \boldsymbol{x}\triangle p)\,\mathrm{d}S\\ &= -\frac{1}{\mathcal{A}(t)}\int_{\mathscr{D}(t)} \begin{pmatrix}\operatorname{div}(p,0)^{\mathrm{T}}\\ \operatorname{div}(0,p)^{\mathrm{T}}\end{pmatrix}\mathrm{d}S = -\frac{1}{\mathcal{A}(t)}\int_{\mathscr{C}(t)} p\boldsymbol{N}\,\mathrm{d}s = -\frac{\gamma}{\mathcal{A}(t)}\int_{\mathscr{C}(t)} k\boldsymbol{N}\,\mathrm{d}s\\ &= \frac{\gamma}{\mathcal{A}(t)}\int_{\mathscr{C}(t)} \partial_s\boldsymbol{T}\,\mathrm{d}s = \boldsymbol{0},\end{aligned}$$

where we have used the Frenet formula. □

Proof of Proposition 6.2.3. Take R large enough so that a circle $\mathscr{C}_R = \{\boldsymbol{x}\in\mathbb{R}^2 \mid |\boldsymbol{x}| = R\}$ encloses $\mathscr{D}(t)$. Let $\mathscr{D}_R(t)$ be the doubly-connected region surrounded by $\mathscr{C}_R$ and $-\mathscr{C}(t)$. Denote the enclosed area of $\mathscr{D}_R(t)$ by $\mathcal{A}_R(t)$. Then we have

$$\dot{\mathcal{A}}_R(t) = \int_{\partial\mathscr{D}_R(t)} V\,\mathrm{d}s = \int_{-\mathscr{C}(t)} V\,\mathrm{d}s = -\int_{-\mathscr{C}(t)} \nabla p\cdot\boldsymbol{N}\,\mathrm{d}s.$$

Here we have used the fact that $V = 0$ on $\mathscr{C}_R$ because $\mathscr{C}_R$ is a fixed boundary. On the other hand, we obtain

$$0 = \int_{\mathscr{D}_R(t)} \triangle p\,\mathrm{d}S = \int_{\partial\mathscr{D}_R(t)} \nabla p\cdot\boldsymbol{N}\,\mathrm{d}s = \int_{\mathscr{C}_R} \nabla p\cdot\boldsymbol{N}\,\mathrm{d}s + \int_{-\mathscr{C}(t)} \nabla p\cdot\boldsymbol{N}\,\mathrm{d}s$$

Therefore we have

$$\dot{\mathcal{A}}_R(t) = \int_{\mathscr{C}_R} \nabla p\cdot\boldsymbol{N}\,\mathrm{d}s.$$

Here, note that for the fundamental solution E of the Laplace operator, we have

$$\int_{\mathscr{C}_R} \nabla(qE)\cdot\boldsymbol{N}\,\mathrm{d}s = \frac{q}{2\pi}\int_{\mathscr{C}_R} \frac{\boldsymbol{x}}{R^2}\cdot\frac{\boldsymbol{x}}{R}\,\mathrm{d}s = \frac{q}{2\pi R}\int_{\mathscr{C}_R} \mathrm{d}s = q.$$

Then we can prove that

$$\int_{\mathscr{C}_R} \nabla p \cdot \boldsymbol{N} \, \mathrm{d}s \longrightarrow q \quad \text{as} \quad R \to \infty.$$

Since $\mathcal{A}(t) = |\mathscr{D}_R| - \mathcal{A}_R(t)$, we obtain $\dot{\mathcal{A}}(t) = -q$. □

Proof of Proposition 6.2.4. For simplicity, we prove the case $m = 1$, and denote $\boldsymbol{\xi} = \boldsymbol{\xi}_1$ and $q = q_1$. Take sufficiently small positive number ϵ so that the disk $B(\boldsymbol{\xi}, \epsilon) = \{\boldsymbol{x} \in \mathbb{R}^2 \mid |\boldsymbol{x} - \boldsymbol{\xi}| < \epsilon\}$ is contained in $\mathscr{D}(t)$, and denote the doubly-connected region surrounded by $\mathscr{C}(t)$ and $-\partial B(\boldsymbol{\xi}, \epsilon)$ by $\mathscr{D}_\epsilon(t)$. Then we have

$$0 = \int_{\mathscr{D}_\epsilon(t)} \triangle p \, \mathrm{d}S = \int_{\mathscr{C}(t)} \nabla p \cdot \boldsymbol{N} \, \mathrm{d}s + \int_{-\partial B(\boldsymbol{\xi}, \epsilon)} \nabla p \cdot \boldsymbol{N} \, \mathrm{d}s.$$

Denoting the pressure function p as the sum of $qE(\boldsymbol{x} - \boldsymbol{\xi})$ and a harmonic function $\tilde{p}$, we obtain

$$\begin{aligned}\dot{\mathcal{A}}(t) &= \int_{\mathscr{C}(t)} V \, \mathrm{d}s = \int_{-\partial B(\boldsymbol{\xi}, \epsilon)} \nabla p \cdot \boldsymbol{N} \, \mathrm{d}s = \int_{-\partial B(\boldsymbol{\xi}, \epsilon)} \left(\nabla \tilde{p} \cdot \boldsymbol{N} + \frac{q(\boldsymbol{x} - \boldsymbol{\xi}) \cdot \boldsymbol{N}}{2\pi |\boldsymbol{x} - \boldsymbol{\xi}|^2} \right) \mathrm{d}s \\ &= -\int_{B(\boldsymbol{\xi}, \epsilon)} \triangle \tilde{p} \, \mathrm{d}S + \int_{-\partial B(\boldsymbol{x}, \epsilon)} \frac{q(\boldsymbol{x} - \boldsymbol{\xi})}{2\pi |\boldsymbol{x} - \boldsymbol{\xi}|^2} \cdot \frac{-(\boldsymbol{x} - \boldsymbol{\xi})}{|\boldsymbol{x} - \boldsymbol{\xi}|} \, \mathrm{d}s = -q.\end{aligned}$$

□

6.3 Numerical scheme for the one-phase interior Hele-Shaw problem (6.1.1)

We approximate the boundary curve $\mathscr{C}(t)$ by polygonal curve, say $\Gamma(t)$, and consider the evolution of it.

Let $\Gamma(t) = \bigcup_{i=1}^n \Gamma_i(t)$ be an n-sided closed polygonal Jordan curve, where $\Gamma_i(t)$ is the i-th edge of $\Gamma(t)$ defined as

$$\Gamma_i(t) = [\boldsymbol{x}_{i-1}(t), \boldsymbol{x}_i(t)] := \{(1 - \lambda)\boldsymbol{x}_{i-1}(t) + \lambda \boldsymbol{x}_i(t) \mid \lambda \in [0, 1]\}$$

and $\boldsymbol{x}_i(t)$ the i-th vertex of $\Gamma(t)$ ($i = 1, 2, \ldots, n$; $\boldsymbol{x}_0(t) = \boldsymbol{x}_n(t)$, $\boldsymbol{x}_{n+1}(t) = \boldsymbol{x}_1(t)$; $t \geq 0$). See Figure 6.2. $\Gamma(t)$ moves according the following evolution law, the polygonal version of (6.2.3):

$$\dot{\boldsymbol{x}}_i(t) = \alpha_i(t)\boldsymbol{T}_i(t) + V_i(t)\boldsymbol{N}_i(t) \quad (i = 1, 2, \ldots, n), \tag{6.3.1}$$

where $\boldsymbol{T}_i(t)$ and $\boldsymbol{N}_i(t) = -\boldsymbol{T}_i(t)^\perp$ denote the unit tangent and the unit outward normal vectors of $\Gamma(t)$ at the i-th vertex $\boldsymbol{x}_i(t)$, respectively. The tangent vector $\boldsymbol{T}_i(t)$ is not well-defined at this stage, and its definition will be given later. Hereafter we abbreviate a notation for function $\mathsf{F}(t)$ as F unless there is confusion.

6.3.1 Algorithm

Since $\boldsymbol{N}_i = -\boldsymbol{T}_i^\perp$, we can rewrite the evolution law (6.3.1) as follows:

$$\dot{\boldsymbol{x}}_i = \alpha_i \boldsymbol{T}_i - V_i \boldsymbol{T}_i^\perp \quad (i = 1, 2, \ldots, N). \tag{6.3.2}$$

As we will see in the following sections, the all quantities $\{\boldsymbol{T}_i\}_{i=1}^n$, $\{\alpha_i\}_{i=1}^n$ and $\{V_i\}_{i=1}^n$ in the right hand side can be expressed as functions of $\{\boldsymbol{x}_i\}_{i=1}^n$. Therefore the time evolution equations (6.3.2) can be rewritten as a system of ordinary differential equations:

$$\dot{\boldsymbol{X}} = \boldsymbol{F}(\boldsymbol{X}(t)), \quad \begin{cases} \boldsymbol{X}(t) = (\boldsymbol{x}_i(t))_{i=1}^n = (\boldsymbol{x}_1(t), \boldsymbol{x}_2(t), \ldots, \boldsymbol{x}_n(t)) \in \mathbb{R}^{2\times n}, \\ \boldsymbol{F} = (\boldsymbol{f}_1, \boldsymbol{f}_2, \ldots, \boldsymbol{f}_n) \colon \mathbb{R}^{2\times n} \to \mathbb{R}^{2\times n};\ \boldsymbol{X} \mapsto \boldsymbol{F}(\boldsymbol{X}), \end{cases}$$

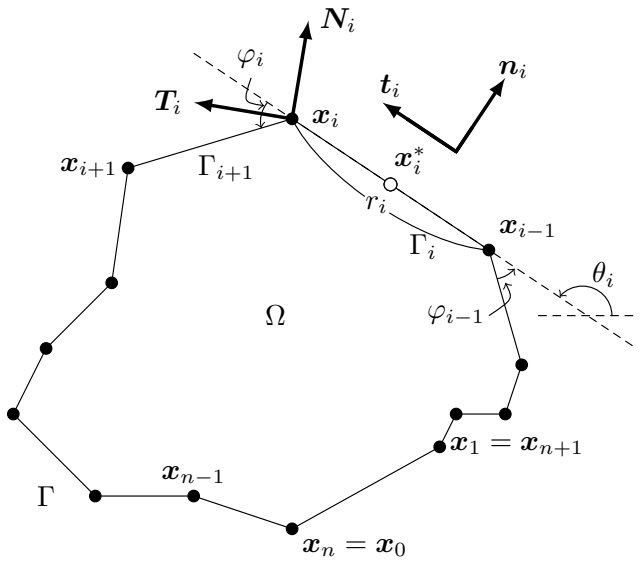

Notation

$$r_i = |\boldsymbol{x}_i - \boldsymbol{x}_{i-1}|$$
$$\boldsymbol{t}_i = \frac{\boldsymbol{x}_i - \boldsymbol{x}_{i-1}}{r_i} = \begin{pmatrix}\cos\theta_i \\ \sin\theta_i\end{pmatrix}$$
$$\boldsymbol{T}_i = \begin{pmatrix}\cos\theta_i^* \\ \sin\theta_i^*\end{pmatrix}$$
$$\theta_i^* = \frac{\theta_i + \theta_{i+1}}{2} = \theta_i + \frac{\varphi_i}{2}$$
$$\boldsymbol{x}_i^* = \frac{\boldsymbol{x}_{i-1} + \boldsymbol{x}_i}{2}$$
$$r_i^* = \frac{r_i + r_{i+1}}{2}$$
$$c_i = \cos\frac{\varphi_i}{2}, \quad s_i = \sin\frac{\varphi_i}{2}$$
$$k_i = \frac{\tan(\varphi_{i-1}/2) + \tan(\varphi_i/2)}{r_i}$$

Figure 6.2: Description of the symbols

where $f_i(\boldsymbol{X}(t)) = \alpha_i(t)\boldsymbol{T}_i(t) - V_i(t)\boldsymbol{T}_i(t)^\perp$, in which $\boldsymbol{T}_i(t) = \boldsymbol{T}_i(\boldsymbol{X}(t)) = (\cos\theta_i^*, \sin\theta_i^*)^{\mathrm{T}}$ is defined by the following Step 1 and in the subsequent subsection, $V_i(t) = V_i(\boldsymbol{X}(t))$ is defined by (6.3.3) and (6.3.13) via the solution $\mathscr{P}$ of (6.3.15) and (6.3.16), which is the structure-preserving scheme (see Section 6.3.4.1), or the one P of (6.3.18) and (6.3.20), which is the practical computational scheme (see Section 6.3.4.3), and $\alpha_i(t) = \alpha_i(\boldsymbol{X}(t))$ defined by (6.3.21) (see the following Step 3 and Section 6.3.5). In our numerical computation, we use the usual fourth order Runge-Kutta method to solve it. Namely, denoting by $\boldsymbol{X}_\tau^m$ the solution at the m-th step with time increment τ ($\boldsymbol{X}_\tau^m \approx \boldsymbol{X}(m\tau)$), then the solutions at the next time step can be obtained as follows:

$$\boldsymbol{X}_\tau^{m+1} = \boldsymbol{X}_\tau^m + \frac{1}{6}(\boldsymbol{K}_1 + 2\boldsymbol{K}_2 + 2\boldsymbol{K}_3 + \boldsymbol{K}_4), \quad \boldsymbol{X}_\tau^0 = \boldsymbol{X}(0),$$

where

$$\boldsymbol{K}_1 = \boldsymbol{F}(\boldsymbol{X}_\tau^m), \quad \boldsymbol{K}_2 = \boldsymbol{F}(\boldsymbol{X}_\tau^m + \boldsymbol{K}_1/2), \quad \boldsymbol{K}_3 = \boldsymbol{F}(\boldsymbol{X}_\tau^m + \boldsymbol{K}_2/2), \quad \boldsymbol{K}_4 = \boldsymbol{F}(\boldsymbol{X}_\tau^m + \boldsymbol{K}_3).$$

As mentioned above, the quantities $\{\boldsymbol{T}_i\}_{i=1}^n$, $\{\alpha_i\}_{i=1}^n$ and $\{V_i\}_{i=1}^n$ are computed as in the following way.

Step 1: Let θ_i be the i-th tangent angle on the i-th edge Γ_i, that is, θ_i satisfies the relation $(\boldsymbol{x}_i - \boldsymbol{x}_{i-1})/r_i = (\cos\theta_i, \sin\theta_i)^{\mathrm{T}}$, where $r_i = |\boldsymbol{x}_i - \boldsymbol{x}_{i-1}|$ is the length of the i-th edge Γ_i. Then we define $\boldsymbol{T}_i$ as follows:

$$\boldsymbol{T}_i = \begin{pmatrix}\cos\theta_i^* \\ \sin\theta_i^*\end{pmatrix}, \quad \theta_i^* = \frac{\theta_i + \theta_{i+1}}{2}.$$

See Section 6.3.2.

Step 2: The i-th normal velocity V_i is computed by MFS. Namely, when we consider the one-phase interior Hele-Shaw problem, the approximation of the pressure p at $\boldsymbol{x} \in \Omega$ is given by

$$Q_0 + \sum_{j=1}^n Q_j E_j(\boldsymbol{x}), \quad E_j(\boldsymbol{x}) = E(\boldsymbol{x} - \boldsymbol{y}_j) - E(\boldsymbol{x} - \boldsymbol{z}_j),$$

where $\{\boldsymbol{y}_j\}_{j=1}^n$ and $\{\boldsymbol{z}_j\}_{j=1}^n$ are the singular and dummy points located in $\mathbb{R}^2 \setminus \overline{\Omega}$, in which Ω denotes the bounded n-polygonal region surrounded by Γ here and hereafter. Coefficients $\{Q_j\}_{j=0}^n$ are determined by solving some system of linear, or quadratic, equations. See Section 6.3.4.

Step 3: The i-th tangential velocity α_i is computed by UDM. Indeed, the tangential velocities can be represented by some linear relations in which the normal velocities obtained in Step 2 appear. See Section 6.3.5.

6.3.2 Step 1: Compute $\{\boldsymbol{T}_i\}_{i=1}^n$

Let r_i be the length of the i-th edge Γ_i, that is, $r_i = |\boldsymbol{x}_i - \boldsymbol{x}_{i-1}|$. Then the i-th tangent vector $\boldsymbol{t}_i$ of Γ on the i-th edge Γ_i can be computed as $\boldsymbol{t}_i = (\boldsymbol{x}_i - \boldsymbol{x}_{i-1})/r_i$. Let θ_i be the i-th tangent angle of Γ; $\boldsymbol{t}_i = (\cos\theta_i, \sin\theta_i)^{\mathrm{T}}$. From these relations, we compute $\{\theta_i\}_{i=0}^{n+1}$ as in the following procedure: Firstly, from $\boldsymbol{t}_1 = (t_{11}, t_{12})^{\mathrm{T}}$, we have $\theta_1 = -\arccos t_{11}$ if $t_{12} < 0$; $\theta_1 = \arccos t_{11}$ if $t_{12} \geq 0$. Secondly, for $i = 1, 2, \ldots, n$ we successively compute θ_{i+1} from θ_i as follows:

$$\theta_{i+1} = \theta_i + (\operatorname{sgn} D) \arccos I,$$

where $D = \det(\boldsymbol{t}_i, \boldsymbol{t}_{i+1})$ and $I = \boldsymbol{t}_i \cdot \boldsymbol{t}_{i+1}$. Note that the sgn function is defined as follows:

$$\operatorname{sgn} a = \begin{cases} 1 & \text{if } a > 0, \\ 0 & \text{if } a = 0, \\ -1 & \text{if } a < 0. \end{cases}$$

Finally, we obtain $\theta_0 = \theta_1 - (\theta_{n+1} - \theta_n)$, since $\theta_n = \theta_0 + 2\pi$ and $\theta_{n+1} = \theta_1 + 2\pi$ hold.

Let us introduce the i-th "dual" edge Γ_i^* of the i-th edge Γ_i as $\Gamma_i^* = [\boldsymbol{x}_i^*, \boldsymbol{x}_i] \cup [\boldsymbol{x}_i, \boldsymbol{x}_{i+1}^*]$, where $\boldsymbol{x}_i^* = (\boldsymbol{x}_{i-1} + \boldsymbol{x}_i)/2$ is the mid point of Γ_i. The length r_i^* of the i-th dual edge Γ_i^* is $r_i^* = (r_i + r_{i+1})/2$. We define the i-th dual tangent angle θ_i^* by the following relation: $\theta_i^* = (\theta_i + \theta_{i+1})/2 = \theta_i + \varphi_i/2$, where $\varphi_i = \theta_{i+1} - \theta_i$ is the angle between adjacent two edges Γ_i and Γ_{i+1}. Thus the i-th dual unit tangent vector $\boldsymbol{T}_i$ is defined as in Step 1. See Figure 6.2 for geometrical descriptions.

6.3.3 Time evolution of the total length, the enclosed area and the barycenter

The total length L of Γ is

$$L = \sum_{i=1}^n r_i.$$

The enclosed area A of Ω can be computed as

$$A = \frac{1}{2}\sum_{i=1}^n (\boldsymbol{x}_i \cdot \boldsymbol{n}_i) r_i = \frac{1}{2}\sum_{i=1}^n \left(\boldsymbol{x}_i \cdot \frac{-(\boldsymbol{x}_i - \boldsymbol{x}_{i-1})^\perp}{r_i} \right) r_i = \frac{1}{2}\sum_{i=1}^n \boldsymbol{x}_{i-1}^\perp \cdot \boldsymbol{x}_i.$$

The barycenter $\boldsymbol{G}$ of Ω can be computed as

$$\boldsymbol{G} = \frac{1}{3A}\sum_{i=1}^n (\boldsymbol{x}_{i-1}^\perp \cdot \boldsymbol{x}_i)\boldsymbol{x}_i^*.$$

Indeed, direct computation yields that

$$\boldsymbol{G} = \frac{1}{A}\int_\Omega \boldsymbol{x}\,\mathrm{d}S = \frac{1}{3A}\int_\Omega \begin{pmatrix}\mathrm{div}(x\boldsymbol{x})\\ \mathrm{div}(y\boldsymbol{x})\end{pmatrix}\mathrm{d}S = \frac{1}{3A}\sum_{i=1}^n \int_{\Gamma_i} \boldsymbol{x}(\boldsymbol{x}\cdot\boldsymbol{n}_i)\,\mathrm{d}s = \frac{1}{3A}\sum_{i=1}^n (\boldsymbol{x}_{i-1}\cdot\boldsymbol{n}_i) r_i \boldsymbol{x}_i^*$$
$$= \frac{1}{3A}\sum_{i=1}^n (\boldsymbol{x}_{i-1}^\perp\cdot\boldsymbol{x}_i)\boldsymbol{x}_i^*.$$

Hereafter we use the following abbreviations:

$$c_i = \cos\frac{\varphi_i}{2}, \quad s_i = \sin\frac{\varphi_i}{2}.$$

Let $\boldsymbol{n}_i = -\boldsymbol{t}_i^\perp$ be the i-th unit outward normal vector of Γ on the i-th edge Γ_i. Then we can easily derive the following relations between the unit tangent and the unit outward normal vectors of Γ on the edges and the ones on the dual edges by virtue of addition theorem of trigonometric functions:

$$\boldsymbol{t}_i = c_i\boldsymbol{T}_i + s_i\boldsymbol{N}_i, \quad \boldsymbol{t}_{i+1} = c_i\boldsymbol{T}_i - s_i\boldsymbol{N}_i, \quad \boldsymbol{n}_i = -s_i\boldsymbol{T}_i + c_i\boldsymbol{N}_i, \quad \boldsymbol{n}_{i+1} = s_i\boldsymbol{T}_i + c_i\boldsymbol{N}_i.$$

Now we are ready to show a polygonal version of Theorem 6.2.1. For smooth curve $\mathscr{C}$ the curvature k can be defined from the first equation in Theorem 6.2.1: $\dot{\mathcal{L}} = \int_{\mathscr{C}} kV\,\mathrm{d}s$, rather than the Frenet type definition $\partial_s\boldsymbol{T} = -k\boldsymbol{N}$. In the same manner, for polygonal curve Γ the discrete curvature k_i on Γ_i can be defined from

$$\dot{L} = \sum_{i=1}^n \dot{r}_i = \sum_{i=1}^n \frac{1}{r_i}(\dot{\boldsymbol{x}}_i - \dot{\boldsymbol{x}}_{i-1})\cdot(\boldsymbol{x}_i - \boldsymbol{x}_{i-1}) = \sum_{i=1}^n (\dot{\boldsymbol{x}}_i - \dot{\boldsymbol{x}}_{i-1})\cdot\boldsymbol{t}_i = \sum_{i=1}^n \dot{\boldsymbol{x}}_i\cdot(\boldsymbol{t}_i - \boldsymbol{t}_{i+1})$$
$$= \sum_{i=1}^n (\alpha_i\boldsymbol{T}_i + V_i\boldsymbol{N}_i)\cdot 2s_i\boldsymbol{N}_i = 2\sum_{i=1}^n V_i s_i = 2\sum_{i=1}^n v_i\left(\tan\frac{\varphi_i}{2} + \tan\frac{\varphi_{i-1}}{2}\right) = \sum_{i=1}^n k_i v_i r_i,$$

when the normal velocity V_i is defined by

$$V_i = \frac{v_i + v_{i+1}}{2c_i}, \quad i = 1, 2, \ldots, n, \tag{6.3.3}$$

where v_i will be defined later as the constant normal velocity Γ_i (see (6.3.13) or (6.3.19)) and, as a result, k_i is defined by

$$k_i = \frac{\tan(\varphi_{i-1}/2) + \tan(\varphi_i/2)}{r_i}, \quad i = 1, 2, \ldots, n. \tag{6.3.4}$$

This is so-called the polygonal curvature when Γ_i is in an equivalent class [11, 56], and the crystalline curvature when Γ is in an admissible class [4, 99].

The following proposition, a polygonal analogue of Theorem 6.2.1, offers us explicit formulae for the time derivatives of the length L, the area A and the barycenter $\boldsymbol{G}$.

Proposition 6.3.1. *We have*

$$\dot{L} = \sum_{i=1}^n k_i v_i r_i, \tag{6.3.5}$$

$$\dot{A} = \sum_{i=1}^n v_i r_i + \mathrm{err}_A, \tag{6.3.6}$$

$$\dot{\boldsymbol{G}} = -\frac{\dot{A}}{A}\boldsymbol{G} + \frac{1}{A}\sum_{i=1}^n \boldsymbol{x}_i^* v_i r_i + \mathbf{err}_{\boldsymbol{G}}, \tag{6.3.7}$$

where err_A *and* $\mathbf{err}_{\boldsymbol{G}} := \mathbf{err}^1_{\boldsymbol{G}} + \mathbf{err}^2_{\boldsymbol{G}}$ *are the error terms:*

$$\mathrm{err}_A = \sum_{i=1}^{n} \left(\alpha_i s_i - \frac{v_{i+1} - v_i}{2} \right) \frac{r_{i+1} - r_i}{2}, \tag{6.3.8}$$

$$\mathbf{err}^1_{\boldsymbol{G}} = \frac{1}{6A} \sum_{i=1}^{n} \left(\alpha_i s_i - \frac{v_{i+1} - v_i}{2} \right) c_i (r_i^2 + r_{i+1}^2) \boldsymbol{T}_i, \tag{6.3.9}$$

$$\mathbf{err}^2_{\boldsymbol{G}} = \frac{1}{6A} \sum_{i=1}^{n} \left(\alpha_i s_i - \frac{v_{i+1} - v_i}{2} \right) (3\boldsymbol{x}_i - 2 s_i r_i^* \boldsymbol{N}_i)(r_{i+1} - r_i). \tag{6.3.10}$$

Proof. (6.3.5) is clear since the discrete curvatures $\{k_i\}_{i=1}^n$ are defined to satisfy (6.3.5).

By direct calculation, we obtain

$$\begin{aligned}
\dot{A} &= \frac{1}{2} \sum_{i=1}^{n} \left((\dot{\boldsymbol{x}}_{i-1})^\perp \cdot \boldsymbol{x}_i + \boldsymbol{x}_{i-1}^\perp \cdot \dot{\boldsymbol{x}}_i \right) = \frac{1}{2} \sum_{i=1}^{n} (\boldsymbol{x}_{i-1} - \boldsymbol{x}_{i+1})^\perp \cdot \dot{\boldsymbol{x}}_i \\
&= \frac{1}{2} \sum_{i=1}^{n} \left[(\boldsymbol{x}_i - r_i(c_i \boldsymbol{T}_i + s_i \boldsymbol{N}_i)) - (\boldsymbol{x}_i + r_{i+1}(c_i \boldsymbol{T}_i - s_i \boldsymbol{N}_i)) \right]^\perp \cdot (\alpha_i \boldsymbol{T}_i + V_i \boldsymbol{N}_i) \\
&= \frac{1}{2} \sum_{i=1}^{n} ((r_{i+1} - r_i) s_i \boldsymbol{T}_i + (r_{i+1} + r_i) c_i \boldsymbol{N}_i) \cdot \left(\alpha_i \boldsymbol{T}_i + \frac{v_i + v_{i+1}}{2c_i} \boldsymbol{N}_i \right) \\
&= \frac{1}{4} \sum_{i=1}^{n} (v_i + v_{i+1})(r_{i+1} + r_i) + \sum_{i=1}^{n} \alpha_i s_i \frac{r_{i+1} - r_i}{2} \\
&= \frac{1}{2} \sum_{i=1}^{n} v_i r_i + \frac{1}{4} \sum_{i=1}^{n} (v_i r_{i+1} + v_{i+1} r_i) + \sum_{i=1}^{n} \alpha_i s_i \frac{r_{i+1} - r_i}{2} \\
&= \sum_{i=1}^{n} v_i r_i + \sum_{i=1}^{n} \alpha_i s_i \frac{r_{i+1} - r_i}{2} + \frac{1}{4} \sum_{i=1}^{n} (v_i r_{i+1} + v_{i+1} r_i) - \frac{1}{4} \sum_{i=1}^{n} (v_i r_i + v_{i+1} r_{i+1}) \\
&= \sum_{i=1}^{n} v_i r_i + \sum_{i=1}^{n} \alpha_i s_i \frac{r_{i+1} - r_i}{2} - \sum_{i=1}^{n} \frac{v_{i+1} - v_i}{2} \frac{r_{i+1} - r_i}{2} \\
&= \sum_{i=1}^{n} v_i r_i + \sum_{i=1}^{n} \left(\alpha_i s_i - \frac{v_{i+1} - v_i}{2} \right) \frac{r_{i+1} - r_i}{2},
\end{aligned}$$

which is nothing but (6.3.6).

Concerning the time derivative of the barycenter, we have

$$\dot{\boldsymbol{G}} = -\frac{\dot{A}}{3A^2} \sum_{i=1}^{n} (\boldsymbol{x}_{i-1}^\perp \cdot \boldsymbol{x}_i) \boldsymbol{x}_i^* + \frac{1}{3A} \frac{\mathrm{d}}{\mathrm{d}t} \left(\sum_{i=1}^{n} (\boldsymbol{x}_{i-1}^\perp \cdot \boldsymbol{x}_i) \boldsymbol{x}_i^* \right) = -\frac{\dot{A}}{A} \boldsymbol{G} + \frac{1}{3A} \frac{\mathrm{d}}{\mathrm{d}t} \left(\sum_{i=1}^{n} (\boldsymbol{x}_{i-1}^\perp \cdot \boldsymbol{x}_i) \boldsymbol{x}_i^* \right),$$

therefore

$$6A \left(\dot{\boldsymbol{G}} + \frac{\dot{A}}{A} \boldsymbol{G} \right) = 2 \frac{\mathrm{d}}{\mathrm{d}t} \left(\sum_{i=1}^{n} (\boldsymbol{x}_{i-1}^\perp \cdot \boldsymbol{x}_i) \boldsymbol{x}_i^* \right)$$

holds. In the following, we compute the right hand side in the above equality. Using the evolution equation (6.3.1) and the relation (6.3.3), we have

$$2 \frac{\mathrm{d}}{\mathrm{d}t} \left(\sum_{i=1}^{n} (\boldsymbol{x}_{i-1}^\perp \cdot \boldsymbol{x}_i) \boldsymbol{x}_i^* \right)$$

$$
\begin{aligned}
&= 2\sum_{i=1}^{n}\left(\dot{\boldsymbol{x}}_{i-1}^{\perp}\cdot\boldsymbol{x}_i+\boldsymbol{x}_{i-1}^{\perp}\cdot\dot{\boldsymbol{x}}_i\right)\boldsymbol{x}_i^*+\sum_{i=1}^{n}(\boldsymbol{x}_{i-1}^{\perp}\cdot\boldsymbol{x}_i)(\dot{\boldsymbol{x}}_{i-1}+\dot{\boldsymbol{x}}_i)\\
&= 2\sum_{i=1}^{n}(\dot{\boldsymbol{x}}_i^{\perp}\cdot\boldsymbol{x}_{i+1})\boldsymbol{x}_{i+1}^*+2\sum_{i=1}^{n}(\boldsymbol{x}_{i-1}^{\perp}\cdot\dot{\boldsymbol{x}}_i)\boldsymbol{x}_i^*+\sum_{i=1}^{n}\dot{\boldsymbol{x}}_i\left(\boldsymbol{x}_{i-1}^{\perp}\cdot\boldsymbol{x}_i+\boldsymbol{x}_i^{\perp}\cdot\boldsymbol{x}_{i+1}\right)\\
&= 2\sum_{i=1}^{n}\left(\dot{\boldsymbol{x}}_i^{\perp}\cdot(\boldsymbol{x}_i+r_{i+1}\boldsymbol{t}_{i+1})\right)\boldsymbol{x}_{i+1}^*+2\sum_{i=1}^{n}[\dot{\boldsymbol{x}}_i\cdot(\boldsymbol{x}_i-r_i\boldsymbol{t}_i)^{\perp}]\boldsymbol{x}_i^*\\
&\qquad\qquad+\sum_{i=1}^{n}\dot{\boldsymbol{x}}_i[\boldsymbol{x}_i\cdot(\boldsymbol{x}_i-r_i\boldsymbol{t}_i)^{\perp}]+\sum_{i=1}^{n}\dot{\boldsymbol{x}}_i[\boldsymbol{x}_i^{\perp}\cdot(\boldsymbol{x}_i+r_{i+1}\boldsymbol{t}_{i+1})]\\
&= 2\sum_{i=1}^{n}(\dot{\boldsymbol{x}}_i^{\perp}\cdot\boldsymbol{x}_i)\boldsymbol{x}_{i+1}^*+2\sum_{i=1}^{n}\left[(V_i\boldsymbol{T}_i-\alpha_i\boldsymbol{N}_i)\cdot r_{i+1}(c_i\boldsymbol{T}_i-s_i\boldsymbol{N}_i)\right]\boldsymbol{x}_{i+1}^*+2\sum_{i=1}^{n}(\dot{\boldsymbol{x}}_i\cdot\boldsymbol{x}_i^{\perp})\boldsymbol{x}_i^*\\
&\quad+2\sum_{i=1}^{n}\left[(\alpha_i\boldsymbol{T}_i+V_i\boldsymbol{N}_i)\cdot r_i(-s_i\boldsymbol{T}_i+c_i\boldsymbol{N}_i)\right]\boldsymbol{x}_i^*+\sum_{i=1}^{n}\dot{\boldsymbol{x}}_i(\boldsymbol{x}_i\cdot r_i\boldsymbol{n}_i)+\sum_{i=1}^{n}\dot{\boldsymbol{x}}_i(\boldsymbol{x}_i^{\perp}\cdot r_{i+1}\boldsymbol{t}_{i+1})\\
&= -2\sum_{i=1}^{n}(\dot{\boldsymbol{x}}_i\cdot\boldsymbol{x}_i^{\perp})\boldsymbol{x}_{i+1}^*+2\sum_{i=1}^{n}(\alpha_is_i+V_ic_i)r_{i+1}\boldsymbol{x}_{i+1}^*+2\sum_{i=1}^{n}(\dot{\boldsymbol{x}}_i\cdot\boldsymbol{x}_i^{\perp})\boldsymbol{x}_i^*\\
&\qquad\qquad+2\sum_{i=1}^{n}(-\alpha_is_i+V_ic_i)r_i\boldsymbol{x}_i^*+\sum_{i=1}^{n}\dot{\boldsymbol{x}}_i(\boldsymbol{x}_i\cdot\boldsymbol{n}_i)r_i+\sum_{i=1}^{n}\dot{\boldsymbol{x}}_i(\boldsymbol{x}_i\cdot\boldsymbol{n}_{i+1})r_{i+1}\\
&= -2\sum_{i=1}^{n}(\dot{\boldsymbol{x}}_i\cdot\boldsymbol{x}_i^{\perp})(\boldsymbol{x}_{i+1}^*-\boldsymbol{x}_i^*)+2\sum_{i=1}^{n}V_ic_i(r_{i+1}\boldsymbol{x}_{i+1}^*+r_i\boldsymbol{x}_i^*)+2\sum_{i=1}^{n}\alpha_is_i(r_{i+1}\boldsymbol{x}_{i+1}^*-r_i\boldsymbol{x}_i^*)\\
&\qquad\qquad+\sum_{i=1}^{n}\dot{\boldsymbol{x}}_i[\boldsymbol{x}_i\cdot(r_i\boldsymbol{n}_i+r_{i+1}\boldsymbol{n}_{i+1})].
\end{aligned}
$$

Using the relations

$$
\begin{aligned}
2(\boldsymbol{x}_{i+1}^*-\boldsymbol{x}_i^*)&=\boldsymbol{x}_i+\boldsymbol{x}_{i+1}-(\boldsymbol{x}_{i-1}+\boldsymbol{x}_i)=\boldsymbol{x}_{i+1}-\boldsymbol{x}_{i-1}=r_i\boldsymbol{t}_i+r_{i+1}\boldsymbol{t}_{i+1}\\
&=r_i(c_i\boldsymbol{T}_i+s_i\boldsymbol{N}_i)+r_{i+1}(c_i\boldsymbol{T}_i-s_i\boldsymbol{N}_i)=(r_i+r_{i+1})c_i\boldsymbol{T}_i+(r_i-r_{i+1})s_i\boldsymbol{N}_i
\end{aligned}
$$

and

$$
r_i\boldsymbol{n}_i+r_{i+1}\boldsymbol{n}_{i+1}=r_i(-s_i\boldsymbol{T}_i+c_i\boldsymbol{N}_i)+r_{i+1}(s_i\boldsymbol{T}_i+c_i\boldsymbol{N}_i)=(r_{i+1}-r_i)s_i\boldsymbol{T}_i+(r_i+r_{i+1})c_i\boldsymbol{N}_i,
$$

we have

$$
\begin{aligned}
&2\frac{\mathrm{d}}{\mathrm{d}t}\left(\sum_{i=1}^{n}(\boldsymbol{x}_{i-1}^{\perp}\cdot\boldsymbol{x}_i)\boldsymbol{x}_i^*\right)\\
&\quad=\sum_{i=1}^{n}(\dot{\boldsymbol{x}}_i^{\perp}\cdot\boldsymbol{x}_i)[c_i(r_i+r_{i+1})\boldsymbol{T}_i+(r_i-r_{i+1})s_i\boldsymbol{N}_i]\\
&\qquad\qquad+\sum_{i=1}^{n}\dot{\boldsymbol{x}}_i[s_i(r_{i+1}-r_i)(\boldsymbol{x}_i\cdot\boldsymbol{T}_i)+c_i(r_i+r_{i+1})(\boldsymbol{x}_i\cdot\boldsymbol{N}_i)]\\
&\qquad\qquad+\sum_{i=1}^{n}(v_ir_{i+1}\boldsymbol{x}_{i+1}^*+v_ir_i\boldsymbol{x}_i^*+v_{i+1}r_{i+1}\boldsymbol{x}_{i+1}^*+v_{i+1}r_i\boldsymbol{x}_i^*)\\
&\qquad\qquad+\sum_{i=1}^{n}\alpha_is_i[r_{i+1}(\boldsymbol{x}_i+\boldsymbol{x}_{i+1})-r_i(\boldsymbol{x}_{i-1}+\boldsymbol{x}_i)]
\end{aligned}
$$

$$
\begin{aligned}
&= \sum_{i=1}^{n}[V_i c_i(r_i + r_{i+1})(\boldsymbol{x}_i \cdot \boldsymbol{T}_i)\boldsymbol{T}_i + V_i s_i(r_i - r_{i+1})(\boldsymbol{x}_i \cdot \boldsymbol{T}_i)\boldsymbol{N}_i \\
&\qquad - \alpha_i c_i(r_i + r_{i+1})(\boldsymbol{x}_i \cdot \boldsymbol{N}_i)\boldsymbol{T}_i - \alpha_i s_i(r_i - r_{i+1})(\boldsymbol{x}_i \cdot \boldsymbol{N}_i)\boldsymbol{N}_i] \\
&\qquad + \sum_{i=1}^{n}[\alpha_i s_i(r_{i+1} - r_i)(\boldsymbol{x}_i \cdot \boldsymbol{T}_i)\boldsymbol{T}_i + \alpha_i c_i(r_i + r_{i+1})(\boldsymbol{x}_i \cdot \boldsymbol{N}_i)\boldsymbol{T}_i \\
&\qquad\quad + V_i s_i(r_{i+1} - r_i)(\boldsymbol{x}_i \cdot \boldsymbol{T}_i)\boldsymbol{N}_i + V_i c_i(r_i + r_{i+1})(\boldsymbol{x}_i \cdot \boldsymbol{N}_i)\boldsymbol{N}_i] \\
&\qquad + 2\sum_{i=1}^{n} \boldsymbol{x}_i^* v_i r_i + \sum_{i=1}^{n}[(v_{i+1} - v_i) r_i \boldsymbol{x}_i^* + v_i r_i \boldsymbol{x}_i^* + v_i r_{i+1} \boldsymbol{x}_{i+1}^*] \\
&\qquad + \sum_{i=1}^{n} \alpha_i s_i(r_{i+1} - r_i)\boldsymbol{x}_i + \sum_{i=1}^{n} \alpha_i s_i[r_{i+1}(\boldsymbol{x}_i + r_{i+1}\boldsymbol{t}_{i+1}) - r_i(\boldsymbol{x}_i - r_i \boldsymbol{t}_i)] \\
&= 2\sum_{i=1}^{n} V_i c_i r_i^* \boldsymbol{x}_i + \sum_{i=1}^{n} \alpha_i s_i(r_{i+1} - r_i)\boldsymbol{x}_i + 3\sum_{i=1}^{n} \boldsymbol{x}_i^* v_i r_i + \sum_{i=1}^{n}(v_{i+1} - v_i) r_i \boldsymbol{x}_i \\
&\qquad - \sum_{i=1}^{n} \frac{v_{i+1} - v_i}{2} r_i^2 \boldsymbol{t}_i + \sum_{i=1}^{n} v_i r_{i+1} \boldsymbol{x}_i + \frac{1}{2}\sum_{i=1}^{n} v_i r_{i+1}^2 \boldsymbol{t}_{i+1} + 2\sum_{i=1}^{n} \alpha_i s_i(r_{i+1} - r_i)\boldsymbol{x}_i \\
&\qquad + \sum_{i=1}^{n} \alpha_i s_i[c_i(r_{i+1}^2 + r_i^2)\boldsymbol{T}_i - s_i(r_{i+1}^2 - r_i^2)\boldsymbol{N}_i] \\
&= \underline{\sum_{i=1}^{n}(v_i + v_{i+1})\frac{r_i + r_{i+1}}{2}\boldsymbol{x}_i} + 3\sum_{i=1}^{n} \alpha_i s_i(r_{i+1} - r_i)\boldsymbol{x}_i \ \underline{+ 3\sum_{i=1}^{n} \boldsymbol{x}_i^* v_i r_i + \sum_{i=1}^{n}(v_{i+1} - v_i) r_i \boldsymbol{x}_i} \\
&\qquad \underline{- \sum_{i=1}^{n} \frac{v_{i+1} - v_i}{2} r_i^2 (c_i \boldsymbol{T}_i + s_i \boldsymbol{N}_i) + \sum_{i=1}^{n}[v_{i+1} - (v_{i+1} - v_i)] r_{i+1} \boldsymbol{x}_i} \\
&\qquad \underline{+ \frac{1}{2}\sum_{i=1}^{n}[(v_i - v_{i+1}) + v_{i+1}] r_{i+1}^2 (c_i \boldsymbol{T}_i - s_i \boldsymbol{N}_i)} + \sum_{i=1}^{n} \alpha_i s_i c_i (r_{i+1}^2 + r_i^2)\boldsymbol{T}_i \\
&\qquad - 2\sum_{i=1}^{n} \alpha_i s_i^2 r_i^*(r_{i+1} - r_i)\boldsymbol{N}_i.
\end{aligned}
$$

The underlined part, say ①, can be computed as follows:

$$
\begin{aligned}
① &= -\sum_{i=1}^{n} \frac{v_{i+1} - v_i}{2}(r_i^2 + r_{i+1}^2) c_i \boldsymbol{T}_i + \sum_{i=1}^{n} \frac{v_{i+1} - v_i}{2}(r_{i+1}^2 - r_i^2) s_i \boldsymbol{N}_i + \sum_{i=1}^{n} v_i r_i \boldsymbol{x}_i^* \\
&\qquad + \frac{1}{2}\sum_{i=1}^{n}(v_i r_{i+1} + v_{i+1} r_i)\boldsymbol{x}_i + 3\sum_{i=1}^{n} \boldsymbol{x}_i^* v_i r_i + \sum_{i=1}^{n}(v_{i+1} - v_i)(r_i - r_{i+1})\boldsymbol{x}_i \\
&\qquad + \sum_{i=1}^{n} v_{i+1} r_{i+1} \boldsymbol{x}_i + \frac{1}{2}\sum_{i=1}^{n} v_{i+1} r_{i+1}^2 (c_i \boldsymbol{T}_i - s_i \boldsymbol{N}_i) \\
&= -\sum_{i=1}^{n} \frac{v_{i+1} - v_i}{2}(r_i^2 + r_{i+1}^2) c_i \boldsymbol{T}_i + \sum_{i=1}^{n} \frac{v_{i+1} - v_i}{2}(r_{i+1}^2 - r_i^2) s_i \boldsymbol{N}_i + 6\sum_{i=1}^{n} \boldsymbol{x}_i^* v_i r_i \\
&\qquad \underline{- \sum_{i=1}^{n}(\boldsymbol{x}_{i-1} + \boldsymbol{x}_i) v_i r_i + \frac{1}{2}\sum_{i=1}^{n}(v_i r_{i+1} + v_{i+1} r_i + 2 v_{i+1} r_{i+1})\boldsymbol{x}_i}
\end{aligned}
$$

$$+\sum_{i=1}^{n}\frac{v_{i+1}-v_i}{2}(r_i-r_{i+1})3\boldsymbol{x}_i\underline{-\sum_{i=1}^{n}\frac{v_{i+1}-v_i}{2}(r_i-r_{i+1})\boldsymbol{x}_i+\frac{1}{2}\sum_{i=1}^{n}v_{i+1}r_{i+1}^2\boldsymbol{t}_{i+1}}$$

The underlined part, say ②, is equal to $\mathbf{0}$. Indeed, we have

$$\begin{aligned}
② &= -\sum_{i=1}^{n}\boldsymbol{x}_i v_i r_i-\sum_{i=1}^{n}(\boldsymbol{x}_i-r_i\boldsymbol{t}_i)v_i r_i-2\sum_{i=1}^{n}v_i r_{i+1}^2\boldsymbol{t}_i\\
&\qquad+\frac{1}{2}\sum_{i=1}^{n}(v_i r_{i+1}+v_{i+1}r_i+2v_i r_i-v_{i+1}r_i+v_{i+1}r_{i+1}+v_i r_i-v_i r_{i+1})\boldsymbol{x}_i\\
&=-2\sum_{i-1}^{n}\boldsymbol{x}_i v_i r_i+\sum_{i=1}^{n}v_i r_i^2\boldsymbol{t}_i+\frac{3}{2}\sum_{i=1}^{n}\boldsymbol{x}_i v_{i+1}r_{i+1}+\frac{1}{2}\sum_{i=1}^{n}\boldsymbol{x}_i v_i r_i+\frac{1}{2}\sum_{i=1}^{n}v_i r_i^2\boldsymbol{t}_i\\
&=\frac{3}{2}\sum_{i=1}^{n}(v_i r_i^2\boldsymbol{t}_i+v_i r_i\boldsymbol{x}_{i-1}-v_i r_i\boldsymbol{x}_i)=\mathbf{0}.
\end{aligned}$$

Summarizing the above relations, we obtain

$$\begin{aligned}
&6A\left(\dot{\boldsymbol{G}}+\frac{\dot{A}}{A}\boldsymbol{G}\right)\\
&\quad=3\sum_{i=1}^{n}\alpha_i s_i(r_{i+1}-r_i)\boldsymbol{x}_i+\sum_{i=1}^{n}\alpha_i s_i c_i(r_{i+1}^2+r_i^2)\boldsymbol{T}_i-2\sum_{i-1}^{n}\alpha_i s_i^2 r_i^*(r_{i+1}-r_i)\boldsymbol{N}_i\\
&\qquad\quad-\sum_{i=1}^{n}\frac{v_{i+1}-v_i}{2}c_i(r_i^2+r_{i+1}^2)\boldsymbol{T}_i+\sum_{i=1}^{n}\frac{v_{i+1}-v_i}{2}2s_i r_i^*(r_{i+1}-r_i)\boldsymbol{N}_i\\
&\qquad\quad+6\sum_{i=1}^{n}\boldsymbol{x}_i^* v_i r_i-\sum_{i=1}^{n}\frac{v_{i+1}-v_i}{2}(r_{i+1}-r_i)3\boldsymbol{x}_i\\
&\quad=\sum_{i=1}^{n}\left(\alpha_i s_i-\frac{v_{i+1}-v_i}{2}\right)c_i(r_i^2+r_{i+1}^2)\boldsymbol{T}_i\\
&\qquad\quad+\sum_{i=1}^{n}\left(\alpha_i s_i-\frac{v_{i+1}-v_i}{2}\right)(3\boldsymbol{x}_i-2s_i r_i^*\boldsymbol{N}_i)(r_{i+1}-r_i)+6\sum_{i=1}^{n}\boldsymbol{x}_i^* v_i r_i,
\end{aligned}$$

which completes the proof of Proposition 6.3.1. □

Remark 6.3.2. Note that under UDM, $r_i\equiv L/n$ holds for all i, then we have $\mathrm{err}_A=0$ and $\mathbf{err}_{\boldsymbol{G}}^2=\mathbf{0}$, and if $\dot{A}=0$, then we have $\dot{\boldsymbol{G}}=\mathbf{0}$ by MFS (see Section 6.3.4.1). We also note that if $\alpha_i=(v_{i+1}-v_i)/(2s_i)$, then $\mathrm{err}_A=0$ and $\mathbf{err}_{\boldsymbol{G}}=\mathbf{0}$ simultaneously [11, 56]. In this case, Γ is restricted in the equivalent class, since $v_i=\dot{\boldsymbol{x}}_i\cdot\boldsymbol{n}_i=\dot{\boldsymbol{x}}_{i-1}\cdot\boldsymbol{n}_i$ hold. Indeed, by the evolution law (6.2.3), we have

$$\begin{aligned}
\dot{\boldsymbol{x}}_i\cdot\boldsymbol{n}_i&=(\alpha_i\boldsymbol{T}_i+V_i\boldsymbol{N}_i)\cdot(-s_i\boldsymbol{T}_i+c_i\boldsymbol{N}_i)=-\alpha_i s_i+V_i c_i=-\frac{v_{i+1}-v_i}{2s_i}s_i+\frac{v_i+v_{i+1}}{2c_i}c_i=v_i,\\
\dot{\boldsymbol{x}}_{i-1}\cdot\boldsymbol{n}_i&=(\alpha_{i-1}\boldsymbol{T}_i+V_{i-1}\boldsymbol{N}_{i-1})\cdot(s_{i-1}\boldsymbol{T}_{i-1}+c_{i-1}\boldsymbol{N}_{i-1})=\alpha_{i-1}s_{i-1}+V_{i-1}s_{i-1}\\
&=\frac{v_i-v_{i-1}}{2s_{i-1}}s_{i-1}+\frac{v_{i-1}+v_i}{2c_{i-1}}c_{i-1}=v_i.
\end{aligned}$$

Direct computation yields

$$\begin{aligned}\dot{\boldsymbol{t}}_i &= \frac{\mathrm{d}}{\mathrm{d}t}\left(\frac{\boldsymbol{x}_i-\boldsymbol{x}_{i-1}}{r_i}\right) = -\frac{1}{r_i^2}\left[(\dot{\boldsymbol{x}}_i-\dot{\boldsymbol{x}}_{i-1})\cdot\boldsymbol{t}_i\right](\boldsymbol{x}_i-\boldsymbol{x}_{i-1})+\frac{1}{r_i}(\dot{\boldsymbol{x}}_i-\dot{\boldsymbol{x}}_{i-1})\\ &= -\frac{1}{r_i}\left[(\alpha_i\boldsymbol{T}_i+V_i\boldsymbol{N}_i)\cdot(c_i\boldsymbol{T}_i+s_i\boldsymbol{N}_i)-(\alpha_{i-1}\boldsymbol{T}_{i-1}+V_{i-1}\boldsymbol{N}_{i-1})\cdot(c_{i-1}\boldsymbol{T}_{i-1}-s_{i-1}\boldsymbol{N}_{i-1})\right]\boldsymbol{t}_i\\ &\qquad +\frac{1}{r_i}\left(\alpha_i\boldsymbol{T}_i+V_i\boldsymbol{N}_i-(\alpha_{i-1}\boldsymbol{T}_{i-1}+V_{i-1}\boldsymbol{N}_{i-1})\right)\\ &= -\frac{1}{r_i}\underline{(\alpha_ic_i+V_is_i-\alpha_{i-1}c_{i-1}+V_{i-1}s_{i-1})\,\boldsymbol{t}_i}+\frac{1}{r_i}\left(\alpha_i\boldsymbol{T}_i+V_i\boldsymbol{N}_i-\alpha_{i-1}\boldsymbol{T}_{i-1}-V_{i-1}\boldsymbol{N}_{i-1}\right).\end{aligned}$$

The underlined part, say ①, can be computed as

$$\begin{aligned}①&=(\alpha_ic_i+V_is_i)(c_i\boldsymbol{T}_i+s_i\boldsymbol{N}_i)-(\alpha_{i-1}c_{i-1}-V_{i-1}s_{i-1})(c_{i-1}\boldsymbol{T}_{i-1}-s_{i-1}\boldsymbol{N}_{i-1})\\ &=\alpha_i(1-s_i^2)\boldsymbol{T}_i+\alpha_ic_is_i\boldsymbol{N}_i+V_ic_is_i\boldsymbol{N}_i+V_i(1-c_i^2)\boldsymbol{N}_i\\ &\qquad-\alpha_{i-1}(1-s_{i-1}^2)\boldsymbol{T}_i+\alpha_{i-1}c_{i-1}s_{i-1}\boldsymbol{N}_i+V_{i-1}c_{i-1}s_{i-1}\boldsymbol{T}_{i-1}-V_{i-1}(1-c_{i-1}^2)\boldsymbol{N}_{i-1}.\end{aligned}$$

Therefore we have

$$\begin{aligned}\dot{\boldsymbol{t}}_i &= \frac{1}{r_i}\big(\alpha_is_i^2\boldsymbol{T}_i-\alpha_ic_is_i\boldsymbol{N}_i-V_ic_is_i\boldsymbol{T}_i+V_ic_i^2\boldsymbol{N}_i-\alpha_{i-1}s_{i-1}^2\boldsymbol{T}_{i-1}-\alpha_{i-1}c_{i-1}s_{i-1}\boldsymbol{N}_{i-1}\\ &\qquad -V_{i-1}c_{i-1}s_{i-1}\boldsymbol{T}_{i-1}-V_{i-1}c_{i-1}^2\boldsymbol{N}_{i-1}\big)\\ &= \frac{1}{r_i}\left[s_i\left(\frac{v_{i+1}-v_i}{2s_i}s_i-\frac{v_i+v_{i+1}}{2c_i}c_i\right)\boldsymbol{T}_i+c_i\left(-\frac{v_{i+1}-v_i}{2s_i}s_i+\frac{v_i+v_{i+1}}{2c_i}c_i\right)\boldsymbol{N}_i\right.\\ &\left.-s_{i-1}\left(\frac{v_i-v_{i-1}}{2s_{i-1}}s_{i-1}+\frac{v_{i-1}+v_i}{2c_{i-1}}c_{i-1}\right)\boldsymbol{T}_{i-1}-c_{i-1}\left(\frac{v_i-v_{i-1}}{2s_{i-1}}s_{i-1}+\frac{v_{i-1}+v_i}{2c_{i-1}}c_{i-1}\right)\boldsymbol{N}_{i-1}\right]\\ &= \frac{1}{r_i}\left(-v_is_i\boldsymbol{T}_i+v_ic_i\boldsymbol{N}_i-v_is_{i-1}\boldsymbol{T}_{i-1}-v_ic_{i-1}\boldsymbol{N}_{i-1}\right)\\ &= \frac{v_i}{r_i}\left[-s_i\boldsymbol{T}_i+c_i\boldsymbol{N}_i-(s_{i-1}\boldsymbol{T}_{i-1}+c_{i-1}\boldsymbol{N}_{i-1})\right]=\boldsymbol{0},\end{aligned}$$

which concludes that Γ is restricted in the equivalent class.

6.3.4 Step 2: Compute $\{V_i\}_{i=1}^n$ by MFS

Fix the time t and give the approximation of the pressure function $p(\cdot,t)$ by using the method of fundamental solutions.

6.3.4.1 Structure-preserving scheme

Let $\Omega(t)$ be the region surrounded by $\Gamma(t)$. Under MFS, the solution of (6.1.1) is approximated by $\mathscr{P}$ such as

$$\mathscr{P}(\boldsymbol{x}) = \mathscr{Q}_0+\sum_{j=1}^{n}\mathscr{Q}_jE_j(\boldsymbol{x}),\quad E_j(\boldsymbol{x})=E(\boldsymbol{x}-\boldsymbol{y}_j)-E(\boldsymbol{x}-\boldsymbol{z}_j),\quad \boldsymbol{x}\in\overline{\Omega}(t), \tag{6.3.11}$$

$$\langle(\mathscr{P}-\gamma k_i)\nabla\mathscr{P}\rangle_i\cdot\boldsymbol{n}_i=0,\quad i=1,2,\ldots,n, \tag{6.3.12}$$

$$v_i=-\langle\nabla\mathscr{P}\rangle_i\cdot\boldsymbol{n}_i,\quad i=1,2,\ldots,n, \tag{6.3.13}$$

where $\{\mathscr{Q}_j\}_{j=0}^n$ are unknown coefficients, $\boldsymbol{y}_j$'s are the singular points defined as

$$\boldsymbol{y}_j=\boldsymbol{x}_j^*+d\boldsymbol{n}_j,\quad j=1,2,\ldots,n, \tag{6.3.14}$$

$d > 0$ is a parameter controlling accuracy of MFS, and $\{\boldsymbol{z}_j\}_{j=1}^n$ are "dummy" points located in $\mathbb{R}^2 \setminus \overline{\Omega}(t)$ which are not equal to the singular points $\{\boldsymbol{y}_j\}_{j=1}^n$. Here $\langle \mathsf{F} \rangle_i = r_i^{-1} \int_{\Gamma_i} \mathsf{F} \, \mathrm{d}s$ is the average of F on Γ_i. Te normal velocities $\{V_i\}_{i=1}^n$ are determined by (6.3.3) and the above $\{v_i\}_{i=1}^n$. Note that $\triangle \mathscr{P} = 0$ holds in $\Omega(t)$ and we have direct calculation such as $\nabla \mathscr{P} = \sum_{j=1}^n \mathscr{Q}_j \nabla E_j$. Note also that if we put $[\mathscr{P}]_i = \langle \mathscr{P} \nabla \mathscr{P} \rangle \cdot \boldsymbol{n}_i / \langle \nabla \mathscr{P} \rangle_i \cdot \boldsymbol{n}_i$, then (6.3.12) can be expressed as $[\mathscr{P}]_i = \gamma k_i$ when $\langle \nabla \mathscr{P} \rangle_i \cdot \boldsymbol{n}_i \neq 0$. We can see that the conditions (6.3.12) are weak forms of the original boundary condition in some sense.

The coefficients $\{\mathscr{Q}_j\}_{j=0}^n$ are determined from $(n+1)$'s quadratic equations: n's quadratic equations (6.3.12) expressed by

$$(\mathscr{Q}_0 - \gamma k_i) \sum_{j=1}^n a_{ij} \mathscr{Q}_j + \sum_{j=1}^n \sum_{l=1}^n a_{ilj} \mathscr{Q}_l \mathscr{Q}_j = 0, \quad i = 1, 2, \ldots, n, \tag{6.3.15}$$

where $a_{ij} = \langle \nabla E_j \rangle_i \cdot \boldsymbol{n}_i$, $a_{ilj} = \langle E_l \nabla E_j \rangle_i \cdot \boldsymbol{n}_i$, and one more equation derived from the second term in (6.3.7) and the first error term (6.3.9):

$$\left| \frac{1}{A} \sum_{i=1}^n \boldsymbol{x}_i^* v_i r_i + \mathbf{err}_{\boldsymbol{G}}^1 \right| = 0,$$

which is the same as the following quadratic equation

$$\sum_{j=1}^n \sum_{l=1}^n \boldsymbol{b}_l \cdot \boldsymbol{b}_j \mathscr{Q}_l \mathscr{Q}_j + 2 \sum_{j=1}^n \boldsymbol{b} \cdot \boldsymbol{b}_j \mathscr{Q}_j + |\boldsymbol{b}|^2 = 0. \tag{6.3.16}$$

Here vectors $\boldsymbol{b}$ and $\{\boldsymbol{b}_j\}_{j=1}^n$ are calculated from (6.3.21) as follows:

$$\begin{aligned}
&\boldsymbol{b} = \sum_{i=2}^n \boldsymbol{\mu}_i \left(\frac{i-1}{n} L - \sum_{l=2}^i r_l \right) \omega, \quad \boldsymbol{b}_j = \boldsymbol{\lambda}_j + \sum_{i=2}^n \boldsymbol{\mu}_i \sum_{l=2}^i b_{lj}, \quad \boldsymbol{\tau}_i = \frac{r_i^2 + r_{i+1}^2}{6} \boldsymbol{T}_i, \\
&\boldsymbol{\mu}_i = s_i \boldsymbol{\tau}_i - \frac{1}{c_i} \left(\sum_{j=1}^n \frac{1}{c_j} \right)^{-1} \left(\sum_{l=1}^n s_l \boldsymbol{\tau}_l \right), \quad \boldsymbol{\lambda}_j = \sum_{i=1}^n \left(-a_{ij} \boldsymbol{x}_i^* r_i + \frac{a_{i+1,j} - a_{ij}}{2} c_i \boldsymbol{\tau}_i \right), \\
&b_{lj} = \frac{\tan(\varphi_l/2)}{2} a_{l+1,j} + \frac{k_l r_l}{2} a_{lj} + \frac{\tan(\varphi_{l-1}/2)}{2} a_{l-1,j} - \frac{1}{n} \sum_{i=1}^n k_i a_{ij} r_i, \quad l = 1, 2, \ldots, n,
\end{aligned}$$

for $i, j = 1, 2, \ldots, n$. Using these normal velocities, we will see in Proposition 6.3.3 that CS-, AP- and BF-properties are satisfied, however, it is hard to compute a_{ij} and a_{ilj} analytically so that we have to do some numerical integration. Moreover, we have to solve $(n+1)$'s nonlinear equations, and it is hard to discuss the existence of solutions of (6.3.15) and (6.3.16). Hence we propose simpler scheme we only have to solve $(n+1)$'s linear equations. Using this scheme, we will see in Proposition 6.3.4 that CS-, AP- and BF-properties hold asymptotically, and in section 6.6 that it offers satisfactory numerical results.

6.3.4.2 Derivation of the equations (6.3.15) and (6.3.16)

Direct computation yields

$$\begin{aligned}
\langle \mathscr{P}\nabla\mathscr{P}\rangle_i \cdot \boldsymbol{n}_i &= \frac{1}{r_i}\int_{\Gamma_i} \mathscr{P}\nabla\mathscr{P}\,\mathrm{d}s\cdot\boldsymbol{n}_i = \frac{1}{r_i}\int_{\Gamma_i}\left(\mathscr{Q}_0+\sum_{l=1}^{n}\mathscr{Q}_l E_l(\boldsymbol{x})\right)\sum_{j=1}^{n}\mathscr{Q}_j\nabla E_j(\boldsymbol{x})\,\mathrm{d}s\cdot\boldsymbol{n}_i \\
&= \mathscr{Q}_0\sum_{j=1}^{n}\mathscr{Q}_j\frac{1}{r_i}\int_{\Gamma_i}\nabla E_j(\boldsymbol{x})\,\mathrm{d}s\cdot\boldsymbol{n}_i + \sum_{l=1}^{n}\sum_{j=1}^{n}\mathscr{Q}_l\mathscr{Q}_j\frac{1}{r_i}\int_{\gamma_i}E_l(\boldsymbol{x})\nabla E_j(\boldsymbol{x})\,\mathrm{d}s\cdot\boldsymbol{n}_i \\
&= \mathscr{Q}_0\sum_{j=1}^{n}\mathscr{Q}_j\langle\nabla E_j\rangle_i\cdot\boldsymbol{n}_i + \sum_{l=1}^{n}\sum_{j=1}^{n}\mathscr{Q}_l\mathscr{Q}_j\langle E_l\nabla E_j\rangle_i\cdot\boldsymbol{n}_i \\
&= \mathscr{Q}_0\sum_{j=1}^{n}a_{ij}\mathscr{Q}_j + \sum_{l=1}^{n}\sum_{j=1}^{n}a_{ilj}\mathscr{Q}_l\mathscr{Q}_j, \\
\langle\nabla\mathscr{P}\rangle_i\cdot\boldsymbol{n}_i &= \frac{1}{r_i}\int_{\Gamma_i}\sum_{j=1}^{n}\mathscr{Q}_j\nabla E_j(\boldsymbol{x})\,\mathrm{d}s\cdot\boldsymbol{n}_i = \sum_{j=1}^{n}\mathscr{Q}_j\langle\nabla E_j\rangle_i\cdot\boldsymbol{n}_i = \sum_{j=1}^{n}a_{ij}\mathscr{Q}_j.
\end{aligned}$$

Hence we obtain

$$\begin{aligned}
\langle(\mathscr{P}-\gamma k_i)\nabla\mathscr{P}\rangle_i\cdot\boldsymbol{n}_i &= \langle\mathscr{P}\nabla\mathscr{P}\rangle_i\cdot\boldsymbol{n}_i - \gamma k_i\langle\nabla\mathscr{P}\rangle_i\cdot\boldsymbol{n}_i \\
&= \mathscr{Q}_0\sum_{j=1}^{n}a_{ij}\mathscr{Q}_j + \sum_{l=1}^{n}\sum_{j=1}^{n}a_{ilj}\mathscr{Q}_l\mathscr{Q}_j - \gamma k_i\sum_{j=1}^{n}a_{ij}\mathscr{Q}_j \\
&= (\mathscr{Q}_0-\gamma k_i)\sum_{j=1}^{n}a_{ij}\mathscr{Q}_j + \sum_{l=1}^{n}\sum_{j=1}^{n}a_{ilj}\mathscr{Q}_l\mathscr{Q}_j.
\end{aligned}$$

As to the expression (6.3.16), we firstly have

$$\left|\frac{1}{A}\sum_{i=1}^{n}\boldsymbol{x}_i^* v_i r_i + \mathbf{err}_{\boldsymbol{G}}^1\right|^2 = \left|\frac{1}{A}\sum_{i=1}^{n}\boldsymbol{x}_i^* v_i r_i\right|^2 + \frac{2}{A}\sum_{i=1}^{n}\boldsymbol{x}_i^* v_i r_i\cdot\mathbf{err}_{\boldsymbol{G}}^1 + |\mathbf{err}_{\boldsymbol{G}}^1|^2.$$

We hereafter expand and tidy up the above expression.

$$\begin{aligned}
\frac{1}{A}\sum_{i=1}^{n}\boldsymbol{x}_i^* v_i r_i &= -\frac{1}{A}\sum_{i=1}^{n}\boldsymbol{x}_i^*\langle\nabla P\rangle_i\cdot\boldsymbol{n}_i r_i = -\frac{1}{A}\sum_{i=1}^{n}\boldsymbol{x}_i^*\left(\sum_{j=1}^{n}a_{ij}\mathscr{Q}_j\right)r_i \\
&= \frac{1}{A}\sum_{j=1}^{n}\left(\sum_{i=1}^{n}-a_{ij}\boldsymbol{x}_i^* r_i\right)\mathscr{Q}_j, \\
\mathbf{err}_{\boldsymbol{G}}^1 &= \frac{1}{6A}\sum_{i=1}^{n}\left(\alpha_i s_i - \frac{v_{i+1}-v_i}{2}\right)c_i(r_i^2+r_{i+1}^2)\boldsymbol{T}_i \\
&= \underline{\frac{1}{6A}\sum_{i=1}^{n}\alpha_i s_i c_i(r_i^2+r_{i+1}^2)\boldsymbol{T}_i} - \underline{\underline{\frac{1}{6A}\sum_{i=1}^{n}\frac{v_{i+1}-v_i}{2}c_i(r_i^2+r_{i+1}^2)\boldsymbol{T}_i}}
\end{aligned}$$

The underlined and doubly-underlined parts, say ① and ②, respectively, can be computed as follows:

$$\begin{aligned}
① &= \alpha_1 s_1 c_1 (r_1^2 + r_2^2)\boldsymbol{T}_1 + \sum_{i=2}^{n} \alpha_i s_i c_i (r_i^2 + r_{i+1}^2)\boldsymbol{T}_i \\
&= \alpha_1 c_1 \sum_{i=1}^{n} s_i (r_i^2 + r_{i+1}^2)\boldsymbol{T}_i + \sum_{i=2}^{n} \Psi_i s_i (r_i^2 + r_{i+1}^2)\boldsymbol{\tau}_i \\
&= -6\frac{\sum_{i=2}^{n} \Psi_i / c_i}{c_1 \sum_{l=1}^{n} 1/c_l} c_1 \sum_{i=1}^{n} s_i \boldsymbol{\tau}_i + 6\sum_{i=2}^{n} \Psi_i s_i \boldsymbol{\tau}_i = 6\sum_{i=2}^{n} \left[s_i \boldsymbol{\tau}_i - \frac{1}{c_i} \left(\sum_{j=1}^{n} \frac{1}{c_j} \right)^{-1} \left(\sum_{l=1}^{n} s_l \boldsymbol{\tau}_l \right) \right].
\end{aligned}$$

Here $\Psi_i = \sum_{l=2}^{i} \psi_l$ for $i = 2, 3, \ldots, n$, and ψ_l can be written concretely by their definitions as follows:

$$\begin{aligned}
\psi_l &= -V_l s_l - V_{l-1} s_{l-1} + \frac{\dot{L}}{n} + \left(\frac{L}{n} - r_l \right) \omega \\
&= -\frac{v_l + v_{l+1}}{2c_l} s_l - \frac{v_{l-1} + v_l}{2c_{l-1}} s_{l-1} + \frac{1}{n} \sum_{i=1}^{n} k_i v_i r_i + \left(\frac{L}{n} - r_l \right) \omega \\
&= -\frac{\tan(\varphi_l/2)}{2} \left(-\sum_{j=1}^{n} a_{lj} \mathscr{Q}_j - \sum_{j=1}^{n} a_{l+1,j} \mathscr{Q}_j \right) - \frac{\tan(\varphi_{l-1}/2)}{2} \left(-\sum_{j=1}^{n} a_{l-1,j} \mathscr{Q}_j - \sum_{j=1}^{n} a_{lj} \mathscr{Q}_j \right) \\
&\qquad + \frac{1}{n} \sum_{i=1}^{n} k_i \left(-\sum_{j=1}^{n} a_{ij} \mathscr{Q}_j \right) r_i + \left(\frac{L}{n} - r_l \right) \omega \\
&= \sum_{j=1}^{n} \left(\frac{\tan(\varphi_l/2)}{2} a_{l+1,j} + \frac{1}{2} \frac{\tan(\varphi_l/2) + \tan(\varphi_{l-1}/2)}{r_l} a_{lj} r_l + \frac{\tan(\varphi_{l-1}/2)}{2} a_{l-1,j} \right. \\
&\qquad \left. - \frac{1}{n} \sum_{i=1}^{n} k_i a_{ij} r_i \right) \mathscr{Q}_j + \left(\frac{L}{n} - r_l \right) \omega \\
&= \sum_{j=1}^{n} b_{lj} \mathscr{Q}_j + \left(\frac{L}{n} - r_l \right) \omega,
\end{aligned}$$

therefore we obtain that

$$\begin{aligned}
① &= 6\sum_{i=2}^{n} \Psi_i \boldsymbol{\mu}_i = 6\sum_{i=2}^{n} \sum_{l=2}^{i} \left[\sum_{j=1}^{n} b_{lj} \mathscr{Q}_j + \left(\frac{L}{n} - r_l \right) \omega \right] \boldsymbol{\mu}_i \\
&= 6\sum_{i=2}^{n} \left[\sum_{l=2}^{i} \sum_{j=1}^{n} b_{lj} \boldsymbol{\mu}_i \mathscr{Q}_j + \left(\frac{i-1}{n} L - \sum_{l=2}^{i} r_l \right) \omega \boldsymbol{\mu}_i \right].
\end{aligned}$$

We also have that

$$② = \sum_{i=1}^{n} \frac{1}{2} \left(-\sum_{j=1}^{n} a_{i+1,j} \mathscr{Q}_j + \sum_{j=1}^{n} a_{ij} \mathscr{Q}_j \right) c_i (r_i^2 + r_{i+1}^2)\boldsymbol{T}_i = -6\sum_{j=1}^{n} \left(\sum_{i=1}^{n} \frac{a_{i+1,j} - a_{ij}}{2} c_i \boldsymbol{\tau}_i \right) \mathscr{Q}_j.$$

Summarizing the above relations, we reach

$$\begin{aligned}\mathbf{err}_{\boldsymbol{G}}^1 &= \frac{1}{A}\sum_{j=1}^{n}\left(\sum_{i=2}^{n}\boldsymbol{\mu}_i\sum_{l=2}^{i}b_{lj}+\sum_{i=1}^{n}\frac{a_{i+1,j}-a_{ij}}{2}c_i\boldsymbol{\tau}_i\right)\mathscr{Q}_j+\frac{1}{A}\sum_{i=2}^{n}\boldsymbol{\mu}_i\left(\frac{i-1}{n}L-\sum_{l=2}^{i}r_l\right)\omega\\ &= \frac{1}{A}\sum_{j=1}^{n}\left(\sum_{i=2}^{n}\boldsymbol{\mu}_i\sum_{l=2}^{i}b_{lj}+\sum_{i=1}^{n}\frac{a_{i+1,j}-a_{ij}}{2}c_i\boldsymbol{\tau}_i\right)\mathscr{Q}_j+\boldsymbol{b}.\end{aligned}$$

Thus we have

$$\left|\frac{1}{A}\sum_{i=1}^{n}\boldsymbol{x}_i^*v_ir_i\right|^2=\frac{1}{A^2}\sum_{l=1}^{n}\sum_{j=1}^{n}\left(\sum_{i=1}^{n}-a_{il}\boldsymbol{x}_i^*r_i\right)\cdot\left(\sum_{i=1}^{n}-a_{ij}\boldsymbol{x}_i^*r_i\right)\mathscr{Q}_l\mathscr{Q}_j,$$

$$\begin{aligned}&\frac{2}{A}\sum_{i=1}^{n}\boldsymbol{x}_i^*v_ir_i\cdot\mathbf{err}_{\boldsymbol{G}}^1\\ &\quad=\frac{2}{A^2}\left[\sum_{l=1}^{n}\left(\sum_{i=1}^{n}-a_{il}\boldsymbol{x}_i^*r_i\right)\mathscr{Q}_l\right]\cdot\left[\sum_{j=1}^{n}\left(\sum_{i=2}^{n}\boldsymbol{\mu}_i\sum_{l=2}^{i}b_{lj}+\sum_{i=1}^{n}\frac{a_{i+1,j}-a_{ij}}{2}c_i\boldsymbol{\tau}_i\right)\mathscr{Q}_j+\boldsymbol{b}\right]\\ &\quad=\frac{2}{A^2}\left[\sum_{l=1}^{n}\sum_{j=1}^{n}\left(\sum_{i=1}^{n}-a_{il}\boldsymbol{x}_i^*r_i\right)\cdot\left(\sum_{i=2}^{n}\boldsymbol{\mu}_i\sum_{l'=2}^{i}b_{l'j}+\sum_{i=1}^{n}\frac{a_{i+1,j}-a_{ij}}{2}c_i\boldsymbol{\tau}_i\right)\mathscr{Q}_l\mathscr{Q}_j\right.\\ &\qquad\left.+\sum_{j=1}^{n}\left(\sum_{i=1}^{n}-a_{ij}\boldsymbol{x}_i^*r_i\right)\cdot\boldsymbol{b}\mathscr{Q}_j\right]\end{aligned}$$

$$\begin{aligned}|\mathbf{err}_{\boldsymbol{G}}^1|^2=&\frac{1}{A^2}\sum_{l=1}^{n}\sum_{j=1}^{n}\left(\sum_{i=2}^{n}\boldsymbol{\mu}_i\sum_{l'=2}^{i}b_{l'l}+\sum_{i=1}^{n}\frac{a_{i+1,l}-a_{il}}{2}c_i\boldsymbol{\tau}_i\right)\\ &\cdot\left(\sum_{i=2}^{n}\boldsymbol{\mu}_i\sum_{l''=2}^{i}b_{l''j}+\sum_{i=1}^{n}\frac{a_{i+1,j}-a_{ij}}{2}c_i\boldsymbol{\tau}_i\right)\mathscr{Q}_l\mathscr{Q}_j\\ &+\frac{2}{A^2}\sum_{j=1}^{n}\left(\sum_{i=2}^{n}\boldsymbol{\mu}_i\sum_{l=2}^{i}b_{lj}+\sum_{i=1}^{n}\frac{a_{i+1,j}-aij}{2}c_i\boldsymbol{\tau}_i\right)\cdot\boldsymbol{b}\mathscr{Q}_j+\frac{|\boldsymbol{b}|^2}{A^2}.\end{aligned}$$

Hence we finally obtain

$$\begin{aligned}&\left|\frac{1}{A}\sum_{i=1}^{n}\boldsymbol{x}_i^*v_ir_i+\mathbf{err}_{\boldsymbol{G}}^1\right|^2\\ &\quad=\frac{1}{A^2}\sum_{l=1}^{n}\sum_{j=1}^{n}\left[\left(\sum_{i=1}^{n}-a_{il}\boldsymbol{x}_i^*r_i\right)\cdot\left(\sum_{i=1}^{n}-a_{ij}\boldsymbol{x}_i^*r_i\right)\right.\\ &\qquad+2\left(\sum_{i=1}^{n}-a_{il}\boldsymbol{x}_i^*r_i\right)\cdot\left(\sum_{i=2}^{n}\boldsymbol{\mu}_i\sum_{l'=2}^{i}b_{l'j}+\sum_{i=1}^{n}\frac{a_{i+1,j}-a_{ij}}{2}c_i\boldsymbol{\tau}_i\right)\\ &\qquad+\left(\sum_{i=2}^{n}\boldsymbol{\mu}_i\sum_{l'=2}^{i}b_{l'l}+\sum_{i=1}^{n}\frac{a_{i+1,l}-a_{il}}{2}c_i\boldsymbol{\tau}_i\right)\\ &\qquad\left.\cdot\left(\sum_{i=2}^{n}\boldsymbol{\mu}_i\sum_{l''=2}^{i}b_{l'j}+\sum_{i=1}^{n}\frac{a_{i+1,j}-a_{ij}}{2}c_i\boldsymbol{\tau}_i\right)\right]\mathscr{Q}_l\mathscr{Q}_j\end{aligned}$$

$$+\frac{2}{A^2}\sum_{j=1}^{n}\left[\sum_{i=1}^{n}\left(-a_{ij}\boldsymbol{x}_i^* r_i+\frac{a_{i+1,j}-a_{ij}}{2}c_i\boldsymbol{\tau}_i\right)+\sum_{i=2}^{n}\boldsymbol{\mu}_i\sum_{l=2}^{i}b_{lj}\right]\cdot\boldsymbol{b}\mathscr{Q}_j+\frac{|\boldsymbol{b}|^2}{A^2}$$
$$=\frac{1}{A^2}\left(\sum_{l=1}^{n}\sum_{j=1}^{n}\boldsymbol{b}_l\cdot\boldsymbol{b}_j\mathscr{Q}_l\mathscr{Q}_j+2\sum_{j=1}^{n}\boldsymbol{b}\cdot\boldsymbol{b}_j\mathscr{Q}_j+|\boldsymbol{b}|^2\right),$$

which is nothing but the equation (6.3.16).

6.3.4.3 Practical computational scheme

The approximate solution P has of the form

$$P(\boldsymbol{x})=Q_0+\sum_{j=1}^{n}Q_jE_j(\boldsymbol{x}),\quad E_j(\boldsymbol{x})=E(\boldsymbol{x}-\boldsymbol{y}_j)-E(\boldsymbol{x}-\boldsymbol{z}_j),\quad \boldsymbol{x}\in\overline{\Omega}(t). \tag{6.3.17}$$

The boundary condition and the normal velocity are approximated as follows:

$$P(\boldsymbol{x}_i^*)=\gamma k_i,\quad i=1,2,\dots,n, \tag{6.3.18}$$
$$v_i=-\nabla P(\boldsymbol{x}_i^*)\cdot\boldsymbol{n}_i,\quad i=1,2,\dots,n. \tag{6.3.19}$$

Then the normal velocities $\{V_i\}_{i=1}^n$ are determined by the same manner as before. The above equations (6.3.18) and (6.3.19) can be obtained by approximating the average $\langle\mathsf{F}\rangle_i$ in (6.3.12) and (6.3.13) as the mid-point value $\mathsf{F}(\boldsymbol{x}_i^*)$ of F on Γ_i, respectively.

The coefficients $\{Q_j\}_{j=0}^n$ are determined from $(n+1)$'s linear equations: n's linear equations (6.3.18) expressed by

$$Q_0+\sum_{j=1}^{n}Q_jE_j(\boldsymbol{x}_i^*)=\gamma k_i,\quad i=1,2,\dots,n,$$

and one linear equation given by

$$\sum_{j=1}^{n}Q_jH_j=0,\quad H_j=-\sum_{i=1}^{n}\nabla E_j(\boldsymbol{x}_i^*)\cdot\boldsymbol{n}_i r_i,\quad j=1,2,\dots,n, \tag{6.3.20}$$

which means $\sum_{i=1}^n v_i r_i=\sum_{j=1}^n Q_jH_j=0$ with $v_i=-\sum_{j=1}^n Q_j\nabla E_j(\boldsymbol{x}_i^*)\cdot\boldsymbol{n}_i$. The existence of solutions of (6.3.18) and (6.3.19) are discussed in Chapter 5.

Note that our approximation is a kind of Murota's invariant scheme [73, 74], in which zero-average condition $\sum_{j=1}^n Q_j=0$ was utilized instead of (6.3.20). We, however, use (6.3.20) since this means $\sum_{i=1}^n v_i r_i=0$ and $\dot{A}=0$ holds if $\mathrm{err}_A=0$ in (6.3.6).

To realize $\mathrm{err}_A=0$, we use UDM in the next Step 3.

6.3.5 Step 3: Compute $\{\alpha_i\}_{i=1}^n$ by UDM

Under the following UDM, tangential velocities $\{\alpha_i\}_{i=1}^n$ are computed by

$$\begin{aligned}
&\alpha_i=\frac{\Psi_i+\alpha_1c_1}{c_i},\quad \Psi_i=\sum_{l=2}^{i}\psi_l,\quad i=2,3,\dots,n,\\
&\psi_l=-V_ls_l-V_{l-1}s_{l-1}+\frac{\dot{L}}{n}+\left(\frac{L}{n}-r_l\right)\omega,\quad l=2,3,\dots,n,\\
&\alpha_1=-\frac{\sum_{i=2}^n\Psi_i/c_i}{c_1\sum_{l=1}^n 1/c_l},
\end{aligned} \tag{6.3.21}$$

where $\omega = \omega(n,t)$ is a relaxation term defined by $\omega(n,t) = \partial_t f(n,t)$, and if we assume $\lim_{t\to T_{\max}} f(n,t) = \infty$ with the final computation time $T_{\max}$, then $\int_0^{T_{\max}} \omega(n,t)\,\mathrm{d}t = \infty$ is satisfied. When $T_{\max} = \infty$, ω can be taken a constant. In our numerical computation, we take $f(n,t) = 10nt$, that is, $\omega = 10n$ (see Section 6.6).

Tangential velocities (6.3.21) are derived from the following criterion [93]:

$$r_i(t) - \frac{L(t)}{n} = \eta_i \exp(-f(n,t)), \quad i = 1,2,\dots,n, \tag{6.3.22}$$

where $f(n,t)$ satisfies $\lim_{t\to T_{\max}} f(n,t) = \infty$ and one can add the assumption $\lim_{n\to\infty} f(n,t) = \infty$, and $\{\eta_i\}_{i=1}^n$ satisfies $\sum_{i=1}^n \eta_i = 0$ and $|\eta_i| \le 1$ for all i. Differentiating (6.3.22) with respect to time, we obtain

$$\dot r_i(t) - \frac{\dot L(t)}{n} = \left(\frac{L(t)}{n} - r_i(t)\right)\omega(n,t). \tag{6.3.23}$$

On the other hand, we obtain from the evolution equation (6.3.1) that

$$\dot r_i = (\dot{\boldsymbol{x}}_i - \dot{\boldsymbol{x}}_{i-1})\cdot \boldsymbol{t}_i = V_i s_i + V_{i-1}s_{i-1} + \alpha_i c_i - \alpha_{i-1}c_{i-1}. \tag{6.3.24}$$

Combining the relations (6.3.23) and (6.3.24) with the zero-average condition $\sum_{i=1}^n \alpha_i = 0$, the tangential velocities $\{\alpha_i\}_{i=1}^n$ can be determined. See also [34, 52, 70, 71, 72] for utilization of nontrivial tangential velocities.

As we can see from (6.3.23), if $\omega \equiv 0$, then $\dot r_i(t) - \dot L(t)/n = 0$ holds, which yields that

$$r_i(t) - \frac{L(t)}{n} = r_i(0) - \frac{L(0)}{n}, \quad i = 1,2,\dots,n; \quad t \in [0, T_{\max}).$$

Thus, if the distribution of initial vertices are "completely" uniform, then it will be kept theoretically in all time. However, in the real numerical computation, uniformness would be broken since numerical error accumulate. From this point of view, it would be preferred to use this type of technique, known as the asymptotic uniform distribution method:

$$r_i(t) - \frac{L(t)}{n} \longrightarrow 0, \quad i = 1,2,\dots,n; \quad \text{as } \ t \to T_{\max}.$$

It can also be examined in similar way that (6.3.23) keeps $r_i(t) = r_{i+1}(t)$ for all i and all time t if uniform distribution is achieved at initial time.

6.3.6 CS-, AP- and BF-properties

Under our algorithm in Section 6.3.1, it can be shown that discrete analogue of Proposition 6.2.2, that is, CS-, AP- and BF-properties hold when the normal velocities are computed by structure-preserving scheme (see Section 6.3.4.1), and that they hold asymptotically when the normal velocities are computed by practical computational scheme (see Section 6.3.4.3) as follows.

Proposition 6.3.3 (CS-, AP- and BF-properties)**.** *Suppose that there exists an approximate solution $\mathscr{P}$ of the form* (6.3.11) *satisfying* (6.3.15) *and* (6.3.16) *for each time t, and that the distribution of the initia vertices is uniform, that is, $r_i(0) \equiv L(0)/n$ holds for all i. The normal velocities $\{v_i\}_{i=0}^n$ on edges are computed by* (6.3.13)*. Then we have*

$$\dot L = -\frac{1}{\gamma}\|\nabla \mathscr{P}\|^2_{L^2(\Omega)} \le 0, \quad \dot A = 0, \quad \dot{\boldsymbol{G}} = \boldsymbol{0}.$$

Namely, CS-, AP- and BF-properties hold.

Proof. Using the expression (6.3.5) for $\dot{L}$ and the condition (6.3.12), we have

$$\begin{aligned}\dot{L} &= -\sum_{i=1}^{n} k_i \langle \nabla \mathscr{P} \rangle_i \cdot \boldsymbol{n}_i r_i = -\frac{1}{\gamma} \sum_{i=1}^{n} \langle \mathscr{P} \nabla \mathscr{P} \rangle_i \cdot \boldsymbol{n}_i r_i = -\frac{1}{\gamma} \sum_{i=1}^{n} \int_{\Gamma_i} \mathscr{P} \nabla \mathscr{P} \cdot \boldsymbol{n}_i \, \mathrm{d}s \\ &= -\frac{1}{\gamma} \int_{\Omega} \operatorname{div}(\mathscr{P} \nabla \mathscr{P}) \, \mathrm{d}S = -\frac{1}{\gamma} \int_{\Omega} \left(|\nabla \mathscr{P}|^2 + \mathscr{P} \triangle \mathscr{P} \right) \mathrm{d}S \le 0,\end{aligned}$$

where we have used the fact that $\mathscr{P}$ is smooth in some neighborhood of $\overline{\Omega}$ and harmonic in Ω. As to the enclosed area, we have

$$\dot{A} = -\sum_{i=1}^{n} \langle \nabla \mathscr{P} \rangle_i \cdot \boldsymbol{n}_i r_i = -\sum_{i=1}^{n} \int_{\Gamma_i} \nabla \mathscr{P} \cdot \boldsymbol{n}_i \, \mathrm{d}s = -\int_{\Omega} \operatorname{div}(\nabla \mathscr{P}) \, \mathrm{d}S = 0$$

from the expression (6.3.6) for $\dot{A}$. Here err_A vanishes since the distribution of vertices is uniform. The barycenter $\boldsymbol{G}$ of Ω does not move since $\dot{A} = 0$, (6.3.16) and $\mathbf{err}_{\boldsymbol{G}}^2 = \mathbf{0}$ (by UDM) hold. □

Proposition 6.3.4 (AP-, and asymptotic CS- and BF-properties)**.** *Suppose that* $\sup_{t \in [0, T_{\max})} L(t) < +\infty$ *holds, that there exists an approximate solution* P *of the form* (6.3.17) *satisfying* (6.3.18) *and* (6.3.20) *for each time* t*, that the distribution of the initial vertices is uniform, that is,* $r_i(0) \equiv L(0)/n$ *holds for all* i*, and that the following angle condition (AC) and non self-intersection condition (NSIC) hold:*

(AC) *there exists some (small) positive constant* δ *such that* $|\varphi_i| \le \pi - \delta$ *holds for all* $i = 1, 2, \ldots, n$*;*

(NSIC) *there exists some positive constant* $\tilde{\delta}$ *such that* $\operatorname{dist}(\Gamma_i, \Gamma_j) \ge \tilde{\delta}$ *holds for all* $i, j = 1, 2, \ldots, n$ *with* $|i - j| \ge 2$*.*

The normal velocities $\{v_i\}_{i=1}^n$ *on edges are computed by* (6.3.19)*. Then*

$$\dot{L} \le -\frac{1}{\gamma} \|\nabla P\|_{L^2(\Omega)}^2 + \frac{C_1}{n}, \quad \dot{A} = 0, \quad |\dot{\boldsymbol{G}}| \le \frac{C_2}{n}$$

hold for sufficiently small d *and sufficiently large* $\tilde{d}$*, where* $\tilde{d}$ *is a parameter to arrange the dummy points* $\{z_j\}_{j=1}^n$ *as*

$$\boldsymbol{z}_j = \boldsymbol{x}_j^* + \tilde{d} \boldsymbol{n}_j, \quad j = 1, 2, \ldots, n,$$

where the constants C_1 *and* C_2 *are defined as*

$$\begin{aligned}C_1 &= \frac{L^2}{\pi \gamma d^2} \left(\sum_{j=1}^{n} |Q_j| \right)^2 \sqrt{\frac{2}{\pi^2} + 5 \left(\log \frac{L + \tilde{d}}{d} \right)^2}, \\ C_2 &= \frac{L^2}{A \pi d} \left(\sum_{j=1}^{n} |Q_j| \right) \left(\frac{\sqrt{2}(\tilde{C}_2 + 1)}{3} + \sqrt{2 + \frac{5 \|\boldsymbol{x}\|_{L^\infty(\Gamma)}}{d^2}} + \frac{1}{\sqrt{2}} \right),\end{aligned}$$

in which

$$\begin{aligned}\tilde{C}_2 &= \max \left\{ \frac{1}{c_1 \sum_{l=1}^{n} 1/c_l} \sum_{m=2}^{n} \frac{C'_{2m}}{c_m}, \max_{i=1,2,\ldots,n} \frac{1}{c_i} \left(C'_{2i} + \frac{1}{\sum_{l=1}^{n} 1/c_l} \sum_{m=2}^{n} \frac{C'_{2m}}{c_m} \right) \right\}, \\ C'_{2i} &= \sum_{l=2}^{i} \left(\left| \tan \frac{\varphi_l}{2} \right| + \left| \tan \frac{\varphi_{l-1}}{2} \right| + 2 \sum_{j=1}^{n} \left| \tan \frac{\varphi_j}{2} \right| \right).\end{aligned}$$

Namely, AP-property holds, and CS- and BF-properties hold asymptotically.

Remark 6.3.5. We conjecture that the sum $\sum_{j=0}^{n}|Q_j|$ of the absolute values of coefficients Q_j is order of 1, that is, it can be bounded by some constant which is independent of n. Indeed, when we consider the case where Γ is a regular n-gon, then we obtain the following numerical results (see Figure 6.3), which enable us to present the above conjecture. In the numerical experiment, Γ is a regular n-gon

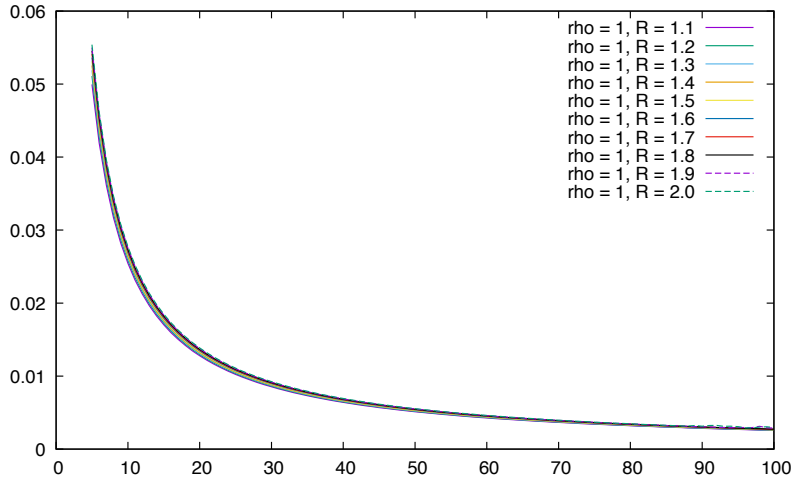

Figure 6.3: Numerical computation of the sum of the coefficients in the case where Γ is a regular n-gon.

with radius of inscribed circle being equal to 1, which means that the collocation points $\{\boldsymbol{x}_i^*\}_{i=1}^n$ are expressed by $\boldsymbol{x}_i^* = \boldsymbol{\omega}_i$, and the singular and dummy points are distributed as follows:

$$\boldsymbol{y}_j = \boldsymbol{x}_j^* + d\boldsymbol{y}_j = R\boldsymbol{\omega}_j, \quad \boldsymbol{z}_j = R'\boldsymbol{\omega}_j, \quad \boldsymbol{\omega}_j = \begin{pmatrix}\cos(2\pi(j-1)/n)\\ \sin(2\pi(j-1)/n)\end{pmatrix}, \quad j = 1, 2, \ldots, n,$$

in which $R' = 1000$ and $R = 1.1, 1.2, \ldots, 2$.

In order to prove the above proposition, we need the following lemma which gives bounds for $L^\infty(\Gamma_i)$ norms of P, ∇P, ∇P_x and ∇P_y.

Lemma 6.3.6. *Suppose that the same hypothesis in Proposition 6.3.4 hold except for the uniform distribution of the initial vertices. Then we have following estimates:*

$$\|P\|_{L^\infty(\Gamma_i)} \le \left(\sum_{j=0}^{n}|Q_j|\right)\log\frac{L+\tilde{d}}{d}, \quad \|\nabla P\|^2_{L^\infty(\Gamma_i)} \le \frac{2}{\pi^2}\left(\sum_{j=1}^{n}|Q_j|\right)^2\frac{1}{d^2},$$

$$\|\nabla P_x\|^2_{L^\infty(\Gamma_i)},\ \|\nabla P_y\|^2_{L^\infty(\Gamma_i)} \le \frac{5}{\pi^2}\left(\sum_{j=1}^{n}|Q_j|\right)^2\frac{1}{d^4}.$$

Here $\|\boldsymbol{f}\|_{L^\infty(\Gamma_i)}$ *is defined by* $\|\boldsymbol{f}\|_{L^\infty(\Gamma_i)} = \|f_1\|^2_{L^\infty(\Gamma_i)} + \|f_2\|^2_{L^\infty(\Gamma_i)}$ *for vector-valued function* $\boldsymbol{f} = (f_1, f_2)^{\mathrm{T}}$ *(or* $\boldsymbol{f} = (f_1, f_2)$*).*

Proof. Note that $d \le |\boldsymbol{x} - \boldsymbol{y}_j|$ holds as $d \to 0$ for all $j = 1, 2, \ldots, n$ and all $\boldsymbol{x} \in \Gamma_i$, and

$$|\boldsymbol{x} - \boldsymbol{z}_j| = |\boldsymbol{x} - (\boldsymbol{x}_j^* + \tilde{d}\boldsymbol{n}_j)| \le |\boldsymbol{x} - \boldsymbol{x}_j^*| + \tilde{d} \le L + \tilde{d}.$$

Then we have

$$\begin{aligned}\|P\|_{L^\infty(\Gamma_i)} &\le |Q_0| + \sum_{j=1}^n |Q_j| \|E_j\|_{L^\infty(\Gamma_i)} \le |Q_0| + \frac{1}{2\pi}\sum_{j=1}^n |Q_j| \log \frac{\sup_{\boldsymbol{x}\in\Gamma_i} |\boldsymbol{x}-\boldsymbol{z}_j|}{\inf_{\boldsymbol{x}\in\Gamma_i} |\boldsymbol{x}-\boldsymbol{y}_j|} \\ &\le \left(\sum_{j=0}^n |Q_j|\right) \log \frac{L+\tilde{d}}{d}\end{aligned}$$

for sufficiently small d and sufficiently large $\tilde{d}$. Next, direct computation yields that

$$\nabla P(\boldsymbol{x}) = \frac{1}{2\pi}\sum_{j=1}^n Q_j \left(\frac{\boldsymbol{x}-\boldsymbol{y}_j}{|\boldsymbol{x}-\boldsymbol{y}_j|^2} - \frac{\boldsymbol{x}-\boldsymbol{z}_j}{|\boldsymbol{x}-\boldsymbol{z}_j|^2}\right).$$

Thus we obtain

$$\begin{aligned}\|\nabla P\|^2_{L^\infty(\Gamma_i)} &\le \sum_{l=1}^2 \left[\frac{1}{2\pi}\sum_{j=1}^n |Q_j| \sup_{\boldsymbol{x}\in\Gamma_i}\left(\frac{|x_l - y_{jl}|}{|\boldsymbol{x}-\boldsymbol{y}_j|^2} + \frac{|x_l - z_{jl}|}{|\boldsymbol{x}-\boldsymbol{z}_j|^2}\right)\right]^2 \\ &\le 2\left[\frac{1}{2\pi}\sum_{j=1}^n |Q_j| \sup_{\boldsymbol{x}\in\Gamma_i}\left(\frac{1}{|\boldsymbol{x}-\boldsymbol{y}_j|} + \frac{1}{|\boldsymbol{x}-\boldsymbol{z}_j|}\right)\right]^2 \le \frac{2}{\pi^2}\left(\sum_{j=1}^n |Q_j|\right)^2 \frac{1}{d^2}.\end{aligned}$$

We again have by direct computation that

$$\begin{aligned}P_{xx} &= \frac{1}{2\pi}\sum_{j=1}^n Q_j \left(\frac{-(x_1-y_{j1})^2 + (x_2-y_{j2})^2}{|\boldsymbol{x}-\boldsymbol{y}_j|^4} - \frac{-(x_1-z_{j1})^2 + (x_2-z_{j2})^2}{|\boldsymbol{x}-\boldsymbol{z}_j|^4}\right), \\ P_{xy} &= -\frac{1}{\pi}\sum_{j=1}^n Q_j \left(\frac{(x_1-y_{j1})(x_2-y_{j2})}{|\boldsymbol{x}-\boldsymbol{y}_j|^4} - \frac{(x_1-z_{j1})(x_2-z_{j2})}{|\boldsymbol{x}-\boldsymbol{z}_j|^4}\right),\end{aligned}$$

therefore we obtain

$$\begin{aligned}\|\nabla P_x\|^2_{L^\infty(\Gamma_i)} \le{}& \left[\frac{1}{2\pi}\sum_{j=1}^n |Q_j| \sup_{\boldsymbol{x}\in\Gamma_i}\left(\frac{(x_1-y_{j1})^2 + (x_2-y_{j2})^2}{|\boldsymbol{x}-\boldsymbol{y}_j|^4} + \frac{(x_1-z_{j1})^2 + (x_2-z_{j2})^2}{|\boldsymbol{x}-\boldsymbol{z}_j|^4}\right)\right]^2 \\ &+ \left[-\frac{1}{\pi}\sum_{j=1}^n |Q_j| \sup_{\boldsymbol{x}\in\Gamma_i}\left(\frac{|x_1-y_{j1}||x_2-y_{j2}|}{|\boldsymbol{x}-\boldsymbol{y}_j|^4} + \frac{|x_1-z_{j1}||x_2-z_{j2}|}{|\boldsymbol{x}-\boldsymbol{z}_j|^4}\right)\right]^2 \\ \le{}& \frac{5}{4\pi^2}\left[\sum_{j=1}^n |Q_j| \sup_{\boldsymbol{x}\in\Gamma_i}\left(\frac{1}{|\boldsymbol{x}-\boldsymbol{y}_j|^2} + \frac{1}{|\boldsymbol{x}-\boldsymbol{z}_j|^2}\right)\right]^2 \le \frac{5}{\pi^2}\left(\sum_{j=1}^n |Q_j|\right)^2 \frac{1}{d^4}.\end{aligned}$$

The estimate on $\|\nabla P_y\|^2_{L^\infty(\Gamma_i)}$ can be obtained in similar way. □

Proof of Proposition 6.3.4. Put $f_{1,i}(\boldsymbol{a}) = P(\boldsymbol{a})\nabla P(\boldsymbol{a})\cdot\boldsymbol{n}_i$. Note that $f_{1,i}$ is smooth in some neighborhood of $\overline{\Omega}(t)$ since P is so. Then we have

$$f_{1,i}(\boldsymbol{x}) - f_{1,i}(\boldsymbol{x}_i^*) = \int_0^1 \frac{\partial f_{1,i}}{\partial \boldsymbol{a}}((1-\mu)\boldsymbol{x}_i^* + \mu\boldsymbol{x})\,\mathrm{d}\mu\,(\boldsymbol{x}-\boldsymbol{x}_i^*)$$

for all $\boldsymbol{x} \in \Gamma_i$. Therefore

$$|f_{1,i}(\boldsymbol{x}) - f_{1,i}(\boldsymbol{x}_i^*)| \le \int_0^1 \left| \frac{\partial f_{1,i}}{\partial \boldsymbol{a}}((1-\mu)\boldsymbol{x}_i^* + \mu \boldsymbol{x}) \right| \mathrm{d}\mu \, |\boldsymbol{x} - \boldsymbol{x}_i^*| \le \left\| \frac{\partial f_{1,i}}{\partial \boldsymbol{a}} \right\|_{L^\infty(\Gamma_i)} \cdot \frac{L}{2n}$$

holds for all $\boldsymbol{x} \in \Gamma_i$. Owing to Lemma 6.3.6, $\|\partial f/\partial \boldsymbol{a}\|_{L^\infty(\Gamma_i)}$ can be bounded as follows:

$$\begin{aligned}
\left\| \frac{\partial f_{1,i}}{\partial \boldsymbol{a}} \right\|_{L^\infty(\Gamma_i)} &= \|\nabla P(\boldsymbol{x})(\nabla P(\boldsymbol{x}) \cdot \boldsymbol{n}_i) + P(\boldsymbol{x})(\operatorname{Hess} P(\boldsymbol{x}))\boldsymbol{n}_i\|_{L^\infty(\Gamma_i)} \\
&= \sqrt{\|P_x \nabla P \cdot \boldsymbol{n}_i + P \nabla P_x \cdot \boldsymbol{n}_i\|_{L^\infty(\Gamma_i)}^2 + \|P_y \nabla P \cdot \boldsymbol{n}_i + P \nabla P_y \cdot \boldsymbol{n}_i\|_{L^\infty(\Gamma_i)}^2} \\
&\le \sqrt{2(\|P_x\|_{L^\infty(\Gamma_i)}^2 + \|\nabla P_y\|_{L^\infty(\Gamma_i)}^2)\|\nabla P \cdot \boldsymbol{n}_i\|_{L^\infty(\Gamma_i)}^2} \\
&\qquad \overline{+2\|P\|_{L^\infty(\Gamma_i)}^2 \left(\|\nabla P_x \cdot \boldsymbol{n}_i\|_{L^\infty(\Gamma_i)}^2 + \|\nabla P_y \cdot \boldsymbol{n}_i\|_{L^\infty(\Gamma_i)}^2 \right)} \\
&\le \sqrt{2\|\nabla P\|_{L^\infty(\Gamma_i)}^2 + 2\|P\|_{L^\infty(\Gamma_i)}^2 \left(\|\nabla P_x\|_{L^\infty(\Gamma_i)}^2 + \|\nabla P_y\|_{L^\infty(\Gamma_i)}^2 \right)} \\
&\le \sqrt{2 \left[\frac{4}{\pi^4} \left(\sum_{j=1}^n |Q_j| \right)^4 \frac{1}{d^4} + \left(\sum_{j=0}^n |Q_j| \right)^2 \left(\log \frac{L+\tilde{d}}{d} \right)^2 \cdot \frac{10}{\pi^2} \left(\sum_{j-1}^n |Q_j| \right)^2 \frac{1}{d^4} \right]} \\
&= \left[\frac{2}{\pi} \left(\sum_{j=1}^n |Q_j| \right)^2 \sqrt{\frac{2}{\pi^2} + 5 \left(\log \frac{L+\tilde{d}}{d} \right)^2} \right] \frac{1}{d^2}.
\end{aligned}$$

Using a relation

$$\dot{L} = \sum_{i=1}^n k_i v_i r_i = -\frac{1}{\gamma} \sum_{i=1}^n P(\boldsymbol{x}_i^*) \nabla P(\boldsymbol{x}_i^*) \cdot \boldsymbol{n}_i r_i,$$

we obtain

$$\begin{aligned}
\dot{L} + \frac{1}{\gamma} \int_\Omega |\nabla P(\boldsymbol{x})|^2 \, \mathrm{d}\Omega &= \left| \frac{1}{\gamma} \int_\Omega |\nabla P(\boldsymbol{x})|^2 \, \mathrm{d}\Omega + \dot{L} \right| \\
&\le \left| \frac{1}{\gamma} \sum_{i=1}^n \int_{\Gamma_i} (P(\boldsymbol{x}) \nabla P(\boldsymbol{x}) - P(\boldsymbol{x}_i^*) \nabla P(\boldsymbol{x}_i^*)) \cdot \boldsymbol{n}_i \, \mathrm{d}s \right| \\
&= \left| \frac{1}{\gamma} \sum_{i=1}^n \int_{\Gamma_i} (f_{1,i}(\boldsymbol{x}) - f_{1,i}(\boldsymbol{x}_i^*)) \, \mathrm{d}s \right| \\
&\le \frac{1}{\gamma} \sum_{i=1}^n \int_{\Gamma_i} \left[\frac{2}{\pi} \left(\sum_{j=1}^n |Q_j| \right)^2 \sqrt{\frac{2}{\pi^2} + 5 \left(\log \frac{L+\tilde{d}}{d} \right)^2} \right] \frac{1}{d^2} \cdot \frac{L}{2n} \, \mathrm{d}s \le \frac{C_1}{n},
\end{aligned}$$

where

$$C_1 = \frac{L^2}{\pi \gamma d^2} \left(\sum_{j=1}^n |Q_j| \right)^2 \sqrt{\frac{2}{\pi^2} + 5 \left(\log \frac{L+\tilde{d}}{d} \right)^2}.$$

Hence we obtain the desired estimate for $\dot{L}$.

Since we use UDM, we obtain $\mathrm{err}_A = 0$. $\sum_{i=1}^n v_i r_i$ is equal to 0 because of the constraint (6.3.20). Hence we obtain AP-property.

As to the barycenter, since we use UDM, $\dot{A} = 0$ and $\mathbf{err}_{\boldsymbol{G}}^2 = \mathbf{0}$ hold. $\mathbf{err}_{\boldsymbol{G}}^1$ can be evaluated as follows:

$$|\mathbf{err}_{\boldsymbol{G}}^1| \le \frac{1}{6A}\sum_{i=1}^n \left(|\alpha_i| + \frac{|v_{i+1}|+|v_i|}{2}\right)(r_i^2 + r_{i+1}^2) \le \frac{(\|\boldsymbol{\alpha}\|_\infty + \|\boldsymbol{v}\|_\infty)L^2}{3An},$$

where $\boldsymbol{\alpha} = (\alpha_1, \alpha_2, \dots, \alpha_n)^{\mathrm{T}}$ and $\boldsymbol{v} = (v_1, v_2, \dots, v_n)^{\mathrm{T}}$. By definition of tangential velocities, we have

$$\begin{aligned}
\alpha_1 &= -\frac{1}{c_1\sum_{l=1}^n 1/c_l}\sum_{i=2}^n \frac{1}{c_i}\sum_{l=2}^i \left(-\frac{v_l + v_{l+1}}{2c_l}s_l - \frac{v_{l-1}+v_l}{2c_{l-1}}s_{l-1} + \frac{1}{n}\sum_{j=1}^n k_j v_j r_j\right),\\
\alpha_i &= \frac{1}{c_i}\left(\sum_{l=2}^i \left(-\frac{v_l + v_{l+1}}{2c_l}s_l - \frac{v_{l-1}+v_l}{2c_{l-1}}s_{l-1} + \frac{1}{n}\sum_{j=1}^n k_j v_j r_j\right) + \alpha_1 c_1\right), \quad i = 2, 3, \dots, n.
\end{aligned}$$

Therefore we obtain estimates

$$\begin{aligned}
|\alpha_1| &\le \frac{1}{c_i\sum_{l=1}^n 1/c_l}\sum_{i=2}^n \frac{1}{c_i}\sum_{l=2}^i \left(\frac{|v_l|+|v_{l+1}|}{2}\left|\tan\frac{\varphi_l}{2}\right| + \frac{|v_{l-1}|+|v_l|}{2}\left|\tan\frac{\varphi_{l-1}}{2}\right|\right.\\
&\qquad\left. + \frac{1}{n}\sum_{j=1}^n \left(\left|\tan\frac{\varphi_{j-1}}{2}\right| + \left|\tan\frac{\varphi_j}{2}\right|\right)|v_j|\right)\\
&\le \frac{\sum_{m=2}^n C'_{2m}/c_m}{c_1\sum_{l=1}^n 1/c_l}\|\boldsymbol{v}\|_\infty
\end{aligned}$$

and

$$|\alpha_i| \le \frac{1}{c_i}\left(C'_{2i} + \frac{\sum_{m=2}^n C'_{2m}/c_m}{\sum_{l=1}^n 1/c_l}\right)\|\boldsymbol{v}\|_\infty, \quad i = 2, 3, \dots, n,$$

where

$$C'_{2i} = \sum_{l=2}^i \left(\left|\tan\frac{\varphi_l}{2}\right| + \left|\tan\frac{\varphi_{l-1}}{2}\right| + \frac{2}{n}\sum_{j=1}^n \left|\tan\frac{\varphi_j}{2}\right|\right), \quad i = 2, 3, \dots, n.$$

Summarizing the above, we obtain

$$\|\boldsymbol{\alpha}\|_\infty \le \tilde{C}_2\|\boldsymbol{v}\|_\infty, \quad \tilde{C}_2 = \max\left\{\frac{\sum_{m=2}^n C'_{2m}/c_m}{c_1\sum_{l=1}^n 1/c_l}, \max_{i=2,3,\dots,n}\frac{1}{c_i}\left(C'_{2i} + \frac{\sum_{m=2}^n C'_{2m}/c_m}{\sum_{l=1}^n 1/c_l}\right)\right\}.$$

The normal velocities $\{v_i\}_{i=1}^n$ can be estimated as

$$|v_i| = |-\nabla P(\boldsymbol{x}_i^*)\cdot\boldsymbol{n}_i| \le \|\nabla P\|_{L^\infty(\Gamma_i)}, \quad \text{that is,} \quad \|\boldsymbol{v}\|_\infty \le \|\nabla P\|_{L^\infty(\Gamma_i)}.$$

Therefore we obtain

$$|\mathbf{err}_{\boldsymbol{G}}^1| \le \frac{C_{21}}{n}, \quad C_{21} = \frac{\sqrt{2}(\tilde{C}_2+1)L^2}{3A\pi d}\left(\sum_{j=1}^n |Q_j|\right).$$

The second term in the expression (6.3.7) for $\dot{\boldsymbol{G}}$ can be evaluated as follows:

$$\begin{aligned}\left|\frac{1}{A}\sum_{i=1}^{n} v_i r_i \boldsymbol{x}_i^*\right| &= \left|-\frac{1}{A}\sum_{i=1}^{n}\int_{\Gamma_i} \boldsymbol{x}_i^* \nabla P(\boldsymbol{x}_i^*)\cdot \boldsymbol{n}_i\right| \\ &\le \left|\frac{1}{A}\sum_{i=1}^{n}\int_{\Gamma_i} (\boldsymbol{x}\nabla P(\boldsymbol{x})^{\mathrm{T}}\boldsymbol{n}_i - \boldsymbol{x}_i^*\nabla P(\boldsymbol{x}_i^*)\boldsymbol{n}_i)\,\mathrm{d}s\right| \\ &\qquad + \left|-\frac{1}{A}\sum_{i=1}^{n}\int_{\Gamma_i} (P(\boldsymbol{x}) - P(\boldsymbol{x}_i^*))\boldsymbol{n}_i\,\mathrm{d}s\right|,\end{aligned} \tag{6.3.25}$$

where we have used the relations

$$\sum_{i=1}^{n}\int_{\Gamma_i} \boldsymbol{x}\nabla P(\boldsymbol{x})\cdot\boldsymbol{n}_i\,\mathrm{d}s = \sum_{i=1}^{n}\int_{\Gamma_i} P\boldsymbol{n}_i\,\mathrm{d}s$$

and

$$\begin{aligned}\sum_{i=1}^{n}\int_{\Gamma_i} P(\boldsymbol{x}_i^*)\boldsymbol{n}_i\,\mathrm{d}s &= \gamma\sum_{i=1}^{n} k_i\boldsymbol{n}_i r_i = \gamma\sum_{i=1}^{n}\left(\tan\frac{\varphi_{i-1}}{2} + \tan\frac{\varphi_i}{2}\right)\boldsymbol{n}_i = \gamma\sum_{i=1}^{n}\frac{s_i}{c_i}(\boldsymbol{n}_{i+1}+\boldsymbol{n}_i) \\ &= \gamma\sum_{i=1}^{n} 2s_i\boldsymbol{N}_i = \gamma\sum_{i=1}^{n}(\boldsymbol{t}_i - \boldsymbol{t}_{i+1}) = \boldsymbol{0}.\end{aligned}$$

We evaluate (6.3.25) by similar procedures for evaluating $\dot{L}$, and obtain

$$\left|\frac{1}{A}\sum_{i=1}^{n} v_i r_i \boldsymbol{x}_i^*\right| \le \frac{L^2}{A\pi d}\left(1 + \frac{2\|\boldsymbol{x}\|_{L^\infty(\Gamma)}}{d}\right)\frac{1}{n}.$$

Indeed, putting $\boldsymbol{f}_{2,i}(\boldsymbol{a}) := \boldsymbol{a}\nabla P(\boldsymbol{a})^{\mathrm{T}}\boldsymbol{n}_i$ and $f_3(\boldsymbol{a}) := P(\boldsymbol{a})$, we obtain for $\boldsymbol{x}\in\Gamma_i$ that

$$\begin{aligned}\left\|\frac{\partial \boldsymbol{f}_{2,i}}{\partial \boldsymbol{a}}\right\|_{\mathrm{M},L^\infty(\Gamma_i)}^2 &= \|\nabla P\cdot\boldsymbol{n}_1 + x_1\nabla P_x\cdot\boldsymbol{n}_i\|_{L^\infty(\Gamma_i)}^2 + \|x_1\nabla P_y\cdot\boldsymbol{n}_i\|_{L^\infty(\Gamma_i)}^2 + \|x_2\nabla P_x\cdot\boldsymbol{n}_i\|_{L^\infty(\Gamma_i)}^2 \\ &\qquad + \|\nabla P\cdot\boldsymbol{n}_i + x_2\nabla P_y\cdot\boldsymbol{n}_i\|_{L^\infty(\Gamma_i)}^2 \\ &\le 2\left(\|\nabla P\|_{L^\infty(\Gamma_i)}^2 + \|x_1\|_{L^\infty(\Gamma_i)}^2\|\nabla P_x\|_{L^\infty(\Gamma_i)}^2\right) + \|x_1\|_{L^\infty(\Gamma_i)}^2\|\nabla P_y\|_{L^\infty(\Gamma_i)}^2 \\ &\quad + \|x_2\|_{L^\infty(\Gamma_i)}^2\|\nabla P_x\|_{L^\infty(\Gamma_i)}^2 + 2\left(\|\nabla P\|_{L^\infty(\Gamma_i)}^2 + \|x_2\|_{L^\infty(\Gamma_i)}^2\|\nabla P_y\|_{L^\infty(\Gamma_i)}^2\right) \\ &\le 4\|\nabla P\|_{L^\infty(\Gamma_i)}^2 + 2\|\boldsymbol{x}\|_{L^\infty(\Gamma_i)}^2\left(\|\nabla P_x\|_{L^\infty(\Gamma_i)}^2 + \|\nabla P_y\|_{L^\infty(\Gamma_i)}^2\right) \\ &\le \frac{8}{\pi^2}\left(\sum_{j=1}^{n}|Q_j|\right)^2\frac{1}{d^2} + 2\|\boldsymbol{x}\|_{L^\infty(\Gamma)}^2\cdot\frac{10}{\pi^2}\left(\sum_{j=1}^{n}|Q_j|\right)^2\frac{1}{d^4}\end{aligned}$$

and

$$\left\|\frac{\partial f_3}{\partial \boldsymbol{a}}\right\|_{L^\infty(\Gamma_i)}^2 = \|\nabla P\|_{L^\infty(\Gamma_i)}^2 \le \frac{2}{\pi^2}\left(\sum_{j=1}^{n}|Q_j|\right)^2\frac{1}{d^2},$$

which yield that

$$\begin{aligned}\left|\frac{1}{A}\sum_{i=1}^{n}\int_{\Gamma_i}\left(\boldsymbol{x}\nabla P(\boldsymbol{x})^{\mathrm{T}}\boldsymbol{n}_i-\boldsymbol{x}_i^*\nabla P(\boldsymbol{x}_i^*)^{\mathrm{T}}\boldsymbol{n}_i\right)\mathrm{d}s\right| &= \left|\frac{1}{A}\sum_{i=1}^{n}\int_{\Gamma_i}\left(\boldsymbol{f}_{2,i}(\boldsymbol{x})-\boldsymbol{f}_{2,i}(\boldsymbol{x}_i^*)\right)\mathrm{d}s\right| \\ &= \frac{1}{A}\left|\sum_{i=1}^{n}\int_{\Gamma_i}\int_0^1\frac{\partial\boldsymbol{f}_{2,i}}{\partial\boldsymbol{a}}((1-\mu)\boldsymbol{x}_i^*+\mu\boldsymbol{x})\,\mathrm{d}\mu\,(\boldsymbol{x}-\boldsymbol{x}_i^*)\right| \le \frac{1}{A}\sum_{i=1}^{n}\int_{\Gamma_i}\left\|\frac{\partial\boldsymbol{f}_{2,i}}{\partial\boldsymbol{a}}\right\|_{\mathrm{M},L^\infty(\Gamma_i)}\cdot\frac{L}{2n}\,\mathrm{d}s \\ &\le \frac{1}{A}\sum_{i=1}^{n}\int_{\Gamma_i}\frac{2}{\pi}\left(\sum_{j=1}^{n}|Q_j|\right)\sqrt{2+\frac{5\|\boldsymbol{x}\|^2_{L^\infty(\Gamma)}}{d^2}}\frac{1}{d}\cdot\frac{L}{2n}\,\mathrm{d}s=\frac{C_{22}}{n}\end{aligned}$$

and

$$\begin{aligned}\left|-\frac{1}{A}\sum_{i=1}^{n}\int_{\Gamma_i}(P(\boldsymbol{x})-P(\boldsymbol{x}_i^*))\boldsymbol{n}_i\,\mathrm{d}s\right| &= \frac{1}{A}\left|\sum_{i=1}^{n}\int_{\Gamma_i}(f_3(\boldsymbol{x})-f_3(\boldsymbol{x}_i^*))\boldsymbol{n}_i\,\mathrm{d}s\right| \\ &\le \frac{1}{A}\sum_{i=1}^{n}\int_{\Gamma_i}\frac{\sqrt{2}}{\pi}\left(\sum_{j=1}^{n}|Q_j|\right)\frac{1}{d}\cdot\frac{L}{2n}\,\mathrm{d}s=\frac{C_{23}}{n},\end{aligned}$$

where

$$C_{22}=\frac{L^2}{A\pi d}\left(\sum_{j=1}^{n}|Q_j|\right)\sqrt{2+\frac{5\|\boldsymbol{x}\|_{L^\infty(\Gamma)}}{d^2}},\quad C_{23}=\frac{L^2}{\sqrt{2}A\pi d}\left(\sum_{j=1}^{n}|Q_j|\right).$$

Here for matrix-valued function $A=(A_{ij})\in\mathbb{R}^{2\times 2}$, its $L^\infty(\Gamma_i)$-spectral norm $\|A\|_{\mathrm{M},L^\infty(\Gamma_i)}$ is defined as $\|A\|_{\mathrm{M},L^\infty(\Gamma_i)}=\left(\sum_{i=1}^{2}\sum_{j=1}^{2}\|A_{ij}\|^2_{L^\infty(\Gamma_i)}\right)^{1/2}$. Combining the above estimates, we obtain

$$|\dot{\boldsymbol{G}}|\le\frac{C_2}{n},$$

where

$$C_2=C_{21}+C_{22}+C_{23}=\frac{L^2}{A\pi d}\left(\sum_{j=1}^{n}|Q_j|\right)\left(\frac{\sqrt{2}(\tilde{C}_2+1)}{3}+\sqrt{2+\frac{5\|\boldsymbol{x}\|_{L^\infty(\Gamma)}}{d^2}}+\frac{1}{\sqrt{2}}\right)$$

as desired. □

6.4 Numerical scheme for the one-phase exterior Hele-Shaw problem (6.2.1)

Using the clockwise-indexed notation in contrast to the interior problem, we can write down numerical scheme in almost similar way. Therefore we only state how to compute the normal velocities, in which essential difference exists.

The problem to be solved is as follows:

$$\begin{cases}\triangle p=0 & \text{in } \widetilde{\Omega}(t),\\ p=\gamma k_i & \text{on } \Gamma_i(t),\ \ i=1,2,\dots,n,\\ p(\boldsymbol{x})=qE(\boldsymbol{x})+O(1) & \text{as } |\boldsymbol{x}|\to\infty,\end{cases}$$

where $\widetilde{\Omega}(t) = \mathbb{R}^2 \setminus \overline{\Omega}(t)$, and $\Omega(t)$ is a bounded region surrounded by $\Gamma(t)$. For the above problem, we construct the approximate solution P as

$$P(\boldsymbol{x}) = Q_0 + \sum_{j=1}^{n} Q_j E_j(\boldsymbol{x}) + qE(\boldsymbol{x}-\boldsymbol{z}), \quad E_j(\boldsymbol{x}) = E(\boldsymbol{x}-\boldsymbol{y}_j) - E(\boldsymbol{x}-\boldsymbol{z}_j), \quad \boldsymbol{x} \in \widetilde{\Omega}(t) \cup \Gamma(t), \tag{6.4.1}$$

where $\{\boldsymbol{z}_j\}_{j=1}^n$ and $\boldsymbol{z}$ are dummy points located in $\Omega(t)$ and $\boldsymbol{y}_j$'s are the singular points given by (6.3.14), in which $\boldsymbol{n}_j$ denotes the unit "inward" normal vector of Γ on the j-th edge Γ_j. Coefficients $\{Q_j\}_{j=0}^n$ are determined by solving the linear equations (6.3.18) with the following constraint:

$$\sum_{j=1}^{n} Q_j H_j - \sum_{i=1}^{n} q \nabla E(\boldsymbol{x}_i^* - \boldsymbol{z}) = q.$$

Then the speed of time variation of $A(t)$, the area of $\Omega(t)$, is constant $-q$ as follows:

Proposition 6.4.1 (Prescribed area-speed property)**.** *Assuming the uniform distribution of initial vertices, under our practical scheme, we obtain the prescribed area-speed property, that is, $\dot{A}(t) = -q$.*

6.5 Numerical scheme for the one-phase interior Hele-Shaw problem with sink/source points (6.2.2)

The only difference between the one-phase interior Hele-Shaw problem and the one-phase interior Hele-Shaw problem with sink/source points is a problem to be solved:

$$\begin{cases} \triangle p = \displaystyle\sum_{i=1}^{m} q_i \delta(\boldsymbol{x} - \boldsymbol{\xi}_i) & \text{for } \boldsymbol{x} \in \Omega(t), \\ p = \gamma k_i & \text{on } \Gamma_i(t), \ \ i = 1, 2, \ldots, n. \end{cases}$$

We approximate the solution p for the above problem by P which is defined as

$$P(\boldsymbol{x}) = Q_0 + \sum_{j=1}^{n} Q_j E_j^1(\boldsymbol{x}) + \sum_{j=1}^{m} q_j E_j^2(\boldsymbol{x}), \tag{6.5.1}$$

where

$$E_j^1(\boldsymbol{x}) = E(\boldsymbol{x}-\boldsymbol{y}_j) - E(\boldsymbol{x}-\boldsymbol{z}_j), \quad E_j^2(\boldsymbol{x}) = E(\boldsymbol{x}-\boldsymbol{\xi}_j) - E(\boldsymbol{x}-\boldsymbol{z}),$$

in which $\{\boldsymbol{z}_j\}_{j=1}^n$ and $\boldsymbol{z}$ are dummy points located at a sufficiently far position in $\mathbb{R}^2 \setminus \overline{\Omega}(t)$. Coefficients $\{Q_j\}_{j=0}^n$ are determined by solving the linear equations (6.3.18) with the following constraint:

$$\sum_{j=1}^{n} Q_j H_j - \sum_{i=1}^{n} \sum_{j=1}^{m} q_j \nabla E_j^2(\boldsymbol{x}_i^*) \cdot \boldsymbol{n}_i r_i = -\sum_{j=1}^{m} q_j.$$

Then for $A(t)$ the area of $\Omega(t)$, we obtain the following prescribed area-speed property:

Proposition 6.5.1 (Prescribed area-speed property)**.** *Assuming the uniform distribution of initial vertices, under our practical numerical scheme, the prescribed area-speed property, that is, $\dot{A}(t) = -\sum_{j=1}^{m} q_j$ holds.*

6.6 Numerical experiments

In this section, we show some results of our numerical computation. In all numerical computation shown below, we make distribution of the initial vertices into uniform one. For instance, for a given initial closed polygonal curve $\Gamma(0)$ which is not necessarily distributed uniformly, we may use a closed polygonal curve which can be obtained by using Algorithm in Section 6.3.1 with all normal velocities V_i being equal to 0 until uniform distribution is realized. (It can be done within one second.)

6.6.1 One-phase interior Hele-Shaw problem (6.1.1)

Exact solution

Example 6.6.1. When the initial curve $\mathscr{C}(0)$ is a circle with radius R, the Dirichlet problem to be solved at the initial time becomes

$$\begin{cases} \triangle p(\boldsymbol{x}, 0) = 0 & \text{for } \boldsymbol{x} \in \mathscr{D}(0), \\ p(\boldsymbol{x}, 0) = \dfrac{\gamma}{R} & \text{for } \boldsymbol{x} \in \mathscr{C}(0). \end{cases}$$

By the maximum principle for harmonic functions, the solution is the constant function $p = \gamma/R$, therefore the normal velocity V is equal to 0. Hence the solution curve $\mathscr{C}(t)$ does not change from the initial curve $\mathscr{C}(0)$. This is the only known exact solution for the one-phase interior Hele-Shaw problem. Similarly, we only know a trivial solution $P = Q_0$ for the polygonal problem, therefore the normal velocities v_i on the i-th edge Γ_i are equal to 0 for all i. Moreover, we can easily verify that the MFS solution coincides with the exact solution in this case, that is, the following proposition holds:

Proposition 6.6.2. *If $\Gamma(0)$ is a regular n-polygon, then the solution P of* (6.3.18) *and* (6.3.20) *is given by a constant function $P = \gamma/R$. Namely, P coincides with the exact solution p.*

Thus we do not compare our numerical scheme with this exact solution but compare with a result where the normal velocity is computed by using the boundary element method (BEM) instead of MFS, since in the previous work [106], one of the authors offered a scheme for the one-phase interior Hele-Shaw problem with a time-dependent gap, where the normal velocity is computed by BEM.

Numerical results

The parameters are taken as follows:

- $n = 100$ (the number of grid points);
- $\gamma = 1$ (the surface tension coefficient);
- $\boldsymbol{z}_j = 1000\boldsymbol{y}_j$ (the dummy points in MFS approximation (6.3.17));
- $\tau = 1/(10n^2)$ (the time-mesh size);
- $\omega = 10n$ (the relaxation term);
- $d = n^{-1/2}$ (the parameter controlling accuracy of MFS);
- $T_{\max} = 0.9$ (the final computation time).

The initial curve $\mathscr{C}(0)\colon [0,1] \ni u \mapsto \boldsymbol{x}(u) = (x_1(u), x_2(u))^{\mathrm{T}} \in \mathbb{R}^2$ is given by

$$x_1(u) = 1.8\cos(2\pi u), \quad x_2(u) = 0.5\sin(2\pi u) + \sin a_1(u) + a_2(u)\sin(2\pi u) \tag{6.6.1}$$

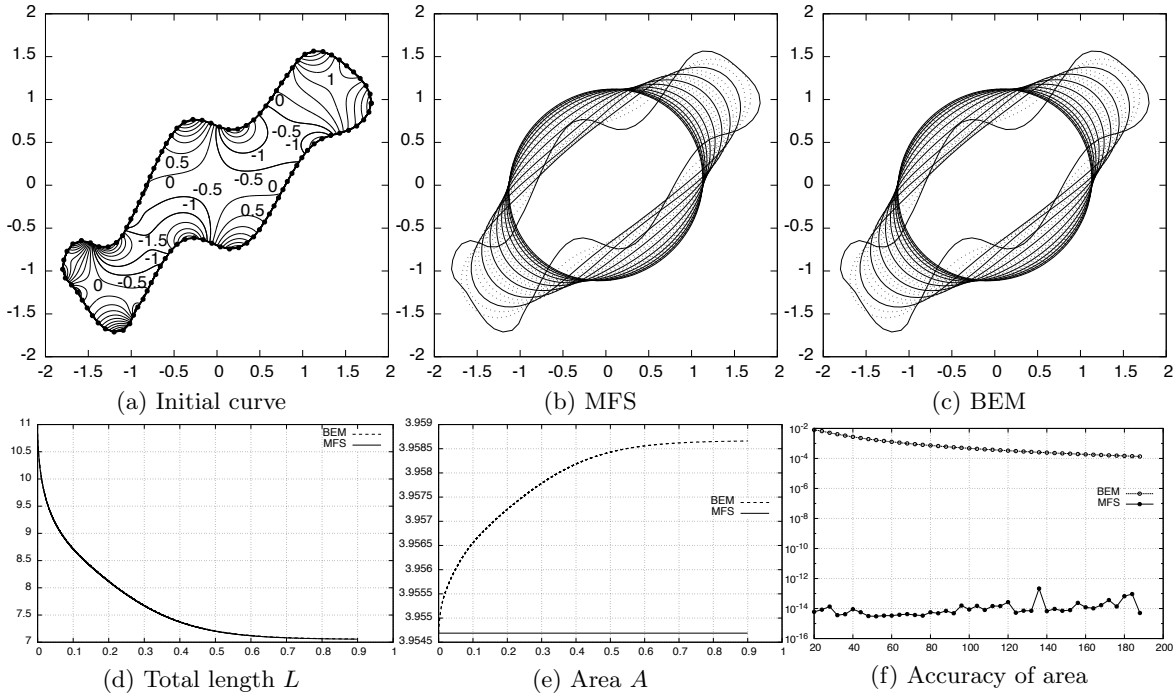

(a) Initial curve (b) MFS (c) BEM

(d) Total length L (e) Area A (f) Accuracy of area

Figure 6.4: Results of numerical computation: (a) the initial curve; time evolution of boundary curves (b) MFS; (c) BEM; (d) time evolution of total length; (e) time evolution of area; (f) the accuracy of area.

where $a_2(u) = 0.2 + \sin(\pi u)\sin(6\pi u)\sin(2a_1(u))$ for $u \in [0,1]$. In Figure 6.4(a), the black points represent vertices of polygon, and the solid lines are contour lines of pressure computed by MFS. The numbers indicate the values of pressure. We summarize the results of our numerical computation for the one-phase interior Hele-Shaw problem.

- Time evolutions of boundary curves are indicated in Figure 6.4(b) and (c), when the normal velocity is computed by MFS and BEM, respectively. The boundary curves converge to circles in both cases, and their size seem to be coincide.
- Figure 6.4(d) shows the time evolution of the total length $L(t)$ of the boundary curve $\Gamma(t)$, where the horizontal axis and the vertical axis represent the time and the total length L, respectively. It can be observed that the total length decreases monotonically for both methods: MFS and BEM (their graphs are overlapped with each other). As we have seen Proposition 6.3.4 in section 6.3.6, when the normal velocity is computed by MFS, we can prove that $\dot{L}$ takes a negative value plus a small error for a large n, since the approximate solution by MFS is smooth in a neighborhood of $\overline{\Omega}$. On the other hand, when the normal velocity is computed by BEM, there exist singularities on the boundary curve Γ, therefore we cannot use a useful mathematical tool such as the divergence theorem, and this makes it difficult to analyze the evolution of the total length. However, CS-property is observed numerically.
- Figure 6.4(e) shows the time evolution of the enclosed area $A(t)$ of the region $\Omega(t)$ bounded by $\Gamma(t)$, where the horizontal axis and the vertical axis represent the time t and the area A, respectively. Concerning the time evolution of the area, there is a big difference. In both methods of MFS and BEM, the tangential velocity is computed by UDM, therefore err_A converges to 0 exponentially as $t \uparrow T_{\max}$ or $n \to \infty$. When we compute the normal velocity by MFS, AP-property is achieved in maximal accuracy in double-precision arithmetic. On the other hand, when the normal velocity is computed by BEM, AP-property does not hold. Indeed, the area increases in time.
- Figure 6.4(f) shows the accuracy of area, where the horizontal axis and the vertical axis represent the number of grid points n and the error $\mathrm{err}(n)$, respectively. The error is measured by

$$\mathrm{err}(n) = \max_{1 \le m \le M} \left| \frac{A_m^{(n)} - A_0^{(n)}}{A_0^{(n)}} \right|, \quad n = 4k \ (k = 5, 6, \ldots, 47),$$

  where $A_m^{(n)}$ denotes the enclosed area of n-polygon at the m-th step, and $M = 1000$ denotes the maximum number of time steps. It can be observed that there are differences of accuracy about 9-12 digits between in two methods, and this implies that our proposal scheme computing the normal velocity by MFS is much better than that by BEM.

Since the pressure function is approximated by MFS as (6.3.17), we can easily visualize the contour lines of pressure. Indeed, we can draw the contour lines of pressure as in Figure 6.5.

Example 6.6.2. We show one more toy example for our numerical scheme. We take the initial curve as "π-like curve", which is given by some one-parameter functions (see for details the web page of Wolfram Alpha). The parameters are taken as follows:

- $n = 100$ (the number of grid points);
- $\gamma = 1$ (the surface tension coefficient);
- $\boldsymbol{z}_j = 1000\boldsymbol{y}_j$ (the dummy points in MFS approximation (6.3.17));
- $\tau = 1/(10n^2)$ (the time-mesh size);

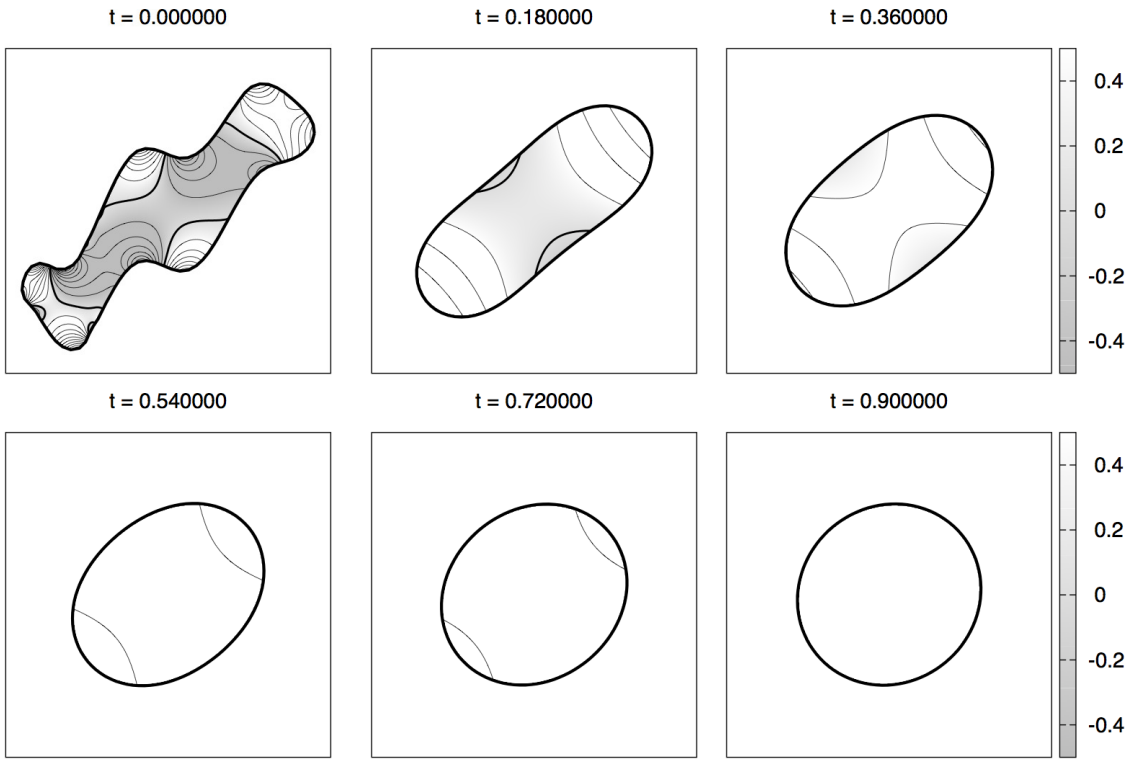

Figure 6.5: Contour lines of pressure corresponding to Figure 6.4.

- $\omega = 10n$ (the relaxation term);
- $d = n^{-1/2}$ (the parameter controlling accuracy of MFS);
- $T_{\max} = 3.0$ (the final computation time).

The results are shown in Figure 6.5, where the white circles represent the positions of the singular points.

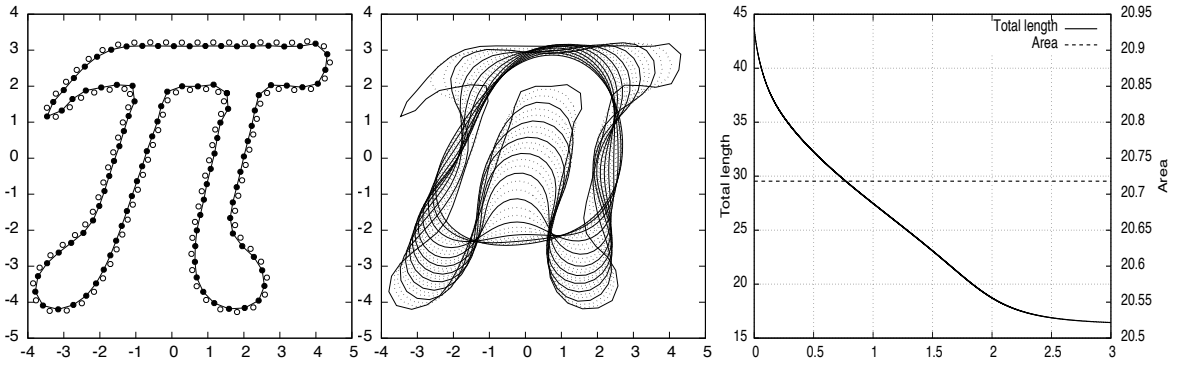

(a) initial curve (b) Evolution of curves (c) Total length L and area A

Figure 6.6: Results of numerical computation in which the initial curve is taken as the π-like curve: (a) initial curve; (b) the evolution of boundary curves; (c) time evolution of length; (d) time evolution of area.

6.6.2 One-phase exterior Hele-Shaw problem (6.2.1)

Exact solution

Example 6.6.3. We can construct a nontrivial exact solution for the one-phase exterior Hele-Shaw problem when the initial curve is a circle, especially we seek a self-similar solution for (6.2.1). Let $\mathscr{C}(t)$ be a circle with radius $R(t)$ having the origin as its center: $\mathscr{C}(t) = B_{R(t)} := \{|\boldsymbol{x}| = R(t)\}$. Then our problem is to find a self-similar solution p and a radius $R(t)$ for (6.2.1), that is, we seek a solution p of the form

$$p(r,t) = C + \frac{q}{2\pi}\log r \quad (R(t) \le r < +\infty),$$

where C is a constant. Since the curvature k is equal to $-1/R(t)$, the boundary condition becomes

$$p(R(t),t) = -\frac{\gamma}{R(t)}.$$

Then we can determine the constant C, and obtain

$$p(r,t) = -\frac{\gamma}{R(t)} + \frac{q}{2\pi}\log\frac{r}{R(t)} \quad (R(t) \le r < +\infty).$$

The normal velocity V of the curve $\mathscr{C}(t)$ can be computed as

$$V = \dot{\boldsymbol{x}} \cdot \boldsymbol{N} = -\dot{R}(t) = -\nabla p \cdot \boldsymbol{N} = \partial_r p(R(t),t).$$

Therefore we obtain the initial-value problem for ordinary differential equation:

$$\dot{R}(t) = -\frac{q}{2\pi R(t)}, \quad R(0) \text{ is given.}$$

Solving this problem yields

$$R(t) = \sqrt{R(0)^2 - \frac{q}{\pi}t}.$$

These p and $R(t)$ are the exact solutions for (6.2.1).

On the other hand, for polygonal problem, we can seek the solution by using MFS. Let $\Gamma(t)$ be a circumscribed regular n-polygon of $B_{a(t)}$. We take the singular points $\{\boldsymbol{y}_j\}_{j=1}^n$ as follows:

$$\boldsymbol{y}_j = \mu \boldsymbol{x}_j^*, \quad j = 1, 2, \ldots, n,$$

where $\mu \in]0, 1[$. See for settings Figure 6.7. Since the length r_i of the i-th edge Γ_i and the angle φ_i

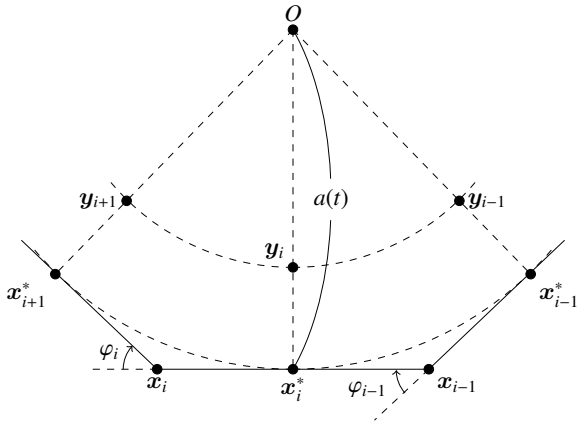

Figure 6.7: Our settings for the polygonal exterior problem.

between adjacent two edges Γ_i and Γ_{i+1} are calculated as $r_i(t) = 2a(t)\tan(\pi/N)$ and $\varphi_i = -2\pi/N$ for all i, respectively, we have

$$k_i = \frac{\tan(\varphi_{i-1}/2) + \tan(\varphi_i/2)}{r_i} = -\frac{1}{a(t)}.$$

Therefore the problem is written as follows:

$$\begin{cases} \triangle p(\boldsymbol{x}, t) = 0 & \text{for } \boldsymbol{x} \in \tilde{\Omega}(t),\ t \in [0, T[, \\ p(\boldsymbol{x}, t) = -\dfrac{\gamma}{a(t)} & \text{for } \boldsymbol{x} \in \Gamma(t), \\ p(\boldsymbol{x}, t) = qE(\boldsymbol{x}) + O(1) & \text{as } |\boldsymbol{x}| \to \infty,\ t \in [0, T[. \end{cases}$$

We seek the approximate solution P by MFS, that is, P at time t has of the form

$$P(\boldsymbol{x}) = Q_0 + \sum_{j=1}^{n} \frac{Q_j}{2\pi} \log \frac{|\boldsymbol{x} - \boldsymbol{y}_j|}{|\boldsymbol{x}|} + \frac{q}{2\pi} \log |\boldsymbol{x}|,$$

where the dummy points $\{\boldsymbol{z}_j\}_{j=0}^n$ and $\boldsymbol{z}$ are taken as the origin. The boundary condition (6.3.18) is

$$P(\boldsymbol{x}_i^*) = -\frac{\gamma}{a(t)}, \quad i = 1, 2, \ldots, n.$$

Taking into account of the symmetry, we can take Q_j, $j = 1, 2, \ldots, n$ as the same value C, and can determine Q_0. After taking $C = 0$, and similar procedure for smooth curve yields

$$P(\boldsymbol{x}) = -\frac{\gamma}{a(t)} + \frac{q}{2\pi} \log \frac{|\boldsymbol{x}|}{a(t)}, \quad a(t) = \sqrt{a(0)^2 - \frac{q}{\pi}t}. \tag{6.6.2}$$

We can observe that this solution for polygonal curve coincides with that for smooth curve. As you can see from the above argument, if the initial curve is a circle, where we can write down the exact solution, then the corresponding solution for polygonal problem can be constructed by using MFS, that is, MFS is a numerical solver which contains the exact solution. Namely, the following proposition holds:

Proposition 6.6.5. *If $\Gamma(t)$ is a circumscribed regular n-polygon of $B_{a(t)}$, then the solution P of* (6.3.18) *and* (6.3.20) *is given by* (6.6.2)*. Namely, P coincides with the exact solution p when $a(0) = R(0)$.*

Numerical results

Example 6.6.4. Taking the initial curve as the same for the interior problem (6.6.1), we perform a numerical computation using our numerical scheme, where the parameters are taken as follows:

- $n = 100$ (the number of grid points);
- $\gamma = 1$ (the surface tension coefficient);
- $\boldsymbol{z} = \boldsymbol{z}_j = n^{-1} \sum_{i=1}^{n} \boldsymbol{y}_i$ (the dummy points in MFS approximation (6.4.1));
- $\tau = 1/(10n^2)$ (the time-mesh size);
- $\omega = 10n$ (the relaxation term);
- $d = n^{-1/2}$ (the parameter controlling accuracy of MFS);
- $q = 1$ ($\dot{A}(t) = -q$);
- $T_{\max} = 0.9$ (the final computation time).

The results are depicted in Figure 6.8 and Figure 6.9.

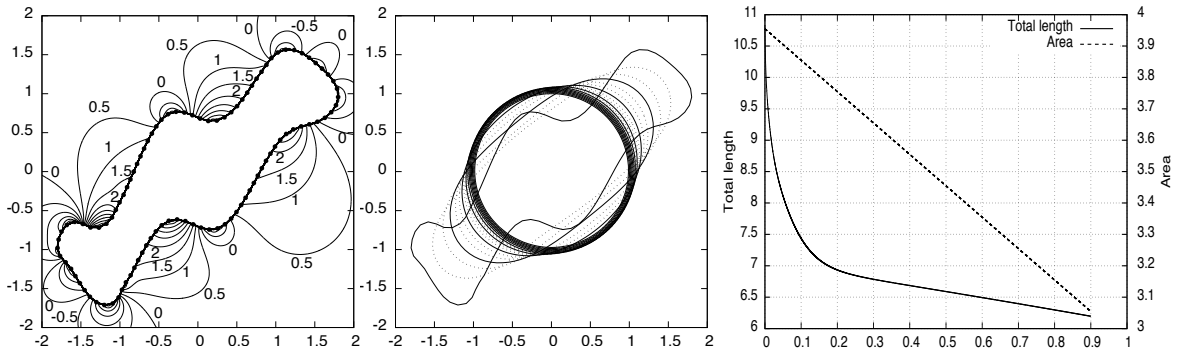

(a) Initial curve (b) Evolution of curves (c) Total length L and area A

Figure 6.8: Results of numerical computation: (a) the initial curve; (b) the evolution of boundary curves; (c) time evolution of total length and area.

Example 6.6.5. Another toy example is the exterior Hele-Shaw problem with "dolphin-like curve" as its initial curve (see for details the web page of Wolfram Alpha). The parameters are taken as follows:

- $n = 100$ (the number of grid points);
- $\gamma = 1$ (the surface tension coefficient);

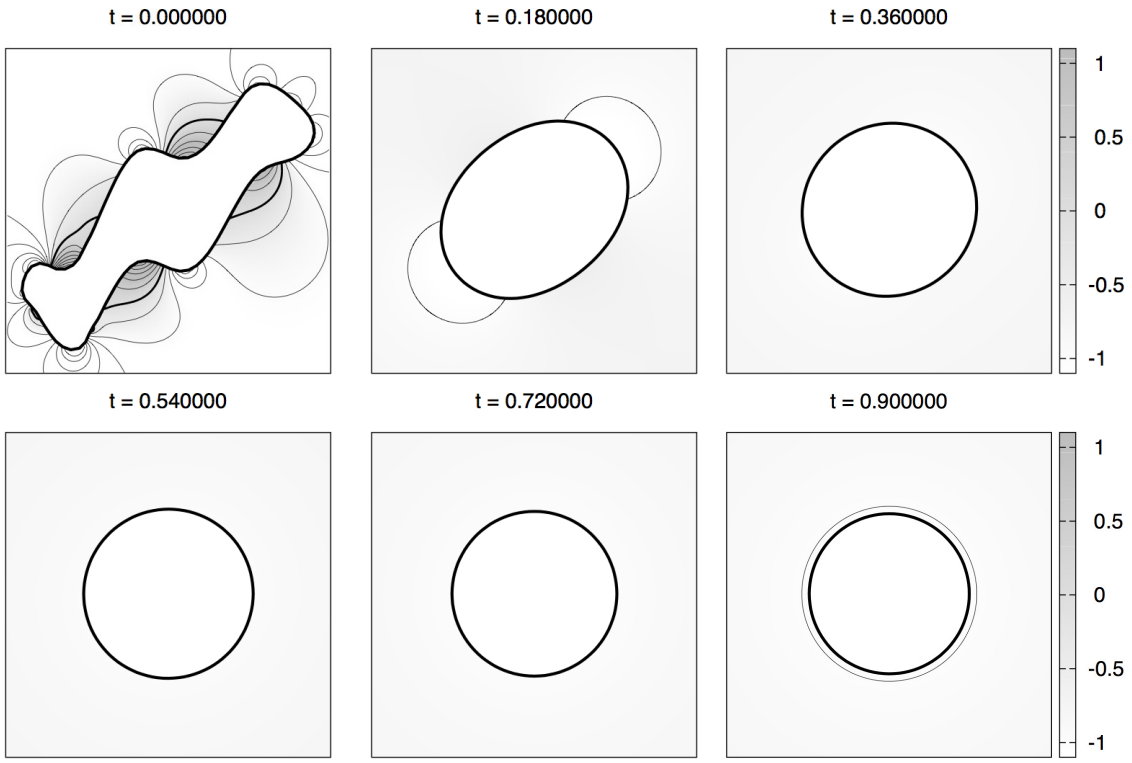

Figure 6.9: Contour lines of pressure corresponding to Figure 6.8.

- $\boldsymbol{z} = \boldsymbol{z}_j = n^{-1} \sum_{i=1}^{n} \boldsymbol{y}_i$ (the dummy points in MFS approximation (6.4.1));
- $\tau = 1/(10n^2)$ (the time-mesh size);
- $\omega = 10n$ (the relaxation term);
- $d = n^{-1/2}$ (the parameter controlling accuracy of MFS);
- $q = 1$ ($\dot{A}(t) = -q$);
- $T_{\max} = 4.8$ (the final computation time).

The results are depicted in Figure 6.10.

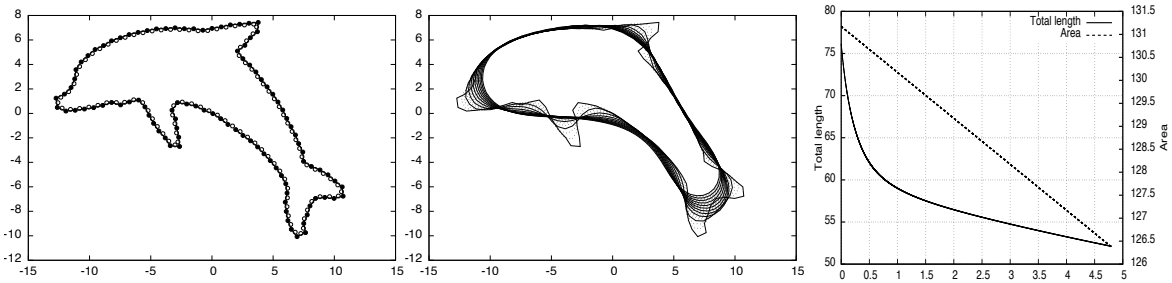

(a) Initial curve (b) Evolution of curves (c) Total length L and area A

Figure 6.10: Results of numerical computation in which the initial curve is take as the dolphin-like curve: (a) the initial curve; (b) the evolution of boundary curves; (c) time evolution of total length and area.

6.6.3 One-phase interior Hele-Shaw problem with sink/source points (6.2.2)

Exact solution

Example 6.6.6. Let the initial curve $\mathscr{C}(0)$ surround the origin and there exists one sink/source point at the origin, that is, we consider the following problem:

$$\begin{cases} \triangle p(\boldsymbol{x}, t) = q_1 \delta(\boldsymbol{x}) & \text{for } \boldsymbol{x} \in \mathscr{D}(t),\ t \in [0, T[, \\ p(\boldsymbol{x}, t) = 0 & \text{for } \boldsymbol{x} \in \mathscr{C}(t),\ t \in [0, T[, \\ V(\boldsymbol{x}, t) = -\nabla p(\boldsymbol{x}, t) \cdot \boldsymbol{N}(\boldsymbol{x}, t) & \text{for } \boldsymbol{x} \in \mathscr{C}(t),\ t \in [0, T[. \end{cases}$$

Note that the surface tension coefficient γ is equal to 0 and that the origin is a suction point if $q_1 > 0$ and an injection point if $q_1 < 0$.

For the above problem, we can construct nontrivial exact solution as follows. Riemann's mapping theorem assures the unique existence of conformal mapping $f(\cdot, t)\colon B(\boldsymbol{0}, 1) \to \Omega(t)$ satisfying $f(0, t) = 0$ and $f_\zeta(0, t) > 0$. Then there exists some holomorphic function $\varphi(\zeta, t)$ such that $f(\zeta, t) = \zeta\varphi(\zeta, t)$ and $\varphi(0, t) \neq 0$. Moreover, we know that $\varphi(\zeta, t) \neq 0$ for all $\zeta \in B(\boldsymbol{0}, 1)$ at each time $t \in [0, T[$ since f is conformal. Since the solution $p(\boldsymbol{x}, t)$ for the above problem can be expressed as the sum of the logarithmic potential $q/(2\pi) \log |\boldsymbol{x}|$ and some harmonic function $\tilde{p}(\boldsymbol{x}, t)$, we have

$$p(f(\zeta, t), t) = \frac{q}{2\pi} \log |f(\zeta, t)| + \tilde{p}(f(\zeta, t), t) = \frac{q}{2\pi} \log |\zeta| + \frac{q}{2\pi} \log |\varphi(\zeta, t)| + \tilde{p}(f(\zeta, t), t).$$

Note that the last two terms $\overline{p}(\zeta,t) := q/(2\pi)\log|\varphi(\zeta,t)| + \tilde{p}(f(\zeta,t),t)$ is a harmonic function since φ is a holomorphic function. In view of the boundary condition, $\overline{p}(\zeta,t) = 0$ for $|\zeta| = 1$, therefore by the maximum principle for harmonic functions, we have $\overline{p}(\zeta,t) = 0$ for $\zeta \in B(\mathbf{0},1)$, that is,

$$p(f(\zeta,t),t) = \frac{q}{2\pi}\log|\zeta|, \quad \zeta \in \overline{B}(\mathbf{0},1).$$

Let $w(\cdot,t) = u(\cdot,t) - \mathrm{i}v(\cdot,t)$ be complex representation of velocity field and $g(\cdot,t) := f^{-1}(\cdot,t)$. Then we have

$$p(z,t) = p(f(g(z,t),t),t) = \frac{q}{2\pi}\log|g(z,t)| = \frac{q}{2\pi}\Re\log g(z,t).$$

Owing to Darcy's law $\boldsymbol{u} = -\nabla p$, we obtain

$$u(z,t) = -\frac{q}{2\pi}\Re\frac{g_z(z,t)}{g(z,t)}, \quad v(z,t) = \frac{q}{2\pi}\Im\frac{g_z(z,t)}{g(z,t)},$$

that is,

$$w(z,t) = u(z,t) - \mathrm{i}v(z,t) = -\frac{q}{2\pi}\frac{g_z(z,t)}{g(z,t)}.$$

Since $g(f(\zeta,t),t) = \zeta$, we clearly have $g_z(f(\zeta,t),t)f_\zeta(\zeta,t) = 1$, that is,

$$w(f(\zeta,t),t) = -\frac{q}{2\pi}\frac{1}{\zeta f_\zeta(\zeta,t)}.$$

Let $\boldsymbol{N}(z,t)$ be the complex representation of the unit outward normal vector of $\mathscr{C}(t)$, that is,

$$\boldsymbol{N}(f(\zeta,t),t) = \frac{\zeta f_\zeta(\zeta,t)}{|f_\zeta(\zeta,t)|}, \quad |\zeta| = 1.$$

Using a relation

$$\frac{\partial p}{\partial \boldsymbol{N}} = \boldsymbol{N}\cdot\nabla p = -\boldsymbol{N}\cdot\boldsymbol{u} = -\Re(Nw),$$

we obtain

$$\frac{\partial p}{\partial \boldsymbol{N}}(f(\zeta,t),t) = \frac{q}{2\pi}\frac{1}{|f_\zeta(\zeta,t)|}, \quad |\zeta| = 1.$$

Since the normal velocity V is represented in two ways as $V = -\partial p/\partial\boldsymbol{N}$ and $V = \Re((\partial_t f)\overline{N})$, we finally obtain the so-called *Polubarinova-Galin equation*:

$$\Re\left(\frac{\partial f}{\partial t}\zeta\overline{\frac{\partial f}{\partial\zeta}}\right) = -\frac{q}{2\pi}, \quad |\zeta| = 1.$$

Particularly, if we seek quadratic conformal mapping $f(\zeta,t) = a(t)\zeta + b(t)\zeta^2$, we obtain from the Polubarinova-Galin equation that

$$a(t)^2 b(t) = a(0)^2 b(0), \quad a(t)^2 + 2b(t)^2 + a(0)^2 + 2b(0)^2 - \frac{Q}{\pi}t.$$

Solving this yields the solution curve

$$\begin{aligned}&\mathscr{C}(t)\colon [0,1] \ni u \mapsto \boldsymbol{x}(u,t) = (x_1(u,t), x_2(u,t))^{\mathrm{T}} \in \mathbb{R}^2;\\ &\qquad x_1(u,t) = a(t)\cos(2\pi u) + b(t)\cos(4\pi u), \quad x_2(u,t) = a(t)\sin(2\pi u) + b(t)\sin(4\pi u).\end{aligned}$$

for each time $t \in [0, T_{\max}[$. See for details Gustafsson and Vasil'ev [26, p. 28] and Varchenko and Etingof [101, p. 62].

Numerical results

Example 6.6.7. We compare a result of our numerical computation with the exact solution. The settings of parameters are as follows:

- $n = 100$ (the number of grid points);
- $\gamma = 0$ (the surface tension coefficient);
- $\boldsymbol{z} = (1000, 0)^{\mathrm{T}}$, $\boldsymbol{z}_j = 1000\boldsymbol{y}_j$ (the dummy points in MFS approximation (6.5.1));
- $m = 1$ (the number of sink/source points), then we have $\dot{A}(t) = -q$;
- $\boldsymbol{\xi}_1 = (0, 0)^{\mathrm{T}}$ (the position of sink/source point);
- $q_1 = 1$ ($\boldsymbol{z}_1$ is a sink point);
- $\tau = 1/(10n^2)$ (the time-mesh size);
- $\omega = 10n$ (the relaxation term);
- $d = n^{-1/2}$ (the parameter controlling accuracy of MFS);
- $T_{\max} = 3.0$ (the final computation time).

The initial curve $\mathscr{C}(0)\colon [0, 1] \ni u \mapsto \boldsymbol{x}(u) = (x_1(u), x_2(u))^{\mathrm{T}} \in \mathbb{R}^2$ is given by

$$x_1(u) = a\cos(2\pi u) + b\cos(4\pi u), \quad x_2(u) = a\sin(2\pi u) + b\sin(4\pi u)$$

where $a = a(0) = 2$ and $b = b(0) = 1/3$. The results of our numerical computation can be found in Figure 6.11 and Figure 6.12, where the velocity field is added in Figure 6.12. In Figure 6.11(a), the

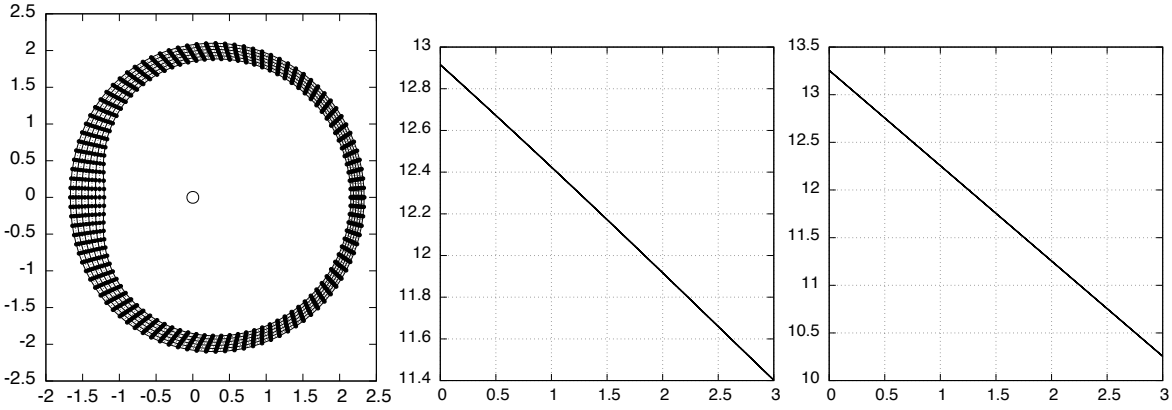

(a) Evolution of curves (the most outside curve is the initial curve)

(b) Total length L

(A) Area A

Figure 6.11: Results of numerical computation for the one-phase interior Hele-Shaw problem with sink/source points: (a) the evolution of boundary curves; (b) time evolution of total length; (c) time evolution of area.

solid and dashed lines are the exact solutions, the points are the numerical solutions and the circle denotes the position of sink point. We can see that the numerical solution matches well with the exact solution. In [53], the similar numerical computation is doen, where the origin is a source point. See

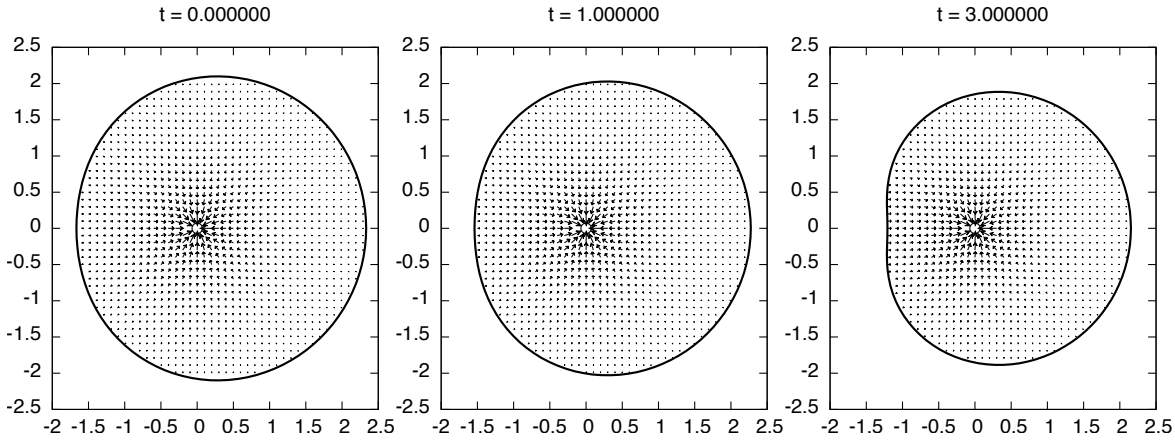

Figure 6.12: Velocity field corresponding to Figure 6.11.

[53, Figure 11]. Furthermore, we compute the error between the exact solution and the numerical solution by using a discrete Hausdorff distance as follows.

Let $\mathscr{C}(t)\colon \boldsymbol{x}(u,t)$ $(u \in [0,1],\ t \in [0, T_{\max}[)$ be the exact solution with the given initial curve. We divide the parameter interval $[0,1]$ into m equal sections, that is, $[0,1] = \bigcup_{i=1}^{m} [u_{i-1}, u_i]$, where $u_i = i/m$ $(i = 0, 1, \ldots, m)$. We then measure the error between $\mathscr{C}(t)$ and $\Gamma(t)$ by the following quantity:

$$d_{\mathrm{H}}^{(n,m)}(\mathscr{C}(t), \Gamma(t)) = \max\left\{ D_1^{(n,m)}(t), D_2^{(n,m)}(t) \right\},$$

where

$$D_1^{(n,m)}(t) = \max_{i=1,2,\ldots,n} \min_{j=1,2,\ldots,m} |\boldsymbol{x}(u_j,t) - \boldsymbol{x}_i(t)|,$$
$$D_2^{(n,m)}(t) = \max_{j=1,2,\ldots,n} \min_{i=1,2,\ldots,n} |\boldsymbol{x}(u_j,t) - \boldsymbol{x}_i(t)|.$$

Take m sufficiently large and fix it. Moreover we define the time-mesh size τ a priori, and define the following quantity:

$$E_r^{(\Lambda)}(n) = \begin{cases} \max\limits_{l=1,2,\ldots,\Lambda} d_{\mathrm{H}}^{(n,m)}(\mathscr{C}(t_l), \Gamma(t_l)) & \text{if } r = \infty, \\ \left(\dfrac{1}{\Lambda} \displaystyle\sum_{l=1}^{\Lambda} d_{\mathrm{H}}^{(n,m)}(\mathscr{C}(t_l), \Gamma(t_l))^r \tau \right)^{1/r} & \text{if } 1 \le r < \infty, \end{cases}$$

where Λ is a positive integer and $t_l = l\tau$. It can be seen that $E_r^{(\Lambda)}(n)$ corresponds to the time ℓ^r norm of the discrete Hausdorff distance $d_{\mathrm{H}}^{(n,m)}(\mathscr{C}(t), \Gamma(t))$. In our numerical scheme, the pressure p is approximated by MFS, therefore the error for approximation of p can be expected to decay exponentially with respect to n. On the other hand, the time discretization is done by the usual fourth order Runge-Kutta method. Therefore we can expect that the error $E_r^{(\Lambda)}(n)$ decays algebraically with respect to n. If we assume that $E_r^{(\Lambda)}(n) = Cn^{-a_r}$ $(a_r > 0)$ holds, then we have

$$a_r = \log_2 \frac{E_r^{(\Lambda)}(n)}{E_r^{(\Lambda)}(2n)} =: \mathrm{EOC}_r(n),$$

in which the right hand side $\mathrm{EOC}_r(n)$ is the experimental order of convergence.

We show the results of our numerical computation. The settings for parameters are as follows:

- $n = 10, 20, \ldots, 200$ (the number of grid points);
- $\tau = 1/(10 \cdot (200)^2) = 2.5 \cdot 10^{-6}$ (the time-mesh size);
- $d = n^{-1/2}$ (the parameter controlling accuracy of MFS);
- $m = 1000$ (the number of divisions of parameter interval $[0, 1]$);
- $\Lambda = 0.001/\tau = 400$ (the number of steps of computation).

In the previous numerical computation, the time-mesh size τ depended on n, more precisely, it was defined as $\tau = (10n^2)^{-1}$. However, we here define τ as the case where $n = 200$, and compute the same number of steps Λ, and compute $E_\infty^{(\Lambda)}(n)$, $E_1^{(\Lambda)}(n)$ and $E_2^{(\Lambda)}(n)$ (see Table 6.1). We can see in Table

n	$\mathrm{EOC}_\infty(n)$	$\mathrm{EOC}_1(n)$	$\mathrm{EOC}_2(n)$
20	1.004146	1.004411	1.004411
30	0.998665	0.998819	0.998816
40	0.999435	0.999709	0.999710
50	0.997245	0.997025	0.997032
60	0.999651	0.999914	0.999915
70	0.999844	1.000614	1.000624
80	0.994698	0.994774	0.994775
90	0.997119	0.998162	0.998164
100	1.004909	1.006235	1.006227

Table 6.1: Experimental order of convergence

6.1 that $E_\infty^{(\Lambda)}(n)$, $E_1^{(\Lambda)}(n)$ and $E_2^{(\Lambda)}(n)$ are of order n^{-1}. In the previous work, Kimura and Notsu [55] computed the one-phase exterior Hele-Shaw problem with the use of signed distance function, and the experimental order was almost equal to 1, which agrees with our numerical results. Then we can say that our proposal scheme has good accuracy, together with asymptotic structure preserving properties. Furthermore, its implementation and computation are easier than other known numerical schemes.

Example 6.6.8. We show two more results of our numerical experiments. The one is the case where the initial curve $\mathscr{C}(0)\colon [0,1] \ni u \mapsto \boldsymbol{x}(u) = (x_1(u), x_2(u))^{\mathrm{T}} \in \mathbb{R}^2$ is an ellipse

$$x_1(u) = a\cos(2\pi u), \quad x_2(u) = b\sin(2\pi u),$$

where $a = 1$ and $b = 2$, which was studied in [53]. The parameters are taken as follows:

- $n = 50$ (the number of grid points);
- $\gamma = 0.2$ (the surface tension coefficient);
- $\boldsymbol{z} = (1000, 0)^{\mathrm{T}}$, $\boldsymbol{z}_j = 1000\boldsymbol{y}_j$ (the dummy points in MFS approximation (6.5.1));
- $m = 1$ (the number of sink/source points), then we have $\dot{A}(t) = -q_1$;
- $\boldsymbol{\xi}_1 = (0, 0)^{\mathrm{T}}$ (the position of sink/source point);
- $q_1 = 2$ ($\boldsymbol{z}_1$ is a sink point);
- $\tau = 1/(10n^2)$ (the time-mesh size);
- $\omega = 10n$ (the relaxation term);

- $d = n^{-1/2}$ (the parameter controlling accuracy of MFS);
- $T_{\max} = 2.1$ (the final computation time).

The results are shown in Figure 6.13 and Figure 6.14. We can say that our result agrees with the one

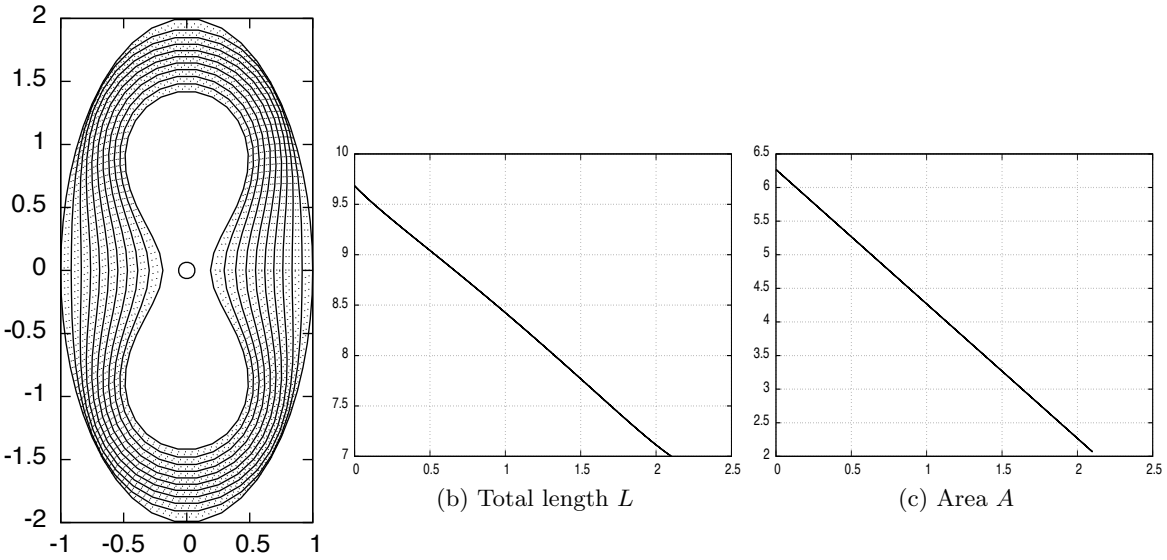

(a) Evolution of curves (the most outside curve is the initial curve)

(b) Total length L

(c) Area A

Figure 6.13: Results of numerical computation for the one-phase interior Hele-Shaw problem with sink/source points: (a) the evolution of boundary curves; (b) time evolution of total length; (c) time evolution of area.

obtained in [53] (see Figure 9 and Figure 10 in [53]).

Example 6.6.9. The other one is the case where the initial curve $\mathscr{C}(0)\colon [0,1] \ni u \mapsto \boldsymbol{x}(u) = (x_1(u), x_2(u))^{\mathrm{T}} \in \mathbb{R}^2$ is given by

$$x_1(u) = 2\cos(2\pi u), \quad x_2(u) = 4\sin(2\pi u) - 3.98\sin^3(2\pi u).$$

The parameters are taken as follows:

- $n = 100$ (the number of grid points);
- $\gamma = 1$ (the surface tension coefficient);
- $\boldsymbol{z} = (1000, 0)^{\mathrm{T}}$, $\boldsymbol{z}_j = 1000\boldsymbol{y}_j$ (the dummy points in MFS approximation (6.5.1));
- $m = 2$ (the number of sink/source points), then we have $\dot{A}(t) = -q_1 - q_2$;
- $\boldsymbol{\xi} = (1.2, 0)^{\mathrm{T}}$, $\boldsymbol{\xi}_2 = (-1.2, 0)^{\mathrm{T}}$;
- $q_1 = -1$, $q_2 = 1$ ($\boldsymbol{z}_1$ is a source point and $\boldsymbol{z}_2$ is a sink point);
- $\tau = 1/(10n^2)$ (the time-mesh size);
- $\omega = 10n$ (the relaxation term);

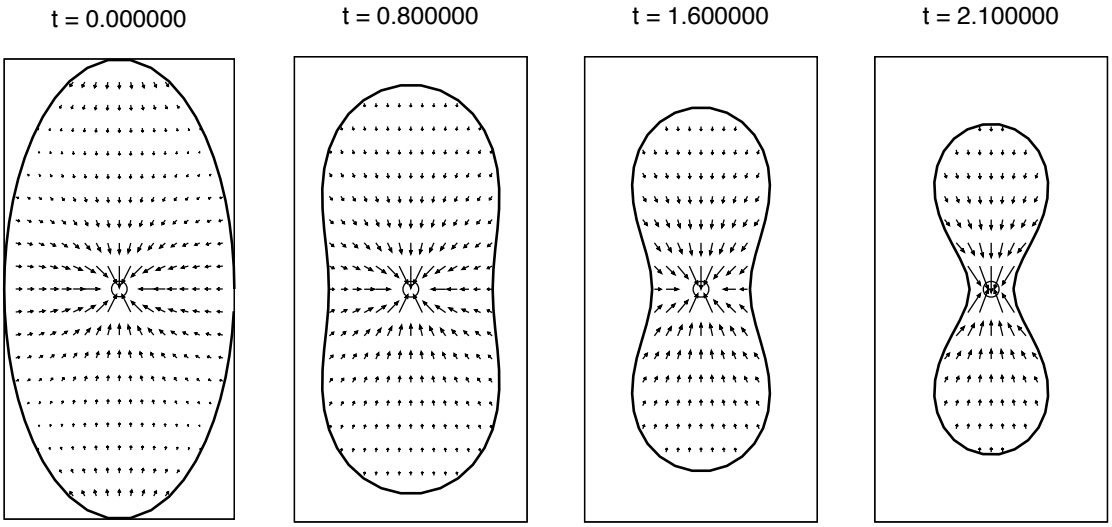

Figure 6.14: Velocity field corresponding to Figure 6.13.

- $d = n^{-1/2}$ (the parameter controlling accuracy of MFS);
- $T_{\max} = 0.9$ (the final computation time).

The results are shown in Figure 6.15 and Figure 6.16.

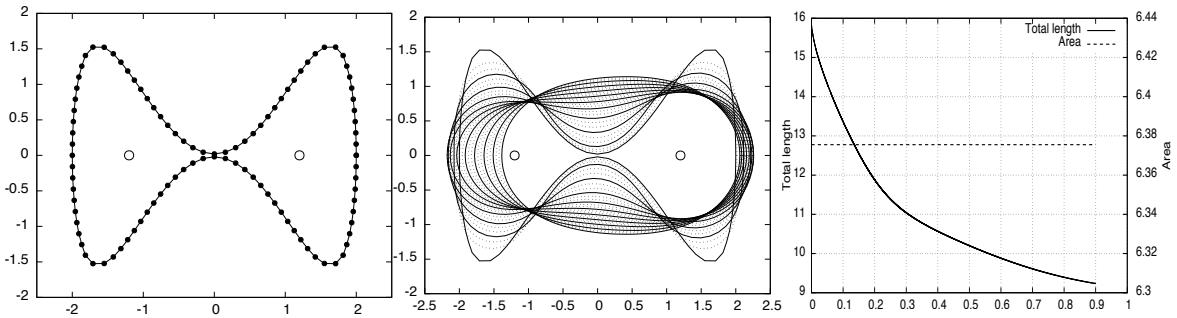

(a) Initial curve (b) Evolution of curves (c) Total length L and area A

Figure 6.15: Results of numerical computation for the one-phase interior Hele-Shaw problem with sink/source points: (a) initial curve; (b) the evolution of boundary curves; (c) time evolution of total length and area.

6.7 Concluding remarks

In this chapter, solutions to the several one-phase Hele-Shaw problems are discretized in space by means of MFS combined with UDM, and our scheme satisfies variational structures such as CS-, AP- and BF-properties under some ideal situations, and asymptotically under practical computational situations, in a discrete sense. As we have seen in Section 6.6, it is easy to make pressure field and vector field without generating mesh in the fluid region in each computational step. This is one of powerful and useful feature of MFS. Application of MFS to moving boundary problems has been done

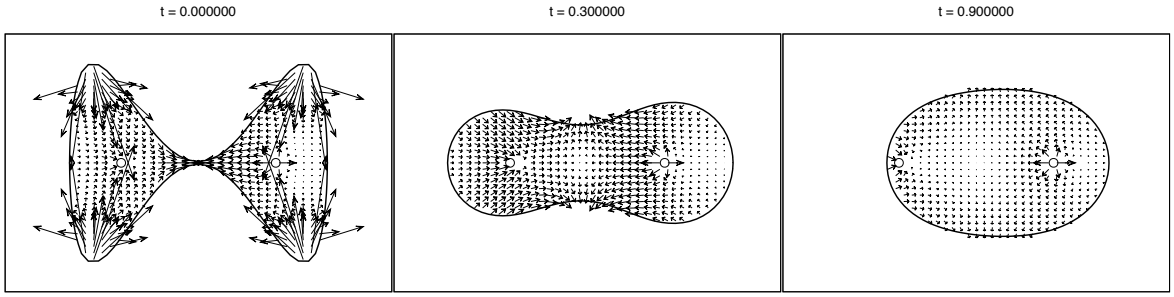

Figure 6.16: Velocity field corresponding to Figure 6.15.

in quite a few papers, but our present attempt will open up a new strategy in numerical computation for moving boundary problems. In this sense, we have many future works. The following are selected future works directly connected to the present paper: (1) to analyze the value of EOC (why it takes "around" 1 and does not "converge" to 1 as n tends to infinity), (2) to treat two-phase Hele-Shaw and other potential problems, (3) to track the exact solution curve (Figure 6.11(a)) of one-phase Hele-Shaw problem with sink until it forms cusp singularity.

Chapter 7

Numerical conformal mapping based on the dipole simulation method

Abstract

In this chapter, we propose a method for numerical conformal mapping based on the dipole simulation method. The proposed method offers us simpler numerical scheme compared with Amano's method based on the method of fundamental solutions, in which we have to compute suitable branch of complex logarithmic function. Several numerical experiments exemplify the effectiveness of our proposed method. This chapter is based on the following paper in preparation:

- K. Sakakibara and M. Katsurada, *Numerical conformal mapping based on the dipole simulation method*, in preparation.

7.1 Introduction

Conformal mapping is a fundamental and important concepts in the field of complex analysis, and it has been applied to science and engineering. Therefore, it is preferable to obtain "analytic expression" of conformal mapping. However, it is impossible to do it except for some simple region, so we have to compute conformal mapping "numerically" in general. Thus, numerical computation of conformal mapping is a hot research topic in numerical analysis. Among several numerical methods, Symm [98] offered an efficient numerical scheme, in which we have to solve first kind of Fredholm integral equation. Afterward, several techniques based on spline function, FFT, and so on, to solve it have been developed (see, for instance, [31, 35, 36]). As a result, high precision numerical conformal mapping could be obtained. On the other hand, their numerical procedures are complex, and their applicable region is so limited. In view of the affairs stated above, Amano [2] offered very simple and accurate numerical scheme based on the method of fundamental solutions. Hereafter, we explain the concept of his method.

Mathematical formulation

Let Ω be a Jordan region in the complex plane $\mathbb{C}$. Riemann mapping theorem assures the existence of conformal mapping f of Ω onto D_1. Taking $z_0 \in \Omega$ arbitrarily, fixing it, and imposing the normalized

condition

$$f(z_0) = 0, \quad f'(z_0) > 0, \tag{7.1.1}$$

a conformal mapping f is determined uniquely. Since the boundary $\partial\Omega$ of Ω is a Jordan curve, f can be continued to an isomorphism of $\overline{\Omega}$ onto $\overline{D}_1$ by virtue of Osgood-Carathéodory theorem. We here consider a function g defined as

$$g(z) = \frac{f(z)}{z - z_0}.$$

According to the normalized condition (7.1.1), $g(z) \neq 0$ for all $z \in \Omega$. Since Ω is simply-connected, there exists a single-valued branch of $\log g(z)$. Denote its real, and imaginary parts by u, and v, respectively:

$$u(z) = \Re \log \frac{f(z)}{z - z_0}, \quad v(z) = \Im \log \frac{f(z)}{z - z_0}.$$

Namely, we obtain an expression $f(z) = (z - z_0)\exp[u(z) + \mathrm{i}v(z)]$. Since $\partial\Omega$ is mapped onto ∂B_1, the function u can be characterized as the solution for the following boundary value problem:

$$\begin{cases} \triangle u = 0 & \text{in } \Omega, \\ u(z) = -\log|z - z_0| & \text{on } \partial\Omega. \end{cases} \tag{7.1.2}$$

The function v is a conjugate harmonic function of u, and satisfies a condition $v(z_0) \equiv 0 \pmod{2\pi}$ since $f'(z_0) > 0$, the second equation in (7.1.1), is assumed. Summarizing the above, we can construct the conformal mapping f by solving the boundary value problem (7.1.2), which yields u, and compute the conjugate harmonic function v of u satisfying $v(z_0) = 0$.

Amano's method

Amano [2] offered a simple numerical method for computing conformal mapping based on MFS, which does not require any numerical integration. Namely, taking singular points $\{\zeta_k\}_{k=1}^N \subset \mathbb{C}\backslash\overline{\Omega}$ "suitably", an approximation $u^{(N)}$ of u is given by

$$u^{(N)}(z) = \sum_{k=1}^{N} \log|z - \zeta_k|.$$

Coefficients $\{Q_k\}_{k=1}^N$ are determined by collocation method, that is, take the collocation points $\{z_j\}_{j=1} \subset \partial\Omega$ "suitably", and impose the following approximate boundary conditions, which are termed the collocation equations:

$$u^{(N)}(z_j) = -\log|z_j - z_0|, \quad j = 1, 2, \ldots, N.$$

Solving the above system yields $u^{(N)}$. Then, we can obtain $v^{(N)}$, which is an approximation of v, as follows:

$$v^{(N)}(z) = \tilde{v}^{(N)}(z) - \tilde{v}^{(N)}(z_0), \quad \tilde{v}^{(N)}(z) = \sum_{k=1}^{N} Q_k \arg(z - \zeta_k).$$

Here, the value of arg function should be determined so that it would be continuous in Ω. If Ω is starlike with respect to z_0, then we have

$$v^{(N)}(z) = \sum_{k=1}^{N} Q_k \operatorname{Arg}\left(\frac{z - \zeta_k}{z_0 - \zeta_k}\right),$$

where Arg is a principal value of arg. Therefore, it is easy to program the above scheme. However, if Ω is not starlike with respect to z_0, then it would be a hard task to choose suitable branch of arg function. In order to resolve this difficulty, the following "continuous scheme" has been developed in [3]. An approximation $u^{(N)}$ of u is given by invariant scheme for MFS:

$$u^{(N)}(z) = Q_0 + \sum_{k=1}^{N} Q_k \log|z - \zeta_k|, \quad \sum_{k=1}^{N} Q_k = 0.$$

We here rewrite $u^{(N)}$ by using Abel transformation, which yields the following expression.

$$u^{(N)}(z) = Q_0 + \sum_{k=1}^{N-1} Q^{(k)} \log\left|\frac{z-\zeta_k}{z-\zeta_{k+1}}\right|, \quad Q^{(k)} := \sum_{l=1}^{k} Q_l.$$

Since the function $z \mapsto \mathrm{Arg}((z-\zeta_k)/(z-\zeta_{k+1}))$ is a harmonic function defined in $\mathbb{C} \setminus [\zeta_k, \zeta_{k+1}]$, if $[\zeta_k, \zeta_{k+1}]$ is contained in $\mathbb{C} \setminus \overline{\Omega}$ for all $k = 1, 2, \ldots, N$, then

$$\tilde{v}^{(N)}(z) = \sum_{k=1}^{N-1} Q^{(k)} \mathrm{Arg}\left(\frac{z-\zeta_k}{z-\zeta_{k+1}}\right)$$

is a conjugate harmonic function of $u^{(N)}$. Hence, defining $v^{(N)} := \tilde{v}^{(N)} - \tilde{v}^{(N)}(z_0)$, we obtain the desired approximation.

Based on the idea described above, simple and high-precision numerical conformal mappings have been studied in several regions. Nevertheless, we always keep in mind that the singular points $\{\zeta_k\}_{k=1}^{N}$ should be chosen so that all the line segment $[\zeta_k, \zeta_{k+1}]$ are in the exterior of Ω, in which some craftsmanship would be required. The aim of this chapter is to construct numerical conformal mapping with same accuracy and without any difficulty in implementation. Concretely speaking, we adopt DSM instead of MFS. This is the only but essential idea of our numerical scheme. The contents of this chapter are as follows. In Section 7.2, we briefly explain our method for numerical conformal mapping. In Section 7.3, we investigate the accuracies of our method and Amano's method by using Hilbert transform. In 7.4, we extend our numerical scheme to multiply-connected region. The efficiency of our numerical scheme will be verified in Section 7.5. We finally summarize this chapter and present future works in Section 7.6.

7.2 Numerical conformal mapping based on DSM

In Amano's method, approximation $u^{(N)}$ of u is given by MFS. If we use DSM instead of MFS, $u^{(N)}$ has of the form

$$u^{(N)}(z) = \sum_{k=1}^{N} Q_k \Re\left(\frac{n_k}{z-\zeta_k}\right).$$

The most important fact is that the following function $\tilde{v}^{(N)}$ becomes a conjugate harmonic function of $u^{(N)}$.

$$\tilde{v}^{(N)}(z) = \sum_{k=1}^{N} Q_k \Im\left(\frac{n_k}{z-\zeta_k}\right).$$

Therefore, defining $v^{(N)}(z) := \tilde{v}^{(N)}(z) - \tilde{v}^{(N)}(z_0)$ and $f^{(N)}(z) = (z-z_0)\exp[u^{(N)}(z) + \mathrm{i}v^{(N)}(z)]$, we obtain the desired numerical conformal mapping. A noteworthy point of this method is that arg function does not appear in the expression for $v^{(N)}$. This implies that we can compute numerical conformal mapping easier than Amano's method.

7.3 Accuracy

In both Amano's method and our method, approximation $u^{(N)}$ of u is given by MFS and DSM, respectively, and approximation $v^{(N)}$ of v is given by the conjugate harmonic function of $u^{(N)}$ satisfying $v^{(N)}(z_0) = 0$. In this section, we investigate the accuracy of such approximations.

7.3.1 Accuracy of $u^{(N)}$

It has been studied in previous studies [49, 45, 46, 47, 50, 48, 79, 84] and in this thesis, Chapters 2 and 3, that if we define the singular points, the collocation points, and the dipole moments suitably, then the approximation error decays exponentially with respect to the number of the singular points. Therefore, we do not turn attention to the accuracy of real part, and we next study the approximation error of imaginary part.

7.3.2 Accuracy of $v^{(N)}$

In previous studies, the behavior of approximation error of imaginary part have not been studied theoretically. The following theorem tells us that it will be completely dominated by the approximation error of real part.

Theorem 7.3.1. *Let Ω be a Jordan region in the complex plane, whose boundary $\partial\Omega$ is analytic, and denote its analytic parameteziation by $\Psi\colon [0,1] \to \mathbb{C}$. Let u be a solution for the following boundary value problem:*

$$\begin{cases} \triangle u = 0 & \text{in } \Omega, \\ u = f & \text{on } \partial\Omega, \end{cases} \tag{7.3.1}$$

where f is a given data, which satisfies the regularity condition $f \circ \Psi \in \mathscr{X}_{\xi,\sigma}$ for $(\xi,\sigma) > (1, 1/2)$. Let v be a conjugate harmonic function of u satisfying $v(z_0) = 0$. Denote by $u^{(N)}$ an approximation of u by MFS or DSM, and by $v^{(N)}$ the conjugate harmonic function of $u^{(N)}$ satisfying $v^{(N)}(z_0) = 0$. Then, there exists some positive constant C such that the following estimate holds for all $s \in \mathbb{R}$:

$$\|v - v^{(N)}\|_{H^s(\partial\Omega)} \le C\|u - u^{(N)}\|_{H^s(\partial\Omega)}.$$

Proof. We only consider the case where Ω is a unit disk D_1, in which the constant C is indeed equal to 1. The general case can be shown via the conformal mapping of Ω onto the unit disk.

Define $F(\tau) = f(\mathrm{e}^{2\pi \mathrm{i}\tau})$ for $\tau \in S^1$. Then, using the Fourier coefficients $\{\hat{F}(n)\}_{n\in\mathbb{Z}}$ of F, we can explicitly write the exact solution u for (7.3.1) as follows:

$$u(z) = \sum_{n=-\infty}^{\infty} \hat{F}(n) r^{|n|} \mathrm{e}^{2\pi \mathrm{i} n\theta} \quad (z = r\mathrm{e}^{2\pi\mathrm{i}\theta}).$$

Let $u^{(N)}$ be an approximation of u by MFS or DSM, and define $\phi^{(N)}(\tau) := u^{(N)}(\mathrm{e}^{2\pi\mathrm{i}\tau})$ for $\tau \in S^1$. Then, $\phi^{(N)}$ can expanded into Fourier series as follows:

$$\phi^{(N)}(\tau) = \sum_{n=-\infty}^{\infty} \hat{\phi}^{(N)}(n) \mathrm{e}^{2\pi \mathrm{i} n\tau}.$$

Then, we have

$$\|F - \phi^{(N)}\|^2_{\mathscr{X}_{\epsilon,s}} = |\hat{F}(0) - \hat{\phi}^{(N)}(0)|^2 + \sum_{n\in\mathbb{Z}^*} |\hat{F}(n) - \hat{\phi}^{(N)}(n)|^2 \epsilon^{2|n|} (2\pi|n|)^{2s}.$$

We here define the Hilbert transform G of F, that is, G is defined as

$$G(\tau) = \sum_{n=-\infty}^{\infty} \sigma_n \hat{F}(n) \mathrm{e}^{2\pi \mathrm{i} n\tau}, \quad \tau \in S^1,$$

where σ_n is a signum function, which is defined as

$$\sigma_n = \begin{cases} 1 & \text{if } n > 0, \\ 0 & \text{if } n = 0, \\ -1 & \text{otherwise.} \end{cases}$$

Similarly, the Hilbert transfor $\psi^{(N)}$ of $\phi^{(N)}$ can be defined as

$$\psi^{(N)}(\tau) = \sum_{n=-\infty}^{\infty} \sigma_n \hat{\phi}^{(N)}(n) \mathrm{e}^{2\pi \mathrm{i} n\tau}, \quad \tau \in S^1.$$

Hence, we obtain

$$\begin{aligned} \|G - \psi^{(N)}\|_{\epsilon,s}^2 &= \sum_{n\in\mathbb{Z}^*} |\sigma_n \hat{F}(n) - \sigma_n \hat{\phi}^{(N)}(n)|^2 \epsilon^{2|n|} (2\pi|n|)^{2s} \\ &= \sum_{n\in\mathbb{Z}^*} |\hat{F}(n) - \hat{\phi}^{(N)}(n)|^2 \epsilon^{2|n|} (2\pi|n|)^{2s} \leq \|F - \phi^{(N)}\|_{\epsilon,s}^2, \end{aligned}$$

which implies the desired estimate. □

7.3.3 Accuracy of $f^{(N)}$

Using the above theorem, we immediately obtain the following estimate.

Theorem 7.3.2. *Under the same condition in Theorem 7.3.1, there exists some positive constant C such that the following estimate holds for all $s \in \mathbb{R}$:*

$$\left\| \log \frac{f(z)}{f^{(N)}(z)} \right\|_{H^s(\partial\Omega)} \leq 2\|u - u^{(N)}\|_{H^s(\partial\Omega)}.$$

Note that we can observe from the numerical experiments in Section 7.5 that the behavior of the error for $f^{(N)}$ is almost the same as that for $u^{(N)}$. Therefore, it can be conjectured that

$$\|f - f^{(N)}\|_{H^s(\partial\Omega)} = \|u - u^{(N)}\|_{H^s(\partial\Omega)} \tag{7.3.2}$$

holds.

7.4 Numerical conformal mapping in multiply-connected regions

In the above sections, we have considered the case where Ω is a simply-connected region. However, numerical conformal mapping in multiply-connected region is actively used in practical applications, for instance, computation of potential flow. Thus, in this section, we aim to extend our method to multiply-connected region.

7.4.1 Doubly-connected region

Let Ω be a nondegenerate doubly-connected region. Namely, assume that there exist two disjoint connected components K_1 and K_2 such that $\hat{\mathbb{C}} \setminus \Omega = K_1 \sqcup K_2$, K_1 is unbounded, and neither K_1 nor K_2 is reduced to a single point. Then, the following theorem holds, which assures the existence of conformal mapping in doubly-connected region.

Theorem 7.4.1 (Henrici [33, Theorem 17.1a]). *There uniquely exists $\mu \in]0,1[$, which is called the modulus of Ω, such that there exists a conformal mapping f of Ω onto the annular region $\mathcal{R}_{\mu,1}$.*

If both $C_1 = \partial K_1$ and $C_2 = \partial K_2$ are Jordan curves, f can be extended to isomorphism of $\overline{\Omega}$ onto $\overline{\mathcal{R}}_{\mu,1}$ by virtue of Osgood-Carathéodory theorem. Hereafter, assume that $0 \in K_2$ just for simplicity.

We are also able to assume that the conformal mapping f has of the form

$$f(z) = z \exp[u(z) + \mathrm{i}v(z)],$$

which is the same for the case where Ω is a Jordan region. Since $f(C_1) = \gamma_1$ and $f(C_2) = \gamma_\mu$ holds, following boundary conditions for u are derived.

$$\begin{aligned} u(z) &= -\log|z| && \text{for } z \in C_1, \\ u(z) - \log\mu &= -\log|z| && \text{for } z \in C_2. \end{aligned}$$

When Ω is a simply-connected region, the existence of conjugate harmonic function v of u can be assured easily. On the other hand, when Ω is not a simply-connected region, it is not easy to ensure the existence of the conjugate harmonic function. However, in general, the following theorem is well known.

Theorem 7.4.2 (Henrici [33, Theorem 15.1d]). *A harmonic function u in a finitely connected region Ω has a conjugate harmonic function in Ω if and only if the conjugate periods with respect to all bounded components of the complement of Ω are equal to zero.*

We hereafter construct numerical scheme for numerical conformal mapping with keeping the above theorem in mind. We give approximation $u^{(N)}$ of u by MFS or DSM, that is,

$$u^{(N)}(z) = \sum_{\nu=1}^{2}\sum_{k=1}^{N} Q_{\nu k} \log|z - \zeta_{\nu k}| \quad \text{or} \quad u^{(N)}(z) = \sum_{\nu=1}^{2}\sum_{k=1}^{N} Q_{\nu k} \Re\left(\frac{n_{\nu k}}{z - \zeta_{\nu k}}\right),$$

where $\{\zeta_{\nu k}\}_{k=1}^{N} \subset \mathring{K}_\nu$ are singular points, and $\{n_{\nu k}\}_{k=1}^{N}$ are dipole moments for $\nu = 1, 2$. Coefficients $\{Q_{\nu k}\}_{\nu=1,2}^{k=1,2,\ldots,N}$ are determined by the collocation method, that is, take the collocation points $\{z_{\mu j}\}_{j=1}^{N} \subset C_\mu$ for $\mu = 1, 2$, and impose the following collocation equations.

$$u^{(N)}(z_{1j}) = -\log|z_{1j}| \qquad (j = 1, 2, \ldots, N), \tag{7.4.1a}$$

$$u^{(N)}(z_{2j}) - \log M = -\log|z_{2j}| \qquad (j = 1, 2, \ldots, N). \tag{7.4.1b}$$

Here, note that the modulus μ of Ω cannot be obtained analytically in general. Therefore, we regard it as the unknown quantity, say M, and obtain it together with u, and v. In order to derive one more equation, we recall Theorem 7.4.2. When we consider the case where an approximation $u^{(N)}$ of u is given by MFS, a conjugate harmonic function $v^{(N)}$ has of the form if it exists:

$$v^{(N)}(z) = \sum_{\nu=1}^{2}\sum_{k=1}^{N} Q_{\nu k} \arg(z - \zeta_{\nu k}) + c,$$

where c is an arbitrary constant. Defining $f^{(N)}$ as $f^{(N)}(z) := z\exp[u^{(N)}(z) + \mathrm{i}v^{(N)}(z)]$, we have

$$\int_{C_2}\left(\frac{(f^{(N)})'(z)}{f(z)} - \frac{1}{z}\right)\mathrm{d}z = \int_{C_2}\sum_{\nu=1}^{2}\sum_{k=1}^{N}\frac{Q_{\nu k}}{z-\zeta_{\nu k}}\,\mathrm{d}z = 2\pi\mathrm{i}\sum_{k=1}^{N}Q_{2k},$$

which implies that the conjugate period of $u^{(N)}$ with respect to K_2 is equal to $2\pi\sum_{k=1}^{N}Q_{2k}$. Therefore, if we impose the condition

$$\sum_{k=1}^{N}Q_{2k} = 0, \tag{7.4.1c}$$

then the existence of $v^{(N)}$ is assured. Therefore, solving the linear system (7.4.1a), (7.4.1b), (7.4.1c), we can obtain numerical conformal mapping and approximation M of the modulus μ. We here also note that it would be required to choose suitable branch of arg function in programming. On the other hand, if we use DSM, then

$$\int_{C_2}\left(\frac{(f^{(N)})'(z)}{f(z)} - \frac{1}{z}\right)\mathrm{d}z = \int_{C_2}\sum_{\nu=1}^{2}\sum_{k=1}^{N}\frac{-Q_{\nu k}n_{\nu k}}{(z-\zeta_{\nu k})^2}\,\mathrm{d}z = 0,$$

which implies that the conjugate period of $u^{(N)}$ with respect to K_2 is always equal zero. Therefore there exists possibility to obtain better numerical conformal mapping than Amano's method, and it would be expected that this advantage could be used effectively when we apply our method to potential flow problem, and so on. However, we here adopt the same condition (7.4.1c) just for simplicity. Since there does not appear arg function in $v^{(N)}$ obtained by DSM, it is easy to implement our method.

7.4.2 $n$ly-connected region, where $n \geq 3$

We here consider more general situation, which appears in practical application. Let Ω be an n-ly connected region in the complex plane $\mathbb{C}$, where $n \geq 3$. Namely, there exist n disjoint connected components K_j $(j = 1, 2, \ldots, n)$ such that $\hat{\mathbb{C}} \setminus \Omega = K_1 \sqcup K_2 \sqcup \cdots \sqcup K_n$, K_1 is unbounded, and none of them is reduced to a single point. Then, the following theorem holds.

Theorem 7.4.3 (Henrici [33, Theorem 17.1b]). *Under the above hypothesis, there exist $n-1$ real numbers μ_j, $j = 1, 2, \ldots, n-1$, such that $0 < \mu_{n-1} < \mu_j < 1$, $j = 1, 2, \ldots, n-2$, such that there exists a conformal mapping f of Ω onto the annulus $\mathcal{R}_{\mu_{n-1},1}$, cut along $n-2$ mutually disjoint arcs Λ_j located on the circles $|w| = \mu_j$, $j = 1, 2, \ldots, n-2$. The mapping function f can be extended analytically to the curves ∂K_j bounding Ω. The images of ∂K_1 and ∂K_n are circles $\Lambda_1 \colon |w| = 1$ and $\Lambda_n \colon |w| = \mu_{n-1}$, respectively. The images of the curves ∂K_j are the arcs Λ_j, $j = 1, 2, \ldots, n-2$.*

We can also obtain numerical conformal mapping in this case by similar procedures in Section 7.4.1. We also here assume that $0 \in K_n$ just for simplicity.

We construct an approximation $u^{(N)}$ of u by I-MFS or DSM, that is,

$$u^{(N)}(z) = Q_0 + \sum_{\nu=1}^{n}\sum_{k=1}^{N}Q_{\nu k}\log|z-\zeta_{\nu k}| \quad \text{or} \quad u^{(N)}(z) = \sum_{\nu=1}^{n}\sum_{k=1}^{N}Q_{\nu k}\Re\left(\frac{n_{\nu k}}{z-\zeta_{\nu k}}\right).$$

Using the collocation method, we obtain the following collocation equations.

$$\begin{aligned} &u^{(N)}(z_{1j}) = -\log|z_{1j}| && (j = 1, 2, \ldots, N),\\ &u^{(N)}(z_{\mu j}) - \log M_\mu = -\log|z_{\mu j}| && (\mu = 2, \ldots, n;\ j = 1, 2, \ldots, N). \end{aligned}$$

We first consider the case where $u^{(N)}$ is computed by MFS. Since

$$\int_{\partial K_j}\left(\frac{(f^{(N)})'(z)}{f(z)}-\frac{1}{z}\right)\mathrm{d}z=\int_{\partial K_j}\left(\sum_{\nu=1}^{n}\sum_{k=1}^{N}\frac{Q_{\nu k}}{z-\zeta_{\nu k}}\right)=2\pi\mathrm{i}\sum_{k=1}^{N}Q_{jk},$$

the conjugate period of $u^{(N)}$ with respect to K_j is equal to $2\pi\sum_{k=1}^{N}Q_{jk}$ for each $j=2,3,\ldots,n$. Therefore, we impose the following conditions.

$$\sum_{k=1}^{N}Q_{jk}=0,\quad j=2,3,\ldots,n. \tag{7.4.2}$$

In order to derive one more condition, we focus on the scaling invariance of conformal mapping. Here, the scaling invariance means that for arbitrary given positive constant α, define a region Ω_α as

$$\Omega_\alpha=\{w\in\mathbb{C}\mid w=\alpha z,\ z\in\Omega\}=\alpha\Omega.$$

Then, the conformal mapping f_α of Ω_α onto $\mathcal{R}_{\mu_{n-1},1}\setminus\bigcup_{j=1}^{n-2}\Lambda_j$ is given by $f_\alpha(w)=f(z)$, $w=\alpha z$. We would like to require numerical conformal mapping $f^{(N)}$ to satisfy the above property. Since

$$f^{(N)}(z)=f^{(N)}(z;\zeta_{11},\ldots,\zeta_{nN},z_{11},\ldots,z_{nN})=z\exp\left[Q_0+\sum_{\nu=1}^{n}\sum_{k=1}^{N}Q_{jk}\log(z-\zeta_{\nu k})\right],$$

the approximation of f_α is given by

$$f_\alpha^{(N)}(w)=F(w;\alpha\zeta_{11},\ldots,\alpha\zeta_{nN},z_{11},\ldots,z_{nN}).$$

Using the condition (7.4.2), we have

$$\begin{aligned}f_\alpha^{(N)}(w)&=\alpha z\exp\left[Q_0+\sum_{\nu=1}^{n}\sum_{k=1}^{N}Q_{\nu k}\log(\alpha(z-\zeta_{\nu k}))\right]\\&=\alpha z\exp\left[Q_0+\sum_{\nu=1}^{n}\sum_{k=1}^{N}Q_{\nu k}\log\alpha+\sum_{\nu=1}^{n}\sum_{k=1}^{N}Q_{\nu k}\log(z-\zeta_{\nu k})\right]\\&=F(z)\alpha\exp\left[\sum_{k=1}^{N}Q_{1k}\log\alpha\right].\end{aligned}$$

Therefore, if we impose the condition

$$\sum_{k=1}^{N}Q_{1k}=-1 \tag{7.4.3}$$

the numerical conformal mapping $f^{(N)}$ satisfies the scaling invariance property.

If we use DSM, numerical conformal mapping $f^{(N)}$ satisfies the above properties naturally. Therefore, there are several possibilities of constructing better numerical conformal mapping to meet a request for the considered problem. We here adopt the conditions (7.4.2) and (7.4.3).

7.5 Numerical experiments

In this section, we show results of numerical experiments.

7.5.1 Collocation points, singular points, and dipole moments

We arrange the singular points, the collocation points, and the dipole moments as in the following procedure, which is influenced by Amano's method [3]. For the sake of simplicity, let Ω be a Jordan region with analytic boundary curve $\partial\Omega$. Denote the analytic parameterization of $\partial\Omega$ by $\Psi\colon [0,1] \to \mathbb{C}$. Then, we arrange the collocation points $\{z_j\}_{j=1}^N$ as follows:

$$z_j = \Psi(j/N), \quad j = 1, 2, \ldots, N. \tag{7.5.1}$$

Then, the singular points $\{\zeta_k\}_{k=1}^N$ and the dipole moments $\{n_k\}_{k=1}^N$ are defined automatically from the collocation points $\{z_j\}_{j=1}^N$. Namely, they are defined as follows:

$$\zeta_k = z_k - \frac{\mathrm{i}r_z}{2}(\zeta_{k+1} - \zeta_{k-1}), \quad n_k = -\mathrm{i}\frac{\zeta_{k+1} - \zeta_{k-1}}{|\zeta_{k+1} - \zeta_{k-1}|}, \quad k = 1, 2, \ldots, N, \tag{7.5.2}$$

where $r_z = rN$, and r is a positive parameter. It can be observed that the singular points $\{\zeta_k\}_{k=1}^N$ and the dipole moments $\{n_k\}_{k=1}^N$ thus defined are approximations of those obtained by using conformal mappings. Therefore, the above methods offer simple and good arrangements of the collocation points, the singular points, and the dipole moments.

7.5.2 Ω: Cassini's oval

We firstly consider the case where Ω is a Cassini's oval, which is defined as

$$\{(x, y) \in \mathbb{R}^2 \mid \{(x+1)^2 + y^2\}\{(x-1)^2 + y^2\} < a^4\},$$

where a is a parameter greater thatn 1. It is known that the explicit form of the conformal mapping f is given by

$$f(z) = \frac{az}{\sqrt{a^4 - 1 + z^2}},$$

where $z_0 = 0$. The boundary $\partial\Omega$ can be parameterized as follows:

$$\partial\Omega = \{r(\theta)\exp(\mathrm{i}\theta) \mid \theta \in [0, 2\pi]\}, \quad r(\theta) = \sqrt{\cos(2\theta) + \sqrt{\cos^2(2\theta) + a^4 - 1}}.$$

Therefore, we determine the collocation points $\{z_j\}_{j=1}^N$ by (7.5.1), and the singular points $\{\zeta_k\}_{k=1}^N$ and the dipole moments $\{n_k\}_{k=1}^N$ by (7.5.2). The configurations of the region Ω, the collocation points $\{z_j\}_{j=1}^N$, and the singular points $\{\zeta_k\}_{k=1}^N$ are depicted in Figure 7.1 (a), and the images of numerical conformal mapping are in Figure 7.1 (b). The behavior of the error can be found in Figure 7.2. It can be observed that the error $\|v - v^{(N)}\|_{L^\infty(\partial\Omega)}$ of $v^{(N)}$ is a little bit smaller than the error $\|u - u^{(N)}\|_{L^\infty(\partial\Omega)}$ of $u^{(N)}$. Moreover, it can be found that the error $\|f - f^{(N)}\|_{L^\infty(\partial\Omega)}$ of $f^{(N)}$ agrees with $\|u - u^{(N)}\|_{L^\infty(\partial\Omega)}$, which implies that the relation (7.3.2) might hold.

7.5.3 Ω: doubly-connected region surrounded by two ellipses

We next show numerical results for the case where Ω is a doubly-connected region surrounded by two ellipses. More precisely, define two curves C_μ $(\mu = 1, 2)$ as

$$C_\mu = \left\{(x, y) \in \mathbb{R}^2 \;\middle|\; \frac{x^2}{a_\mu^2} + \frac{y^2}{b_\mu^2} < 1\right\} \quad (\mu = 1, 2;\ a_1 > a_2,\ b_1 > b_2,\ a_\mu > b_\mu),$$

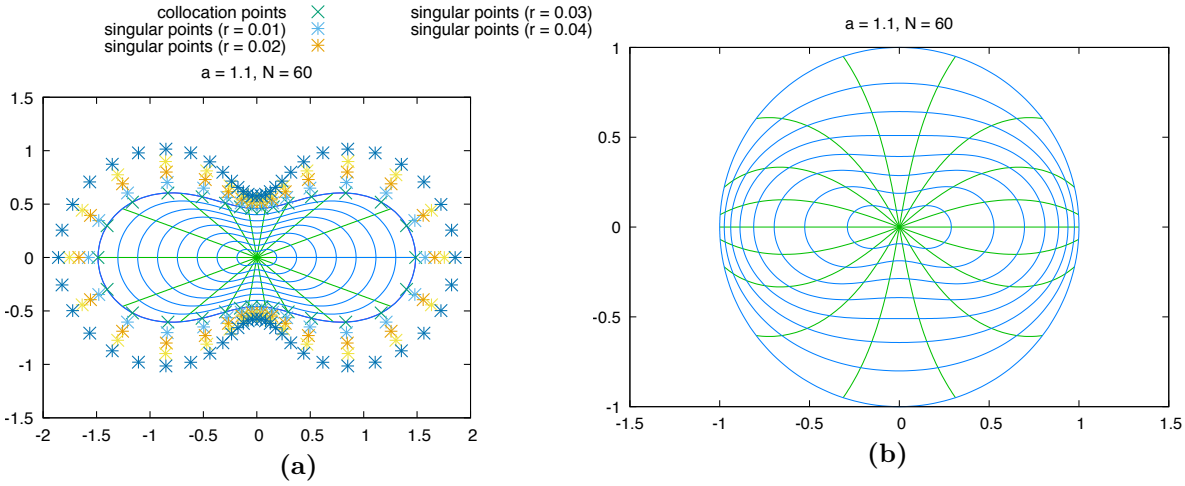

Figure 7.1: Numerical conformal mapping from Cassini's oval onto the unit disk, where $a = 1.1$ and $N = 60$. **a** Configurations and the preimage of numerical conformal mapping. **b** Image of numerical conformal mapping.

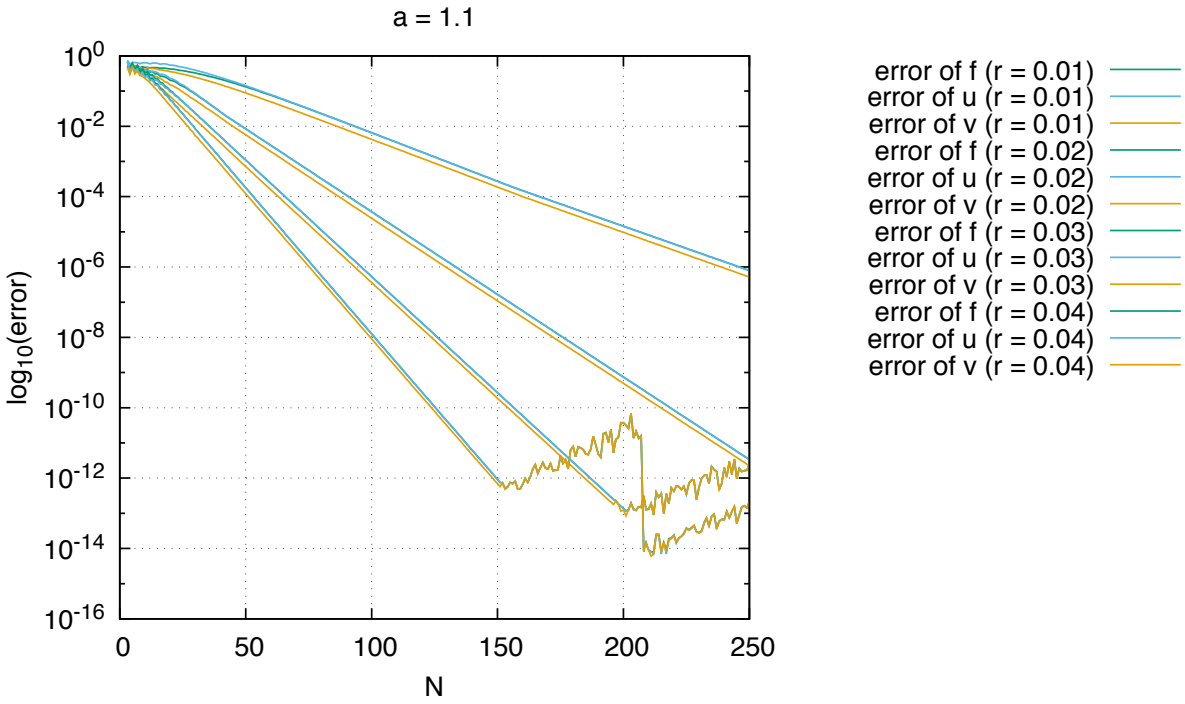

Figure 7.2: N-$\log_{10}$(error) plots, where Ω is Cassini's oval. The lines correspond to the case where $r = 0.01$, 0.02, 0.03, and 0.04 from the above.

and define Ω as the interior doubly-connected region surrounded by C_1 and C_2, which we call doubly-elliptic region hereafter. If two ellipses C_μ $(\mu = 1, 2)$ has the same foci, which means that $a_1^2 - b_1^2 = a_2^2 - b_2^2$ hold, then the exact conformal mapping can be represented by the following formula:

$$f(z) = \frac{z + \sqrt{z^2 - (a_1^2 + b_1^2)}}{a_1 + b_1},$$

where the values of square roots $\sqrt{z^2 - (a_1^2 + b_1^2)}$ should be chosen so that $\sqrt{z^2 - (a_1^2 + b_1^2)}$ is continuous in Ω. Also, the exact value of the modulus μ is given by

$$\mu = \frac{a_2 + b_2}{a_1 + b_1}.$$

We have taken the parameters a_1, b_1, a_2, and b_2 as 7, 5, 5, 1, respectively. The configurations of the region Ω, the collocation points $\{z_j\}_{j=1}^N$, the singular points $\{\zeta_k\}_{k=1}^N$, and the dipole moments $\{n_k\}_{k=1}^N$ are depicted in Figure 7.3 (a). Images of numerical conformal mapping can be found in Figure 7.3 (b), and the behaviors of errors are shown in Figure 7.4.

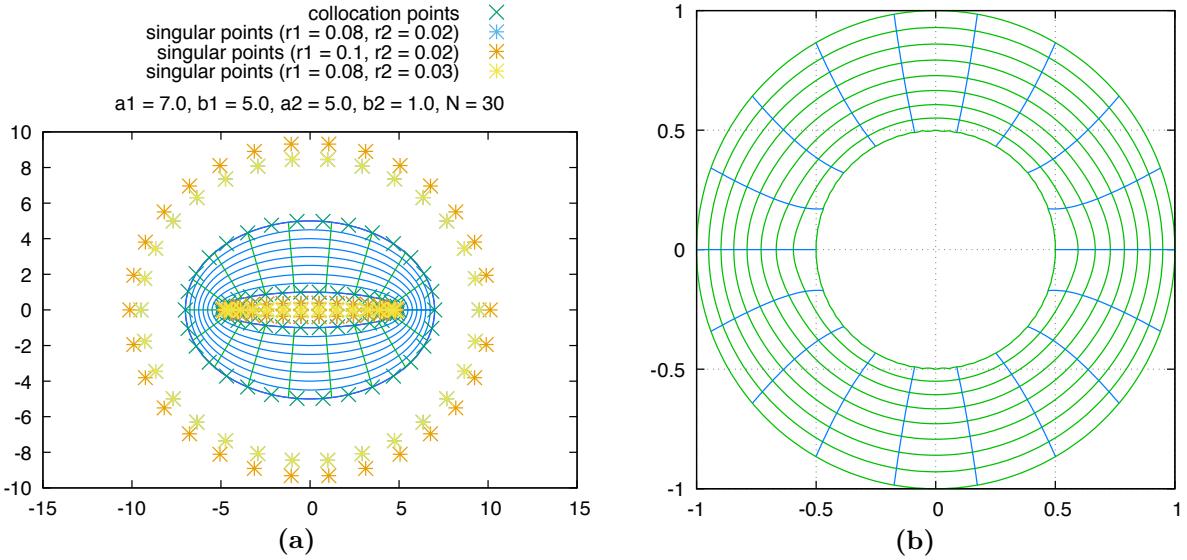

Figure 7.3: Numerical conformal mapping from doubly-elliptic region onto the annulus, where $a_1 = 7$, $b_1 = 5$, $a_2 = 5$, $b_2 = 1$, and $N = 30$. **a** Configurations and the preimage of numerical conformal mapping. **b** Image of numerical conformal mapping.

7.6 Concluding remarks

In this chapter, we have developed scheme for numerical conformal mapping based on DSM, and proved that approximation errors of v and f are completely governed by that of u. Results of numerical experiments in Section 7.5 verify the effectiveness of our proposed numerical scheme. Although we have omitted the details of the application for another multiply-connected regions, we just comment here that our present scheme works well for such regions. Namely, we could construct numerical scheme for conformal mapping which does not require any special techniques in computation but offers us high-precision results.

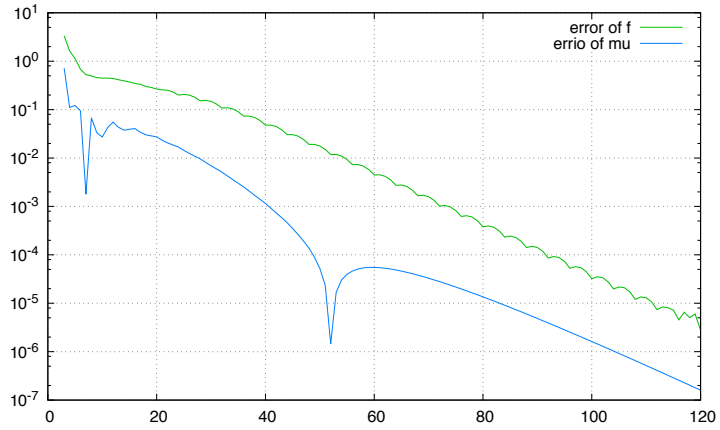

Figure 7.4: $N - \log_{10}(\text{error})$ plots, where Ω is doubly-elliptic region, and the parameters are $a_1 = 7$, $b_1 = 5$, $a_2 = 5$, and $b_2 = 1$.

There are possibilities for our numerical scheme to apply several problems. The first thing is to construct numerical scheme for Poisson equation in arbitrary Jordan region. Since the exact solution can be obtained by using Green function and it can be represented by using conformal mapping, it can be expected that another numerical scheme for solving Poisson equation can be obtained by combining our numerical conformal mapping and some quadrature rule, such as the double exponential formula. We also expect that numerical scheme for moving boundary problem can be obtained by applying our method. For instance, if we consider water wave problem in bounded region in the plane, its motion can be represented by using conformal mapping. Therefore, our numerical conformal mapping may develop new numerical scheme for such a kind of moving boundary problems.

Chapter 8

A mathematical analysis of the complex dipole simulation method

Abstract

We propose the complex dipole simulation method (CDSM) which approximates a holomorphic function by linear combination of $1/(z-\zeta)$ with the use of its boundary values. In this chapter, we deal with a function f which is holomorphic in Ω and continuous on $\overline{\Omega}$ in the case where Ω is a disk or the exterior region of a disk. Then, we establish the following fact: if f is holomorphic in some neighborhood of $\overline{\Omega}$, the error of an approximate function $f^{(N)}$ decays exponentially with respect to N, where N is the number of the singular points. This chapter is based on the following published paper:

- K. Sakakibara and M. Katsurada, *A mathematical analysis of the complex dipole simulation method*, Tokyo J. Math. **38** (2015), no. 2, 309–326.

8.1 Introduction

The objectives of this chapter are to propose the complex dipole simulation method (CDSM) which is an approximation technique for holomorphic function f by using its boundary values, to prove the unique existence of the approximate function $f^{(N)}$ and the exponential decay of the error of $f^{(N)}$, and to exemplify the effectiveness of CDSM by numerical experiments.

As we have explained in Chapter 3, DSM offers an approximate solution for the potential problem in the following form.

$$u^{(N)}(\boldsymbol{x}) = \sum_{k=1}^{N} Q_k D(\boldsymbol{x}, \boldsymbol{y}_k; \boldsymbol{n}_k), \quad D(\boldsymbol{x}, \boldsymbol{y}_k; \boldsymbol{n}_k) = \frac{1}{2\pi} \frac{(\boldsymbol{n}_k \mid \boldsymbol{x} - \boldsymbol{y}_k)}{\|\boldsymbol{x} - \boldsymbol{y}_k\|^2}.$$

We here rewrite the DSM approximate solutions in terms of the real part of the holomorphic function:

$$u^{(N)}(\boldsymbol{x}) = \Re \left(\sum_{k=1}^{N} \frac{-1}{2\pi} \frac{Q_k}{z - \zeta_k} \right),$$

where

$$Q_k = p_k + \mathrm{i} q_k, \quad z = x + \mathrm{i} y, \quad \zeta_k = \xi_k + \mathrm{i} \eta_k,$$

in which

$$Q_k \boldsymbol{n}_k = (p_k, q_k)^{\mathrm{T}}, \quad \boldsymbol{x} = (x, y)^{\mathrm{T}}, \quad \boldsymbol{y}_k = (\xi_k, \eta_k)^{\mathrm{T}}.$$

In view of this expression, we propose CDSM for approximating holomorphic functions. In detail, let Ω be a region in the complex plane and f be a function which is holomorphic in Ω and continuous on $\overline{\Omega}$. CDSM gives an approximate function for f as

$$f^{(N)}(z) = \sum_{k=1}^{N} \frac{Q_k}{z - \zeta_k}, \tag{8.1.1}$$

where $\{\zeta_k\}_{k=1}^N$ are taken from the exterior of Ω and the complex coefficients $\{Q_k\}_{k=1}^N$ are determined by the collocation method, that is, we take N points $\{z_j\}_{j=1}^N$ on $\partial\Omega$ and determine $\{Q_k\}_{k=1}^N$ by the equations below:

$$f^{(N)}(z_j) = f(z_j), \quad j = 1, 2, \ldots, N. \tag{8.1.2}$$

This is an algorithm of CDSM. We call $\{\zeta_k\}_{k=1}^N$, $\{z_j\}_{j=1}^N$, and the equations (8.1.2) the singular points, the collocation points, and the collocation equations, respectively.

The readers may think that a holomorphic function can be approximated by DSM by considering its real part and imaginary part separately. Indeed, when we write the boundary values of $f = u + \mathrm{i}v$ as $f|_{\partial\Omega} = \phi + \mathrm{i}\psi$, then u and v are characterized by two Dirichlet problems:

$$\begin{aligned} \triangle u = 0 \quad &\text{in} \quad \Omega, \quad u = \phi \quad \text{on} \quad \partial\Omega, \\ \triangle v = 0 \quad &\text{in} \quad \Omega, \quad v = \psi \quad \text{on} \quad \partial\Omega. \end{aligned}$$

Although the collocation equations

$$f^{(N)}(z_j) = f(z_j), \quad j = 1, 2, \ldots, N$$

are solvable, the collocation equations

$$\Re f^{(N)}(z_j) = f(z_j), \quad j = 1, 2, \ldots, N$$

are not solvable. Furthermore, since the error of CDSM's approximate function $f^{(N)}$ is evaluated as

$$\sup_{z \in \overline{\Omega}} \left| f(z) - f^{(N)}(z) \right| \leq C \left(\frac{\rho}{R} \right)^N + C' \left(\frac{\rho}{r_0} \right)^N,$$

(we will show details in Theorems 8.2.3 and 8.2.6), where C and C' are constants independent of N, comparing (8.1) with the error estimate for DSM, we see that the convergence rates are different from each other. Therefore the theory of CDSM are not followed from the one of DSM.

This chapter consists of six sections. In Section 8.2, we state theorems on the convergence and error estimates and we prove them in Section 8.3. In Section 8.4, we calculate the condition number of the coefficient matrix for the linear system (8.1.2) explicitly. In Section 8.5, we show some numerical experiments in the case where Ω is a disk, and moreover we compare the results for CDSM with DSM. In Section 8.6, we summarize this chapter and give some concluding remarks.

8.2 Main results

We prepare some notations in advance.

Notations 8.2.1. For a positive number r, we define

$$D_r := \{z \in \mathbb{C} \mid |z| < r\}, \quad \gamma_r := \{z \in \mathbb{C} \mid |z| = r\}, \quad D_r^* := \{z \in \mathbb{C} \mid |z| > r\}.$$

We first consider the case where $\Omega = D_\rho$, where ρ is a positive number. The singular points $\{\zeta_k\}_{k=1}^N$, and the collocation points $\{z_j\}_{j=1}^N$ are located at $R\omega^{k-1}$ $(k = 1, 2, \ldots, N)$, and $\rho\omega^{j-1}$ $(j = 1, 2, \ldots, N)$, respectively, where $R > \rho$ and $\omega = \exp(2\pi \mathrm{i}/N)$. We assume that a function f is holomorphic in Ω and continuous on $\overline{\Omega}$.

We seek an approximate function $f^{(N)}$ within the function space $\mathscr{X}^{(N)}$ which is defined as follows:

$$\mathscr{X}^{(N)} = \mathscr{X}^{(N)}(\{\zeta_k\}_{k=1}^N) = \left\{ \sum_{k=1}^N Q_k H(\cdot, \zeta_k) \;\middle|\; (Q_1, Q_2, \ldots, Q_N)^{\mathrm{T}} \in \mathbb{C}^N \right\},$$

where

$$H(z, \zeta) = \frac{1}{z - \zeta}.$$

We introduce a norm $\|\cdot\|_r \colon X \to \mathbb{R}$ for each $r \in]0, +\infty[$ as follows:

$$\|f\|_r = \sum_{n=0}^\infty |a_n| r^n,$$

where X is a function space whose elements are holomorphic functions in D_ρ and

$$f(z) = \sum_{n=0}^\infty a_n z^n \quad (f \in X;\ z \in D_\rho).$$

We are now in a position to state the theorems:

Theorem 8.2.2. *We can determine $f^{(N)} \in \mathscr{X}^{(N)}$ by* (8.1.2) *uniquely.*

Theorem 8.2.3. *Assume that f is holomorphic in some neighborhood of $\overline{\Omega}$. If we choose $r_0 > \rho$ so that $\|f\|_{r_0} < +\infty$, then we have the inequality*

$$\left\| f - f^{(N)} \right\|_{L^\infty(\Omega)} \leq \frac{2\|f\|_\rho}{1 - (\rho/R)^N} \left(\frac{\rho}{R}\right)^N + 2\|f\|_{r_0} \left(\frac{\rho}{r_0}\right)^N$$

for the approximate function $f^{(N)}$ in Theorem 8.2.2.

We next consider the case $\Omega = D_\rho^*$, where ρ is a positive number. We take the singular points $\{\zeta_k\}_{k=1}^N$, and the collocation points $\{z_j\}_{j=1}^N$ similarly in the case $\Omega = D_\rho$, where $0 < R < \rho$. We assume that a function f is holomorphic and bounded in Ω and continuous in $\overline{\Omega}$.

We seek an approximate function $f^{(N)}$ within the function space $\mathscr{Y}^{(N)}$ which is defined as follows:

$$\mathscr{Y}^{(N)} = \mathscr{Y}^{(N)}(\{\zeta_k\}_{k=1}^N) = \left\{ \sum_{k=1}^N Q_k \Gamma(\cdot, \zeta_k) \;\middle|\; (Q_1, Q_2, \ldots, Q_N)^{\mathrm{T}} \in \mathbb{C}^N \right\},$$

where

$$\Gamma(z, \zeta) = \frac{z}{z - \zeta}.$$

Remark 8.2.4. We cannot use $H(\cdot, \cdot)$ as a substitute for $\Gamma(\cdot, \cdot)$ in $\mathscr{Y}^{(N)}$ since if we use $H(\cdot, \cdot)$, then the value at the point at infinity becomes zero. Inversely we cannot use $\Gamma(\cdot, \cdot)$ instead of $H(\cdot, \cdot)$ in $\mathscr{X}^{(N)}$ since if we use $\Gamma(\cdot, \cdot)$, then the value at the origin becomes zero. However, we can use $\mathcal{H}(z, \zeta) = \zeta/(z - \zeta)$ in place of $H(z, \zeta)$ in $\mathscr{X}^{(N)}$ and obtain similar theorems with Theorems 8.2.2 and 8.2.3.

We introduce the norm $\|\cdot\|_r \colon Y \to \mathbb{R}$ for each $r \in]0, +\infty[$ as follows:

$$\|f\|_r = \sum_{n=0}^{\infty} |b_{-n}| r^{-n},$$

where Y is a function space whose elements are holomorphic and bounded in Ω and

$$f(z) = \sum_{n=0}^{\infty} b_{-n} z^{-n} \quad (f \in Y;\ z \in D_\rho^*).$$

We can state the theorems:

Theorem 8.2.5. *We can determine $f^{(N)} \in Y^{(N)}$ by (8.1.2) uniquely.*

Theorem 8.2.6. *Assume that f is holomorphic in some neighborhood of $\overline{\Omega}$. If we choose $0 < r_0 < \rho$ so that $\|f\|_{r_0} < +\infty$, then we have the inequality*

$$\left\| f - f^{(N)} \right\|_{L^\infty(\Omega)} \leq \frac{2\|f\|_\rho}{1 - (R/\rho)^N} \left(\frac{R}{\rho} \right)^N + 2\|f\|_{r_0} \left(\frac{r_0}{\rho} \right)^N$$

for the approximate function $f^{(N)}$ in Theorem 8.2.5.

8.3 Proofs of theorems

The proof techniques employed here are based on the ones due to [49].

8.3.1 Proof of Theorem 8.2.2

We rewrite the collocation equations (8.1.2) as follows:

$$\sum_{k=1}^{N} \frac{1}{\omega^{j-1}} \frac{Q_k}{\varrho R \omega^{k-j}} = f(z_j), \quad j = 1, 2, \ldots, N,$$

therefore (8.1.2) is equivalent to the linear system

$$G\boldsymbol{Q} = \boldsymbol{f}, \tag{8.3.1}$$

where $\boldsymbol{Q} = (Q_1, Q_2, \ldots, Q_N)^{\mathrm{T}} \in \mathbb{C}^N$, $\boldsymbol{f} = (f(z_1), \omega f(z_2), \ldots, \omega^{N-1} f(z_N))^{\mathrm{T}} \in \mathbb{C}^N$, and G is an $N \times N$ complex matrix with the entries $g_{jk} = 1/(\rho - R\omega^{k-j})$ $(j, k = 1, 2, \ldots, N)$. Let $W = (W_{jk} \mid j, k = 1, 2, \ldots, N)$ be an N-dimensional discrete Fourier transform, that is,

$$W_{jk} = \frac{1}{N^{1/2}} \omega^{(j-1)(k-1)}, \quad j, k = 1, 2, \ldots, N.$$

Note that G is a circulant matrix whose (j, k) entry depends on $k - j \pmod N$. In general, circulant matrices can be diagonalized by discrete Fourier transform, indeed we see

$$W^{-1} G W = \operatorname{diag}\left(\varphi_0^{(N)}(\rho), \varphi_1^{(N)}(\rho), \ldots, \varphi_{N-1}^{(N)}(\rho) \right), \tag{8.3.2}$$

where

$$\varphi_p^{(N)}(z) = \sum_{k=1}^{N} \omega^{p(k-1)} H(z, \zeta_k) \quad (z \in \mathbb{C} \setminus \{\zeta_k\}_{k=1}^N;\ p \in \mathbb{Z}). \tag{8.3.3}$$

The function $\varphi_p^{(N)}$ plays a fundamental role in the following analysis. We first prove the following lemma.

Lemma 8.3.1. (i) $\varphi_p^{(N)}$ *is periodic with respect to* p *with period* N.

(ii) *We have*

$$\varphi_p^{(N)}(z) = -\frac{N}{R}\left(\frac{z}{R}\right)^{p-1}\frac{1}{1-(z/R)^N} \quad (z \in D_R)$$

for all $p \in \{1, 2, \ldots, N\}$.

Proof. (i) $\varphi_p^{(N)} = \varphi_q^{(N)}$ follows from (8.3.3) if $p \equiv q \pmod N$ since $\omega^N = 1$.

(ii) To begin with, we expand $H(z, \zeta_k)$ as

$$H(z,\zeta_k) = \frac{-1}{R\omega^{k-1}}\frac{1}{1-z/(R\omega^{k-1})} = -\frac{1}{R}\sum_{n=0}^{\infty}\left(\frac{z}{R}\right)^n \omega^{-(k-1)(n+1)} \quad (z \in D_R).$$

Hence we have

$$\begin{aligned}\varphi_p^{(N)}(z) &= \sum_{k=1}^{N}\omega^{p(k-1)}H(z,\zeta_k) = \sum_{k=1}^{N}\omega^{p(k-1)}\left[-\frac{1}{R}\sum_{n=0}^{\infty}\left(\frac{z}{R}\right)^n\omega^{-(k-1)(n+1)}\right]\\ &= -\frac{1}{R}\sum_{n=0}^{\infty}\left(\frac{z}{R}\right)^n\sum_{k=1}^{N}\omega^{-(n-(p-1))(k-1)} = -\frac{N}{R}\sum_{\substack{n\equiv p-1 \pmod N\\ n\geq 0}}\left(\frac{z}{R}\right)^N\\ &= -\frac{N}{R}\left(\frac{z}{R}\right)^{p-1}\frac{1}{1-(z/R)^N}\end{aligned}$$

for all $p \in \{1, 2, \ldots, N\}$. □

Proof of Theorem 8.2.2. By (8.3.2) and Lemma 8.3.1, we can compute the determinant of G as

$$\det G = \prod_{p=0}^{N-1}\varphi_p^{(N)}(\rho) = \prod_{p=1}^{N}\varphi_p^{(N)}(\rho).$$

By Lemma 8.3.1 (ii), we know $\varphi_p^{(N)}(\rho) < 0$ $(p = 1, 2, \ldots, N)$. Hence $\det G \neq 0$ follows and this completes the proof of Theorem 8.2.2. □

8.3.2 Proof of Theorem 8.2.3

By (8.3.2), the inverse matrix of G is as follows:

$$G^{-1} = W\,\mathrm{diag}\left(\frac{1}{\varphi_0^{(N)}(\rho)}, \frac{1}{\varphi_1^{(N)}(\rho)}, \ldots, \frac{1}{\varphi_{N-1}^{(N)}(\rho)}\right)W^{-1}.$$

A direct calculation yields

$$[G^{-1}]_{kj} = \frac{1}{N}\sum_{p=1}^{N}\frac{\omega^{(k-j)(p-1)}}{\varphi_{p-1}^{(N)}(\rho)} \quad (j, k = 1, 2, \ldots, N),$$

where $[G^{-1}]_{kj}$ denotes the (k, j) element of G^{-1}. This makes it possible to solve (8.3.1) as

$$\begin{aligned}Q_k &= \sum_{j=1}^{N}[G^{-1}]_{kj}[\boldsymbol{f}]_j = \sum_{j=1}^{N}\left(\frac{1}{N}\sum_{p=1}^{N}\frac{\omega^{(k-j)(p-1)}}{\varphi_{p-1}^{(N)}(\rho)}\right)\omega^{j-1}f(z_j)\\ &= \frac{1}{N}\sum_{j,p=1}^{N}\frac{\omega^{(k-1)(p-1)-(j-1)(p-2)}}{\varphi_{p-1}^{(N)}(\rho)}f(z_j).\end{aligned}$$

Hence we have

$$\begin{aligned} f^{(N)}(z) &= \sum_{k=1}^{N} Q_k H(z,\zeta_k) = \sum_{k=1}^{N} \left(\frac{1}{N} \sum_{j,p=1}^{N} \frac{\omega^{(k-1)(p-1)-(j-1)(p-2)}}{\varphi_{p-1}^{(N)}(\rho)} f(z_j) \right) H(z,\zeta_k) \\ &= \frac{1}{N} \sum_{j,p=1}^{N} \omega^{-(j-1)(p-2)} \frac{\varphi_{p-1}^{(N)}(z)}{\varphi_{p-1}^{(N)}(\rho)} \sum_{n=0}^{\infty} a_n \rho^n \omega^{(j-1)n} \\ &= \frac{1}{N} \sum_{p=1}^{N} \frac{\varphi_{p-1}^{(N)}(z)}{\varphi_{p-1}^{(N)}(\rho)} \sum_{n=0}^{\infty} a_n \rho^n \left(\sum_{j=1}^{N} \omega^{(n-(p-2))(j-1)} \right) \\ &= \sum_{p=1}^{N} \frac{\varphi_{p-1}^{(N)}(z)}{\varphi_{p-1}^{(N)}(\rho)} \sum_{\substack{n \equiv p-2 \pmod N \\ n \geq 0}} a_n \rho^n = \sum_{n=0}^{\infty} a_n \rho^n \frac{\varphi_{n+1}^{(N)}(z)}{\varphi_{n+1}^{(N)}(\rho)}. \end{aligned}$$

Consequently we can write the error function $e^{(N)} = f - f^{(N)}$ as

$$e^{(N)}(z) = \sum_{n=0}^{\infty} a_n \rho^n \left[\left(\frac{z}{\rho} \right)^n - \frac{\varphi_{n+1}^{(N)}(z)}{\varphi_{n+1}^{(N)}(\rho)} \right].$$

Since $e^{(N)}$ is holomorphic in Ω and continuous on $\overline{\Omega}$, we obtain by the maximum modulus principle for holomorphic functions

$$\|e^{(N)}\|_{L^\infty(\Omega)} \leq \sum_{n=0}^{\infty} |a_n| \rho^n g_{n,\rho}^{(N)}, \tag{8.3.4}$$

where

$$g_{n,\rho}^{(N)} := \sup_{z \in \gamma_\rho} \left| \left(\frac{z}{\rho} \right)^n - \frac{\varphi_{n+1}^{(N)}(z)}{\varphi_{n+1}^{(N)}(\rho)} \right|.$$

At this stage, we claim the following Lemma 8.3.2 concerning $g_{n,\rho}^{(N)}$.

Lemma 8.3.2. (i) *For all $n \in \mathbb{N} \cup \{0\}$, we have*

$$g_{n,\rho}^{(N)} \leq 2. \tag{8.3.5}$$

(ii) *For all $p \in \{0, 1, \ldots, N-1\}$, we have*

$$g_{p,\rho}^{(N)} \leq \frac{2(\rho/R)^N}{1-(\rho/R)^N}. \tag{8.3.6}$$

Proof. (i) We know by Lemma 8.3.1 that the inequality

$$|\varphi_p^{(N)}(z)| \leq |\varphi_p^{(N)}(|z|)|$$

holds for all $p \in \mathbb{Z}$ and for all $z \in D_R$. Therefore we see

$$\left| \left(\frac{z}{\rho} \right)^n - \frac{\varphi_{n+1}^{(N)}(z)}{\varphi_{n+1}^{(N)}(\rho)} \right| \leq \left(\frac{|z|}{\rho} \right)^n + \frac{|\varphi_{n+1}^{(N)}(z)|}{|\varphi_{n+1}^{(N)}(\rho)|} \leq 2$$

for all $z \in \gamma_\rho$. This establishes (8.3.5).

(ii) By Lemma 8.3.1, we have

$$\left|\left(\frac{z}{\rho}\right)^p - \frac{\varphi_{p+1}^{(N)}(z)}{\varphi_{p+1}^{(N)}(\rho)}\right| = \left|\left(\frac{z}{\rho}\right)^p \frac{(\rho/R)^N - (z/R)^N}{1-(z/R)^N}\right| \le \frac{2(\rho/R)^N}{1-(\rho/R)^N}$$

for all $z \in \gamma_\rho$. Thus (8.3.6) is shown and this completes the proof of Lemma 8.3.2. □

Proof. By (8.3.4) and Lemma 8.3.2, we have

$$\begin{aligned}\|f - f^{(N)}\|_{L^\infty(\Omega)} &\le \left[\sum_{n=0}^{N-1} + \sum_{n=N}^{\infty}\right] |a_n|\rho^n g_{n,\rho}^{(N)} \le \sum_{n=0}^{N-1} |a_n|\rho^n \frac{2(\rho/R)^N}{1-(\rho/R)^N} + \sum_{n=N}^{\infty} |a_n|\rho^n \cdot 2 \\ &\le \sum_{n=0}^{\infty} |a_n|\rho^n \frac{2(\rho/R)^N}{1-(\rho/R)^N} + 2\sum_{n=N}^{\infty} |a_n| r_0^n \left(\frac{\rho}{r_0}\right)^n \\ &\le \frac{2\|f\|_\rho}{1-(\rho/R)^N}\left(\frac{\rho}{R}\right)^N + 2\|f\|_{r_0}\left(\frac{\rho}{r_0}\right)^N.\end{aligned}$$

□

8.3.3 Proofs of Theorems 8.2.5 and 8.2.6

Theorems 8.2.5 and 8.2.6 are proved as well as Theorems 8.2.2 and 8.2.3, respectively. Therefore we only sketch out the proofs of them.

We rewrite the collocation equations (8.1.2) into (8.3.1) similarly, where $\boldsymbol{Q} = (Q_1, Q_2, \dots, Q_N)^{\mathrm{T}} \in \mathbb{C}^N$, $\boldsymbol{f} = (f(z_1), f(z_2), \dots, f(z_N))^{\mathrm{T}} \in \mathbb{C}^N$, and G is an $N \times N$ complex matrix with the entries $g_{jk} = \Gamma(z_j, \zeta_k)$ $(j,k = 1,2,\dots,N)$. G is a circulant matrix whose (j,k) entry depends on $k-j \pmod N$. Therefore we see

$$W^{-1}GW = \operatorname{diag}\left(\psi_0^{(N)}(\rho), \psi_1^{(N)}(\rho), \dots, \psi_{N-1}^{(N)}(\rho)\right), \tag{8.3.7}$$

where

$$\psi_p^{(N)}(z) := \sum_{k=1}^{N} \omega^{p(k-1)}\Gamma(z, \zeta_k) \quad (z \in \mathbb{C} \setminus \{\zeta_k\}_{k=1}^N;\ p \in \mathbb{Z}).$$

We have the following Lemma 8.3.3 as to the function $\psi_p^{(N)}$.

Lemma 8.3.3. (i) *$\psi_p^{(N)}$ is periodic with respect to p with period N.*

(ii) *We have*

$$\psi_p^{(N)}(z) = N\left(\frac{R}{z}\right)^{N-p} \frac{1}{1-(R/z)^N} \quad (z \in D_R^*)$$

for all $p \in \{1,2,\dots,N\}$.

By (8.3.7), G^{-1} can be represented as follows:

$$G^{-1} = W \operatorname{diag}\left(\frac{1}{\psi_0^{(N)}(\rho)}, \frac{1}{\psi_1^{(N)}(\rho)}, \dots, \frac{1}{\psi_{N-1}^{(N)}(\rho)}\right) W^{-1}.$$

A direct calculation yields

$$[G^{-1}]_{kj} = \frac{1}{N}\sum_{p=1}^{N} \frac{\omega^{(k-j)(p-1)}}{\psi_{p-1}^{(N)}(\rho)} \quad (j,k = 1,2,\dots,N).$$

This makes it possible to solve (8.3.1) for Q_k $(k = 1, 2, \ldots, N)$ as

$$Q_k = \frac{1}{N} \sum_{j,p=1}^{N} \frac{\omega^{(k-1)(p-1)-(j-1)(p-1)}}{\psi_{p-1}^{(N)}(\rho)} f(z_j).$$

Hence we have

$$f^{(N)}(z) = \sum_{n=0}^{\infty} b_{-n} \rho^{-n} \frac{\psi_{-n}^{(N)}(z)}{\psi_{-n}^{(N)}(\rho)}.$$

Consequently we can write the error function $e^{(N)} = f - f^{(N)}$ as

$$e^{(N)}(z) = \sum_{n=0}^{\infty} b_{-n} \rho^{-n} \left[\left(\frac{\rho}{z} \right)^n - \frac{\psi_{-n}^{(N)}(z)}{\psi_{-n}^{(N)}(\rho)} \right].$$

We obtain by the maximum modulus principle for holomorphic functions

$$\sup_{z \in \overline{\Omega}} |e^{(N)}(z)| \leq \sum_{n=0}^{\infty} |b_{-n}| \rho^{-n} g_{n,\rho}^{(N)}, \tag{8.3.8}$$

where

$$g_{n,\rho}^{(N)} = \sup_{z \in \gamma_\rho} \left| \left(\frac{\rho}{z} \right)^n - \frac{\psi_{-n}^{(N)}(z)}{\psi_{-n}^{(N)}(\rho)} \right|.$$

At this stage we claim the following Lemma 8.3.4 concerning $g_{n,\rho}^{(N)}$.

Lemma 8.3.4. (i) *For all $n \in \mathbb{N} \cup \{0\}$, we have*

$$g_{n,\rho}^{(N)} \leq 2.$$

(ii) *For all $p \in \{0, 1, \ldots, N-1\}$, we have*

$$g_{p,\rho}^{(N)} \leq \frac{2(R/\rho)^N}{1 - (R/\rho)^N}.$$

By (8.3.8) and Lemma 8.3.4, we complete a proof of Theorem 8.2.6.

8.4 Condition numbers

In this section, we calculate the condition number of the coefficient matrix G for the linear system (8.3.1).

(I) In the case $\Omega = D_\rho$. Since the coefficient matrix G is an Hermitian matrix, if we take a norm for N-dimensional vectors as

$$\|\boldsymbol{x}\| := \sqrt{\sum_{j=1}^{N} |x_j|^2} \quad (\boldsymbol{x} = (x_1, x_2, \ldots, x_N)^{\mathrm{T}}),$$

we can calculate the condition number of G as

$$\operatorname{cond} G = \|G\| \cdot \|G^{-1}\| = \frac{\max_{p=1,2,\ldots,N} |\varphi_p^{(N)}(\rho)|}{\min_{p=1,2,\ldots,N} |\varphi_p^{(N)}(\rho)|} = \frac{|\varphi_1^{(N)}(\rho)|}{|\varphi_N^{(N)}(\rho)|} = \left(\frac{R}{\rho} \right)^{N-1}.$$

(II) In the case $\Omega = D_\rho^*$. We can calculate $\operatorname{cond} G$ similarly in the case (I) as

$$\operatorname{cond} G = \left(\frac{\rho}{R}\right)^{N-1}.$$

We know from (I) and (II) that $\operatorname{cond} G$ increases exponentially with respect to N. Therefore, the linear system (8.3.1) is ill-conditioned. Nevertheless, as we shall see in Section 8.5, numerical computations perform well.

On the other hand, in MFS, $\operatorname{cond} G = O((R/\rho)^{N/2})$ or $O((\rho/R)^{N/2})$ in the case $\Omega = D_\rho$ or $\Omega = D_\rho^*$, respectively. Therefore, the linear system for Q_ks is ill-conditioned, too. There are results abount the numerical stability of CSM by Kitagawa [57, 58]. Studying the numerical stability of CDSM will be expected, too.

8.5 Numerical experiments

In this section, we present results for our numerical experiments in the case $\Omega = D_\rho$. Since errors of MFS and DSM show almost similar behavior, we show results for DSM, and compare it with that for CDSM. A corresponding Dirichlet problem which is solved numerically by DSM is as follows:

$$\begin{aligned} \triangle u &= 0, \quad \text{in } \Omega, \\ u &= \Re f, \quad \text{on } \partial\Omega. \end{aligned}$$

The singular points $\{\zeta_k\}_{k=1}^N$ and the collocation points $\{z_j\}_{j=1}^N$ are defined by

$$\zeta_k = R\omega^{k-1} \quad (k = 1, 2, \ldots, N) \quad z_j = \rho\omega^{j-1} \quad (j = 1, 2, \ldots, N),$$

where R is a parameter which satisfies $R > \rho$. In order to estimate the error $\|f - f^{(N)}\|_{L^\infty(\Omega)}$ numerically, we use the Monte Carlo method. In other words, we adopt the following quantity as an approximation of the error:

$$\tilde{e}^{(N)} := \max_{z\in\Lambda} \left| f(z) - f^{(N)}(z) \right|,$$

where Λ is a set of points chosen from γ_ρ. To be more concrete, we prepare a set $\Theta := \{\theta_k\}_{k=1}^M \subset [0, 1[$ (M is equal to $10 \cdot \max N$) by using pseudo-random numbers, and put

$$\Lambda := \{\rho \mathrm{e}^{2\pi \mathrm{i}\theta} \mid \theta \in \Theta\}.$$

Likewise, we set up

$$\tilde{e}_{\mathrm{D}}^{(N)} := \max_{z\in\Lambda} \left| u(z) - u^{(N)}(z) \right|$$

as an approximation of the error for DSM. Test 1, 2-(i), 3, and 4-(i) were performed by using MATLAB, and Test 2-(ii), and 4-(ii) by C++ programs using the multiple-precision arithmetic library "exflib" (see Fujiwara [21]).

In each numerical experiment, we compute $\tilde{e}^{(N)}$ and $\tilde{e}_{\mathrm{D}}^{(N)}$, and plot graphs whose horizontal axis represents N and vertical axis $\log_{10} \tilde{e}^{(N)}$ or $\log_{10} \tilde{e}_{\mathrm{D}}^{(N)}$.

Test 1. In this test we deal with the case where f is a power function whose exponent is a non-negative integer:

$$f(z) = z^m,$$

where $m \in \{0, 1, \ldots, 5\}$ is a parameter. In Figure 8.1, we find these graphs are almost linear. This

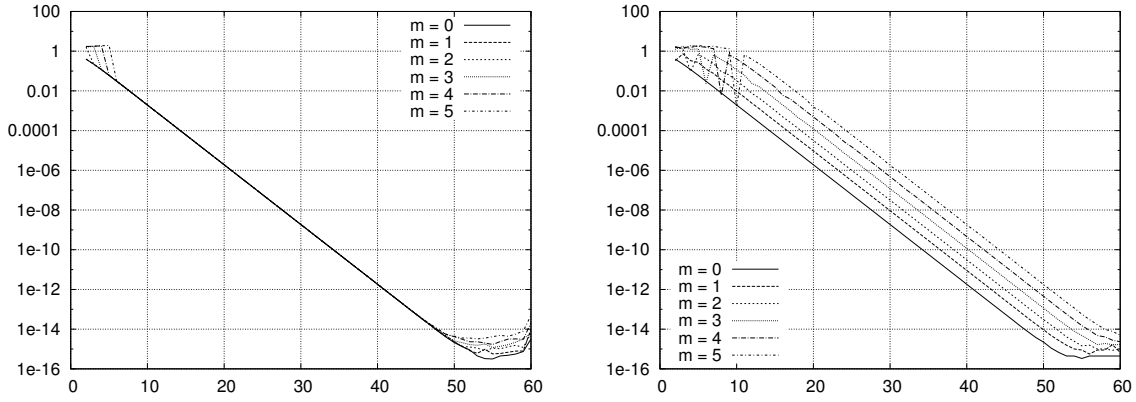

(a) CDSM **(b) DSM**

Figure 8.1: $f(z) = z^m$, where $m \in \{0, 1, \ldots, 5\}$, $N \in \{2, 3, \ldots, 60\}$, $\rho = 1$, and $R = 2$

implies that $\tilde{e}^{(N)}$ and $\tilde{e}_{\mathrm{D}}^{(N)}$ behave as

$$\tilde{e}^{(N)} \sim C\tau^N, \quad \tilde{e}_{\mathrm{D}}^{(N)} \sim C'\tau'^N \quad (N \to \infty). \tag{8.5.1}$$

We know that τ and τ' are almost equal to ρ/R in this case since f is holomorphic and u harmonic in the entire plane.

Test 2. In this test we deal with the case where f is an exponential function composed with a power function whose exponent is a non-negative integer:

$$f(z) = \exp(z^m),$$

where $m \in \{0, 1, \ldots, 5\}$ is a parameter.

(i) We compute $\tilde{e}^{(N)}$ and $\tilde{e}_{\mathrm{D}}^{(N)}$ for all $N \in \{2, 3, \ldots, 60\}$ when $(\rho, R) = (1, 2)$, and $N \in \{2, 3, \ldots, 100\}$ when $(\rho, R) = (1, 1.5)$ (see Figure 8.2).

Since f is holomorphic and u harmonic in the entire plane, τ and τ' are both almost equal to ρ/R as well as Test 1. However, we cannot see from Figures 8.2 (a) and (b) that $\tilde{e}^{(N)}$ and $\tilde{e}_{\mathrm{D}}^{(N)}$ behave as (8.5.1). On the other hand, from Figure 8.2 (c), $\tilde{e}^{(N)}$ behaves as (8.5.1) for $m \in \{0, 1, 2, 3, 4\}$. Simultaneously, from Figure 8.2 (d), $\tilde{e}_{\mathrm{D}}^{(N)}$ behaves as (8.5.1) for $m \in \{0, 1, 2, 3\}$. Hence we can investigate that $\tilde{e}^{(N)}$ and $\tilde{e}_{\mathrm{D}}^{(N)}$ behave as (8.5.1) for sufficiently large N.

In order to clear up this investigation, we compute $\tilde{e}^{(N)}$ with $(\rho, R) = (1, 2)$ and $\tilde{e}_{\mathrm{D}}^{(N)}$ with (ρ, R) for large N using multiple-precision arithmetic.

(ii) We compute $\tilde{e}^{(N)}$ and $\tilde{e}_{\mathrm{D}}^{(N)}$ for all $N \in \{2, 3, \ldots, 400\}$ in 120 digits by C++ programs using exflib (see Figure 8.3). We can see from Figure 8.3 that $\tilde{e}^{(N)}$ and $\tilde{e}_{\mathrm{D}}^{(N)}$ behave as (8.5.1).

Test 3. In this test we deal with the case where f is a rational function:

$$f(z) = \frac{1}{z - p(m)}, \quad p(m) = \rho + 0.1 + 0.2m,$$

where $m \in \{0, 1, \ldots, 10\}$ is a parameter. f has a simple pole at $p(m)$. We find from Figure 8.4 that $\tilde{e}^{(N)}$ and $\tilde{e}_{\mathrm{D}}^{(N)}$ behave as (8.5.1), and τ and τ' are equal to $\max\{\rho/R, \rho/p(m)\}$ and $\max\{\rho/R, \sqrt{\rho/p(m)}\}$, respectively.

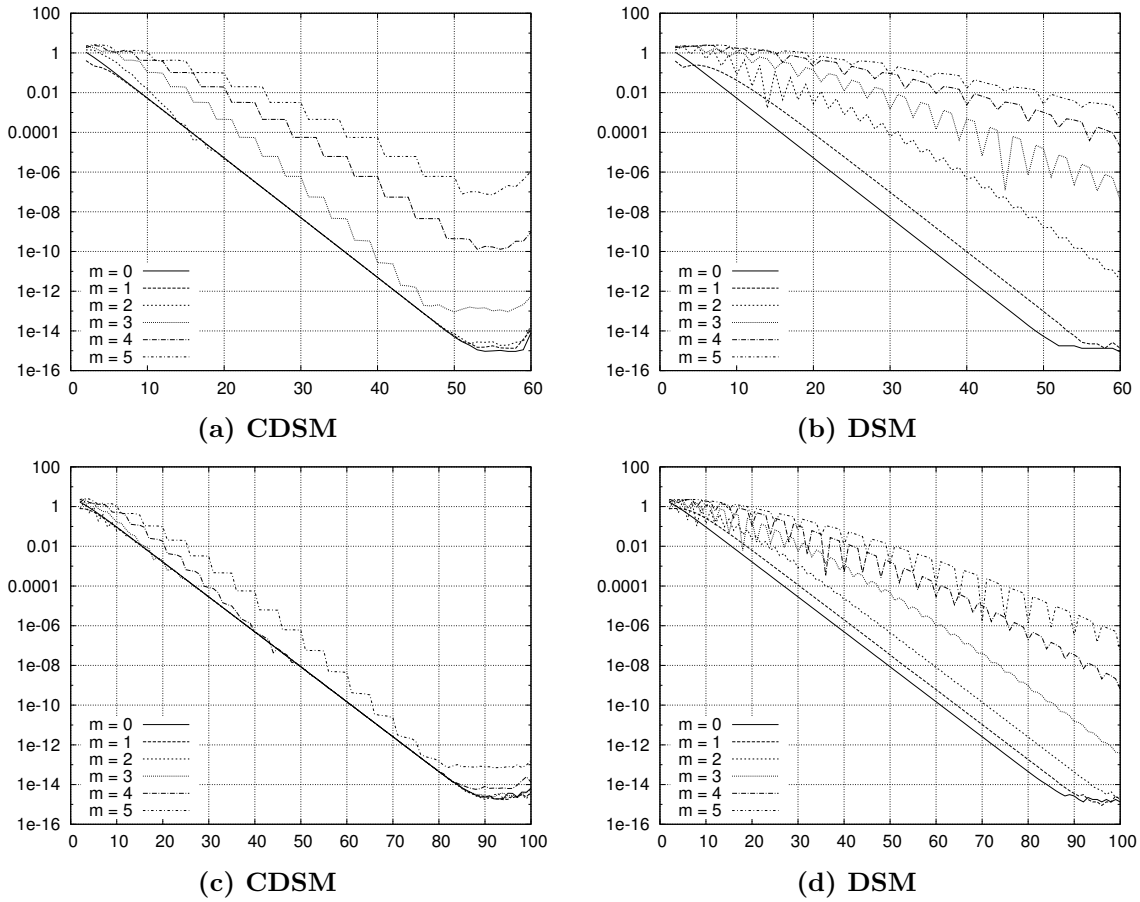

(a) CDSM **(b) DSM**

(c) CDSM **(d) DSM**

Figure 8.2: $f(z) = \exp(z^m)$ where $m \in \{0, 1, \ldots, 5\}$, in double-precision: (a), (b) $N \in \{2, 3, \ldots, 060\}$, $\rho = 1$, and $R = 2$; (c), (d) $N \in \{2, 3, \ldots, 100\}$, $\rho = 1$, and $R = 1.5$

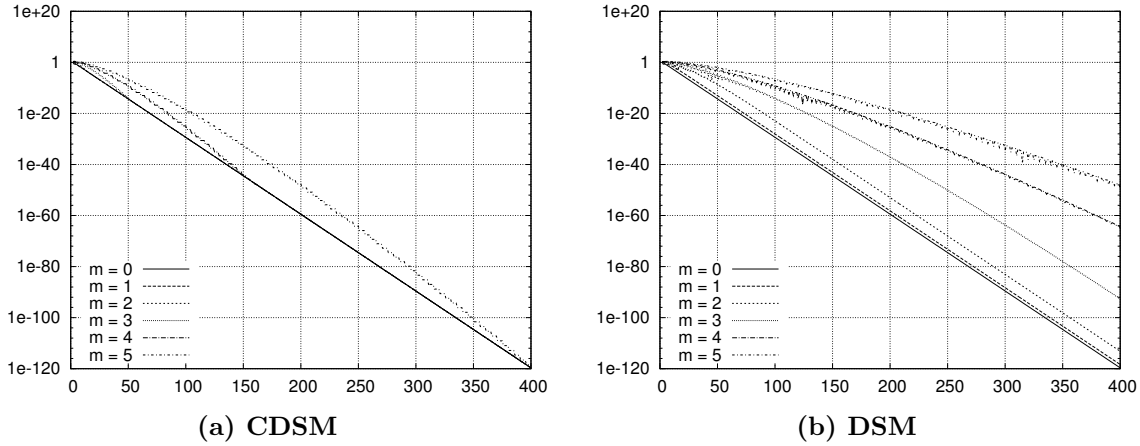

(a) CDSM **(b) DSM**

Figure 8.3: $f(z) = \exp(z^m)$ where $m \in \{0, 1, \ldots, 5\}$, $N \in \{2, 3, \ldots, 400\}$, in multiple-precision (120 digits): (a) $\rho = 1$ and $R = 2$; (b) $\rho = 1$ and $R = 1.5$

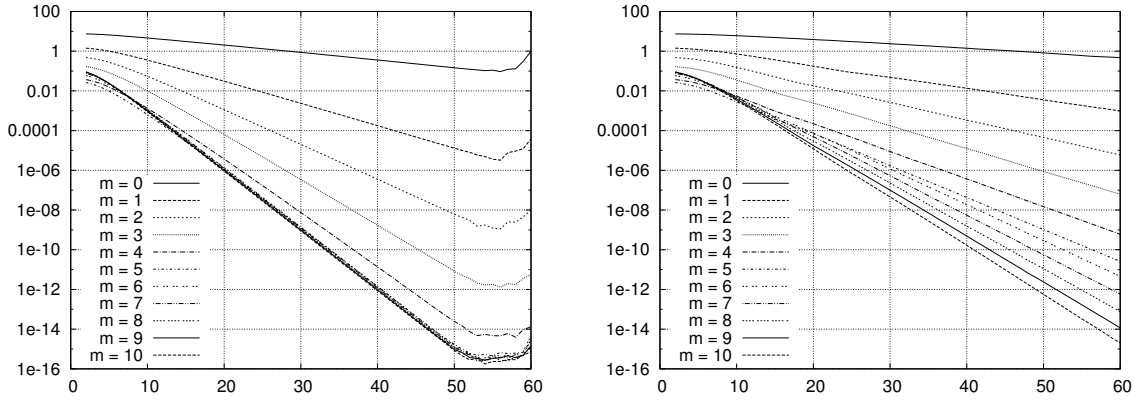

(a) CDSM **(b) DSM**

Figure 8.4: $f(z) = 1/(z - p(m))$ where $m \in \{0, 1, \ldots, 10\}$, $N \in \{2, 3, \ldots, 60\}$, $\rho = 1$ and $R = 2$

Test 4. In this test we deal with the case where f is an exponential function composed with a rational function:

$$f(z) = \exp\left(\frac{1}{z - p(m)}\right), \quad p(m) = \rho + 0.1 + 0.2m,$$

where $m \in \{0, 1, \ldots, 10\}$ is a parameter. f has an essential singularity at $p(m)$.

(i) We compute $\tilde{e}^{(N)}$ and $\tilde{e}_{\mathrm{D}}^{(N)}$ for all $N \in \{2, 3, \ldots, 60\}$. See Figure 8.5.

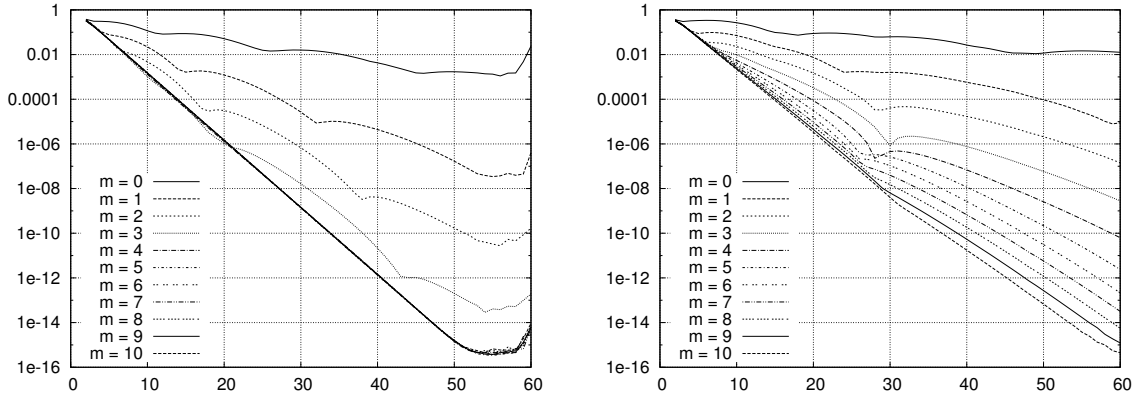

(a) CDSM **(b) DSM**

Figure 8.5: $f(z) = \exp(1/(z - p(m)))$ where $m \in \{0, 1, \ldots, 10\}$, $N \in \{2, 3, \ldots, 60\}$, in double-precision: $\rho = 1$ and $R = 2$

(ii) In order to elucidate the same investigation of Test 2, we compute $\tilde{e}^{(N)}$ and $\tilde{e}_{\mathrm{D}}^{(N)}$ for al $N \in \{2, 3, \ldots, 400\}$ in 120 digits precision by C++ programs using exflib. We find from Figure 8.6 that $\tilde{e}^{(N)}$ and $\tilde{e}_{\mathrm{D}}^{(N)}$ behave as (8.5.1), and $\dagger$ and τ' are equal to $\max\{\rho/R, \rho/p(m)\}$ and $\max\{\rho/R, \sqrt{\rho/p(m)}\}$, respectively, in this case.

We summarize the results of our numerical experiments.

- The behaviors of $\tilde{e}^{(N)}$ and $\tilde{e}_{\mathrm{D}}^{(N)}$ are what we can expect from the error estimate.

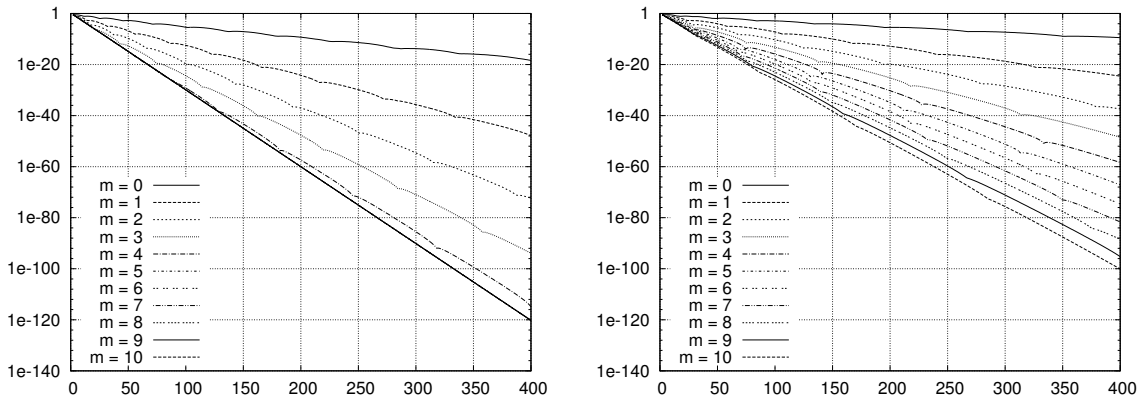

(a) CDSM **(b) DSM**

Figure 8.6: $f(z) = \exp(1/(z - p(m)))$ where $m \in \{0, 1, \ldots, 10\}$, $N \in \{2, 3, \ldots, 400\}$, in multiple-precision (120 digits), $\rho = 1$, and $R = 2$

- $\tilde{e}^{(N)}$ decays exponentially with respect to N, and the gradient of the straight section of N-$\log_{10} \tilde{e}^{(N)}$ curve is almost equal to

$$\max\left\{\log_{10}\frac{\rho}{R}, \log_{10}\frac{\rho}{r_0}\right\}.$$

  Simultaneously, $\tilde{e}_{\mathrm{D}}^{(N)}$ decays exponentially with respect to N, and the gradient of the straight section of N-$\log_{10} \tilde{e}_{\mathrm{D}}^{(N)}$ curve is almost equal to

$$\max\left\{\log_{10}\frac{\rho}{R}, \frac{1}{2}\log_{10}\frac{\rho}{r_0}\right\}.$$

- Best selection of Rs for CDSM and DSM is $R = r_0$ and $R = \sqrt{\rho r_0}$, respectively. Hence, the fastest decaying speed of the error for CDSM and DSM is $(\rho/r_0)^N$ and $(\rho/r_0)^{N/2}$, respectively. In the light of this fact, the convergence rate for CDSM is faster than that for DSM, and to incarnate it, we have to choose largish R, but we can achieve the smallest error for smaller N.

8.6 Concluding remarks

In the previous sections, we proposed CDSM which approximates a holomorphic function f by a linear combination of $1/(z - \zeta)$ of the form (8.1.1) using boundary values of f. A mathematical analysis showed the exponential convergence of the approximate function which is constructed by CDSM, and the result of our numerical experiments exemplified the effectiveness of CDSM.

Bibliography

[1] G. Ala, G. Fasshauer, E. Francomano, S. Ganci and M. Mccourt, *The method of fundamental solutions in solving coupled boundary value problems for M/EEG*, SIAM J. Sci. Comput. **37** (2015), no. 4, B570–B590.

[2] K. Amano, *Numerical conformal mapping based on the charge simulation method* (in Japanese), Trans. Inform. Process. Soc. Japan **28** (1987), 697–704.

[3] K. Amano, D. Okano, H. Ogata and M. Sugihara, *Numerical conformal maings onto the linear slit domains*, Jpn. J. Ind. Appl. Math. **29** (2012), no. 2, 165–186.

[4] S. B. Angenent and M. E. Gurtin, *Multiphase thermomechanics with interfacial structure. II. Evolution of an isothermal interface*, Arch. Ration. Mech. Anal. **108** (1989), no. 4, 323–391.

[5] D. N. Arnold, *A spline-trigonometric Galerkin method and an exponentially convergent boundary integral method*, Math. Comp. **41** (1983), no. 164, 383–397.

[6] D. N. Arnold and W. L. Wendland, *The convergence of spline collocation for strongly elliptic equations on curves*, Numer. Math. **47** (1985), no. 3, 317–341.

[7] T. L. Ashbee, J. G. Esler and N. R. McDonald, *Generalized Hamiltonian point vortex dynamics on arbitrary domains using the method of fundamental solutions*, J. Comput. Phys. **246** (2013), 289–303.

[8] S. Axler, P. Bourdon and W. Ramey, *Harmonic function theory*, Second edition, Springer-Verlag, New York, 2001.

[9] R. Ballisti and Ch. Hafner, *The multiple multipole method (MMP) in electro- and magnetostatic problems*, IEEE Transactions on Magnetics **19** (1983), no. 6, 2367–2370.

[10] A. H. Barnett and T. Betcke, *Stability and convergence of the method of fundamental solutions for Helmholtz problems on analytic domains*, J. Comput. Phys. **227** (2008), no. 14, 7003–7026.

[11] M. Beneš, M. Kimura and S. Yazaki, *Second order numerical scheme for motion of polygonal curves with constant area speed*, Interfaces Free Bound. **11** (2009), no. 4, 515–536.

[12] S. Bock and K. Gürlebeck, *On a spatial generalization of the Kolosov-Muskhelishvili formulae*, Math. Methods Appl. Sci. **32** (2009), no. 2, 223–240.

[13] A. Bogomolny, *Fundamental solutions method for ellitic boundary value problems*, SIAM J. Numer. Anal. **22** (1985), no. 4, 644–669.

[14] C. S. Chen, X. Jiang, W. Chen and G. Yao, *Fast solution for solving the modified Helmholtz equation with the method of fundamental solutions*, Commun. Comput. Phys. **17** (2015), no. 3, 867–886.

[15] W. Chen and F. Z. Wang, *A method of fundamental solutions without fictitious boundary*, Eng. Anal. Bound. Elem. **34** (2010), no. 5, 530–532.

[16] W. Chen, J. Lin and C. S. Chen, *The method of fundamental solutions for solving exterior axisymmetric Helmholtz Problems with high wave-number*, Adv. Appl. Math. Mech. **5** (2013), no. 4, 477–493.

[17] M. I. Comodi and R. Mathon, *A boundary approximation method for fourth order problems*, Math. Models Methods Appl. Sci. **1** (1991), no. 4, 437–445.

[18] C. L. Epstein and M. Gage, *The curve shortening flow*, Math. Sci. Res. Inst. Publ. **7** (1987), 15–59.

[19] G. B. Folland, *Introduction to partial differential equations*, 2nd edn., Princeton University Press, Princeton (1995).

[20] G. Fairweather and A. Karageorghis, *The method of fundamental solutions for elliptic boundary value problems*, Adv. Comput. Math. **9** (1998), no. 1–2, 69–95.

[21] H. Fujiwara, `http://www-an.acs.i.kyoto-u.ac.jp/~fujiwara/exflib/`

[22] G. Gáspár, *A regularized multi-level technique for solving potential problems by the method of fundamental solutions*, Eng. Anal. Bound. **57** (2015), 66–71.

[23] L. Greengard and J.-Y. Lee, *A direct adaptive Poisson solver of arbitrary order accuracy*, J. Comput. Phys. **125** (1996), no. 2, 415–424.

[24] Y. Gu, W. Chen, Z.-J. Fu and B. Zhang, *The singular boundary method: mathematical background and application in orthotropic elastic problems*, Eng. Anal. Bound. Elem. **44** (2014), 152–160.

[25] M. E. Gurtin, *Thermomechanics of evolving phase boundaries in the plane*, Oxford, 1993.

[26] B. Gustafsson and A. Vasil'ev, *Conformal and potential analysis in Hele-Shaw cells*, Birkhäuser, 2006.

[27] M. A. Golberg, *The method of fundamental solutions for Poisson's equation*, Eng. Anal. Bound. Elem. **16** (1995), no. 3, 205–213.

[28] E. Goursat, *Sur l'équation* $\triangle\triangle u = 0$, Bull. Soc. Math. France **26** (1898), 236-237.

[29] Ch. Hafner, *The generalized multipole technique for computational electromagnetics*, Artech House Books, Boston, 1990, 312pp.

[30] S. A. A. A.-Hatemi, A. H. M. Murid and M. M. S. Nasser, *A boundary integral equation with the generalized Neumann kernel for a mixed boundary value problem in unbounded multiply connected regions*, Bound. Value Probl. **54** (2013), 2013:54, 17 pp.

[31] J. K. Hayes, D. K. Kahaner, and R. G. Kellner, *An improved method for numerical conformal mapping*, Math. Comput. **26** (1972), no. 118, 327–334.

[32] H. S. Hele-Shaw, *The flow of water*, Nature **58** (1898), no. 1489, 34–36.

[33] P. Henrici, *Applied and computational complex analysis, vol. 3*, John Wiley & Sons, New York, 1986.

[34] T. Y. Hou, J. S. Lowengrub and M. J. Shelley, *Removing the stiffness from interfacial flows with surface tension*, J. Comput. Phys. **114** (1994), no. 2, 312–338.

[35] D. M. Hough and N. Papamichael, *The use of splines and singular functions in an integral equation method for conformal mapping*, Numer. Math. **37** (1981), 133–147.

[36] D. M. Hough and N. Papamichael, *An integral equation method for the numerical conformal mapping of interior, exterior and doubly-connected domains*, Numer. Math. **41** (1983), 287–307.

[37] B. T. Johansson, D. Lesnic and T. Reeve, *The method of fundamental solutions for the two-dimensional inverse Stefan problem*, Inverse Probl. Sci. Eng. **22** (2014), no. 1, 112–129.

[38] U. Kangro, *Convergence of collocation method with delta functions for integral equations of first kind*, Integr. Equ. Oper. Theory **66** (2010), no. 2, 265–282.

[39] A. Karageorghis, *Efficient MFS algorithms for inhomogeneous polyharmonic problems*, J. Sci. Comput. **46** (2011), no. 3, 519–541.

[40] A. Karageorghis, *The method of fundamental solutions for elliptic problems in circular domains with mixed boundary conditions*, Numer. Algor. **68** (2015), 185–211.

[41] A. Karageorghis and G. Fairweather, *The method of fundamental solutions for the numerical solution of the biharmonic equation*, J. Comput. Phys. **69** (1987), 434–459.

[42] A. Karageorghis and G. Fairweather, *The Almansi method of fundamental solutions for solving biharmonic problems*, Int. J. Numer. Methods Eng. **26** (1988), no. 7, 1665–1682.

[43] A. Karageorghis and G. Fairweather, *The method of fundamental solutions for the solution of nonlinear plane potential problems*, IMA J. Numer. Anal. **9** (1989), no. 2, 231–242.

[44] A. Karageorghis, D. Lesnic and L. Marin, *A survey of applications of the MFS to inverse problems*, Inverse Probl. Sci. Eng. **19** (2011), no. 3, 309–336.

[45] M. Katsurada, *A mathematical study of the charge simulation method II*, J. Fac. Sci. Univ. Tokyo Sect. IA Math. **36** (1989), no. 1, 135–162.

[46] M. Katsurada, *Asymptotic error analysis of the charge simulation method in a Jordan region with an analytic boundary*, J. Fac. Sci. Univ. Tokyo Sect. IA Math. **37** (1998), no. 8, 195–212.

[47] M. Katsurada, *Charge simulation method using exterior maing functions*, Jpn. J. Indust. Appl. Math. **11** (1994), no. 1, 47–61.

[48] M. Katsurada, *A mathematical study of the charge simulation method by use of peripheral conformal mappings*, Mem. Inst. Sci. Tech. Meiji Univ. **35** (1998), no. 3, 195–212.

[49] M. Katsurada and H. Okamoto, *A mathematical study of the charge simulation method I*, J. Fac. Sci. Univ. Tokyo Sect. IA Math. **35** (1988), no. 3, 507–518.

[50] M. Katsurada and H. Okamoto, *The collocation points of the fundamental solution method for the potential roblem*, Comput. Math. Appl. **31** (1996), no. 1, 123–137.

[51] A. K. Khambampati, Y.-L. Lee, K. Y. Kim, D. W. Jerng and S. Kim, *A meshless improved boundary distributed source method for two-phase flow monitoring using electrical resistance tomography*, Eng. Anal. Bound. Elem. **52** (2015), 1–15.

[52] M. Kimura, *Accurate numerical scheme for the flow by curvature*, Appl. Math. Lett. **7** (1994), no. 1, 69–73.

[53] M. Kimura, *Numerical analysis of moving boundary problems using the boundary tracking method*, Jpn. J. Indust. Appl. Math. **14** (1997), no. 3, 373–398.

[54] M. Kimura, *Geometry of hypersurfaces and moving hypersurfaces in $\mathbb{R}^m$ for the study of moving boundary problems*, Topics in mathematical modeling, Jindřich Nečas Cent. Math. Model. Lect. Notes **4**, Matfyzpress (2008), 39–93.

[55] M. Kimura and H. Notsu, *A level set method using the signed distance function*, Jan. J. Indust. Appl. Math. **19** (2002), no. 2, 415–446.

[56] M. Kimura, D. Tagami and S. Yazaki, *Polygonal Hele-Shaw problem with surface tension*, Interfaces and Free Boundaries **15** (2013), no. 1, 77–93.

[57] T. Kitagawa, *On the numerical stability of the method of fundamental solutions applied to the Dirichlet problem*, Japan. J. Appl. Math. **5** (1988), no. 1, 123–133.

[58] T. Kitagawa, *Asymptotic stability of the fundamental solution method*, Proceedings of the International Symposium on Computational Mathematics (Matsuyama 1990), J. Comput. Appl. Math. **38** (1991), no. 1–3, 263–269.

[59] J. A. Kołodziej and M. Mierzwiczak, *Transient heat conduction by different version of the method of fundamental solutions — a comparison study*, Comput. Assist. Mech. Eng. Sci. **17** (2010), no. 1, 75–88.

[60] J. A. Kołodziej and J. K. Grabski, *Application of the method of fundamental solutions and the radial basis functions for viscous laminar flow in wavy channel*, Eng. Anal. Bound. Elem. **57** (2015), 58–65.

[61] M. Krakowski and A. Charnes, *Stokes' paradox and biharmonic flows*, Report **37**, Carnegie Institute of Technology, Department of Mathematics, Pittsuburgh, PA (1953).

[62] H. Lamb, *Hydrodynamics*, 6th edition, Dover Publications, 1945.

[63] M. Li, C. S. Chen, C. C. Chu and D. L. Young, *Transient 3D heat conduction in functionally graded materials by the method of fundamental solutions*, Eng. Anal. Bound. Elem. **45** (2014), 62–67.

[64] M. Li, C. S. Chen and A. Karageorghis, *The MFS for the solution of harmonic boundary value problems with non-harmonic boundary conditions*, Comput. Math. Appl. **66** (2013), no. 11, 2400–2424.

[65] W. Li, M. Li, C. S. Chen and X. Lu, *Compactly supported radial basis functions for solving high order partial differential equations in 3D*, Eng. Anal. Bound. Elem. **55** (2015), 2–9.

[66] Z.-C. Li, *The method of fundamental solutions for annluar shaped domains*, J. Comput. Appl. Math. **228** (2009), no. 1, 355–372.

[67] Z.-C. Li, M.-G. Lee, J. Y. Chiang and Y. P. Liu, *The Trefftz method using fundamental solutions for biharmonic equations*, J. Comput. Appl. Math. **235** (2011), no. 15, 4350–4367.

[68] Z.-C. Li, R. Mathon and . Sermer, *Boundary methods for solving elliptic problems with singularities and interfaces*, SIAM J. Numer. Anal. **24** (1987), no. 3, 487–498.

[69] J. Lin, W. Chen and C. S. Chen, *A new scheme for the solution of reaction diffusion and wave propagation problems*, Appl. Math. Model. **38** (2014), no. 23, 5651–5664.

[70] K. Mikula and D. Ševčovič, *Evolution of plane curves driven by a nonlinear function of curvature and anisotropy*, SIAM J. Appl. Math. **61** (2001), no. 5, 1473–1501.

[71] K. Mikula and D. Ševčovič, *A direct method for solving an anisotropic mean curvature flow of plane curve with an external force*, Math. Meth. Appl. Sci. **27** (2004), no. 13, 1545–1565.

[72] K. Mikula and D. Ševčovič, *Evolution of curves on a surface driven by the geodesic curvature and external force*, Appl. Anal. **85** (2006), no. 4, 345–362.

[73] K. Murota, *On "invariance" of schemes in the fundamental solution method* (Japanese), Information Processing Society of Japan **34** (1993), no. 3, 533–535.

[74] K. Murota, *Comparison of conventional and "invariant" schemes of fundamental solutions method for annular domains*, Jpn. J. Indust. Appl. Math. **12** (1995), no. 1, 61–85.

[75] M. M. S. Nasser, A. H. M. Muric, M. Ismail and E. M. A. Alejaily, *Boundary integral equations with the generalized Neumann kernel for Laplace's equation in multiply connected regions*, Appl. Math. Comput. **217** (2011), no. 9, 4710–4727.

[76] K. Nishida, *Mathematical and numerical analysis of charge simulation method in* 2*-dimensional ellitic domains*, Trans. Jpn. Soc. Ind. Appl. Math. **5** (1995), no. 3, 185–198.

[77] H. Ogata, *Dipole simulation method for two-dimensional potential problems*, NOLTA, IEICE **5** (2014), no. 1, 2–14.

[78] H. Ogata, F. Chiba and T. Ushijima, *A new theoretical error estimate of the method of fundametal solutions applied o reduced wave problems in the exterior region of a disk*, J. Comput. Appl. Math. **235** (2011), no. 12, 3395–3412.

[79] H. Ogata and M. Katsurada, *Convergence of the invariant scheme of the method of fundamental solutions for two-dimensional potential problems in a Jordan region*, Jpn. J. Ind. Appl. Math. **31** (2014), no. 1, 231–262.

[80] T. Ohe and K. Ohnaka, *Uniqueness and convergence of numerical solution of the Cauchy roblem for the Laplace equation by a charge simulation method*, Jpn. J. Indust. Appl. Math. **31** (2014), no. 1, 231–262.

[81] I. G. Petrovsky, *Lectures on partial differential equations*, Dover Publications, Inc., New York (1991).

[82] T. Reeve and B. T. Johansson, *The method of fundamental solutions for a time-dependent two-dimensional Cauchy heat conduction problem*, Eng. Anal. Bound. Elem. **37** (2013), no. 3, 569–578.

[83] T. Sakajo and Y. Amaya, *Numerical construction of potential flows in multily connected channel domains*, Computat. Methods and Funct. Theory **11** (2011), no. 2, 415–438.

[84] K. Sakakibara, *Analysis of the dipole simulation method for two-dimensional Dirichlet problems in Jordan regions with analytic boundaries*, BIT Numer. Math. **56** (2016), no. 4, 1369–1400.

[85] K. Sakakibara, *Asymptotic analysis of the conventional and invariant schemes for the method of fundamental solutions applied to potential problems in doubly-connected regions*, accepted by Jpn. J. Indust. Appl. Math.

[86] K. Sakakibara, *Method of fundamental solutions for biharmonic equation based on Almansi-type decomposition*, submitted.

[87] K. Sakakibara and M. Katsurada, *A mathematical analysis of the complex dipole simulation method*, Tokyo J. Math. **38** (2015), no. 2, 309–326.

[88] K. Sakakibara and M. Katsurada, *Numerical conformal mapping based on the dipole simulation method*, in preparation.

[89] K. Sakakibara and S. Yazaki, *A charge simulation method for the computation of Hele-Shaw problem*, RIMS Kôkyûroku **1957** (2015), 116–133.

[90] K. Sakakibara and S. Yazaki, *Structure-preserving numerical scheme for the one phase Hele-Shaw problems by the method of fundamental solutions*, submitted revised version to Numer. Math.

[91] K. Sakakibara and S. Yazaki, *Method of fundamental solutions with weighted average condition and dummy points*, submitted revised vertion to JSIAM Lett.

[92] D. Ševčovič and S. Yazaki, *Evolution of plane curves with a curvature adjusted tangential velocity*, Jpn. J. Indust. Appl. Math. **28** (2011), no. 3, 413–442.

[93] D. Ševčovič and S. Yazaki, *On a gradient flow of plane curves minimizing the anisoperimetric ratio*, IAENG Int. J. Appl. Math. **43** (2013), no. 3, 160–171.

[94] M. J. Shelley, F.-R. Tian and K. Wlodarski, *Hele-Shaw flow and pattern formation in a time-dependent gap*, Nonlinearity **10** (1997), no. 6, 1471–1495.

[95] Y.-S. Smyrlis, *The method of fundamental solutions: A weighted least-squares approach*, no. 1, BIT Numer. Math. **46** (2006), 163–194.

[96] Y. Sun, *Modified method of fundamental solutions for the Cauchy problem connected with the Laplace equation*, Int. J. Comput. Math. **91** (2014), no. 10, 2185–2198.

[97] Y. Sun, F. Ma and X. Zhou, *An invariant method of fundamental solutions for the Cauchy problem in two-dimensional isotropic linear elasticity*, J. Sci. Comput. **64** (2015), no. 1, 197–215.

[98] S. G. Symm, *An integral equation method in conformal mapping*, Numer. Math. **9** (1956), 250–258.

[99] J. E. Taylor, *Motion of curves by crystalline curvature, including triple junctions and boundary points*, Proc. Sympos. Pure Math. 54, Amer. Math. Soc. (1993), Part 1, 417–438.

[100] C. C. Tsai, Y. C. Lin, D. L. Young and S. N. Atluri, *Investigations on the accuracy and condition number for the method of fundamental solutions*, CMES **16** (2006), no. 2, 103–114.

[101] A. N. Varchenko and P. I. Etingof, *Why the boundary of a round drop becomes a curve of order four*, University Lecture Series **3** (1992), Amer. Math. Soc.

[102] T. Wei and Y. Zhou, *Convergence analysis for the Cauchy roblem of Laplace's equation by a regularized method of fundamental solutions*, Adv. Comput. Math. **33** (2010), no. 4, 491–510.

[103] J. Wen, M. Yamamoto and T. Wei, *Simultaneous determination of a time-dependent heat source and the initial temperature in an inverse heat conduction problem*, Inverse Probl. Sci. Eng. **21** (2013), no. 3, 485–499.

[104] C. Xenophontos, M. Elliotis and G. Georgious, *A singular function boundary integral method for Laplacian problems with boundary singularities*, SIAM J. Sci. Comput. **28** (2006), no. 2, 517–532.

[105] L. Yan and F. Yang, *Efficient Kansa-type MFS algorithm for time-fractional inverse diffusion problems*, Comput. Math. Appl. **67** (2014), no. 8, 1507–1520.

[106] S. Yazaki, *A numerical scheme for the Hele-Shaw flow with a time-dependent gap by a curvature adjusted method*, Nonlinear Dynamics in Partial Differential Equations, Adv. Stud. Pure Math. **64** (2015), Math. Soc. Japan, Tokyo, 253–261.

[107] D. L. Young, C. C. Tsai, C. W. Chen and C. M. Fan, *The method of fundamental solutions and condition number analysis for inverse problems of Laplace equation*, Comput. Math. Appl. **55** (2008), no. 6, 1189–1200.

[108] L. Zhang, Z.-C. Li, Y. Wei and J. Y. Chiang, *Cauchy problems of Laplace's equation by the methods of fundamental solutions and particular solutions*, Eng. Anal. Bound. Elem. **37** (2013), no. 4, 765–780.